University of Antwerp

Faculty of Medicine and Health Science

Decoding the Genetic Puzzle of Inherited Cardiac Arrhythmias: Insights from Molecular Autopsy, Genetic Profiling and iPSC-derived Cardiomyocyte Modelling

PhD thesis submitted for the degree of Doctor of Medical Sciences at the University of Antwerp to be defended by Eline Simons

Supervisors:
Prof. Maaike Alaerts, Prof. Bart Loeys, Dr. Dorien Schepers

Antwerp, 2024

Members of the Jury

Promotors

Prof. Maaike Alaerts

Prof. Bart Loeys

Dr. Dorien Schepers

Internal Doctoral Committee

Prof. Caroline Van De Heyning

Prof. Marije Meuwissen

External jury members

Prof. Jolanda Van Hengel

Prof. Paul Volders

Cover by: Bing Image Creator

Table of Contents

Summary

Inherited cardiac arrhythmias (ICA) encompass a group of cardiac diseases with common characteristics such as low prevalence, reduced penetrance and similar but variable phenotypical expression including electrocardiogram (ECG) abnormalities, syncopes, ventricular fibrillations and increased risk for sudden cardiac death (SCD). Most ICAs are autosomal dominantly inherited and are accounted for by roughly 70 genes which demonstrate substantial genetic overlap. The complete genetic architecture of these ICA is not yet fully understood. Even with the rise of next generation sequencing (NGS) techniques, many cases remain genetically unsolved, in part because of more complex genetic inheritance patterns and still unidentified genetic causes, but also due to the substantial number of variants of uncertain significance (VUS) in the known genes. Functional analyses can provide the ultimate proof to reclassify a VUS to either (likely) benign or (likely) pathogenic but as this is labour intensive and expensive, it is not routinely done in a diagnostic setting.

A case of sudden cardiac death was investigated at our Center of Medical Genetics using two diagnostic gene panels including 51 ICA and 51 cardiomyopathy genes to screen for possible causal variants. We detected two VUS in the *KCNQ1* and *DSG2* genes. On research basis, an *in vitro* functional analysis of the *KCNQ1* variant, performed by a master student, did not show any effect on the potassium current. Segregation analysis revealed that the *DSG2* variant was *de novo*, upscaling its classification to likely pathogenic. Both the mother and daughter of the deceased patient carried the *KCNQ1* variant, for which they initially were receiving treatment. However, based on the functional analysis this variant could be reclassified as likely benign and consequently the treatment was discontinued. This case highlights the added value of performing a molecular autopsy and functional analysis of VUS.

Brugada syndrome (BrS) is an ICA displaying extreme variable expressivity and only up to 30% of the patients can be genetically diagnosed. In our Center of Medical Genetics, together with colleagues I collected clinal data from 350 patients' records and examined the genetic diagnostic yield of an ICA gene panel in a BrS cohort and only found a (likely) pathogenic genetic variant in 9% of the patients. These patients showed a more severe clinical phenotype with more spontaneous type I BrS pattern on ECG, prolonged PR interval and QRS segment, ventricular fibrillations and more often presented with a family history of BrS or SCD. If only patients are included with a definite BrS diagnosis following the Shanghai scoring system, a yield of 18% is reached. VUS were found in 31% of the full BrS cohort, but apart from the opportunity to perform segregation analysis, such VUS do not contribute to more informative genetic counselling for the patient and family members.

To better interpret VUS, functional analyses can be performed in heterologous expression systems, as we did for the *KCNQ1* VUS. But a new human cellular model to study variants became available with the advent of induced pluripotent stem cells (iPSC). Using small molecules, these iPSCs can be differentiated into cardiomyocytes (iPSC-CM), providing a disease-specific physiologically relevant cell model for investigation. We generated iPSCs from skin fibroblasts from five BrS patients carrying a Belgian *SCN5A* founder mutation (c.4813+3_4813+6dupGGGT) and two unrelated healthy control individuals. These cells showed their pluripotent nature and were validated using a series of molecular assays. Although the five patients carried the same mutation, they presented with different clinical phenotypes, ranging from being asymptomatic to suffering from SCD. To investigate the effect of the *SCN5A* mutation, iPSCs were differentiated into cardiomyocytes which show spontaneous contraction and express cardiomyocyte-specific markers. iPSC-CMs of patients did not differ significantly from the ones originated from control individuals when comparing total *SCN5A* mRNA and protein expression, sodium current density and action potential (AP) characteristics. The only significant difference we observed was in the expression of the transcripts of *SCN5A* where patient iPSC-CMs expressed two mutant transcripts, one with a 96 base pair (bp) deletion and one with an intronic GTGG retention leading to a frameshift. Only few parameters analysed in the iPSC-CMs of the patients correlated with the clinical severity of the patients. These parameters are the expression of WT and 96 bp deletion *SCN5A* transcripts, AP amplitude, upstroke velocity and AP duration at 90% of repolarization. An important observation was that our ability to identify statistically significant differences and correlations was hampered by the variability of the results. We differentiated two different iPSC clones per individual and performed at least two differentiations per clone and we observed substantial variation in the results between two clones of one individual as well as within one clone. The use of a CRISPR generated isogenic control of one of the severely affected patients, in which absence of the two mutant *SCN5A* transcripts was confirmed, did result in a peak sodium current that was significantly higher in the isogenic control compared to the patient iPSC-CMs. This supports the use of isogenic controls as a promising strategy to study this and other mutations.

With enhanced molecular techniques for investigating the genetic landscape of ICAs, it has become clear that the effect of genetic variants is not always easy to interpret and functional analysis is needed. For this purpose, novel study models such as iPSC-CMs can play an important role as they represent the disease-relevant cell type with full cardiomyocyte-specific molecular machinery, can be patient-specific and isogenic lines can be generated. In this way, also more complex interactions can be studied in a relevant cell model.

Samenvatting

Erfelijke hartritmestoornissen (EHS) vormen een groep van hartziekten met gemeenschappelijke kenmerken zoals een lage prevalentie, beperkte penetrantie en gelijkaardige maar variabele fenotypische expressie waaronder afwijkingen in het elektrocardiogram (ECG), syncopen, ventrikelfibrillaties en een verhoogd risico op plotse hartdood. De meeste EHS worden autosomaal dominant overgeërfd en worden veroorzaakt door ongeveer 70 genen die een aanzienlijke genetische overlap vertonen. De volledige genetische architectuur van deze EHS is nog niet volledig begrepen. Zelfs met de opkomst van next generation sequencing (NGS) technieken, blijven veel gevallen genetisch onopgelost, deels vanwege een complexer genetisch overervingspatroon en nog niet geïdentificeerde genetische oorzaken, maar ook vanwege het substantiële aantal varianten van onzekere betekenis (variants of uncertain significance - VUS) in de bekende genen. Functionele analyses kunnen het ultieme bewijs leveren om een VUS te herclassificeren naar (waarschijnlijk) goedaardig of (waarschijnlijk) pathogeen, maar omdat dit arbeidsintensief en duur is, wordt het niet routinematig gedaan in een diagnostische setting.

Een geval van plotse hartdood werd in ons Centrum voor Medische Genetica onderzocht met behulp van twee diagnostische genpanels met 51 EHS- en 51 cardiomyopathiegenen om te screenen op mogelijke causale varianten. Er werden twee VUS'en gedetecteerd in de genen *KCNQ1* en *DSG2*. Een *in vitro* functionele analyse van de *KCNQ1* variant toonde geen effect op de kaliumstroom. Segregatieanalyse toonde aan dat de *DSG2* variant *de novo* was, waardoor de classificatie verhoogd werd naar waarschijnlijk pathogeen. Zowel de moeder als de dochter van de overleden patiënt waren drager van de *KCNQ1* variant, waarvoor ze aanvankelijk werden behandeld. Op basis van de functionele analyse kon deze variant echter worden geherclassificeerd als waarschijnlijk goedaardig, waardoor de behandeling werd gestaakt. Deze casus benadrukt de toegevoegde waarde van het uitvoeren van een moleculaire autopsie en functionele analyse van VUS.

Brugada syndroom (BrS) is een EHS met zeer variabele expressiviteit en slechts bij 30% van de patiënten kan een genetische diagnose worden gesteld. In ons Centrum voor Medische Genetica onderzochten we de genetische diagnostische opbrengst van een EHS-genenpanel in een BrS cohorte en vonden we slechts bij 9% van de patiënten een (waarschijnlijk) pathogene genetische variant. Deze patiënten vertoonden een ernstiger klinisch fenotype met meer spontaan type I BrS patroon op ECG, verlengd PR-interval en QRS-segment, ventriculaire fibrillaties en hadden ze vaker een familiale voorgeschiedenis van BrS of SCD. Als alleen patiënten worden geïncludeerd met een definitieve BrS diagnose volgens het Shanghai scoresysteem, wordt een opbrengst van 18% bereikt. VUS'en werden gevonden in 31% van de BrS cohorte, maar afgezien van de

mogelijkheid om segregatieanalyse uit te voeren, dragen dergelijke VUS'en niet bij aan een meer informatieve genetische counseling voor de patiënt en familieleden.

Om VUS'en beter te kunnen interpreteren, kunnen functionele analyses worden uitgevoerd in heterologe expressiesystemen, zoals we hebben gedaan voor de *KCNQ1* VUS. Maar een nieuw humaan celmodel om varianten te bestuderen werd beschikbaar met de komst van geïnduceerde pluripotente stamcellen (iPSC). Met behulp van 'small molecules' kunnen deze iPSCs worden gedifferentieerd in cardiomyocyten (iPSC-CM), waardoor een ziektespecifiek fysiologisch relevant celmodel ontstaat. We hebben iPSCs gegenereerd uit huidfibroblasten van vijf BrS patiënten met de Belgische *SCN5A* foundermutatie (c.4813+3_4813+6dupGGGT) en twee niet-verwante gezonde controlepersonen. Deze cellen toonden hun pluripotente aard en werden gevalideerd met behulp van een reeks moleculaire testen. Hoewel de vijf patiënten dezelfde mutatie dragen, vertoonden ze verschillende klinische fenotypes, variërend van asymptomatisch tot plotse hartdood. Om het effect van de *SCN5A* mutatie te onderzoeken, werden iPSCs gedifferentieerd tot cardiomyocyten die spontane contractie vertonen en cardiomyocyt-specifieke markers tot expressie brengen. iPSC-CM van patiënten verschilden niet significant van die afkomstig van controlepersonen bij het vergelijken van de totale *SCN5A* mRNA en eiwitexpressie, natriumstroomdensiteit en actiepotentiaal (AP) karakteristieken. Het enige significante verschil dat we zagen was in de expressie van de transcripten van *SCN5A*, waar iPSC-CMs van patiënten twee gemuteerde transcripten tot expressie brachten, één met een deletie van 96 baseparen (bp) en één met een intronische GTGG retentie wat leidt tot een frameshift. Slechts enkele parameters die in de iPSC-CMs van de patiënten werden geanalyseerd, correleerden met de klinische ernst van de patiënten. Deze parameters zijn de expressie van WT en 96 bp deletie *SCN5A* transcripten, AP amplitude, upstroke snelheid en AP duur bij 90% van de repolarisatie. Een belangrijke observatie was dat ons vermogen om statistisch significante verschillen en correlaties te identificeren gehinderd werd door de variabiliteit van de resultaten. We differentieerden twee verschillende iPSC klonen per individu en voerden ten minste twee differentiaties per kloon uit en we zagen aanzienlijke variatie in de resultaten tussen twee klonen van één individu en binnen één kloon. Het gebruik van een CRISPR-gegenereerde isogene controle van een van de ernstig aangedane patiënten, waarin de afwezigheid van de twee gemuteerde *SCN5A* transcripten werd bevestigd, resulteerde in een piek natriumstroom die significant hoger was in de isogene controle in vergelijking met de iPSC-CMs van de patiënt. Dit ondersteunt het gebruik van isogene controles als een veelbelovende strategie om deze en andere mutaties te bestuderen.

Met verbeterde moleculaire technieken voor het onderzoeken van het genetische landschap van EHS, is het duidelijk geworden dat varianten niet altijd gemakkelijk te

interpreteren zijn en dat functionele analyse nodig is. Voor dit doel kunnen nieuwe studiemodellen zoals iPSC-CM een belangrijke rol spelen, omdat ze het ziekterelevante celtype vertegenwoordigen met een volledige cardiomyocyt-specifieke moleculaire architectuur, patiënt specifiek kunnen zijn en isogene controlelijnen kunnen worden gegenereerd. Op deze manier kunnen ook complexere interacties worden bestudeerd in een relevant celmodel.

Introduction:
iPSC-Derived Cardiomyocytes in Inherited Cardiac Arrhythmias: Pathomechanistic Discovery and Drug Development

Eline Simons, Bart Loeys and Maaike Alaerts

Cardiogenetics Research Group, Center of Medical Genetics, University of Antwerp and Antwerp University Hospital, 2650 Antwerp, Belgium

Adapted from Biomedicines. DOI: 10.3390/biomedicines11020334

Abstract

With the discovery of induced pluripotent stem cell (iPSCs) a wide range of cell types, including iPSC-derived cardiomyocytes (iPSC-CM), can now be generated from an unlimited source of somatic cells. These iPSC-CM are used for different purposes such as disease modelling, drug discovery, cardiotoxicity testing and personalised medicine. The 2D iPSC-CM models have shown promising results, but they are known to be more immature compared to in vivo adult cardiomyocytes. Novel approaches to create 3D models with the possible addition of other (cardiac) cell types are being developed. This will not only improve the maturity of the cells, but also leads to more physiologically relevant models that more closely resemble the human heart. In this review, we focus on the progress in the modelling of inherited cardiac arrhythmias in both 2D and 3D and on the use of these models in therapy development and drug testing

Introduction

Since the discovery of induced pluripotent stem cells (iPSCs) in 2006 by Takahashi and Yamanaka (1), iPSCs have increasingly gained popularity in the scientific field; not only to perform stem cell research but also to create somatic cells derived from these iPSCs such as neurons (2), cardiomyocytes (3) and hepatic cells (4) amongst many others. The numerous advantages, such as access to difficult-to-access human cell types, the development of patient-specific cell types, decreased need for laboratory animals and less ethical concerns compared to embryonal stem cells (ESC), are well-known. However, there are also some drawbacks on the use of these derived cells such as variability, low differentiation efficiency and the immature state of the differentiated cells. Nevertheless, iPSC-derived cells are indispensable in the current cell-biology research community.

In 2009, Zwi et al. presented their work on the development of a way to differentiate iPSCs into cardiomyocytes (3). Their iPSC-derived cardiomyocytes (iPSC-CM) expressed the cardiac specific markers cardiac troponin-I and sarcomeric α-actinin, were electrophysiologically active and they displayed the expected response to the admission of different drugs. Ever since, an increasing number of papers have been published using iPSC-CM to model diseases, perform drug and cardiotoxicity testing and develop new therapies.

In this review, we take a closer look at these recent developments focusing on cardiac arrhythmia disorders and the transition from 2D to 3D culture models (Figure 1).

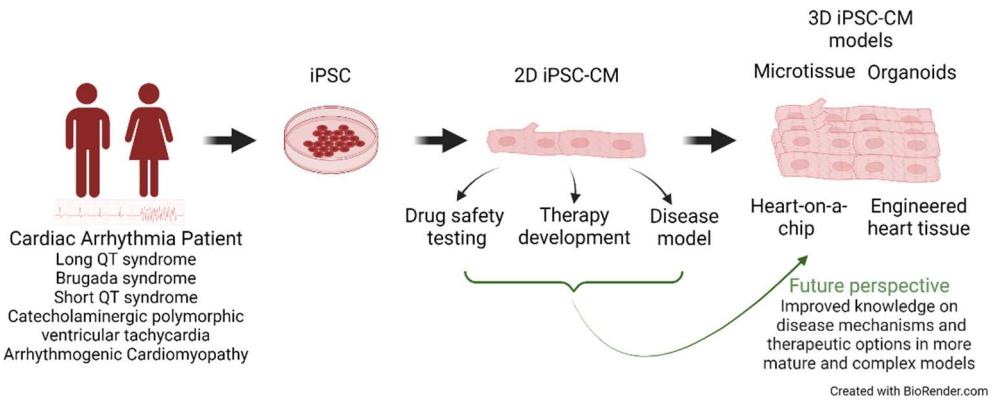

Figure 1. Schematic representation of different applications of iPSC-cardiomyocytes.

iPSC-Derived Cardiomyocytes as Inherited Cardiac Arrhythmia Models

Inherited cardiac arrhythmias (ICAs) are characterised by the dysfunction of cardiac ion channels, their accessory proteins or cell–cell contact proteins which can lead to ventricular arrhythmias and potential sudden cardiac death. The most well-known inherited cardiac arrhythmias (see **Table 1**) include long QT syndrome (LQTS), Brugada syndrome (BrS), catecholaminergic polymorphic ventricular tachycardia (CPVT), short QT syndrome (SQTS) and arrhythmogenic cardiomyopathy (ACM). These diseases are caused by pathogenic variants in genes encoding components or accessory elements of these ion channels or desmosomes. The type of mutation (loss-of-function (LOF) or gain-of-function (GOF)) is also important in defining the disease outcome. In the past, mutations were detected using Sanger sequencing, which is still the gold standard. This technique allows to read the DNA sequence of a gene in several small parts, which is a rather slow process. As such, potential candidate genes were sequenced one by one, starting with the most likely causal one. As soon as next generation sequencing (NGS) techniques were developed, using massive parallel sequencing technology, large amounts of DNA could be read simultaneously and many genes sequenced at the same time. Currently, three different approaches are available in a clinical setting for detecting (causal) variants, namely targeted next generation sequencing (NGS), whole exome sequencing (WES) or whole genome sequencing (WGS). The difference resides in the fact that targeted NGS reads a specific subset of genes that may play a role in the development of ICAs, while WES looks at all exons of all known genes at once. With WGS, the entire genome is examined, including the non-coding sequence and deep intronic variants. In the following section a brief overview of the different ICAs is given.

Long QT syndrome has a prevalence of 1 in 2000 and is clinically diagnosed by a prolongation of the QT interval (heart rate-corrected QT (QTc) interval ≥480 ms) on the electrocardiogram (ECG) (5). Patients present with symptoms like syncopes, palpitations, arrhythmias and typical development of Torsades de pointes that can lead to death. To prevent the development of symptoms, adjustments of lifestyle is advised with the addition of beta-blockers to reduce the risk of sudden cardiac death (SCD), and avoidance of any medication that could have a QT-prolonging effect. In case symptoms still occur under the treatment with beta-blockers, an implantable cardioverter defibrillator (ICD) can be implanted (6,7). Currently, there are 17 subtypes of LQTS based on the gene involved and the most common subtypes, responsible for up to 90% of patients with a causative mutation, are LQT1, LQT2 and LQT3, caused by mutations in the *KCNQ1*, *KCNH2* and *SCN5A* genes, respectively (8,9).

Short QT syndrome is diagnosed by a shortening of the QT interval (QTc <340 ms) on the ECG and has a prevalence ranging from 1 in 1000 to 1 in 5000 (10). Clinical symptoms are syncopes, atrial fibrillation, ventricular arrhythmia and SCD (10,11). Causal GOF mutations are mostly found in potassium channel genes such as *KCNH2*, *KCNQ1* and *KCNJ2* (11,12). The disease can be managed with the implantation of an ICD in symptomatic patients. As possible alternative a pharmacological treatment with quinidine or sotalol can be considered to prevent symptoms (13,14).

CPVT most often occurs in young adults and athletes and is triggered by β-adrenergic stimulation related to exercise or emotional stress. It is diagnosed based on an ECG with unexplained catecholamine-induced or stress-induced bidirectional ventricular tachycardia with normal resting ECG and in the absence of structural cardiac anomalies (15). Symptoms such as syncopes, ventricular (tachy)arrhythmias and SCD occur typically during physical activity or emotional stress (15,16). It is mainly caused by mutations in Ca^{2+}-handling related genes such as *RYR2* and *CASQ2* and has an estimated prevalence of 1 in 10.000 (12,17). Both proteins are essential in the Ca^{2+} handling in heart and muscle cells, responsible for the proper contraction of the cells. The preferred treatment is the administration of the beta-blocker nadolol in combination with lifestyle adjustments such as exercise restriction although this cannot prevent all the arrhythmic events in patients. In these cases, ICD implantation can be considered (5).

ACM, previously known as arrhythmogenic right ventricular cardiomyopathy (ARVC), has a prevalence of 1 in 5000 and is characterised by fibrofatty myocardial replacement, leading to impaired ventricular systolic function and ventricular arrhythmias. These can lead to SCD, which is an important cause of death in young athletes (18). Currently, there is no golden standard to diagnose ACM but scoring systems have been proposed, all using multiple parameters such as functional and structural ventricular abnormalities, tissue characterization, electrocardiographic alterations, ventricular arrhythmias, and familial/genetic background (19,20). Mutations in desmosomal genes such as *PKP2, DSG2, DSP, DSC2* and *JUP* play a prominent role in the development of the disease (18). Patients should adjust their lifestyle and not participate in competitive or endurance sport activities. On top of that, beta-blockers are recommended as well as the use of anti-arrhythmic drugs, implantation of an ICD and catheter ablation, all can help to manage the disease (18,21).

Brugada syndrome is a cardiac arrhythmia with a prevalence ranging from 1 in 500 to 1 in 2000 and patients display a specific ST-segment elevation on the ECG (Type I) in more than one right precordial lead (V1-V3), either occurring spontaneously or after administration of a sodium channel blocker like ajmaline or flecainide (22). BrS patients

and affected family members can show a variety of symptoms ranging from being asymptomatic over heart palpitations, syncopes and ventricular fibrillations (VF) which could eventually lead to SCD indicating the reduced penetrance and variable expression, phenomena's well known in BrS. This makes is challenging to apply risk stratification, even within one family. Currently only one gene is considered causal for BrS, namely *SCN5A,* encoding the cardiac sodium channel $Na_V1.5$ (23). Mutations in *SCN5A* account for up to 20–25% of the BrS cases (24,25). Many other genes encoding sodium (*SCN10A, SCN1B, SCN2B, SCN3B*), calcium (*CACNA1C, CACNA2D1, CACNB2B*) and potassium channels (*HCN4, KCND2, KCND3, KCNE3, KCNE5, KCNJ8*) and their associated proteins have been associated with the disease but evidence is lacking to definitely consider them as causal (23). Regarding the treatment and management of BrS, an ICD is advised for BrS patients with previous cardiac arrest or syncopes. All BrS patients should treat fever immediately and avoid drugs that can provoke BrS. Other treatments that might be considered are the use of quinidine and in some cases ablation (5,29).

Table 1: Inherited cardiac arrhythmias

Disease	Genes	Diagnosis	Treatment
LQTS	*KCNQ1* *KCNH2* *SCN5A*	QTc ≥ 480ms	ICD Beta-blockers
SQTS	KCNH2 KCNQ1 KCNJ2	QTc < 340ms	ICD Quinidine Sotalol
CPVT	*RYR2* *CASQ2*	ECG with unexplained catecholamine-induced or stress-induced bidirectional VT	ICD Lifestyle changes (reduces exercise) Beta-blockers (Nadolol)
ACM	*PKP2* *DSG2* *DSP* *DSC2* *JUP*	Scoring system: ventricular abnormalities tissue characterization electrocardiographic alterations ventricular arrhythmias familial/genetic background	ICD Beta-blockers Catheter ablation
BrS	*SCN5A*	Type I ECG with ST-segment elevation	ICD

In the past, mutations/variations were studies in heterologous expression systems where immortalized human or animal cells were used to express a specific ion channel

with or without the mutation in order to study the effect on the functioning of the channel. In some cases, auxiliary subunits are added to resemble more the in vivo situation. However, this technique does not allow to mimic the full physiological state to for example investigate the effect on action potentials generated in cardiac cells. In ICAs, arrhythmias mostly occur in the ventricles, making ventricular cardiomyocytes the most relevant cell type to investigate. Most of the currently used iPSC-CM differentiation protocols generate a mixture of atrial, ventricular and sinoatrial pacemaker cardiomyocytes, but with a clear overrepresentation/higher presence of ventricular cells. Ventricular action potentials (AP) are characterised by a more negative maximum diastolic potential, a rapid AP upstroke, a long plateau phase and an APD90/APD50 ratio ≤1.3/1.4 (30-32). It is also possible to differentiate iPSCs directly into the specific cardiomyocyte types (33).

In 2018, Garg et al. reviewed the published iPSC-CM models of several channelopathies (34) and Pan et al. updated this review with the addition of ACM (**Table S1** (Supplementary Materials)) (35). Here, the overview is updated (see **Table 2)** with more recently published models.

Long QT Syndrome

Over the years, several LQTS iPSC-CM models have been published, the first in 2010 by Moretti et al. (31). The latter investigated patient-specific iPSC-CM of three related LQT1 patients harbouring a p.(Arg190Gln) variant and showed a prolonged action potential duration at 90% of repolarisation (APD90) and lower potassium current densities compared to control individuals. This corresponded to the phenotype observed in the patients. Since then, several papers have been published describing LQTS iPSC-CM models of known pathogenic mutations (reviewed by Garg et al. (34), Table S1). More recently, LQTS iPSC-CM models have been used to investigate the pathogenicity of variants of uncertain significance (VUS). For example, Garg et al. created a LQT2 iPSC-CM model harbouring the VUS p.(Thr983Ile) in the *KCNH2* gene. Using CRISPR/Cas9 technology, they developed both a homozygous VUS cell line as well as an isogenic control line. Both patch-clamp and multi-electrode array (MEA) experiments showed prolonged APD50, APD90 and field potential duration (FPD) in the homozygous as well as in the heterozygous VUS iPSC-CMs . In addition, more beat irregularity or early after depolarisations (EADs) were observed and the phenotype of the homozygous VUS iPSC-CMs resembled that of the known pathogenic p.(Ala561Val) *KCNH2* variant. Potassium (I_{Kr}) current was decreased in the VUS cell line and restored to normal current densities in the isogenic control (36). Chavali et al. took a different CRISPR/Cas9 approach when they introduced a VUS p.(Asn639Thr) in the *CACNA1C* gene into iPSCs to create a patient-

independent iPSC model. Prolonged APD and FPD were recorded due to a slower inactivation of the $Ca_v1.2$ current. As this cellular phenotype recapitulated the patient phenotype, the authors reclassified the VUS as probably pathogenic (37).

Brugada Syndrome

The first report on iPSC-CM in BrS was published by Davis et al. They modelled an iPSC-CM line harbouring a *SCN5A* mutation p.(1798insAsp) from a patient with an overlap syndrome of LQT/BrS and conduction disorder. Reduced and persistent sodium currents, slower upstroke velocity and prolongation of APD90 were observed in patients' iPSC-CMs but not in controls, mimicking the LOF and GOF phenotype of this mutation (38). Later, two iPSC-CM lines from BrS patients with *SCN5A* (p.(Arg620His)+ p.(Arg811His) and c. 4190delA) mutation were evaluated by Liang et al. Both cell lines showed abnormal action potentials (AP) compared to the controls as well as a reduced sodium current (39). In 2021, Nijak et al. published a review on iPSC-CM models generated of BrS patients, included in Table S1 (40). More recently, extra reports on BrS iPSC-CM models harbouring variants in *SCN5A* (p.(Val1405Met), p.(Ser1812X)), *SCN1B* (p.(Ala197Val)) and *CACNB2* (p.(Ser142Phe)) were published. Reduced expression of the encoded proteins was observed as well as reduced sodium or calcium currents leading to reduced action potential amplitude (APA) and maximum upstroke velocity (Vmax) but prolonged APDs (41-43). Calcium imaging showed more proarrhythmic events such as EADs and DADs (early and delayed after depolarisations) in BrS cell lines compared to control cell lines (42). A *SCN5A* p.(Ser1812X) variant resulted in reduced conduction velocity and proarrhythmic events (43).

Short QT Syndrome

The first iPSC-CM model of SQTS was published by El-Battrawy et al. in 2018 where one patient cell line with a p.(Asn588Lys) mutation in the *KCNH2* gene was compared to two control cell lines. They demonstrated an upregulation of the hERG channel expression and increased potassium currents (I_{Kr}) resulting in a shortening of the action potential. During calcium-handling experiments, irregular beating, DAD-like and EAD-like arrhythmic events were recorded more in patient iPSC-CMs compared to control iPSC-CMs (44). Later, the same mutation and another *KCNH2* p.(Thr618Ile) variant were modelled in iPSC-CMs and similar electrophysiological and molecular results were obtained (45,46). An iPSC-based cardiac cell sheet model was created by Shinnawi and colleagues and an increase in susceptibility to the development of re-entrant arrhythmias recorded (45). The p.(Thr618Ile) variant did not give rise to any arrhythmic events. However, there was an increased beat-to-beat variability in the patient cell line (46).

Catecholaminergic Polymorphic Ventricular Tachycardia Type

Different iPSC-CM CPVT models have been developed (reviewed by Garg et al. in 2018 (34), included in Table S1). The first CPVT iPSC-CM model from a patient carrying a *RYR2* pathogenic variant (p.Phe2483Ile) was published in 2011 by Fatima et al. The analysis revealed more DAD events in patient iPSC-CMs compared to control iPSC-CMs and embryonal stem cell-derived cardiomyocytes (ESC-CM), recapitulating the CPVT phenotype. The underlying aberrant sarcoplasmic reticulum (SR) Ca^{2+} release in the iPSC-CMs is responsible for the development of these DADs and arrhythmias (47). The same variant was modelled using CRISPR/Cas9 by Wei et al. and showed longer calcium sparks in both hetero- and homozygous iPSC-CMs, larger SR Ca^{2+} leak levels and smaller load levels which is consistent with higher diastolic Ca^{2+} levels (48). In 2018, Acimovic et al. published an iPSC-CM model of a CPVT patient with a *RYR2* p.(Asp3638Ala) variant. They found an increase in beat rate in the patient cell line compared to both iPSC- and ESC-derived CMs and a weaker response in force contraction upon stress induction. Calcium handling was normal under basal conditions, but upon stress more irregular Ca^{2+}-release events in CPVT iPSC-CMs were recorded. Patch clamp data revealed a prolongation of the AP in basal conditions while during stress, APD, Vmax and the amplitude were lower in CPVT CMs compared to controls (49). Several other reports on *RYR2* variants, either from patient-specific (50,51) or CRIPSR/Cas9-induced iPSC-CMs (52), show similar aberrant Ca^{2+} handling although mutant lines also differ from each other, for example in the magnitude of the Ca^{2+} leak or SR Ca^{2+} content (50-52). Two *CASQ2* (p.(Asp307His)) patient-specific iPSC-CM models showed DADs, oscillatory prepotentials, after-contractions and diastolic $(Ca^{2+})_i$ rises similar to *RYR2* CPVT models (53).

Arrhythmogenic Cardiomyopathy

The first model of ARVC was published in 2013 by Ma et al. They created a patient-specific iPSC-CM model with a *PKP2* p.(Leu614Pro) mutation and showed downregulation of the expression of plakophilin and plakoglobin but no other desmosomal genes (54). El-Battrawy and Buljubasic studied the same patient-derived iPSC-CM ACM model harbouring a mutation in the *DSG2* gene (p.(Gly638Arg)) (55,56). The amplitude and the upstroke velocity of the AP were decreased as well as peak I_{Na}, I_{NCX}, I_{to}, I_{SK} and I_{KATP}, while I_{Kr} on the contrary was enhanced. Mutant iPSC-CMs showed more arrhythmogenic effects compared to control cells (55). In addition, Buljubasic further investigated the underlying molecular mechanisms and revealed upregulation of SK4 channels and NDPK-B resulting in increased I_{SK4}, pacemaker activity and arrhythmic events (56).

Table 2: overview of published 2D iPSC-CM cardiac arrhythmia disease models.

Syndrome	Causal Gene Variant	Experimental Approach	Cellular Phenotype	Ref.
LQTS	*KCNQ1* p.(Arg190Gln)	PC, IF	Prolonged AP, reduced I_{Ks} current, ER retention, increased susceptibility to catecholamine-induced tachyarrhythmia, attenuation of this phenotype with beta blockade	(31)
	KCNH2 p.(Thr983Ile)	PC, MEA, WB, CI	Prolonged APD50 and APD90, beat irregularity, EAD, decreased I_{Kr} density, reduced channel surface expression, higher diastolic Ca^{2+}	(36)
	CACNA1C p.(Asn639Thr)	CardioExcyte 96, PC	Prolonged Maximum Field Potential Duration and APD, slower $Ca_V1.2$ voltage-dependent inactivation	(37)
BrS/LQT	*SCN5A* p.(1798insAsp)	PC,	Reduced I_{Na} peak current, persistent I_{Na}, reduced Vmax, prolonged APD90	(38)
BrS	*SCN5A* p.(Arg620His)+ p.(Arg811His) *SCN5A* (c. 4190delA)	PC, CI	Reductions in I_{Na} and Vmax of AP, increased burden of triggered activity, abnormal calcium transients and beating interval variation	(39)
	CACNB2 p.(Ser142Phe)	PC, CI	Reduction in peak $I_{Ca\text{-}L}$, acceleration recovery of inactivation and altered voltage dependent inactivation, reduced APA and Vmax, reduced protein expression of the *CACNB2* gene, increased arrhythmia-like events, suppression of	(41)

Syndrome	Causal Gene Variant	Experimental Approach	Cellular Phenotype	Ref.
			arrhythmic events by quinidine and bisoprolol	
	SCN5A p.(Val1405Met) *SCNB1* p.(Ala197Val)	PC, CI	Reduction in peak I_{Na} density, reduced APA and V_{max}, prolonged AP, more proarrhythmic events (EAD, DAD-like events), reduced Nav1.5 protein expression	(42)
	SCN5A p.(Ser1812X)	PC, IF, MEA	Reduced I_{Na} and a delayed sodium channel activation, slowed AP upstroke velocity, reduced FP and CV, enhanced I_{to} and an augmented $I_{Ca\text{-}L}$ window current, reduced $Na_V1.5$ protein expression	(43)
SQTS	*KCNH2* p.(Asn588Lys)	PC, IF, CI	Shortening APD, Increased I_{Kr} tail current, arrhythmic events, increased hERG expression, re-entrant arrhythmias	(44, 45)
	KCNH2 p.(Thr618Ile)	PC, WB	Increased I_{kr}, shortened APD, beat-to-beat variability, increased membrane expression	(46)
CPVT	*RYR2* p.(Phe2483Ileu)	PC, MEA, CI	Arrhythmias, DAD, forskolin can rescue these phenotypes	(47)
	RYR2 p.(Phe2483Ile)	CI	Longer Ca^{2+} sparks, higher diastolic Ca^{2+} levels, irregular beating, SR calcium leak and lower load levels	(48)
	RYR2 p.(Asp3638Ala)	AFM, CI, PC,	Higher beat rate, diastolic SR Ca^{2+} leak, weaker force contraction during stress,	(49)

Syndrome	Causal Gene Variant	Experimental Approach	Cellular Phenotype	Ref.
			APD, Vmax and APA decreased during stress	
	RYR2 p.(Arg176Gln)	CI	Aberrant diastolic SR Ca^{2+} release, EAD	(50)
	RYR2 p.(Gln4201Arg) p.(Arg420Gln) p.(Phe2483Ile)	PC, CI, qPCR, WB	p.(Gln4201Arg): decrease mRNA levels RYR2, protein similar, All mutants: longer sparks p.(Arg420Gln): lower spark frequency	(52)
	RYR2 p.(Phe13Leu) p.(Leu14Pro) p.(Arg15Pro) p.(Arg176Gln)	CI, WB, qPCR, MEA LEAP	Increased Ca^{2+} amplitude and upstroke velocity, decrease in calcium transient duration, irregular beating, decreased beat rate	(51)
	CASQ2 p.(Asp307His)	PC, CI, EM	DADs, oscillatory arrhythmic, after-contractions and diastolic $(Ca^{2+})_i$ rise, less organised myofibrils, enlarged SR cisternae and reduced number of caveolae	(53)
ACM	*PKP2* p.(Leu614Pro)	PC, CI, qPCR, IF	Reduction in rate of spontaneous cell contraction and amplitude under nifedipine, reduced expression plakophilin2 and plakoglobin	(54)
	DSG2 p.(Gly638Arg)	IF, PC, CI, qPCR	Lower APA and Vmax, decreased peak I_{Na}, I_{NCX}, I_{to}, I_{SK}, and I_{KATP}, increased I_{Kr}, more arrhythmogenic events	(55)
	DSG2 p.(Gly638Arg)	PC, WB, qPCR	Upregulation of SK4 and NDPK-B, enhanced SK4 channel currents,	(56)

Syndrome	Causal Gene Variant	Experimental Approach	Cellular Phenotype	Ref.
			pacemaker activity and more arrhythmic events	

Adapted and updated from Garg et al. (2018) and Pan et al. (2021) (34,35). PC: patch clamp; IF: immunofluorescence; MEA: Multi electrode array; WB: Western Blot; CI: Calcium imaging; AFM: atomic force microscopy; AP: action potential; I_{Ks}: slow delayed rectifier K+ current; ER: endoplasmic reticulum; APD50-90: Action potential duration at 50%–90% of repolarisation; EAD: early after depolarisation; I_{Kr}: rapid delayed rectifier K+ current; $I_{Ca\text{-}L}$: L-type calcium current; APA: action potential amplitude; Vmax: maximum rate of rise of the action potential; I_{Na}: sodium current; DAD: delayed after repolarisation; FP: field potential; CV: conduction velocity; I_{to}: transient outward current; SR: sarcoplasmic reticulum; EM: electron microscope.

From 2D to 3D

In the iPSC-CM field, immaturity of the created iPSC-CM is a well-known problem. As the cardiomyocytes often only stay in culture for 30 days or less, it is not surprising that the phenotype of these cells does not fully recapitulate the phenotype of a mature native cardiomyocyte that has been developing for many years. Ahmed et al. (2020) reviewed the currently applied methods of maturation and pinpointed the main differences between fetal-like iPSC-CMs and adult cardiomyocytes. Methods to promote maturation include prolonged culture, addition of hormones (e.g., thyroid hormone) or cellular energy source (e.g., fatty acids such as palmitate, oleic acid, linoleic acid), co-culture, extracellular matrix, mechanical or electrical stimulation and 3D culture (57). The latter is not only beneficial for the maturity of the cardiomyocytes but also enables the creation of 3D models that are more similar to native heart tissue. The heart consists of cardiomyocytes, but also various other cell types are present in the tissue such as endothelial cells (EC), fibroblasts (FB), pericytes, smooth muscle cells, immune cells (myeloid and lymphoid), adipocytes, mesothelial cells and neuronal cells (58). Meanwhile, Pinto et al. found that CMs accounted for only 25%–35% of the cells in the heart, ECs for 60% and FBs for less than 20%; Litviňuková found CMs represented 30% to 50% of the cells in atrial and ventricular samples, respectively, while ECs represented 10% and FBs 20% (58,59). Adding these extra cell types to the model will make it even more physiologically relevant and likely more suitable for modelling pathological conditions and downstream applications such as drug or cardiotoxicity screening.

Below, we will discuss the development from 2D to 3D iPSC-CM cultures with or without other cell types using scaffold-free and scaffold-based techniques.

Scaffold-Free 3D Culture

One method to create a 3D cell culture is the scaffold-free hanging droplet method in which iPSC-CMs are placed in a droplet in an ultra-low attachment plate with (60,61) or without (62,63) the addition of other cell types such as cardiac fibroblasts and endothelial cells. Beauchamp et al. and Ergir et al. reported a long-term stable 3D model of iPSC-CMs that was able to respond to electrical, pharmacological, and physical stimuli but Ca^{2+} dyes only partially penetrated the culture and the CMs still displayed more fetal-like features such as shorter sarcomeres (62,63). Sharma et al. combined iPSC-CM with human cardiac fibroblasts (HCFs) and human coronary artery endothelial cells to create cardiac spheroids containing a cardiac endothelial cell network that recapitulated better than the in vivo human heart (61).

Organoids are mainly formed by differentiating iPSC directly to CM (and other cell types) in ultra-low attachment plates. Drakhlis et al. generated a model of heart-forming organoids (HFO) by differentiating free-floating iPSC aggregates into cardiac organoids that resemble the early embryonic heart as they are composed of a myocardial layer and endocardial-like cells. They were able to model a *NKX2*.5 KO which resulted in similar cardiac malformations such as decreased cardiomyocyte adhesion and hypertrophy as observed in in vivo mouse studies (64). A similar HFO protocol by Lewis-Israeli et al. using different small molecules' concentrations and adding one WNT pathway modulation step enabled the generation of multiple cardiac-specific cell lineages such as endo- and epicardial cells, endothelial cells and cardiac fibroblasts (65). Lee at al. started from embryonic bodies and generated chamber-forming HFOs. RNA-seq revealed that they more closely resembled the fetal heart than adult heart tissue, but here as well, several cell types were generated (66). As such, a drawback of this technique is that the iPSC-CMs still display an immature phenotype but the HFOs are well suited to studying cardiac diseases linked to development.

Another scaffold-free method is used to create cardiac microtissues (cMT) where several (previously generated) cell types (CMs, ECs, FBs, …) are combined. Giacomelli et al. combined iPSC-derived ECs, iPSC-derived cardiac FBs and iPSC-CMs to form a microtissue displaying mature iPSC-CM ultrastructures such as elongated tubular myofibrils and T-tubule-like structures (67). RNA-seq indicated a mature expression profile of the iPSC-CMs comparable to that of adult CMs. Electrophysiological maturation was proven by the presence of the typical AP notch, although this has also been observed in 2D cultures (43,68). As a proof-of-concept they created a cMT consisting of healthy iPSC-CMs and iPSC-ECs combined with mutant cardiac FB of an ACM patient with a *PKP2* (c.2013delC, p.(Lys672ArgfsX12)) mutation (**Table 3**) and found reduced Cx43 expression in ACM cMT

as well as arrhythmic behaviour (50), highlighting the importance of the presence of these non-myocytes in the model. In another paper, a LQTS cMT harbouring a *KCNQ1* p.(Arg594Gln) variant, showed a prolonged field potential compared to wild-type cMT (69) proving that the cMT can recapitulate the disease phenotype (**Table 3**). However, as 2D models already showed this phenotype, the MT model was not of specific added value in this case.

Scaffold-Based 3D Culture

Another frequently used method is scaffold-based culture. These scaffolds consist of (decellularised) extracellular matrix (ECM) (70), natural or synthetic polymers (71,72) and can be combined as a hydrogel in an organised well-defined shape or in certain orientations (73). Fong et al. tested the effect of adult and fetal extracellular matrix from decellularised bovine adult and fetal heart tissue on the maturity of the CMs in both 2D and 3D cultures. Adult heart ECM improved maturation, demonstrated by increased expression of several calcium-handling genes and enhanced calcium signalling, both in 2D and 3D culture with the highest expression levels observed in 3D cultured iPSC-CMs. However, there was no improvement on the formation of T-tubules (70).

In engineered heart tissue (EHT) iPSC-CMs are grown on hydrogel scaffolds wrapped around two flexible pillars that have the ability to mechanically stimulate the cells and improve maturation. Several published models indeed prove that CMs grown in EHT present more mature electrophysiological properties such as action potential amplitude and upstroke velocity and more mature rod-shape morphology and sarcomere alignment (74). Expression profiles as well as the cardiac ultrastructure, bioenergetics and t-tubule formation of stimulated EHT are more in line with adult cardiac tissue then fetal cardiac tissue (75). To improve maturation even more, Lu et al. induced progressive stretch on the EHT which led to higher contractility and passive elasticity, more mature excitation/contraction coupling and a higher ratio of beta-myosin heavy chain (MHC) by alpha-MHC mRNA (76). Goldfracht et al. combined the use of ECM with EHT, and in comparison, using a 2D model they found an increased expression of cardiac-related genes and the cardiomyocytes were arranged anisotropically and developed relatively elongated and oriented cell alignments. They created a LQTS2 (*KCNH2* p.(Ala614Val)) and CPVT2 (*CASQ2* p.(Asp307His)) (Table 3) model and using voltage and calcium dyes, AP prolongation in LQTS iPSC-CM was revealed while the CPVT cell model showed abnormal calcium transients and more arrhythmias under stress conditions, indicating that these EHT models can be used to study channelopathies. In comparison with a 2D single cell model, the EHT showed less frequent, severe or complicated arrhythmogenic activity which is clinically more relevant as the extremely high incidence of arrhythmias

as recorded in a single cell model would probably be incompatible with life. Re-entrant arrhythmias were not observed at baseline in the LQT-EHT but they were developed after blocking the I_{Kr}, mimicking the clinical situation in LQT patients challenged with a QT prolonging agent (77). The major advantage of this technique is the maturation state of the CMs, but special equipment for the generation of this EHT is needed, which might not be available for every lab.

Table 3: Overview of published 3D iPSC-CM arrhythmia models.

3D Model	Disease/Gene/ Variant	Cellular Phenotype	Ref.
Cardiac Microtissue	ACM *PKP2* (c.2013delC, p.(Lys672ArgfsX12))	Lower Cx43 expression and arrhythmic behaviour of ACM cMT consisting of control CM and EC and ACM cardiac fibroblasts	(67)
Cardiac Microtissue	LQTS *KCNQ1* p.(Arg594Gln)	Prolonged field potential duration (FPD), β-adrenergic stimulation shortened the RR interval and decreased the FPD	(69)
Engineered heart tissue	LQTS *KCNH2* p.(Ala614Val)	APD prolongation (via ArcLight), re-entrant arrhythmic activity after I_{Kr} blocking with dofetilide	(77)
Engineered heart tissue	CPVT *CASQ2* p.(Asp307His)	More $(Ca2+)_i$ transient abnormalities and arrhythmias compared to control EHT but less than single cell CPVT iPSC-CM	(77)

Heart-on-a-chip

Heart-on-a-chip is a method to culture iPSC-CM—with or without other cell types —in a 2D or 3D manner on a microfluidic device in a chamber with built-in channels for fluids, microactuators and microsensors (78). Microactuators can give either electrical or mechanical stimuli to the cells/tissue, while the sensors record electrophysiological signals or contraction force (78). Heart-on-a-chip has been used for drug toxicity assessments and maturation was shown to be improved through electrical and mechanical stimulation (79). Although some cardiac disease models such as ischaemia and fibrosis have been investigated using the heart-on-a-chip method (80,81), to date there are no publications on its use for inherited cardiac arrhythmias. The technique is currently still under development and the primary focus is on its application for drug cardiotoxicity screening. Even for this application, there are some challenges such as standardisation, reliable tissue manufacturing, high throughput, high content functional readouts and high cost, that still need to be solved before heart-on-a-chip can be more widely used (82,83).

Drug and Gene Therapy Testing

Cardiotoxicity Screening

A first application of iPSC-CMs and their ability to model/display/show arrhythmias and structural pathology is testing of the cardiotoxicity of a drug under development. Cardiotoxicity and arrhythmia induction such as life-threatening Torsade de pointes (TdP) are a main reason for preclinical and clinical drug failure and withdrawal from the market. In 2013, the Comprehensive in Vitro Proarrhythmia Assay (CiPA) initiative was founded to overcome the low specificity of the preclinical studies and clinical trials at that time (84). One of the novel components is testing the effect of a drug in vitro in iPSC-CM. A total of 28 compounds with known cardiac effects were tested in commercially available iPSC-CMs using a MEA system and voltage-sensitive dyes and could be classified as high-, intermediate- and low-risk for TdP (85). To confirm these findings, these drugs were tested over several laboratories/facilities, commercial cardiomyocyte types and different MEA platforms and reproducible concentration-dependent electrophysiological responses were reported, indicating that iPSC-CMs can predict clinical QT prolongation and/or arrhythmogenic potential of drug compounds (86-88). Lee at al showed that addition of a contractility assay (impedance measurement) into the evaluation of cardiotoxicity provides/allows more mechanistic insights on the drug effect (89). As discussed above, 3D heart-on-a-chip models are also being tested, holding promise for even better prediction of cardiotoxic and pro-arrhythmic drug effects as they better recapitulated the clinical effects compared to 2D iPSC-CM models as they present occasionally with arrhythmias that are not reported in adult cardiomyocytes (90,91). Regarding inherited cardiac arrhythmias, variable expressivity is a known characteristic, with many individuals who carry pathogenic variants remaining asymptomatic throughout life. However, specific drugs can also elicit life-threatening arrhythmias in these carriers/patients and patients are recommended to avoid taking them. Using iPSC-CM with such pathogenic variants in cardiotoxicity screening could be a valuable option to predict these adverse effects in a subset of the population.

Drug Testing

In addition to cardiotoxicity, iPSC-CM can also be deployed to test compounds that could (partially) restore the phenotype of inherited cardiac arrhythmias models (Table 4). Two recent publications reported a 2D LQT3 (*SCN5A* p.(Phe1473Cys)) model that was used to test mexiletine and different analogues in their ability to reduce the prolongation of the AP and they found that the analogues were more potent and selective in inhibiting the late sodium current, responsible for the APD prolongation in patients. In addition, they

did not induce AP prolongation or EADs, known off-target effects of mexiletine due to unwanted inhibition of hERG (92), and were still able to suppress arrhythmias (93,94). Verapamil and lidocaine were able to reduced APD in another LQT model harbouring to variants (*KCNQ1* p.(Gly219Glu)/ *TRPM4* p.(Thr160Met)) (95).

Several LQT2 models, with pathogenic variants in the *KCNH2* (hERG channel) have also been used to test drugs. Telmisartan and GW0742 are agonists of the PPARδ pathway, which helps hERG to stabilise the PKA-phosphorylated active state of the channel opening at more negative potentials. Duncan et al. tested these agonists in a patient iPSC-CM model harbouring a *KCNH2* p.(Ala561Thr) variant and found a 20% reduction in APD for both compounds, which is comparable to the observed effect of NS1643 (also 20% APD shortening), a known compound that reduces inactivation of the hERG channel (96). Mehta et al. created iPSC-CMs of five patients with either disrupted *KCNH2* trafficking (p.(Ala561Val), (IVS9-28A/G)) or synthesis (p.(Ser428X), p.(Arg366X)) to test the use of lumacaftor as a treatment option as the drug acts as a chaperone during protein folding. As predicted, they found higher *KCNH2* expression and shortened field potentials after 7 days of treatment with lumacaftor in patients with trafficking defect mutations but not in patients with disrupted synthesis of the hERG channel (97). Two of the patients received treatment with lumacaftor and Ivacaftor and indeed showed a shorter QTc, however this shortening was not as pronounced as in the in vitro model indicating that the translation from in vitro to in vivo is not straightforward (98). Another study also tested lumacaftor on three LQT2 (*KCNH2*) patient iPSC-CM lines with different pathogenic variants and found rescued phenotypes in two (p.(Asn633Ser), p.(Arg685Pro)) of the three lines. For the third one (p.(Gly604Ser)), on the other hand, they saw a prolongation of the AP after administration of the compound, which could be explained by the dominant-negative effect that was observed next to the trafficking defect caused by the third variant (99). Another compound (ICA-105574, a type II I_{Kr} activator) was used by two groups and tested both on VUS (p.(Thr983Ile)) and pathogenic (p.(Ala422Thr) LQT2 iPSC-CM models. They both saw a shortening of the action potential, field potential or calcium transient but with the risk of overcorrection at higher concentrations which might induce arrhythmic events (36,100).

Ajmaline is a class IA anti-arrhythmic drug that can be used to diagnose BrS patients. Studies have already shown that ajmaline can inhibit various currents, including I_{Na}, I_{to} or I_{Kr} (101). In the iPSC-CM of a BrS patient without a known genetic cause ajmaline had the same blocking effect on both the repolarisation and depolarisation caused by an inhibition of both I_{Na} and I_{Kr} as observed in the control iPSC-CMs. In an iPSC-CM model harbouring two *SCN10A* (p.(Arg1268Gln)/p.(Arg1250Gln) variants there was a more pronounced reduction in APA and Vmax compared to control iPSC-CMs (102). The same

was observed in a *SCN1B* (p.(Leu210Pro)/p.(Pro213Thr)) iPSC-CM model (103). Cilostazol and milrinone, two phosphodiesterase III inhibitors, increased I_{Ca} and suppressed I_{to} by increasing the heart rate (104). These were tested on BrS iPSC-CM models from two patients carrying a *SCN5A* p.(Ser1812X) variant, which resulted in a reduction in I_{to} and arrhythmic beating (43). Bisoprolol, a beta blocker, was recently tested in a *CACNB2* p.(Ser142Phe) iPSC-CM model and reduced variation in beat-to-beat interval time as well as arrhythmic events. Quinidine, a class I antiarrhythmic agent, on the other hand, only reduced arrhythmic events (41). The same anti-arrhythmic effect of quinidine was observed in a *SCN5A* (p.(Val1405Met)) and *SCN1B* (p.(Ala197Val)) iPSC-CM model (42).

Guo et al. tested quinidine in an iPSC-CM model of a SQT (*KCNH2*, p.(Thr618Ile)) patient who was already receiving quinidine treatment. The cell model confirmed the beneficial effect of quinidine as APD was prolonged, comparable to the APD of the isogenic control. Next to quinidine, a short peptide derived from a scorpion, BmKKx2, prolonged the APD by targeting the *KCNH2* gene (46). In another model (*KCNH2* p.(Asn588Lys)), quinidine reduced Vmax, prolonged APD and abolished arrhythmic events while sotalol and metoprolol did not have an effect (44). Ivabradine, ajmaline, and mexiletine prolonged APD and reduced arrhythmic events in the same iPSC-CM model (105).

One way to prevent arrhythmias in CPVT is to upregulate the calcium uptake by the mitochondria by, for example, mitochondrial Ca^{2+} uptake enhancers (MiCUp) such as efsevin and kaempferol (106). These MiCUps were tested both in mice and *RYR2* (p.(Ser406Leu)) patient iPSC-CMs and were able to reduce episodes of stress-induced ventricular tachycardia in mice and reduce arrhythmogenic Ca^{2+} waves in iPSC-CMs (106). Two other MiCUps, ezetimibe and disulfiram, suppressed arrhythmogenesis in patient iPSC-CMs (107) (genetic variant not specified). Another way to modulate calcium is by inhibiting the Ca^{2+}/calmodulin-dependent protein kinase II (CaMKII) with a CaMKII inhibitory peptide, which is successful in reducing the abnormal Ca^{2+} release events and frequency of Ca^{2+} sparks in two CPVT *RYR2* (p.(Ser404Arg)/p.(Asn658Ser), p.(Gly3946Ser)/(p.(Gly1885Glu)) iPSC-CMs (108). EL20, a tetracaine derivative and *RYR2* inhibitor, decreased spark activity in iPSC-CMs of a CPVT patient harbouring a *RYR2* (p.(Arg176Gln)) mutation without negatively affecting the Ca^{2+} transient amplitude (50). Stutzman et al. created four iPSC-CM lines of CPVT patients with *RYR2* mutations, (p.(Phe13Leu), p.(Leu14Pro), p.(Arg15Pro) and p.(Arg176Gln)), and treated them with nadolol and flecainide. Both were able to decrease the Ca^{2+} transient amplitude and spark activity (51).

All these reports confirm the great potential of iPSC-CM arrhythmia models to test novel and existing therapies, and also for personalised medicine. In both 2D and 3D, they could also be effectively used for larger drug-library screening experiments.

Table 4: Overview of published drug testing in iPSC-CM arrhythmia models.

Drug	Mode of Action	Disease Gene Mutation	Effect on Phenotype	Ref.
Mexiletine analogues	Class 1B antiarrhythmic drug, inhibits I_{Na}	LQT *SCN5A* p.(Phe1473Cys), p.(Asn406Lys)	Mexiletine: I_{NaL} inhibition and APD shortening at lower dose but modest prolongation at higher dose and proarrhythmic response Analogues 'MexA2' and 'MexA5': more potent and selective for I_{NaL} over I_{NaP} and I_{Kr}, Shortening of APD and suppression of arrhythmia Analogues '13, 14, 25': shortening of APD and no EADs	(92, 93)
Verapamil, Lidocaine	Calcium channel blocker Sodium channel blocker	LQT *KCNQ1* p.(Gly219Glu)/ *TRPM4* p.(Thr160Met)	Reduction in APD	(95)
Telmisarta, GW0742	Agonists of the PPARδ pathway, stabilise the active PKA-phosphorylated state of hERG	LQT *KCNH2* p.(Ala561Thr)	Reduction in APD50 , APD90 and triangularisation	(96)
NS1643	Change the voltage dependence of	LQT *KCNH2* p.(Ala561Thr)	Reductions in APD50, APD90 and triangularisation	(96)

Drug	Mode of Action	Disease Gene Mutation	Effect on Phenotype	Ref.
	inactivation of hERG			
Lumacaftor	Trafficking chaperone during protein folding	LQT *KCNH2* Trafficking p.(Ala561Val), (IVS9-28A/G), p.(Asn633Ser), p.(Arg685Pro), p.(Gly604Ser) Synthesis p.(Ser428X), p.(Arg366X)	*Trafficking variants* Increased membrane localisation, reduced cFPD and APD90, increase in I_{Kr} current densities, reduced calcium transient irregularities and frequency p.(Gly604Ser): increased membrane expression, no effect on APD90 *Other variants* Reduced calcium transient irregularities and frequency, no effect on cFPD	(97, 99)
ICA-105574	Type II I_{Kr} activator (impairs transition to the inactivated state)	LQT *KCNH2* p.(Thr983Ile), p.(Ala422Thr)	Increased I_{Kr}, shortening APD/cFPD in patient and control, shortened calcium transient, at higher concentrations (10-30µM): cessation of the spontaneous calcium transients	(36, 100)
Ajmaline	Class IA anti-arrhythmic drug inhibits I_{Na}, I_{to} or I_{Kr}	BrS Unknown mutation	No difference between patient and control	(101)
		BrS *SCN10A* p.(Arg1268Gln)/ p.(Arg1250Gln)	Prolonged APD50 and APD90, reduced APA and Vmax	(102)
		BrS *SCN1B* p.(Leu210Pro)/ p.(Pro213Thr)	Reduced APA and Vmax	(103)

Drug	Mode of Action	Disease Gene Mutation	Effect on Phenotype	Ref.
Cilostazol, Milrinone	Phosphodiesterase III inhibitors, increase I_{Ca} and suppress I_{to}	BrS *SCN5A* p.(Ser1812X)	Reduction in I_{to}, decreased arrhythmic beating, no EAD- or EAD-triggered activities	(43)
Bisoprolol	Beta blocker	BrS *CACNB2* p.(Ser142Phe)	Reduced arrhythmic events and reduced variation in the beat-to-beat interval time at 30nM	(41)
Quinidine	Class I antiarrhythmic agent, blocking I_{to}	BrS *CACNB2* p.(Ser142Phe)	Reduced arrhythmic events	(41)
		BrS *SCN5A* p.(Val1405Met) *SCN1B* p.(Ala197Val)	Elimination of arrhythmic events (EAD, DAD), Vmax, APA, and RMP reduced in control and patients' groups	(42)
		SQT *KCNH2* p.(Thr618Ile)	Prolonged APD	(46)
		SQT *KCNH2* p.(Asn588Lys)	Reduced Vmax, prolonged APD, elimination of arrhythmic events	(44)
Toxin BmKKx2	Selective I_{Kr} blocker	SQT *KCNH2* p.(Thr618Ile)	Prolonged APD	(46)
Ivabradine, Ajmaline, Mexiletine	Inhibitor of the pacemaker funny current, Class IA anti-arrhythmic drug, inhibits I_{Na}, I_{to} or I_{Kr}	SQT *KCNH2* p.(Asn588Lys)	Prolonged APD90, reduced number of arrhythmic events	(105)

Drug	Mode of Action	Disease Gene Mutation	Effect on Phenotype	Ref.
	Class 1B antiarrhythmic drug			
MiCUps (efsevin, kaempferol, ezetimibe, disulfiram)	Mitochondrial Ca^{2+} uptake enhancers	CPVT *RYR2* p.(Ser406Leu)	Reduced number of cells displaying Ca^{2+} waves and reduced frequency of Ca^{2+} waves	(106)
		CPVT unknown mutation	Reduced Ca^{2+} waves	(107)
Autocamtide-2-related inhibitory peptide (AIP)	Ca^{2+}/calmodulin-dependent protein kinase II (CaMKII) inhibitory peptide	CPVT *RYR2* p.(Ser404Arg)/p.(Asn658Ser), p.(Gly3946Ser)/ p.(Gly1885Glu)	Reduced abnormal Ca^{2+} transients, reduced frequency of Ca^{2+} sparks, restored regular and spontaneous Ca^{2+} transients	(108)
Tetracaine derivative EL20	Targeted inhibition of RyR2	CPVT *RYR2* p.(Arg176Gln)	Reduced the Ca^{2+} spark frequency, prevented pacing-evoked Ca^{2+} oscillations	(50)
Nadolol, Flecainide	Non-selective beta blocker Class IC anti-arrhythmic agent inhibits I_{Na} and I_{Kr}	CPVT *RYR2* p.(Phe13Leu), p.(Leu14Pro), p.(Arg15Pro), p.(Arg176Gln)	Reduced Ca^{2+} transient amplitude, reduced spontaneous Ca^{2+} release, reduced Ca^{2+} sparking activity, decreased irregularities in beat period and spontaneous beat rate	(51)

Gene Therapy Testing

Inherited cardiac arrhythmia iPSC-CM models have also been used to test novel gene therapies, acting straight on the nucleic acid molecular/genetic level.

One way to perform gene therapy is by patient-specific targeting the causal mutation. Matsa et al. used an allele-specific small interfering RNA to knock down the mutated *KCNH2* mRNA in LQTS (*KCNH2* p.(Ala561Thr)) patient iPSC-CMs thereby preventing the dominant negative-trafficking defect. This resulted in a shortening of the AP, increase in K^+ current and rescue of the arrhythmogenic phenotype (109). A more general gene therapy approach was published by Dotzler et al. They developed a novel method with a dual mode of action called suppression-and-replacement (SupRep) *KCNQ1* gene therapy. As the name indicates, first the endogenous alleles were suppressed by short hairpin RNA (shRNA) and in the next step, the *KCNQ1* gene was replaced by expression of a shRNA-immune (shIMM) *KCNQ1* cDNA immune for breakdown by the shRNA. This method was tested in four LQT1 (*KCNQ1* p.(Tyr171X), p.(Val254Met), p.(Ile567Ser) and p.(Ala344Ala/splice variant)) patient iPSC-CM models and showed a shortening of the APD in all 2D patient models. As a proof-of-concept, a 3D cardiac organoid of one of the patient lines (p.(Tyr171X)) was created and here as well, an APD shortening was observed after treatment (110). The same treatment approach was used for *KCNH2* variants, in iPSC-CM models of two LQT2 (p.(Gly604Ser), p.(Asn633Ser)) patients as well as in one SQT (p.(Asn588Lys) patient and resulted in a normal APD90 for both the LQT2 and SQT patients (111).

Discussion and Conclusions

With the advent of iPSC creation, major steps have been taken to differentiate these stem cells into several cell types including iPSC-derived cardiomyocytes. Using this model in inherited cardiac arrhythmia research has increased knowledge on the underlying disease mechanisms and creates opportunities to functionally characterise and interpret the pathogenicity of patient-specific genetic variants and to perform (personalised) drug testing. As a proof-of-concept of this more 'personalised' drug testing, a few 'clinical trials in a dish' have been performed where healthy control individuals and their iPSC-CMs were challenged with known QT-prolonging drugs to compare the effect on the in vitro model to the in vivo situation. Using sotalol, a correlation was found between the in vivo QT interval and in vitro FPD results (112). One study also found such a positive correlation for moxifloxacin (113) while another did not find a correlation between the APD response slopes and clinical QT response to moxifloxacin or dofetilide (114). Using (subject-specific) iPSCs for research and drug testing also requires the use of a comprehensive informed consent explaining future use of created iPSCs and derivatives. The reported 2D iPSC-CM disease models recapitulate the patients' phenotype at the cellular level, however, if the specific tested characteristics are compared over several iPSC-clones or several different papers, quite some variability can be observed (115). In addition, for example, the iPSC-CM models of BrS patients with an unknown genetic

cause did not show any electrophysiological differences compared to healthy control iPSC-CMs (116). The known immature phenotype of iPSC-CMs with immature ion channel expression most likely plays a role in these observations and small changes in ionic currents might not be picked up. More in-depth analysis of the iPSC-CM cellular disease phenotype including transcriptomics or proteomics approaches could be useful to further characterise these models.

In addition, efforts have been made to improve the maturity of iPSC-CMs, with one important strategy to culture them in 3D models such as microtissues, organoids and engineered heart tissue. Amongst others, Kerr et al. showed that iPSC-CM in 3D cultures showed a higher similarity to human adult myocardial transcriptome compared to 2D models and had enhanced cell–cell communication, ECM organisation and vascularisation capacity (117). The addition of other (iPSC-derived) cell types that are present in heart tissue further improves the physiological relevance and maturation state of the model. Use of these 3D models will certainly increase the suitability for disease modelling and drug testing. It should be taken into account, though, that they are more complex at the culture level – complicating the high-throughput needed for larger screenings, so that extra variability is introduced to an already variable model (98) and the complexity of the analysis is also increased. Light for microscopy, fluorescent dyes and drugs need to penetrate deeper and evenly into the 3D culture to reach all cells, more computational power might be needed and more expensive single-cell analysis approaches such as scRNA-seq could be necessary. Indeed, Feng et al. already performed single cell analysis on cardiac organoids and found more differentially expressed genes in iPSC-CMs compared to other cell types present in the organoid between Ebstein's anomaly patients and healthy controls (118).

Despite the immense progress that has been made in iPSC-CM generation and application potential, some limiting factors such as immaturity, genetic and phenotypic heterogeneity and variability still have an impact on their usability and should be kept in mind when translating the results in vivo (115). For clinical application in regenerative medicine the arrhythmogenic potential, immunogenicity, tumorigenicity and heterogeneity of the iPSC-CMs should be taken into consideration (119, 120, 121). In conclusion, iPSC-CMs have been instrumental in modelling inherited cardiac arrhythmias, small-scale testing of disease-specific drugs or gene therapies and cardiotoxicity testing. The transition from 2D to 3D models has improved cellular maturity and physiological relevance, but also increases the complexity of the model and its analysis. Large-scale drug library screenings have not yet been performed, but further automation and high-throughput analysis methods will certainly pave the way for this application. Further evolution of both 2D and 3D iPSC-CM modelling and analysis

techniques will allow the discovery of new treatment options for cardiac arrhythmias in general as well as for personalised medicine.

Supplementary Materials: The following are available online at https://www.mdpi.com/article/10.3390/biomedicines11020334/s1, Table S1: overview of previously published 2D iPSC-CM cardiac arrhythmia disease models. References (122–152) are cited.

Author Contributions: Conceptualization, E.S., M.A. and B.L.; Writing – original draft, E.S.; writing – review and editing, E.S., M.A. and B.L. All authors have read and agreed to the published version of the manuscript.

Funding: E. Simons is a research fellow supported by the Research Foundation—Flanders (FWO, Belgium, 1S25318N). Dr. Loeys holds a consolidator grant from the European Research Council ("Genomia" ERC-COG-2017-771945). This research was largely supported by funding from the University of Antwerp (GOA 33933; Methusalem-OEC grant "Genomed" 40709) and the Research Foundation Flanders (FWO, Belgium, G042321N, G040221N, G044720N).

Conflicts of Interest: The authors declare no conflict of interest.

References

1. Takahashi, K.; Yamanaka, S. Induction of pluripotent stem cells from mouse embryonic and adult fibroblast cultures by defined factors. *Cell* **2006**, *126*, 663-676, doi:10.1016/j.cell.2006.07.024.
2. Iannielli, A.; Luoni, M.; Giannelli, S.G.; Ferese, R.; Ordazzo, G.; Fossati, M.; Raimondi, A.; Opazo, F.; Corti, O.; Prehn, J.H.M.; et al. Modeling native and seeded Synuclein aggregation and related cellular dysfunctions in dopaminergic neurons derived by a new set of isogenic iPSC lines with SNCA multiplications. *Cell Death Dis* **2022**, *13*, 881, doi:10.1038/s41419-022-05330-6.
3. Zwi, L.; Caspi, O.; Arbel, G.; Huber, I.; Gepstein, A.; Park, I.H.; Gepstein, L. Cardiomyocyte differentiation of human induced pluripotent stem cells. *Circulation* **2009**, *120*, 1513-1523, doi:10.1161/CIRCULATIONAHA.109.868885.

4. Lai, X.; Li, C.; Xiang, C.; Pan, Z.; Zhang, K.; Wang, L.; Xie, B.; Cao, J.; Shi, J.; Deng, J.; et al. Generation of functionally competent hepatic stellate cells from human stem cells to model liver fibrosis in vitro. *Stem Cell Reports* **2022**, doi:10.1016/j.stemcr.2022.09.010.
5. Priori, S.G.; Blomstrom-Lundqvist, C.; Mazzanti, A.; Blom, N.; Borggrefe, M.; Camm, J.; Elliott, P.M.; Fitzsimons, D.; Hatala, R.; Hindricks, G.; et al. 2015 ESC Guidelines for the management of patients with ventricular arrhythmias and the prevention of sudden cardiac death: The Task Force for the Management of Patients with Ventricular Arrhythmias and the Prevention of Sudden Cardiac Death of the European Society of Cardiology (ESC). Endorsed by: Association for European Paediatric and Congenital Cardiology (AEPC). *Eur Heart J* **2015**, *36*, 2793-2867, doi:10.1093/eurheartj/ehv316.
6. Shah, S.R.; Park, K.; Alweis, R. Long QT Syndrome: A Comprehensive Review of the Literature and Current Evidence. *Curr Probl Cardiol* **2019**, *44*, 92-106, doi:10.1016/j.cpcardiol.2018.04.002.
7. Janzen, M.L.; Davies, B.; Laksman, Z.W.M.; Roberts, J.D.; Sanatani, S.; Steinberg, C.; Tadros, R.; Cadrin-Tourigny, J.; MacIntyre, C.; Atallah, J.; et al. Management of Inherited Arrhythmia Syndromes: A HiRO Consensus Handbook on Process of Care. *CJC Open* **2023**, *5*, 268-284, doi:10.1016/j.cjco.2023.02.006.
8. Ponce-Balbuena, D.; Deschenes, I. Long QT syndrome - Bench to bedside. *Heart Rhythm O2* **2021**, *2*, 89-106, doi:10.1016/j.hroo.2021.01.006.
9. Schwartz, P.J.; Ackerman, M.J.; Antzelevitch, C.; Bezzina, C.R.; Borggrefe, M.; Cuneo, B.F.; Wilde, A.A.M. Inherited cardiac arrhythmias. *Nat Rev Dis Primers* **2020**, *6*, 58, doi:10.1038/s41572-020-0188-7.
10. Campuzano, O.; Sarquella-Brugada, G.; Cesar, S.; Arbelo, E.; Brugada, J.; Brugada, R. Recent Advances in Short QT Syndrome. *Front Cardiovasc Med* **2018**, *5*, 149, doi:10.3389/fcvm.2018.00149.
11. Hancox, J.C.; Du, C.Y.; Butler, A.; Zhang, Y.; Dempsey, C.E.; Harmer, S.C.; Zhang, H. Pro-arrhythmic effects of gain-of-function potassium channel mutations in the short QT syndrome. *Philos Trans R Soc Lond B Biol Sci* **2023**, *378*, 20220165, doi:10.1098/rstb.2022.0165.
12. Walsh, R.; Adler, A.; Amin, A.S.; Abiusi, E.; Care, M.; Bikker, H.; Amenta, S.; Feilotter, H.; Nannenberg, E.A.; Mazzarotto, F.; et al. Evaluation of gene validity for CPVT and short QT syndrome in sudden arrhythmic death. *Eur Heart J* **2022**, *43*, 1500-1510, doi:10.1093/eurheartj/ehab687.
13. Dewi, I.P.; Dharmadjati, B.B. Short QT syndrome: The current evidences of diagnosis and management. *J Arrhythm* **2020**, *36*, 962-966, doi:10.1002/joa3.12439.
14. Asatryan, B.; Barth, A.S. Sex-related differences in incidence, phenotype and risk of sudden cardiac death in inherited arrhythmia syndromes. *Front Cardiovasc Med* **2022**, *9*, 1010748, doi:10.3389/fcvm.2022.1010748.
15. Priori, S.G.; Wilde, A.A.; Horie, M.; Cho, Y.; Behr, E.R.; Berul, C.; Blom, N.; Brugada, J.; Chiang, C.E.; Huikuri, H.; et al. Executive summary: HRS/EHRA/APHRS expert consensus statement on the diagnosis and management of patients with inherited primary arrhythmia syndromes. *Heart Rhythm* **2013**, *10*, e85-108, doi:10.1016/j.hrthm.2013.07.021.

16. Zaffran, S.; Kraoua, L.; Jaouadi, H. Calcium Handling in Inherited Cardiac Diseases: A Focus on Catecholaminergic Polymorphic Ventricular Tachycardia and Hypertrophic Cardiomyopathy. *Int J Mol Sci* **2023**, *24*, doi:10.3390/ijms24043365.
17. Leenhardt, A.; Denjoy, I.; Guicheney, P. Catecholaminergic polymorphic ventricular tachycardia. *Circ Arrhythm Electrophysiol* **2012**, *5*, 1044-1052, doi:10.1161/CIRCEP.111.962027.
18. Corrado, D.; Basso, C.; Judge, D.P. Arrhythmogenic Cardiomyopathy. *Circ Res* **2017**, *121*, 784-802, doi:10.1161/CIRCRESAHA.117.309345.
19. Corrado, D.; Perazzolo Marra, M.; Zorzi, A.; Beffagna, G.; Cipriani, A.; Lazzari, M.; Migliore, F.; Pilichou, K.; Rampazzo, A.; Rigato, I.; et al. Diagnosis of arrhythmogenic cardiomyopathy: The Padua criteria. *Int J Cardiol* **2020**, *319*, 106-114, doi:10.1016/j.ijcard.2020.06.005.
20. McKenna, W.J.; Thiene, G.; Nava, A.; Fontaliran, F.; Blomstrom-Lundqvist, C.; Fontaine, G.; Camerini, F. Diagnosis of arrhythmogenic right ventricular dysplasia/cardiomyopathy. Task Force of the Working Group Myocardial and Pericardial Disease of the European Society of Cardiology and of the Scientific Council on Cardiomyopathies of the International Society and Federation of Cardiology. *Br Heart J* **1994**, *71*, 215-218, doi:10.1136/hrt.71.3.215.
21. Gaine, S.P.; Calkins, H. Antiarrhythmic Drug Therapy in Arrhythmogenic Right Ventricular Cardiomyopathy. *Biomedicines* **2023**, *11*, doi:10.3390/biomedicines11041213.
22. Antzelevitch, C.; Brugada, P.; Borggrefe, M.; Brugada, J.; Brugada, R.; Corrado, D.; Gussak, I.; LeMarec, H.; Nademanee, K.; Perez Riera, A.R.; et al. Brugada syndrome: report of the second consensus conference: endorsed by the Heart Rhythm Society and the European Heart Rhythm Association. *Circulation* **2005**, *111*, 659-670, doi:10.1161/01.CIR.0000152479.54298.51.
23. Hosseini, S.M.; Kim, R.; Udupa, S.; Costain, G.; Jobling, R.; Liston, E.; Jamal, S.M.; Szybowska, M.; Morel, C.F.; Bowdin, S.; et al. Reappraisal of Reported Genes for Sudden Arrhythmic Death: Evidence-Based Evaluation of Gene Validity for Brugada Syndrome. *Circulation* **2018**, *138*, 1195-1205, doi:10.1161/CIRCULATIONAHA.118.035070.
24. Cerrone, M.; Costa, S.; Delmar, M. The Genetics of Brugada Syndrome. *Annu Rev Genomics Hum Genet* **2022**, *23*, 255-274, doi:10.1146/annurev-genom-112921-011200.
25. Vutthikraivit, W.; Rattanawong, P.; Putthapiban, P.; Sukhumthammarat, W.; Vathesatogkit, P.; Ngarmukos, T.; Thakkinstian, A. Worldwide Prevalence of Brugada Syndrome: A Systematic Review and Meta-Analysis. *Acta Cardiol Sin* **2018**, *34*, 267-277, doi:10.6515/ACS.201805_34(3).20180302B.
26. Bezzina, C.R.; Barc, J.; Mizusawa, Y.; Remme, C.A.; Gourraud, J.B.; Simonet, F.; Verkerk, A.O.; Schwartz, P.J.; Crotti, L.; Dagradi, F.; et al. Common variants at SCN5A-SCN10A and HEY2 are associated with Brugada syndrome, a rare disease with high risk of sudden cardiac death. *Nat Genet* **2013**, *45*, 1044-1049, doi:10.1038/ng.2712.
27. Barc, J.; Tadros, R.; Glinge, C.; Chiang, D.Y.; Jouni, M.; Simonet, F.; Jurgens, S.J.; Baudic, M.; Nicastro, M.; Potet, F.; et al. Genome-wide association analyses identify new Brugada syndrome risk loci and highlight a new mechanism of sodium channel regulation in disease susceptibility. *Nat Genet* **2022**, *54*, 232-239, doi:10.1038/s41588-021-01007-6.

28. Matsumura, H.; Nakano, Y.; Ochi, H.; Onohara, Y.; Sairaku, A.; Tokuyama, T.; Tomomori, S.; Motoda, C.; Amioka, M.; Hironobe, N.; et al. H558R, a common SCN5A polymorphism, modifies the clinical phenotype of Brugada syndrome by modulating DNA methylation of SCN5A promoters. *J Biomed Sci* **2017**, *24*, 91, doi:10.1186/s12929-017-0397-x.
29. Krahn, A.D.; Behr, E.R.; Hamilton, R.; Probst, V.; Laksman, Z.; Han, H.C. Brugada Syndrome. *JACC Clin Electrophysiol* **2022**, *8*, 386-405, doi:10.1016/j.jacep.2021.12.001.
30. Casini, S.; Verkerk, A.O.; Remme, C.A. Human iPSC-Derived Cardiomyocytes for Investigation of Disease Mechanisms and Therapeutic Strategies in Inherited Arrhythmia Syndromes: Strengths and Limitations. *Cardiovasc Drugs Ther* **2017**, *31*, 325-344, doi:10.1007/s10557-017-6735-0.
31. Moretti, A.; Bellin, M.; Welling, A.; Jung, C.B.; Lam, J.T.; Bott-Flugel, L.; Dorn, T.; Goedel, A.; Hohnke, C.; Hofmann, F.; et al. Patient-specific induced pluripotent stem-cell models for long-QT syndrome. *N Engl J Med* **2010**, *363*, 1397-1409, doi:10.1056/NEJMoa0908679.
32. Rajamohan, D.; Kalra, S.; Duc Hoang, M.; George, V.; Staniforth, A.; Russell, H.; Yang, X.; Denning, C. Automated Electrophysiological and Pharmacological Evaluation of Human Pluripotent Stem Cell-Derived Cardiomyocytes. *Stem Cells Dev* **2016**, *25*, 439-452, doi:10.1089/scd.2015.0253.
33. Protze, S.I.; Lee, J.H.; Keller, G.M. Human Pluripotent Stem Cell-Derived Cardiovascular Cells: From Developmental Biology to Therapeutic Applications. *Cell Stem Cell* **2019**, *25*, 311-327, doi:10.1016/j.stem.2019.07.010.
34. Garg, P.; Garg, V.; Shrestha, R.; Sanguinetti, M.C.; Kamp, T.J.; Wu, J.C. Human Induced Pluripotent Stem Cell-Derived Cardiomyocytes as Models for Cardiac Channelopathies: A Primer for Non-Electrophysiologists. *Circ Res* **2018**, *123*, 224-243, doi:10.1161/CIRCRESAHA.118.311209.
35. Pan, Z.; Ebert, A.; Liang, P. Human-induced pluripotent stem cells as models for rare cardiovascular diseases: from evidence-based medicine to precision medicine. *Pflugers Arch* **2021**, *473*, 1151-1165, doi:10.1007/s00424-020-02486-y.
36. Garg, P.; Oikonomopoulos, A.; Chen, H.; Li, Y.; Lam, C.K.; Sallam, K.; Perez, M.; Lux, R.L.; Sanguinetti, M.C.; Wu, J.C. Genome Editing of Induced Pluripotent Stem Cells to Decipher Cardiac Channelopathy Variant. *J Am Coll Cardiol* **2018**, *72*, 62-75, doi:10.1016/j.jacc.2018.04.041.
37. Chavali, N.V.; Kryshtal, D.O.; Parikh, S.S.; Wang, L.; Glazer, A.M.; Blackwell, D.J.; Kroncke, B.M.; Shoemaker, M.B.; Knollmann, B.C. Patient-independent human induced pluripotent stem cell model: A new tool for rapid determination of genetic variant pathogenicity in long QT syndrome. *Heart Rhythm* **2019**, *16*, 1686-1695, doi:10.1016/j.hrthm.2019.04.031.
38. Davis, R.P.; Casini, S.; van den Berg, C.W.; Hoekstra, M.; Remme, C.A.; Dambrot, C.; Salvatori, D.; Oostwaard, D.W.; Wilde, A.A.; Bezzina, C.R.; et al. Cardiomyocytes derived from pluripotent stem cells recapitulate electrophysiological characteristics of an overlap syndrome of cardiac sodium channel disease. *Circulation* **2012**, *125*, 3079-3091, doi:10.1161/CIRCULATIONAHA.111.066092.
39. Liang, P.; Sallam, K.; Wu, H.; Li, Y.; Itzhaki, I.; Garg, P.; Zhang, Y.; Vermglinchan, V.; Lan, F.; Gu, M.; et al. Patient-Specific and Genome-Edited Induced Pluripotent Stem Cell-

Derived Cardiomyocytes Elucidate Single-Cell Phenotype of Brugada Syndrome. *J Am Coll Cardiol* **2016**, *68*, 2086-2096, doi:10.1016/j.jacc.2016.07.779.

40. Nijak, A.; Saenen, J.; Labro, A.J.; Schepers, D.; Loeys, B.L.; Alaerts, M. iPSC-Cardiomyocyte Models of Brugada Syndrome-Achievements, Challenges and Future Perspectives. *Int J Mol Sci* **2021**, *22*, doi:10.3390/ijms22062825.
41. Zhong, R.; Schimanski, T.; Zhang, F.; Lan, H.; Hohn, A.; Xu, Q.; Huang, M.; Liao, Z.; Qiao, L.; Yang, Z.; et al. A Preclinical Study on Brugada Syndrome with a CACNB2 Variant Using Human Cardiomyocytes from Induced Pluripotent Stem Cells. *Int J Mol Sci* **2022**, *23*, doi:10.3390/ijms23158313.
42. Zhu, Y.; Wang, L.; Cui, C.; Qin, H.; Chen, H.; Chen, S.; Lin, Y.; Cheng, H.; Jiang, X.; Chen, M. Pathogenesis and drug response of iPSC-derived cardiomyocytes from two Brugada syndrome patients with different Na v1.5-subunit mutations. *J Biomed Res* **2021**, *35*, 395-407, doi:10.7555/JBR.35.20210045.
43. Li, W.; Stauske, M.; Luo, X.; Wagner, S.; Vollrath, M.; Mehnert, C.S.; Schubert, M.; Cyganek, L.; Chen, S.; Hasheminasab, S.M.; et al. Disease Phenotypes and Mechanisms of iPSC-Derived Cardiomyocytes From Brugada Syndrome Patients With a Loss-of-Function SCN5A Mutation. *Front Cell Dev Biol* **2020**, *8*, 592893, doi:10.3389/fcell.2020.592893.
44. El-Battrawy, I.; Lan, H.; Cyganek, L.; Zhao, Z.; Li, X.; Buljubasic, F.; Lang, S.; Yucel, G.; Sattler, K.; Zimmermann, W.H.; et al. Modeling Short QT Syndrome Using Human-Induced Pluripotent Stem Cell-Derived Cardiomyocytes. *J Am Heart Assoc* **2018**, *7*, doi:10.1161/JAHA.117.007394.
45. Shinnawi, R.; Shaheen, N.; Huber, I.; Shiti, A.; Arbel, G.; Gepstein, A.; Ballan, N.; Setter, N.; Tijsen, A.J.; Borggrefe, M.; et al. Modeling Reentry in the Short QT Syndrome With Human-Induced Pluripotent Stem Cell-Derived Cardiac Cell Sheets. *J Am Coll Cardiol* **2019**, *73*, 2310-2324, doi:10.1016/j.jacc.2019.02.055.
46. Guo, F.; Sun, Y.; Wang, X.; Wang, H.; Wang, J.; Gong, T.; Chen, X.; Zhang, P.; Su, L.; Fu, G.; et al. Patient-Specific and Gene-Corrected Induced Pluripotent Stem Cell-Derived Cardiomyocytes Elucidate Single-Cell Phenotype of Short QT Syndrome. *Circ Res* **2019**, *124*, 66-78, doi:10.1161/CIRCRESAHA.118.313518.
47. Fatima, A.; Xu, G.; Shao, K.; Papadopoulos, S.; Lehmann, M.; Arnaiz-Cot, J.J.; Rosa, A.O.; Nguemo, F.; Matzkies, M.; Dittmann, S.; et al. In vitro modeling of ryanodine receptor 2 dysfunction using human induced pluripotent stem cells. *Cell Physiol Biochem* **2011**, *28*, 579-592, doi:10.1159/000335753.
48. Wei, H.; Zhang, X.H.; Clift, C.; Yamaguchi, N.; Morad, M. CRISPR/Cas9 Gene editing of RyR2 in human stem cell-derived cardiomyocytes provides a novel approach in investigating dysfunctional Ca(2+) signaling. *Cell Calcium* **2018**, *73*, 104-111, doi:10.1016/j.ceca.2018.04.009.
49. Acimovic, I.; Refaat, M.M.; Moreau, A.; Salykin, A.; Reiken, S.; Sleiman, Y.; Souidi, M.; Pribyl, J.; Kajava, A.V.; Richard, S.; et al. Post-Translational Modifications and Diastolic Calcium Leak Associated to the Novel RyR2-D3638A Mutation Lead to CPVT in Patient-Specific hiPSC-Derived Cardiomyocytes. *J Clin Med* **2018**, *7*, doi:10.3390/jcm7110423.
50. Word, T.A.; Quick, A.P.; Miyake, C.Y.; Shak, M.K.; Pan, X.; Kim, J.J.; Allen, H.D.; Sibrian-Vazquez, M.; Strongin, R.M.; Landstrom, A.P.; et al. Efficacy of RyR2 inhibitor EL20 in induced pluripotent stem cell-derived cardiomyocytes from a patient with

catecholaminergic polymorphic ventricular tachycardia. *J Cell Mol Med* **2021**, doi:10.1111/jcmm.16521.

51. Stutzman, M.J.; Kim, C.S.J.; Tester, D.J.; Hamrick, S.K.; Dotzler, S.M.; Giudicessi, J.R.; Miotto, M.C.; Gc, J.B.; Frank, J.; Marks, A.R.; et al. Characterization of N-terminal RYR2 variants outside CPVT1 hotspot regions using patient iPSCs reveal pathogenesis and therapeutic potential. *Stem Cell Reports* **2022**, *17*, 2023-2036, doi:10.1016/j.stemcr.2022.07.002.
52. Zhang, X.H.; Wei, H.; Xia, Y.; Morad, M. Calcium signaling consequences of RyR2 mutations associated with CPVT1 introduced via CRISPR/Cas9 gene editing in human-induced pluripotent stem cell-derived cardiomyocytes: Comparison of RyR2-R420Q, F2483I, and Q4201R. *Heart Rhythm* **2021**, *18*, 250-260, doi:10.1016/j.hrthm.2020.09.007.
53. Novak, A.; Barad, L.; Zeevi-Levin, N.; Shick, R.; Shtrichman, R.; Lorber, A.; Itskovitz-Eldor, J.; Binah, O. Cardiomyocytes generated from CPVTD307H patients are arrhythmogenic in response to beta-adrenergic stimulation. *J Cell Mol Med* **2012**, *16*, 468-482, doi:10.1111/j.1582-4934.2011.01476.x.
54. Ma, D.; Wei, H.; Lu, J.; Ho, S.; Zhang, G.; Sun, X.; Oh, Y.; Tan, S.H.; Ng, M.L.; Shim, W.; et al. Generation of patient-specific induced pluripotent stem cell-derived cardiomyocytes as a cellular model of arrhythmogenic right ventricular cardiomyopathy. *Eur Heart J* **2013**, *34*, 1122-1133, doi:10.1093/eurheartj/ehs226.
55. El-Battrawy, I.; Zhao, Z.; Lan, H.; Cyganek, L.; Tombers, C.; Li, X.; Buljubasic, F.; Lang, S.; Tiburcy, M.; Zimmermann, W.H.; et al. Electrical dysfunctions in human-induced pluripotent stem cell-derived cardiomyocytes from a patient with an arrhythmogenic right ventricular cardiomyopathy. *Europace* **2018**, *20*, f46-f56, doi:10.1093/europace/euy042.
56. Buljubasic, F.; El-Battrawy, I.; Lan, H.; Lomada, S.K.; Chatterjee, A.; Zhao, Z.; Li, X.; Zhong, R.; Xu, Q.; Huang, M.; et al. Nucleoside Diphosphate Kinase B Contributes to Arrhythmogenesis in Human-Induced Pluripotent Stem Cell-Derived Cardiomyocytes from a Patient with Arrhythmogenic Right Ventricular Cardiomyopathy. *J Clin Med* **2020**, *9*, doi:10.3390/jcm9020486.
57. Ahmed, R.E.; Anzai, T.; Chanthra, N.; Uosaki, H. A Brief Review of Current Maturation Methods for Human Induced Pluripotent Stem Cells-Derived Cardiomyocytes. *Front Cell Dev Biol* **2020**, *8*, 178, doi:10.3389/fcell.2020.00178.
58. Litvinukova, M.; Talavera-Lopez, C.; Maatz, H.; Reichart, D.; Worth, C.L.; Lindberg, E.L.; Kanda, M.; Polanski, K.; Heinig, M.; Lee, M.; et al. Cells of the adult human heart. *Nature* **2020**, *588*, 466-472, doi:10.1038/s41586-020-2797-4.
59. Pinto, A.R.; Ilinykh, A.; Ivey, M.J.; Kuwabara, J.T.; D'Antoni, M.L.; Debuque, R.; Chandran, A.; Wang, L.; Arora, K.; Rosenthal, N.A.; et al. Revisiting Cardiac Cellular Composition. *Circ Res* **2016**, *118*, 400-409, doi:10.1161/CIRCRESAHA.115.307778.
60. Bai, Y.; Yeung, E.; Lui, C.; Ong, C.S.; Pitaktong, I.; Huang, C.; Inoue, T.; Matsushita, H.; Ma, C.; Hibino, N. A Net Mold-based Method of Scaffold-free Three-Dimensional Cardiac Tissue Creation. *J Vis Exp* **2018**, doi:10.3791/58252.
61. Sharma, P.; Gentile, C. Cardiac Spheroids as in vitro Bioengineered Heart Tissues to Study Human Heart Pathophysiology. *J Vis Exp* **2021**, doi:10.3791/61962.

62. Beauchamp, P.; Moritz, W.; Kelm, J.M.; Ullrich, N.D.; Agarkova, I.; Anson, B.D.; Suter, T.M.; Zuppinger, C. Development and Characterization of a Scaffold-Free 3D Spheroid Model of Induced Pluripotent Stem Cell-Derived Human Cardiomyocytes. *Tissue Eng Part C Methods* **2015**, *21*, 852-861, doi:10.1089/ten.TEC.2014.0376.
63. Ergir, E.; Oliver-De La Cruz, J.; Fernandes, S.; Cassani, M.; Niro, F.; Pereira-Sousa, D.; Vrbsky, J.; Vinarsky, V.; Perestrelo, A.R.; Debellis, D.; et al. Generation and maturation of human iPSC-derived 3D organotypic cardiac microtissues in long-term culture. *Sci Rep* **2022**, *12*, 17409, doi:10.1038/s41598-022-22225-w.
64. Drakhlis, L.; Biswanath, S.; Farr, C.M.; Lupanow, V.; Teske, J.; Ritzenhoff, K.; Franke, A.; Manstein, F.; Bolesani, E.; Kempf, H.; et al. Human heart-forming organoids recapitulate early heart and foregut development. *Nat Biotechnol* **2021**, *39*, 737-746, doi:10.1038/s41587-021-00815-9.
65. Lewis-Israeli, Y.R.; Wasserman, A.H.; Gabalski, M.A.; Volmert, B.D.; Ming, Y.; Ball, K.A.; Yang, W.; Zou, J.; Ni, G.; Pajares, N.; et al. Self-assembling human heart organoids for the modeling of cardiac development and congenital heart disease. *Nat Commun* **2021**, *12*, 5142, doi:10.1038/s41467-021-25329-5.
66. Lee, S.G.; Kim, Y.J.; Son, M.Y.; Oh, M.S.; Kim, J.; Ryu, B.; Kang, K.R.; Baek, J.; Chung, G.; Woo, D.H.; et al. Generation of human iPSCs derived heart organoids structurally and functionally similar to heart. *Biomaterials* **2022**, *290*, 121860, doi:10.1016/j.biomaterials.2022.121860.
67. Giacomelli, E.; Meraviglia, V.; Campostrini, G.; Cochrane, A.; Cao, X.; van Helden, R.W.J.; Krotenberg Garcia, A.; Mircea, M.; Kostidis, S.; Davis, R.P.; et al. Human-iPSC-Derived Cardiac Stromal Cells Enhance Maturation in 3D Cardiac Microtissues and Reveal Non-cardiomyocyte Contributions to Heart Disease. *Cell Stem Cell* **2020**, *26*, 862-879 e811, doi:10.1016/j.stem.2020.05.004.
68. Prajapati, C.; Ojala, M.; Lappi, H.; Aalto-Setala, K.; Pekkanen-Mattila, M. Electrophysiological evaluation of human induced pluripotent stem cell-derived cardiomyocytes obtained by different methods. *Stem Cell Res* **2021**, *51*, 102176, doi:10.1016/j.scr.2021.102176.
69. Giacomelli, E.; Sala, L.; Oostwaard, D.W.; Bellin, M. Cardiac microtissues from human pluripotent stem cells recapitulate the phenotype of long-QT syndrome. *Biochem Biophys Res Commun* **2021**, *572*, 118-124, doi:10.1016/j.bbrc.2021.07.068.
70. Fong, A.H.; Romero-Lopez, M.; Heylman, C.M.; Keating, M.; Tran, D.; Sobrino, A.; Tran, A.Q.; Pham, H.H.; Fimbres, C.; Gershon, P.D.; et al. Three-Dimensional Adult Cardiac Extracellular Matrix Promotes Maturation of Human Induced Pluripotent Stem Cell-Derived Cardiomyocytes. *Tissue Eng Part A* **2016**, *22*, 1016-1025, doi:10.1089/ten.TEA.2016.0027.
71. Zhang, M.; Xu, Y.; Chen, Y.; Yan, Q.; Li, X.; Ding, L.; Wei, T.; Zeng, D. Three-Dimensional Poly-(epsilon-Caprolactone) Nanofibrous Scaffolds Promote the Maturation of Human Pluripotent Stem Cells-Induced Cardiomyocytes. *Front Cell Dev Biol* **2022**, *10*, 875278, doi:10.3389/fcell.2022.875278.
72. Chen, Y.; Chan, J.P.Y.; Wu, J.; Li, R.K.; Santerre, J.P. Compatibility and function of human induced pluripotent stem cell derived cardiomyocytes on an electrospun nanofibrous scaffold, generated from an ionomeric polyurethane composite. *J Biomed Mater Res A* **2022**, *110*, 1932-1943, doi:10.1002/jbm.a.37428.

73. Sacchetto, C.; Vitiello, L.; de Windt, L.J.; Rampazzo, A.; Calore, M. Modeling Cardiovascular Diseases with hiPSC-Derived Cardiomyocytes in 2D and 3D Cultures. *Int J Mol Sci* **2020**, *21*, doi:10.3390/ijms21093404.
74. Lemoine, M.D.; Mannhardt, I.; Breckwoldt, K.; Prondzynski, M.; Flenner, F.; Ulmer, B.; Hirt, M.N.; Neuber, C.; Horvath, A.; Kloth, B.; et al. Human iPSC-derived cardiomyocytes cultured in 3D engineered heart tissue show physiological upstroke velocity and sodium current density. *Sci Rep* **2017**, *7*, 5464, doi:10.1038/s41598-017-05600-w.
75. Ronaldson-Bouchard, K.; Ma, S.P.; Yeager, K.; Chen, T.; Song, L.; Sirabella, D.; Morikawa, K.; Teles, D.; Yazawa, M.; Vunjak-Novakovic, G. Advanced maturation of human cardiac tissue grown from pluripotent stem cells. *Nature* **2018**, *556*, 239-243, doi:10.1038/s41586-018-0016-3.
76. Lu, K.; Seidel, T.; Cao-Ehlker, X.; Dorn, T.; Batcha, A.M.N.; Schneider, C.M.; Semmler, M.; Volk, T.; Moretti, A.; Dendorfer, A.; et al. Progressive stretch enhances growth and maturation of 3D stem-cell-derived myocardium. *Theranostics* **2021**, *11*, 6138-6153, doi:10.7150/thno.54999.
77. Goldfracht, I.; Efraim, Y.; Shinnawi, R.; Kovalev, E.; Huber, I.; Gepstein, A.; Arbel, G.; Shaheen, N.; Tiburcy, M.; Zimmermann, W.H.; et al. Engineered heart tissue models from hiPSC-derived cardiomyocytes and cardiac ECM for disease modeling and drug testing applications. *Acta Biomater* **2019**, *92*, 145-159, doi:10.1016/j.actbio.2019.05.016.
78. Yang, Q.; Xiao, Z.; Lv, X.; Zhang, T.; Liu, H. Fabrication and Biomedical Applications of Heart-on-a-chip. *Int J Bioprint* **2021**, *7*, 370, doi:10.18063/ijb.v7i3.370.
79. Varzideh, F.; Mone, P.; Santulli, G. Bioengineering Strategies to Create 3D Cardiac Constructs from Human Induced Pluripotent Stem Cells. *Bioengineering (Basel)* **2022**, *9*, doi:10.3390/bioengineering9040168.
80. Paloschi, V.; Sabater-Lleal, M.; Middelkamp, H.; Vivas, A.; Johansson, S.; van der Meer, A.; Tenje, M.; Maegdefessel, L. Organ-on-a-chip technology: a novel approach to investigate cardiovascular diseases. *Cardiovasc Res* **2021**, *117*, 2742-2754, doi:10.1093/cvr/cvab088.
81. Liu, H.; Bolonduro, O.A.; Hu, N.; Ju, J.; Rao, A.A.; Duffy, B.M.; Huang, Z.; Black, L.D.; Timko, B.P. Heart-on-a-Chip Model with Integrated Extra- and Intracellular Bioelectronics for Monitoring Cardiac Electrophysiology under Acute Hypoxia. *Nano Lett* **2020**, *20*, 2585-2593, doi:10.1021/acs.nanolett.0c00076.
82. Conant, G.; Lai, B.F.L.; Lu, R.X.Z.; Korolj, A.; Wang, E.Y.; Radisic, M. High-Content Assessment of Cardiac Function Using Heart-on-a-Chip Devices as Drug Screening Model. *Stem Cell Rev Rep* **2017**, *13*, 335-346, doi:10.1007/s12015-017-9736-2.
83. Zhao, Y.; Rafatian, N.; Wang, E.Y.; Wu, Q.; Lai, B.F.L.; Lu, R.X.; Savoji, H.; Radisic, M. Towards chamber specific heart-on-a-chip for drug testing applications. *Adv Drug Deliv Rev* **2020**, *165-166*, 60-76, doi:10.1016/j.addr.2019.12.002.
84. Colatsky, T.; Fermini, B.; Gintant, G.; Pierson, J.B.; Sager, P.; Sekino, Y.; Strauss, D.G.; Stockbridge, N. The Comprehensive in Vitro Proarrhythmia Assay (CiPA) initiative - Update on progress. *J Pharmacol Toxicol Methods* **2016**, *81*, 15-20, doi:10.1016/j.vascn.2016.06.002.
85. Blinova, K.; Stohlman, J.; Vicente, J.; Chan, D.; Johannesen, L.; Hortigon-Vinagre, M.P.; Zamora, V.; Smith, G.; Crumb, W.J.; Pang, L.; et al. Comprehensive Translational Assessment of Human-Induced Pluripotent Stem Cell Derived Cardiomyocytes for

Evaluating Drug-Induced Arrhythmias. *Toxicol Sci* **2017**, *155*, 234-247, doi:10.1093/toxsci/kfw200.

86. Millard, D.; Dang, Q.; Shi, H.; Zhang, X.; Strock, C.; Kraushaar, U.; Zeng, H.; Levesque, P.; Lu, H.R.; Guillon, J.M.; et al. Cross-Site Reliability of Human Induced Pluripotent stem cell-derived Cardiomyocyte Based Safety Assays Using Microelectrode Arrays: Results from a Blinded CiPA Pilot Study. *Toxicol Sci* **2018**, *164*, 550-562, doi:10.1093/toxsci/kfy110.
87. Kitaguchi, T.; Moriyama, Y.; Taniguchi, T.; Ojima, A.; Ando, H.; Uda, T.; Otabe, K.; Oguchi, M.; Shimizu, S.; Saito, H.; et al. CSAHi study: Evaluation of multi-electrode array in combination with human iPS cell-derived cardiomyocytes to predict drug-induced QT prolongation and arrhythmia--effects of 7 reference compounds at 10 facilities. *J Pharmacol Toxicol Methods* **2016**, *78*, 93-102, doi:10.1016/j.vascn.2015.12.002.
88. Yamamoto, W.; Asakura, K.; Ando, H.; Taniguchi, T.; Ojima, A.; Uda, T.; Osada, T.; Hayashi, S.; Kasai, C.; Miyamoto, N.; et al. Electrophysiological Characteristics of Human iPSC-Derived Cardiomyocytes for the Assessment of Drug-Induced Proarrhythmic Potential. *PLoS One* **2016**, *11*, e0167348, doi:10.1371/journal.pone.0167348.
89. Lee, S.G.; Kim, J.; Oh, M.S.; Ryu, B.; Kang, K.R.; Baek, J.; Lee, J.M.; Choi, S.O.; Kim, C.Y.; Chung, H.M. Development and validation of dual-cardiotoxicity evaluation method based on analysis of field potential and contractile force of human iPSC-derived cardiomyocytes / multielectrode assay platform. *Biochem Biophys Res Commun* **2021**, *555*, 67-73, doi:10.1016/j.bbrc.2021.03.039.
90. Visone, R.; Lozano-Juan, F.; Marzorati, S.; Rivolta, M.W.; Pesenti, E.; Redaelli, A.; Sassi, R.; Rasponi, M.; Occhetta, P. Predicting human cardiac QT alterations and pro-arrhythmic effects of compounds with a 3D beating heart-on-chip platform. *Toxicol Sci* **2022**, doi:10.1093/toxsci/kfac108.
91. Charwat, V.; Charrez, B.; Siemons, B.A.; Finsberg, H.; Jaeger, K.H.; Edwards, A.G.; Huebsch, N.; Wall, S.; Miller, E.; Tveito, A.; et al. Validating the Arrhythmogenic Potential of High-, Intermediate-, and Low-Risk Drugs in a Human-Induced Pluripotent Stem Cell-Derived Cardiac Microphysiological System. *ACS Pharmacol Transl Sci* **2022**, *5*, 652-667, doi:10.1021/acsptsci.2c00088.
92. McKeithan, W.L.; Savchenko, A.; Yu, M.S.; Cerignoli, F.; Bruyneel, A.A.N.; Price, J.H.; Colas, A.R.; Miller, E.W.; Cashman, J.R.; Mercola, M. An Automated Platform for Assessment of Congenital and Drug-Induced Arrhythmia with hiPSC-Derived Cardiomyocytes. *Front Physiol* **2017**, *8*, 766, doi:10.3389/fphys.2017.00766.
93. McKeithan, W.L.; Feyen, D.A.M.; Bruyneel, A.A.N.; Okolotowicz, K.J.; Ryan, D.A.; Sampson, K.J.; Potet, F.; Savchenko, A.; Gomez-Galeno, J.; Vu, M.; et al. Reengineering an Antiarrhythmic Drug Using Patient hiPSC Cardiomyocytes to Improve Therapeutic Potential and Reduce Toxicity. *Cell Stem Cell* **2020**, *27*, 813-821 e816, doi:10.1016/j.stem.2020.08.003.
94. Johnson, M.; Gomez-Galeno, J.; Ryan, D.; Okolotowicz, K.; McKeithan, W.L.; Sampson, K.J.; Kass, R.S.; Mercola, M.; Cashman, J.R. Human iPSC-derived cardiomyocytes and pyridyl-phenyl mexiletine analogs. *Bioorg Med Chem Lett* **2021**, *46*, 128162, doi:10.1016/j.bmcl.2021.128162.
95. Wang, F.; Han, Y.; Sang, W.; Wang, L.; Liang, X.; Wang, L.; Xing, Q.; Guo, Y.; Zhang, J.; Zhang, L.; et al. In Vitro Drug Screening Using iPSC-Derived Cardiomyocytes of a Long QT-

Syndrome Patient Carrying KCNQ1 & TRPM4 Dual Mutation: An Experimental Personalized Treatment. *Cells* **2022**, *11*, doi:10.3390/cells11162495.

96. Duncan, G.; Firth, K.; George, V.; Hoang, M.D.; Staniforth, A.; Smith, G.; Denning, C. Drug-Mediated Shortening of Action Potentials in LQTS2 Human Induced Pluripotent Stem Cell-Derived Cardiomyocytes. *Stem Cells Dev* **2017**, *26*, 1695-1705, doi:10.1089/scd.2017.0172.
97. Mehta, A.; Ramachandra, C.J.A.; Singh, P.; Chitre, A.; Lua, C.H.; Mura, M.; Crotti, L.; Wong, P.; Schwartz, P.J.; Gnecchi, M.; et al. Identification of a targeted and testable antiarrhythmic therapy for long-QT syndrome type 2 using a patient-specific cellular model. *Eur Heart J* **2018**, *39*, 1446-1455, doi:10.1093/eurheartj/ehx394.
98. Schwartz, P.J.; Gnecchi, M.; Dagradi, F.; Castelletti, S.; Parati, G.; Spazzolini, C.; Sala, L.; Crotti, L. From patient-specific induced pluripotent stem cells to clinical translation in long QT syndrome Type 2. *Eur Heart J* **2019**, *40*, 1832-1836, doi:10.1093/eurheartj/ehz023.
99. O'Hare, B.J.; John Kim, C.S.; Hamrick, S.K.; Ye, D.; Tester, D.J.; Ackerman, M.J. Promise and Potential Peril With Lumacaftor for the Trafficking Defective Type 2 Long-QT Syndrome-Causative Variants, p.G604S, p.N633S, and p.R685P, Using Patient-Specific Re-Engineered Cardiomyocytes. *Circ Genom Precis Med* **2020**, *13*, 466-475, doi:10.1161/CIRCGEN.120.002950.
100. Perry, M.D.; Ng, C.A.; Mangala, M.M.; Ng, T.Y.M.; Hines, A.D.; Liang, W.; Xu, M.J.O.; Hill, A.P.; Vandenberg, J.I. Pharmacological activation of IKr in models of long QT Type 2 risks overcorrection of repolarization. *Cardiovasc Res* **2020**, *116*, 1434-1445, doi:10.1093/cvr/cvz247.
101. Miller, D.C.; Harmer, S.C.; Poliandri, A.; Nobles, M.; Edwards, E.C.; Ware, J.S.; Sharp, T.V.; McKay, T.R.; Dunkel, L.; Lambiase, P.D.; et al. Ajmaline blocks I(Na) and I(Kr) without eliciting differences between Brugada syndrome patient and control human pluripotent stem cell-derived cardiac clusters. *Stem Cell Res* **2017**, *25*, 233-244, doi:10.1016/j.scr.2017.11.003.
102. El-Battrawy, I.; Albers, S.; Cyganek, L.; Zhao, Z.; Lan, H.; Li, X.; Xu, Q.; Kleinsorge, M.; Huang, M.; Liao, Z.; et al. A cellular model of Brugada syndrome with SCN10A variants using human-induced pluripotent stem cell-derived cardiomyocytes. *Europace* **2019**, *21*, 1410-1421, doi:10.1093/europace/euz122.
103. El-Battrawy, I.; Muller, J.; Zhao, Z.; Cyganek, L.; Zhong, R.; Zhang, F.; Kleinsorge, M.; Lan, H.; Li, X.; Xu, Q.; et al. Studying Brugada Syndrome With an SCN1B Variants in Human-Induced Pluripotent Stem Cell-Derived Cardiomyocytes. *Front Cell Dev Biol* **2019**, *7*, 261, doi:10.3389/fcell.2019.00261.
104. Li, Y.; Lang, S.; Akin, I.; Zhou, X.; El-Battrawy, I. Brugada Syndrome: Different Experimental Models and the Role of Human Cardiomyocytes From Induced Pluripotent Stem Cells. *J Am Heart Assoc* **2022**, *11*, e024410, doi:10.1161/JAHA.121.024410.
105. Zhao, Z.; Li, X.; El-Battrawy, I.; Lan, H.; Zhong, R.; Xu, Q.; Huang, M.; Liao, Z.; Lang, S.; Zimmermann, W.H.; et al. Drug Testing in Human-Induced Pluripotent Stem Cell-Derived Cardiomyocytes From a Patient With Short QT Syndrome Type 1. *Clin Pharmacol Ther* **2019**, *106*, 642-651, doi:10.1002/cpt.1449.
106. Schweitzer, M.K.; Wilting, F.; Sedej, S.; Dreizehnter, L.; Dupper, N.J.; Tian, Q.; Moretti, A.; My, I.; Kwon, O.; Priori, S.G.; et al. Suppression of Arrhythmia by Enhancing

Mitochondrial Ca(2+) Uptake in Catecholaminergic Ventricular Tachycardia Models. *JACC Basic Transl Sci* **2017**, *2*, 737-747, doi:10.1016/j.jacbts.2017.06.008.

107. Sander, P.; Feng, M.; Schweitzer, M.K.; Wilting, F.; Gutenthaler, S.M.; Arduino, D.M.; Fischbach, S.; Dreizehnter, L.; Moretti, A.; Gudermann, T.; et al. Approved drugs ezetimibe and disulfiram enhance mitochondrial Ca(2+) uptake and suppress cardiac arrhythmogenesis. *Br J Pharmacol* **2021**, *178*, 4518-4532, doi:10.1111/bph.15630.
108. Bezzerides, V.J.; Caballero, A.; Wang, S.; Ai, Y.; Hylind, R.J.; Lu, F.; Heims-Waldron, D.A.; Chambers, K.D.; Zhang, D.; Abrams, D.J.; et al. Gene Therapy for Catecholaminergic Polymorphic Ventricular Tachycardia by Inhibition of Ca(2+)/Calmodulin-Dependent Kinase II. *Circulation* **2019**, *140*, 405-419, doi:10.1161/CIRCULATIONAHA.118.038514.
109. Matsa, E.; Dixon, J.E.; Medway, C.; Georgiou, O.; Patel, M.J.; Morgan, K.; Kemp, P.J.; Staniforth, A.; Mellor, I.; Denning, C. Allele-specific RNA interference rescues the long-QT syndrome phenotype in human-induced pluripotency stem cell cardiomyocytes. *Eur Heart J* **2014**, *35*, 1078-1087, doi:10.1093/eurheartj/eht067.
110. Dotzler, S.M.; Kim, C.S.J.; Gendron, W.A.C.; Zhou, W.; Ye, D.; Bos, J.M.; Tester, D.J.; Barry, M.A.; Ackerman, M.J. Suppression-Replacement KCNQ1 Gene Therapy for Type 1 Long QT Syndrome. *Circulation* **2021**, *143*, 1411-1425, doi:10.1161/CIRCULATIONAHA.120.051836.
111. Bains, S.; Zhou, W.; Dotzler, S.M.; Martinez, K.; John Kim, C.S.; Tester, D.J.; Ye, D.; Ackerman, M.J. Suppression and Replacement Gene Therapy for KCNH2-Mediated Arrhythmias. *Circ Genom Precis Med* **2022**, e003719, doi:10.1161/CIRCGEN.122.003719.
112. Stillitano, F.; Hansen, J.; Kong, C.W.; Karakikes, I.; Funck-Brentano, C.; Geng, L.; Scott, S.; Reynier, S.; Wu, M.; Valogne, Y.; et al. Modeling susceptibility to drug-induced long QT with a panel of subject-specific induced pluripotent stem cells. *Elife* **2017**, *6*, doi:10.7554/eLife.19406.
113. Shinozawa, T.; Nakamura, K.; Shoji, M.; Morita, M.; Kimura, M.; Furukawa, H.; Ueda, H.; Shiramoto, M.; Matsuguma, K.; Kaji, Y.; et al. Recapitulation of Clinical Individual Susceptibility to Drug-Induced QT Prolongation in Healthy Subjects Using iPSC-Derived Cardiomyocytes. *Stem Cell Reports* **2017**, *8*, 226-234, doi:10.1016/j.stemcr.2016.12.014.
114. Blinova, K.; Schocken, D.; Patel, D.; Daluwatte, C.; Vicente, J.; Wu, J.C.; Strauss, D.G. Clinical Trial in a Dish: Personalized Stem Cell-Derived Cardiomyocyte Assay Compared With Clinical Trial Results for Two QT-Prolonging Drugs. *Clin Transl Sci* **2019**, *12*, 687-697, doi:10.1111/cts.12674.
115. Volpato, V.; Webber, C. Addressing variability in iPSC-derived models of human disease: guidelines to promote reproducibility. *Dis Model Mech* **2020**, *13*, doi:10.1242/dmm.042317.
116. Veerman, C.C.; Mengarelli, I.; Guan, K.; Stauske, M.; Barc, J.; Tan, H.L.; Wilde, A.A.; Verkerk, A.O.; Bezzina, C.R. hiPSC-derived cardiomyocytes from Brugada Syndrome patients without identified mutations do not exhibit clear cellular electrophysiological abnormalities. *Sci Rep* **2016**, *6*, 30967, doi:10.1038/srep30967.
117. Kerr, C.M.; Richards, D.; Menick, D.R.; Deleon-Pennell, K.Y.; Mei, Y. Multicellular Human Cardiac Organoids Transcriptomically Model Distinct Tissue-Level Features of Adult Myocardium. *Int J Mol Sci* **2021**, *22*, doi:10.3390/ijms22168482.

118. Feng, W.; Schriever, H.; Jiang, S.; Bais, A.; Wu, H.; Kostka, D.; Li, G. Computational profiling of hiPSC-derived heart organoids reveals chamber defects associated with NKX2-5 deficiency. *Commun Biol* **2022**, *5*, 399, doi:10.1038/s42003-022-03346-4.
119. Liu, X.; Li, W.; Fu, X.; Xu, Y. The Immunogenicity and Immune Tolerance of Pluripotent Stem Cell Derivatives. *Front Immunol* **2017**, *8*, 645, doi:10.3389/fimmu.2017.00645.
120. Fang, Y.H.; Wang, S.P.H.; Chang, H.Y.; Yang, P.J.; Liu, P.Y.; Liu, Y.W. Immunogenicity in Stem Cell Therapy for Cardiac Regeneration. *Acta Cardiol Sin* **2020**, *36*, 588-594, doi:10.6515/ACS.202011_36(6).20200811A.
121. Liew, L.C.; Ho, B.X.; Soh, B.S. Mending a broken heart: current strategies and limitations of cell-based therapy. *Stem Cell Res Ther* **2020**, *11*, 138, doi:10.1186/s13287-020-01648-0.
122. Egashira, T.; Yuasa, S.; Suzuki, T.; Aizawa, Y.; Yamakawa, H.; Matsuhashi, T.; Ohno, Y.; Tohyama, S.; Okata, S.; Seki, T.; et al. Disease characterization using LQTS-specific induced pluripotent stem cells. *Cardiovasc Res* **2012**, *95*, 419-429, doi:10.1093/cvr/cvs206.
123. Ma, D.; Wei, H.; Lu, J.; Huang, D.; Liu, Z.; Loh, L.J.; Islam, O.; Liew, R.; Shim, W.; Cook, S.A. Characterization of a novel KCNQ1 mutation for type 1 long QT syndrome and assessment of the therapeutic potential of a novel IKs activator using patient-specific induced pluripotent stem cell-derived cardiomyocytes. *Stem Cell Res Ther* **2015**, *6*, 39, doi:10.1186/s13287-015-0027-z.
124. Sala, L.; Yu, Z.; Ward-van Oostwaard, D.; van Veldhoven, J.P.; Moretti, A.; Laugwitz, K.L.; Mummery, C.L.; AP, I.J.; Bellin, M. A new hERG allosteric modulator rescues genetic and drug-induced long-QT syndrome phenotypes in cardiomyocytes from isogenic pairs of patient induced pluripotent stem cells. *EMBO Mol Med* **2016**, *8*, 1065-1081, doi:10.15252/emmm.201606260.
125. Itzhaki, I.; Maizels, L.; Huber, I.; Zwi-Dantsis, L.; Caspi, O.; Winterstern, A.; Feldman, O.; Gepstein, A.; Arbel, G.; Hammerman, H.; et al. Modelling the long QT syndrome with induced pluripotent stem cells. *Nature* **2011**, *471*, 225-229, doi:10.1038/nature09747.
126. Lahti, A.L.; Kujala, V.J.; Chapman, H.; Koivisto, A.P.; Pekkanen-Mattila, M.; Kerkela, E.; Hyttinen, J.; Kontula, K.; Swan, H.; Conklin, B.R.; et al. Model for long QT syndrome type 2 using human iPS cells demonstrates arrhythmogenic characteristics in cell culture. *Dis Model Mech* **2012**, *5*, 220-230, doi:10.1242/dmm.008409.
127. Terrenoire, C.; Wang, K.; Tung, K.W.; Chung, W.K.; Pass, R.H.; Lu, J.T.; Jean, J.C.; Omari, A.; Sampson, K.J.; Kotton, D.N.; et al. Induced pluripotent stem cells used to reveal drug actions in a long QT syndrome family with complex genetics. *J Gen Physiol* **2013**, *141*, 61-72, doi:10.1085/jgp.201210899.
128. Ma, D.; Wei, H.; Zhao, Y.; Lu, J.; Li, G.; Sahib, N.B.; Tan, T.H.; Wong, K.Y.; Shim, W.; Wong, P.; et al. Modeling type 3 long QT syndrome with cardiomyocytes derived from patient-specific induced pluripotent stem cells. *Int J Cardiol* **2013**, *168*, 5277-5286, doi:10.1016/j.ijcard.2013.08.015.
129. Fatima, A.; Kaifeng, S.; Dittmann, S.; Xu, G.; Gupta, M.K.; Linke, M.; Zechner, U.; Nguemo, F.; Milting, H.; Farr, M.; et al. The disease-specific phenotype in cardiomyocytes derived from induced pluripotent stem cells of two long QT syndrome type 3 patients. *PLoS One* **2013**, *8*, e83005, doi:10.1371/journal.pone.0083005.

130. Malan, D.; Zhang, M.; Stallmeyer, B.; Muller, J.; Fleischmann, B.K.; Schulze-Bahr, E.; Sasse, P.; Greber, B. Human iPS cell model of type 3 long QT syndrome recapitulates drug-based phenotype correction. *Basic Res Cardiol* **2016**, *111*, 14, doi:10.1007/s00395-016-0530-0.
131. Kuroda, Y.; Yuasa, S.; Watanabe, Y.; Ito, S.; Egashira, T.; Seki, T.; Hattori, T.; Ohno, S.; Kodaira, M.; Suzuki, T.; et al. Flecainide ameliorates arrhythmogenicity through NCX flux in Andersen-Tawil syndrome-iPS cell-derived cardiomyocytes. *Biochem Biophys Rep* **2017**, *9*, 245-256, doi:10.1016/j.bbrep.2017.01.002.
132. Yazawa, M.; Dolmetsch, R.E. Modeling Timothy syndrome with iPS cells. *J Cardiovasc Transl Res* **2013**, *6*, 1-9, doi:10.1007/s12265-012-9444-x.
133. Rocchetti, M.; Sala, L.; Dreizehnter, L.; Crotti, L.; Sinnecker, D.; Mura, M.; Pane, L.S.; Altomare, C.; Torre, E.; Mostacciuolo, G.; et al. Elucidating arrhythmogenic mechanisms of long-QT syndrome CALM1-F142L mutation in patient-specific induced pluripotent stem cell-derived cardiomyocytes. *Cardiovasc Res* **2017**, *113*, 531-541, doi:10.1093/cvr/cvx006.
134. Yamamoto, Y.; Makiyama, T.; Harita, T.; Sasaki, K.; Wuriyanghai, Y.; Hayano, M.; Nishiuchi, S.; Kohjitani, H.; Hirose, S.; Chen, J.; et al. Allele-specific ablation rescues electrophysiological abnormalities in a human iPS cell model of long-QT syndrome with a CALM2 mutation. *Hum Mol Genet* **2017**, *26*, 1670-1677, doi:10.1093/hmg/ddx073.
135. Limpitikul, W.B.; Dick, I.E.; Tester, D.J.; Boczek, N.J.; Limphong, P.; Yang, W.; Choi, M.H.; Babich, J.; DiSilvestre, D.; Kanter, R.J.; et al. A Precision Medicine Approach to the Rescue of Function on Malignant Calmodulinopathic Long-QT Syndrome. *Circ Res* **2017**, *120*, 39-48, doi:10.1161/CIRCRESAHA.116.309283.
136. Cerrone, M.; Lin, X.; Zhang, M.; Agullo-Pascual, E.; Pfenniger, A.; Chkourko Gusky, H.; Novelli, V.; Kim, C.; Tirasawadichai, T.; Judge, D.P.; et al. Missense mutations in plakophilin-2 cause sodium current deficit and associate with a Brugada syndrome phenotype. *Circulation* **2014**, *129*, 1092-1103, doi:10.1161/CIRCULATIONAHA.113.003077.
137. Belbachir, N.; Portero, V.; Al Sayed, Z.R.; Gourraud, J.B.; Dilasser, F.; Jesel, L.; Guo, H.; Wu, H.; Gaborit, N.; Guilluy, C.; et al. RRAD mutation causes electrical and cytoskeletal defects in cardiomyocytes derived from a familial case of Brugada syndrome. *Eur Heart J* **2019**, *40*, 3081-3094, doi:10.1093/eurheartj/ehz308.
138. Kosmidis, G.; Veerman, C.C.; Casini, S.; Verkerk, A.O.; van de Pas, S.; Bellin, M.; Wilde, A.A.; Mummery, C.L.; Bezzina, C.R. Readthrough-Promoting Drugs Gentamicin and PTC124 Fail to Rescue Nav1.5 Function of Human-Induced Pluripotent Stem Cell-Derived Cardiomyocytes Carrying Nonsense Mutations in the Sodium Channel Gene SCN5A. *Circ Arrhythm Electrophysiol* **2016**, *9*, doi:10.1161/CIRCEP.116.004227.
139. Ma, D.; Liu, Z.; Loh, L.J.; Zhao, Y.; Li, G.; Liew, R.; Islam, O.; Wu, J.; Chung, Y.Y.; Teo, W.S.; et al. Identification of an I(Na)-dependent and I(to)-mediated proarrhythmic mechanism in cardiomyocytes derived from pluripotent stem cells of a Brugada syndrome patient. *Sci Rep* **2018**, *8*, 11246, doi:10.1038/s41598-018-29574-5.
140. Selga, E.; Sendfeld, F.; Martinez-Moreno, R.; Medine, C.N.; Tura-Ceide, O.; Wilmut, S.I.; Perez, G.J.; Scornik, F.S.; Brugada, R.; Mills, N.L. Sodium channel current loss of function in induced pluripotent stem cell-derived cardiomyocytes from a Brugada syndrome patient. *J Mol Cell Cardiol* **2018**, *114*, 10-19, doi:10.1016/j.yjmcc.2017.10.002.

141. de la Roche, J.; Angsutararux, P.; Kempf, H.; Janan, M.; Bolesani, E.; Thiemann, S.; Wojciechowski, D.; Coffee, M.; Franke, A.; Schwanke, K.; et al. Comparing human iPSC-cardiomyocytes versus HEK293T cells unveils disease-causing effects of Brugada mutation A735V of Na(V)1.5 sodium channels. *Sci Rep* **2019**, *9*, 11173, doi:10.1038/s41598-019-47632-4.
142. Jung, C.B.; Moretti, A.; Mederos y Schnitzler, M.; Iop, L.; Storch, U.; Bellin, M.; Dorn, T.; Ruppenthal, S.; Pfeiffer, S.; Goedel, A.; et al. Dantrolene rescues arrhythmogenic RYR2 defect in a patient-specific stem cell model of catecholaminergic polymorphic ventricular tachycardia. *EMBO Mol Med* **2012**, *4*, 180-191, doi:10.1002/emmm.201100194.
143. Itzhaki, I.; Maizels, L.; Huber, I.; Gepstein, A.; Arbel, G.; Caspi, O.; Miller, L.; Belhassen, B.; Nof, E.; Glikson, M.; et al. Modeling of catecholaminergic polymorphic ventricular tachycardia with patient-specific human-induced pluripotent stem cells. *J Am Coll Cardiol* **2012**, *60*, 990-1000, doi:10.1016/j.jacc.2012.02.066.
144. Preininger, M.K.; Jha, R.; Maxwell, J.T.; Wu, Q.; Singh, M.; Wang, B.; Dalal, A.; McEachin, Z.T.; Rossoll, W.; Hales, C.M.; et al. A human pluripotent stem cell model of catecholaminergic polymorphic ventricular tachycardia recapitulates patient-specific drug responses. *Dis Model Mech* **2016**, *9*, 927-939, doi:10.1242/dmm.026823.
145. Sasaki, K.; Makiyama, T.; Yoshida, Y.; Wuriyanghai, Y.; Kamakura, T.; Nishiuchi, S.; Hayano, M.; Harita, T.; Yamamoto, Y.; Kohjitani, H.; et al. Patient-Specific Human Induced Pluripotent Stem Cell Model Assessed with Electrical Pacing Validates S107 as a Potential Therapeutic Agent for Catecholaminergic Polymorphic Ventricular Tachycardia. *PLoS One* **2016**, *11*, e0164795, doi:10.1371/journal.pone.0164795.
146. Novak, A.; Barad, L.; Lorber, A.; Gherghiceanu, M.; Reiter, I.; Eisen, B.; Eldor, L.; Itskovitz-Eldor, J.; Eldar, M.; Arad, M.; et al. Functional abnormalities in iPSC-derived cardiomyocytes generated from CPVT1 and CPVT2 patients carrying ryanodine or calsequestrin mutations. *J Cell Mol Med* **2015**, *19*, 2006-2018, doi:10.1111/jcmm.12581.
147. Maizels, L.; Huber, I.; Arbel, G.; Tijsen, A.J.; Gepstein, A.; Khoury, A.; Gepstein, L. Patient-Specific Drug Screening Using a Human Induced Pluripotent Stem Cell Model of Catecholaminergic Polymorphic Ventricular Tachycardia Type 2. *Circ Arrhythm Electrophysiol* **2017**, *10*, doi:10.1161/CIRCEP.116.004725.
148. Kim, C.; Wong, J.; Wen, J.; Wang, S.; Wang, C.; Spiering, S.; Kan, N.G.; Forcales, S.; Puri, P.L.; Leone, T.C.; et al. Studying arrhythmogenic right ventricular dysplasia with patient-specific iPSCs. *Nature* **2013**, *494*, 105-110, doi:10.1038/nature11799.
149. Gao, J.; Makiyama, T.; Yamamoto, Y.; Kobayashi, T.; Aoki, H.; Maurissen, T.L.; Wuriyanghai, Y.; Kashiwa, A.; Imamura, T.; Aizawa, T.; et al. Novel Calmodulin Variant p.E46K Associated With Severe Catecholaminergic Polymorphic Ventricular Tachycardia Produces Robust Arrhythmogenicity in Human Induced Pluripotent Stem Cell-Derived Cardiomyocytes. *Circ Arrhythm Electrophysiol* **2023**, *16*, e011387, doi:10.1161/CIRCEP.122.011387.
150. Sun, Y.; Su, J.; Wang, X.; Wang, J.; Guo, F.; Qiu, H.; Fan, H.; Cai, D.; Wang, H.; Lin, M.; et al. Patient-specific iPSC-derived cardiomyocytes reveal variable phenotypic severity of Brugada syndrome. *EBioMedicine* **2023**, *95*, 104741, doi:10.1016/j.ebiom.2023.104741.
151. Maurissen, T.L.; Kawatou, M.; Lopez-Davila, V.; Minatoya, K.; Yamashita, J.K.; Woltjen, K. Modeling mutation-specific arrhythmogenic phenotypes in isogenic human iPSC-derived cardiac tissues. *Sci Rep* **2024**, *14*, 2586, doi:10.1038/s41598-024-52871-1.

152. Kim, S.L.; Trembley, M.A.; Lee, K.Y.; Choi, S.; MacQueen, L.A.; Zimmerman, J.F.; de Wit, L.H.C.; Shani, K.; Henze, D.E.; Drennan, D.J.; et al. Spatiotemporal cell junction assembly in human iPSC-CM models of arrhythmogenic cardiomyopathy. *Stem Cell Reports* **2023**, *18*, 1811-1826, doi:10.1016/j.stemcr.2023.07.005.

Supplementary Table S1: overview of previously published 2D iPSC-CM cardiac arrhythmia disease models

Syndrome	Causal gene	Experimental approach	Cellular phenotype	Ref
LQTS	*KCNQ1* (c.1893del)	PC, MEA	Reduced I_{Kr}, prolonged APD, reduced wild-type *KCNQ1* mRNA and protein	(122)
	KCNQ1 exon 7 deletion	PC	Reduced I_{Ks}, APD prolongation, reduced wild type *KCNQ1* mRNA and protein, small molecule ML277 partially restored APD and reversed the decreased I_{Ks}.	(123)
	KCNQ1 p.(Arg594Gln) p.(Arg190Gln)	PC, MEA	Prolonged APD, reduced I_{Ks} activation that was reversed by hERG allosteric modulator LUF7346	(124)
	KCNH2 p.(Ala614Val)	PC	Prolonged APD, reduction of I_{Kr}, EADs, arrhythmias and potential improvement with pinacidil	(125)
	KCNH2 p.*(*Arg176Trp*)*	PC, MEA	Prolonged APD, reduced I_{Kr}, demonstrated arrhythmogenic electrical activity	(126)
	KCNH2 p.(Gly1681Ala)	PC	APD prolongation and EADs	(109)
	KCNH2 p.(Asn996Ile)	PC, MEA	Prolonged APD, reduced I_{Kr} activation that was reversed by hERG allosteric modulator LUF7346	(124)
	KCNH2 p.(Asn588Asp)	MEA, 3D culture	Prolonged FP duration, more frequent spontaneous arrhythmias	(151)
	SCN5A p.(Phe1473Cys)	PC	Delayed repolarization, prolonged QT interval with increase in pacing improving the phenotype, increased risk of fatal arrhythmia	(127)

Syndrome	Causal gene	Experimental approach	Cellular phenotype	Ref
	SCN5A p.(Val1763Met)	PC	Prolonged APD, elevated late I_{Na} current, $Na_V1.5$ blocker can reverse related symptom	(128)
	SCN5A p.(Val240Met) p.(Arg535Gln)	PC	Insignificant increase in APD, delayed time to peak I_{Na} inactivation	(129)
	SCN5A p.(Arg1644His)	PC, MEA	Prolonged APD, high EADs, and accelerated recovery from inactivation of Na^+ currents. Rescue of abnormal phenotypeby mexiletine and ranolazine	(130)
	KCNJ2 p.(Arg218Trp) p.(Arg67Trp) p.(Arg218Gln)	MEA, CI	Strong arrhythmic events, higher incidence of irregular Ca^{2+} release. Flecainide, but not pilsicainide, suppressed irregular Ca^{2+} release and arrhythmic events	(131)
	CACNA1C p.(Gly1216Ala)	PC, CI	APD prolongation and DADs, abnormal calcium handling, irregular and slow contraction. Roscovitine rescued abnormal cellular phenotype	(132)
	CALM1 p.(Phe142Leu)	PC, MEA, CI	Prolonged APD, defective $I_{Ca\text{-}L}$ inactivation, altered rate-dependency and response to isoproterenol. Repolarization abnormalities reversed by verapamil	(133)
	CALM2 p.(Asn98Ser)	PC	Lower beating rate, prolonged APD, and impaired $I_{Ca\text{-}L}$ inactivation, correction of the mutant allele rescued abnormal phenotype	(134)
	CALM2 p.(Asp130Gly)	PC, IF	Prolonged APD, disrupted Ca^{2+} cycling properties, and	(135)

Syndrome	Causal gene	Experimental approach	Cellular phenotype	Ref
			diminished Ca^{2+}/CaM-dependent inactivation of I_{Ca-L}. Suppressing the mutant gene rescued abnormal phenotype	
	PKP2 (c.2484C>T)	PA, MEA, CI	Reduced I_{Na}, deficit restored by transfection of WT gene	(136)
	PKP2 p.(Arg101His)	PC	Reduced APD90	(101)
SQT	*KCNH2* p.(Asn588Lys)	MEA, 3D culture	Decreased FP duration, Lower arrhythmogenicity compared to control	(151)
BrS	*RRAD* p.(Arg211His)	PC, CI	Reduced Vmax of AP, prolonged APs and increased incidence of EADs, decreased I_{Na} peak amplitude, increased I_{Na} persistent amplitude, decreased I_{Ca-L} amplitude	(137)
	SCN5A p.(Arg1638X) p.(Trp156X)	PC	Reduced Vmax, reduced I_{Na}	(138)
	SCN5A p.(Ala226Val)+ p.(Arg1629X) *SCN5A* p.(Thr1620Met)	PC	Ala226Val/Arg1629X: Reduced I_{Na}, reduced Vmax and APA Thr1620Met: no effect on I_{Na} and normal AP	(139)
	SCN5A p.(Arg367His)	PC	Reduced I_{Na}, shift in activation and inactivation voltage-dependence curves, faster recovery from inactivation	(140)
	SCN5A p.(Ala735Val)	PC	Reduced APA and Vmax, reduced I_{Na}, shift in activation and inactivation voltage-dependence curves	(141)
	SCN5A p.(ASP356Tyr)	PC, MEA, CI	Arrhythmic waveforms, increased inter-spike interval	(150)

Syndrome	Causal gene	Experimental approach	Cellular phenotype	Ref
			variability, reduced Vmax, reduced APA, reduced conduction velocity, reduced $I_{Na,}$ irregular Ca^{2+} transient	
	SCN10A p.(Arg1250Gln)+ p.(Arg1268Gln)	PC, CI	Reduced peak I_{Na} and I_{NaL}, accelerated recovery from inactivation in patient iPSC-CMs, reduced I_{Ca-L} and I_{Ks}, reduced APA and Vmax, increased EAD-like events	(102)
	SCN1B p.(Leu210Pro)+ p.(Pro213Thr)	PC, CI	Reduced peak I_{Na} and I_{NaL}, positive shift in the voltage dependence of activation and negative shift of the inactivation, reduction in IKs and I_{Kr}, Reduced APA and Vmax, increased arrhythmia like events	(103)
CPVT	*RYR2* p.(Ser406Leu)	PC, CI	Elevated diastolic Ca^{2+} concentrations, a reduced SR Ca^{2+} content, DADs and arrhythmia, dantrolene can restore these phenotype	(142)
	RYR2 p.(Pro2328Ser)	PC, CI	Increased non-alternating variability of Ca^{2+} transients in response to isoproterenol and β-agonists decreased AP upslope velocity	(142)
	RYR2 p.(Met4109Arg)	PC, MEA, CI	DADs were eliminated by flecainide and thapsigargin	(143)
	RYR2 p.(Leu3741Pro)	CI, MEA	Altered intracellular Ca^{2+} homeostasis, β-adrenergic stimulation potentiated spontaneous Ca^{2+} waves and prolonged Ca^{2+} sparks. Flecainide ameliorated disease phenotype	(144)

Syndrome	Causal gene	Experimental approach	Cellular phenotype	Ref
	RYR2 p.(Ile4587Val)	PC, CI	Increased diastolic Ca^{2+} waves and DADs with pacing, while S107 suppressed the DADs	(145)
	CASQ2 p.(Asp307His)	PC, CI	β-adrenergic agonist caused DADs, oscillatory arrhythmic pre-potentials, and diastolic $(Ca^{2+})_i$ rise	(53,146)
	CASQ2 p.(Asp307His)	PC, CI	Ca^{2+} transient irregularities, EADs and reduced threshold for store overload-induced Ca^{2+} release, β-blockers prevented arrhythmia	(147)
	CALM2 p.(Glu46Lys)	PC, CI	EADs and DADs, triggered activities, abnormal Ca^{2+} release, decreased Ca^{2+} transient amplitude, altered intracellular Ca2+ homeostasis	(149)
ACM	*PKP2* (c.2484C>T) *PKP2* (c.2013delC)	CI, seahorse metabolic assay	Abnormal plakoglobin nuclear translocation, decreased β-catenin activity, exaggerated lipogenesis and apoptosis calcium-handling deficits	(148)
	PKP2 p.(Arg413Ter)	cell pair platform, IF, CI	defective cell-cell junction assembly, reduced F-actin sarcomeric α-actinin organization, slower Ca^{2+} wave propagation	(152)

Adapted and updated from Garg et al. (2018) and Pan et al. (2021) (9,10). PC: patch clamp; IF: immunofluorescence; MEA: Multi electrode array; WB: Western Blot; CI: Calcium imaging; AFM: atomic force microscopy; AP: action potential; I_{Ks}: slow delayed rectifier K+ current; ER: endoplasmic reticulum; APD50-90: Action potential duration at 50%–90% of repolarisation; EAD: early after depolarisation; I_{Kr}: rapid delayed rectifier K+ current; $I_{Ca\text{-}L}$: L-type calcium current; APA: action potential amplitude; Vmax: maximum rate of rise of the action potential; I_{Na}: sodium current; DAD: delayed after repolarisation; FP: field potential; CV: conduction velocity; I_{to}: transient outward current; SR: sarcoplasmic reticulum; EM: electron microscope.

Aim of the thesis

Inherited cardiac arrhythmias (ICA) encompass a group of heterogeneous disorders characterized by abnormal heart rhythms that can result in life-threatening complications and sudden cardiac death (SCD). Despite extensive research efforts, a significant proportion of individuals suffering from ICA still lack a definitive genetic diagnosis. The genetic architecture of these syndromes is a subject of ongoing investigation, revealing its complexity, with consequences for both diagnosis and genetic counselling. Even when a clear causal variant is identified in a patient, understanding the full spectrum of symptoms and their variable severity within families remains a puzzle. The identification of these genetic variants predominantly relies on next-generation sequencing (NGS) technology, enabling comprehensive exploration of the exonic sequences and intron-exon boundaries of known ICA-related genes. However, determining the pathogenicity of these variants is still challenging and many identified variants remain 'of uncertain significance'. This is where functional studies play a vital role bridging the gap between genetic findings and clinical implications.

In this thesis, we aim to contribute to the general knowledge on ICA by answering the following research questions:

- Can the cause of sudden cardiac death be determined by molecular autopsy followed by functional analysis and what is the impact on relatives?
- What is the genetic yield of a specific ICA gene panel in a Belgian cohort of Brugada Syndrome patients and how does it correlate to the clinical phenotype?
- Is it possible to model phenotypical differences observed in Brugada syndrome patients carrying the same causal mutation in induced pluripotent stem cell derived cardiomyocytes (iPSC-CMs)?

Chapter 1:
Molecular autopsy and subsequent functional analysis reveal *de novo DSG2* mutation as cause of sudden death

Eline Simons[a], Alain Labro[b,d], Johan Saenen[c], Aleksandra Nijak[a], Ewa Sieliwonczyk[a], Bert Vandendriessche[a], Małgorzata Dąbrowska[b], Emeline M. Van Craenenbroeck[c], Dorien Schepers[a], Lut Van Laer[a], Bart Loeys[a], Maaike Alaerts[a]

[a] Cardiogenetics Research Group, Center of Medical Genetics, University of Antwerp and Antwerp University Hospital, Antwerp, Belgium
[b] Laboratory for Molecular, Cellular and Network Excitability, University of Antwerp, Antwerp, Belgium
[c] Department of Cardiology, Antwerp University Hospital, Antwerp, Belgium
[d] Department of Basic and Applied Medical Sciences, Faculty of Medicine and Health Sciences, Ghent University, Ghent, Belgium

Published in European Journal of Medical Genetics. DOI: 10.1016/j.ejmg.2021.104322

Abstract

Sudden cardiac death (SCD) is a common cause of death in young adults. In up to 80% of cases a genetic cause is suspected. Next-generation sequencing of candidate genes can reveal the cause of SCD, provide prognostic management, and facilitate pre-symptomatic testing and prevention in relatives. Here we present a proband who experienced SCD in his sleep for which molecular autopsy was performed.

We performed a post-mortem genetic analysis of a 49-year-old male who died during sleep after competitive kayaking, using a Cardiomyopathy and Primary Arrhythmia next-generation sequencing panel, each containing 51 candidate genes. Autopsy was not performed.

Genetic testing of the proband resulted in missense variants in *KCNQ1* (c.1449C > A; p.(Asn483Lys)) and *DSG2* (c.2979G > T; p.(Gln993His)), both absent from the gnomAD database. Familial segregation analysis showed de novo occurrence of the *DSG2* variant and presence of the *KCNQ1* variant in the proband's mother and daughter. *KCNQ1* p.(Asn483Lys) was predicted to be pathogenic by MutationTaster. However, none of the *KCNQ1* variant carrying family members showed long QTc on ECG or Holter. We further functionally analysed this variant using patch-clamp in a heterologous expression system (Chinese Hamster Ovary (CHO) cells) expressing the *KCNQ1* mutant in combination with *KCNE1* wild type protein and showed no significant changes in electrophysiological function of Kv7.1.

Based on the above evidence, we concluded that the *DSG2* p.(Gln993His) variant is the most likely cause of SCD in the presented case, and that there is insufficient evidence that the identified *KCNQ1* p.(Asn483Lys) variant would confer risk for SCD in his mother and daughter. Fortunately, the *DSG2* variant was not inherited by the proband's two children. This case report indicates the added value of molecular autopsy and the importance of subsequent functional study of variants to inform patients and family members about the risk of variants they might carry.

Introduction

Sudden cardiac death (SCD) has an estimated annual incidence of 1:1000. In the young (<50 years) in up to 80% of the SCD cases a genetic cause is suspected, with inherited cardiac arrhythmia or cardiomyopathy among the main disease categories (1). Next-generation sequencing (NGS) of candidate genes can reveal the cause of SCD, provide prognostic management, and facilitate pre-symptomatic testing and prevention in relatives. Generally speaking, mutations affecting ion channels involved in generation and conduction of action potentials in the heart's electrical system are underlying cardiac arrhythmias, while cardiomyopathies are caused by mutations affecting structural and/or cell-cell adhesion proteins. Several reports have been published regarding the screening of genes related to inherited cardiac arrhythmias and cardiomyopathies in SCD cases, both in larger cohorts as well as in smaller groups (2-10). In a recent study with 70 individuals, who were tested for 100 arrhythmia and cardiomyopathy related genes, 16% of SCD cases carried pathogenic or likely pathogenic variants (2). In another SCD study where 100 genes related to inherited cardiac diseases were tested in 61 individuals, 21 individuals (34%) carried a variant with a likely functional effect (3). A larger study with 302 SCD cases revealed a yield of 13% after testing 77 genes (4). Functional testing of variants can help with the interpretation of the pathogenicity of the variant, both in variants located in ion channel genes as well as in structural genes expressed in the heart (11,12).

Here we present a male proband who experienced SCD in his sleep for which molecular autopsy was performed to enable the identification of a causative mutation and allow family screening and counselling.

Clinical description

The proband is a 49-year-old man who died suddenly in his sleep. The day before, he participated in a kayaking competition and finished the race without problems. The sudden cardiac death happened abroad, and no additional evaluation was carried out. An autopsy could not be performed due to the embalming of the body. His past medical history was uneventful and two previous pre-participation screening ECGs at rest and during exercise (rowing exercise) showed no abnormalities. His family history did not reveal any instances of unexplained sudden cardiac death in first or second degree relatives. His two children (10 years old son and 13 years old daughter), both competitive sporters as well, underwent cardiac evaluation by ECG, echocardiography, SA-ECG, 24-h holter monitoring and cyclo-ergometry, but no abnormal findings were revealed.

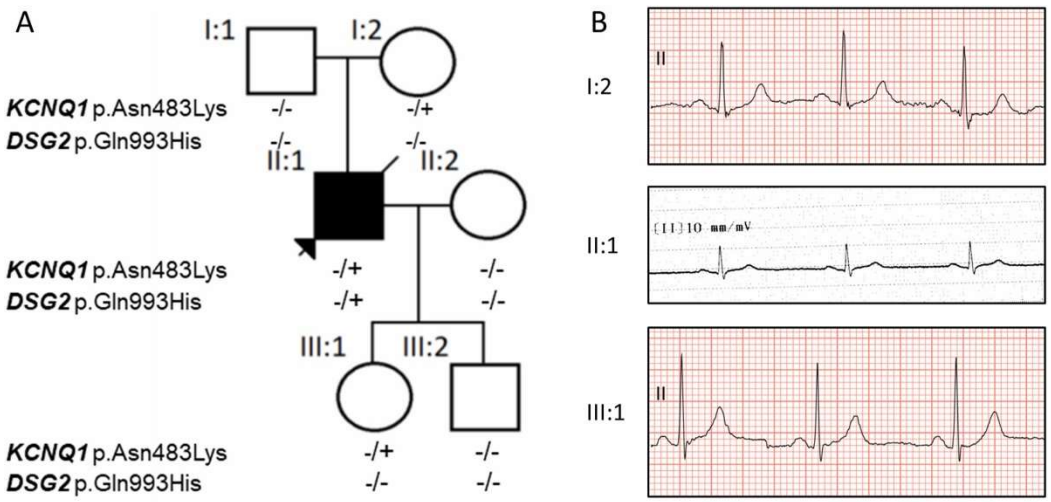

Figure 1. A) Pedigree of the family. Proband is identified with an arrow and a full symbol indicates an affected individual. B) Lead II ECG traces from three individuals (I:2; II:1 and III:1) with the KCNQ1 variant.

From a recent occupational health evaluation two serum tubes were available from the deceased proband. After inverse centrifuging the serum tubes, we were able to recover white blood cells and obtained sufficient quality and amount of DNA. After informed consent and permission of his spouse post-mortem genetic analysis was performed on this sample using next-generation sequencing panels of known cardiomyopathy and primary arrhythmia genes (each n = 51 genes) (13).

The molecular screening revealed two variants of uncertain significance: c.1449C > A (p.(Asn483Lys)) in *KCNQ1* (NM_001943.4, ENST00000155840) encoding the potassium channel Kv7.1 and c.2979G > T (p.(Gln993His)) in *DSG2* (NM_000218.2, ENST00000261590) encoding the cell-cell contact protein desmoglein 2. *KCNQ1* p.(Asn483Lys) was absent in the gnomAD v2.1.1. database (https://gnomad.broadinstitute.org/) and predicted to be damaging by MutationTaster and benign by SIFT and Polyphen-2. *DSG2* p.(Gln993His) was also absent from gnomAD v2.1.1 and only Polyphen-2 scored the variant as probably damaging.

Segregation analysis showed that the *KCNQ1* variant was inherited from the proband's mother and transmitted to the proband's daughter. The *DSG2* variant occurred *de novo* (with proven paternity) and was not inherited by his children (Fig. 1A). The mother and daughter showed normal ECG at rest (Fig. 1B) and during cyclo-ergometry, as well as a 24-h holter registration with normal QTc intervals. Because of the daughter's sport

activities, it was decided to put her on beta-blockers and limit competitive sporting as long as the pathogenicity of the *KCNQ1* variant was not excluded, as intensive sporting is known to be a trigger for arrhythmias in Long QT syndrome type 1 (LQT1) (14).

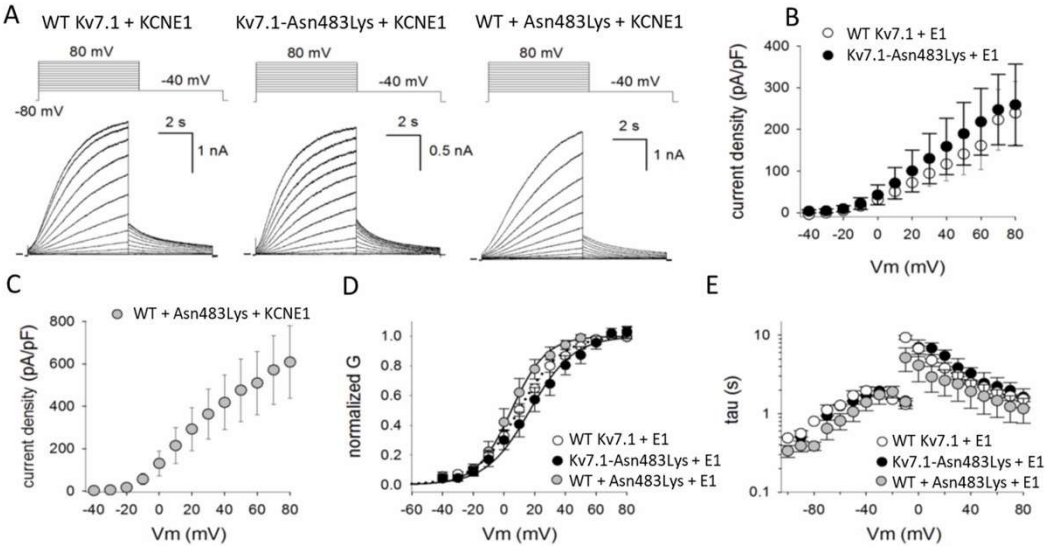

Figure 2. Electrophysiological properties of WT Kv7.1 and Kv7.1-Asn483Lys co-expressed with KCNE1 (representing in vivo I_{Ks} current). A) Displayed from left to right are representative whole cell ionic current recordings of CHO cells expressing WT Kv7.1 + KCNE1, Kv7.1-Asn483Lys + KCNE1 and the co-expression of WT Kv7.1 with Kv7.1-Asn483Lys + KCNE1. The K+ selective currents were elicited with the pulse protocol shown on top. Horizontal bar at the start indicates the zero current level. B) Current density of WT Kv7.1 + KCNE1 (white circles, n = 5) and Kv7.1-Asn483Lys + KCNE1 (black circles, n = 7) obtained by normalizing the peak current amplitudes after 6 s depolarization, from recordings shown in panel b, to the cell capacitance. C) Current density of the co-expression of WT Kv7.1 with Kv7.1-Asn483Lys + KCNE1 (n = 5). In this condition the amount of Kv7.1 a-subunit cDNA doubled compared to the expression of WT Kv7.1 and Kv7.1-Asn483Lys alone. Accordingly, the current density increased a 2-fold compared to the data displayed in panel c. The data from panel c and d indicate that the Asn483Lys mutation does not affect current expression. D) Voltage dependence of channel activation obtained by plotting the normalized amplitudes of the tail currents at −40 mV, elicited after 6 s depolarization as shown in panel b, as a function of the depolarizing potential. E) Voltage-dependent kinetics of channel activation and deactivation. Shown values are the means ± S.E.M. with n the number of cells analysed.

In order to further investigate the pathogenic nature of the *KCNQ1* variant, we tested the variant electrophysiologically in Chinese Hamster Ovarian cells (CHO). Both wild type (WT, Kv7.1) and mutant (MUT, Kv7.1-Asn483Lys) were tested on their own as well as in combination, and we always co-expressed the auxiliary Mink protein encoded by the *KCNE1* gene, that is necessary for proper functioning of the ion channel. Ionic currents were recorded during the following pulse protocol: starting from a −80mV holding potential, a 6s depolarizing pulse from −60 to +80 mV in 10 mV steps was forced to the

cells after which they were repolarized to −40mV to measure the tail current. Whole cell current recordings show no significant differences in current density between the different combinations (WT, MUT, WT/MUT). Normalized tail current amplitudes (I/Imax) were plotted as a function of the depolarizing potential. The resulting voltage dependence of channel activation was not impaired by the variant and also both activation and inactivation kinetics were the same in the different combinations (WT, MUT, WT/MUT) (Fig. 2).

Discussion and conclusions

Genetic analysis of the proband's DNA revealed two possible causal variants for his SCD, namely p.(Asn483Lys) in *KCNQ1* and p.(Gln993His) in *DSG2*. The Kv7.1 potassium channel is responsible for the delayed rectifier current I_{Ks}, important in the repolarization of the cardiac action potential. Mutations in *KCNQ1* are a known cause of LQT1 which can cause ventricular fibrillations and lead to SCD (15). Pathogenic mutations are mostly located in the transmembrane part of the channel as well as the C-terminal domain of the protein (16), where our variant is located. Many variants have been modelled in heterologous expression systems, often showing a loss-of-function or a dominant negative effect on the functioning of Kv7.1 (17-20). Although sometimes, a variant is reported that does not have an effect on the functioning of the channel (21). Wedekind et al. found two variants (p.(Val254Met) and p.(Val417Met)) in a family that were located in cis on the same *KCNQ1* allele and electrophysiological data showed that only p.(Val254Met) had an effect on the function of Kv7.1 (21).

The electrophysiological data we generated in a heterologous expression system indicates that the function of the Kv7.1 protein is not altered by the p.(Asn483Lys) variant, which is consistent with the normal results of the QTc measurements in the proband's mother and daughter. Based on these results, we concluded that there is insufficient evidence that this variant would confer risk for SCD in the mother and daughter of the proband. Beta-blockade was discontinued in the daughter and she was allowed to continue her sports career, with close clinical follow-up.

Desmoglein-2 is a cadherin providing cell-cell contact in cardiac desmosomes. In 2006, Pilichou et al. and Awad et al. were the first to report *DSG2* variants in family members with ARVC (22, 23). ARVC is characterized by fibro-fatty replacement, predominantly in the right ventricle, which can induce ventricular arrhythmias and eventually lead to SCD (22). The *DSG2* p.(Gln993His) variant which occurred de novo in this described case is located in the intracellular repeat unit domain (RUD). Previously, two variants in this RUD were reported. A p.(Val920Gly) variant was found in the father of a boy who died at age

17. Post-mortem analysis of the boy suggested left ventricular involvement in ARVC as the cause of death. The father was asymptomatic but had late potentials on signal-averaged ECG and cardiac imaging revealed hypokinesia of the anterior wall of the right ventricular outflow tract and the apical free wall (24). A functional study showed that this variant reduces cell-cell cohesion in HL-1 cardiomyocytes (25). Another p.(Tyr1047Arg) variant in the same RUD was reported in a patient with ARVC and a family member whose phenotype was not specified in the report (26). Together, these findings support the potential pathogenicity of variants located in the RUD domain of *DSG2*.

The *DSG2* p.(Gln993His) variant occurred *de novo* (with proven paternity) in a proband without family history (PS2 argument). In addition, we can assign PM2 (moderate evidence) for absence in controls and PP2 (supportive evidence) for a missense variant in a gene that has a low rate of benign missense variation and where missense variants are a common mechanism of disease. Overall, the variant is classified as a likely pathogenic variant (according to the ACMG-rule "1 Strong (PS1–PS4) AND 1–2 Moderate (PM1–PM6)") (27). Based on all the mentioned evidence and the fact that ARVC is a typical cause of death in competitive sportsmen, we can conclude that the *DSG2* p.(Gln993His) variant is the most likely cause of SCD in the proband. We proved that the *KCNQ1* variant did not interfere with the function of Kv7.1. As such, the daughter could be taken off the beta-blocker treatment. But since still additional unknown genetic variants not detected by the used gene panels could have contributed to the proband's SCD, close clinical follow-up of the children remains warranted when performing competitive sports. A limitation in this study is the fact that an autopsy was not performed, which could have revealed typical ARVC-related abnormalities in the structure of the proband's heart. This case report indicates the added value of molecular autopsy and the importance of subsequent functional study of detected variants to inform patients and family members about the risk of variants they might carry.

Declaration of competing interest
The authors declare that they have no competing interests.

Acknowledgements
We acknowledge the family of the patient for their cooperation.

Ethics approval and consent to participate
This study was approved by the Ethical Committee of the Antwerp University Hospital.

Consent for publication
Written consent for publication was obtained from the proband's wife.

Availability of data and materials

The datasets used and/or analysed during the current study are available from the corresponding author on reasonable request. Both variants have been submitted to the Clinvar database (*KCNQ1*: VCV000927801; *DSG2*: VCV000996557).

Funding

This research work was supported by funding from the University of Antwerp (GOA FFB160361, Methusalem-OEC grant "Genomed" FFB190208) and the Research Foundation - Flanders (FWO, G.0356.17). Dr. Loeys is senior clinical investigator of the FWO and holds a consolidator grant from the European Research Council ("Genomia" ERC-COG-2017-771945). E. Simons, A. Nijak and E. Sieliwończyk are research fellows supported by the FWO (1S25318N, 1S24317N, 1192019N). D. Schepers is a postdoctoral fellow of the FWO (12R5619N).

Authors' contributions

E.Sim., A.L., J.S., B.L. and M.A: Conceptualization, Methodology; J.S., E.Sie., E.V.C., B.L., M.D.: Investigation; E.Sim.: Writing - Original Draft; A.L., J.S., D.S., L.V.L., B.L. and M.A: Writing - Review & Editing; E.Sim, A.N: Visualization; E.Sim., A.L., A.N., B.V., M.D., D.S. and M.A.: Validation; All authors have read and approved the manuscript.

References

1. Saenen JB, Van Craenenbroeck EM, Proost D, Marchau F, Van Laer L, Vrints CJ, et al. Genetics of sudden cardiac death in the young. Clin Genet. 2015;88(2):101-13.
2. Larsen MK, Christiansen SL, Hertz CL, Frank-Hansen R, Jensen HK, Banner J, et al. Targeted molecular genetic testing in young sudden cardiac death victims from Western Denmark. Int J Legal Med. 2020;134(1):111-21.
3. Christiansen SL, Hertz CL, Ferrero-Miliani L, Dahl M, Weeke PE, LuCamp, et al. Genetic investigation of 100 heart genes in sudden unexplained death victims in a forensic setting. Eur J Hum Genet. 2016;24(12):1797-802.
4. Lahrouchi N, Raju H, Lodder EM, Papatheodorou E, Ware JS, Papadakis M, et al. Utility of Post-Mortem Genetic Testing in Cases of Sudden Arrhythmic Death Syndrome. J Am Coll Cardiol. 2017;69(17):2134-45.
5. Gaertner-Rommel A, Tiesmeier J, Jakob T, Strickmann B, Veit G, Bachmann-Mennenga B, et al. Molecular autopsy and family screening in a young case of sudden cardiac death reveals an unusually severe case of FHL1 related hypertrophic cardiomyopathy. Mol Genet Genomic Med. 2019;7(8):e841.
6. Anderson JH, Tester DJ, Will ML, Ackerman MJ. Whole-Exome Molecular Autopsy After Exertion-Related Sudden Unexplained Death in the Young. Circ Cardiovasc Genet. 2016;9(3):259-65.
7. Hellenthal N, Gaertner-Rommel A, Klauke B, Paluszkiewicz L, Stuhr M, Kerner T, et al. Molecular autopsy of sudden unexplained deaths reveals genetic predispositions for cardiac diseases among young forensic cases. Europace. 2017;19(11):1881-90.

8. Neubauer J, Lecca MR, Russo G, Bartsch C, Medeiros-Domingo A, Berger W, et al. Exome analysis in 34 sudden unexplained death (SUD) victims mainly identified variants in channelopathy-associated genes. Int J Legal Med. 2018;132(4):1057-65.
9. Neubauer J, Haas C, Bartsch C, Medeiros-Domingo A, Berger W. Post-mortem whole-exome sequencing (WES) with a focus on cardiac disease-associated genes in five young sudden unexplained death (SUD) cases. Int J Legal Med. 2016;130(4):1011-21.
10. Hertz CL, Christiansen SL, Ferrero-Miliani L, Fordyce SL, Dahl M, Holst AG, et al. Next-generation sequencing of 34 genes in sudden unexplained death victims in forensics and in patients with channelopathic cardiac diseases. Int J Legal Med. 2015;129(4):793-800.
11. Zou Y, Zhang Q, Zhang J, Chen X, Zhou W, Yang Z, et al. A common indel polymorphism of the Desmoglein-2 (DSG2) is associated with sudden cardiac death in Chinese populations. Forensic Sci Int. 2019;301:382-7.
12. Shafaattalab S, Li AY, Lin E, Stevens CM, Dewar LJ, Lynn FC, et al. In vitro analyses of suspected arrhythmogenic thin filament variants as a cause of sudden cardiac death in infants. Proc Natl Acad Sci U S A. 2019;116(14):6969-74.
13. Proost D, Saenen J, Vandeweyer G, Rotthier A, Alaerts M, Van Craenenbroeck EM, et al. Targeted Next-Generation Sequencing of 51 Genes Involved in Primary Electrical Disease. J Mol Diagn. 2017;19(3):445-59.
14. Schwartz PJ, Priori SG, Spazzolini C, Moss AJ, Vincent GM, Napolitano C, et al. Genotype-phenotype correlation in the long-QT syndrome: gene-specific triggers for life-threatening arrhythmias. Circulation. 2001;103(1):89-95.
15. Priori SG, Wilde AA, Horie M, Cho Y, Behr ER, Berul C, et al. Executive summary: HRS/EHRA/APHRS expert consensus statement on the diagnosis and management of patients with inherited primary arrhythmia syndromes. Heart Rhythm. 2013;10(12):e85-108.
16. Kapa S, Tester DJ, Salisbury BA, Harris-Kerr C, Pungliya MS, Alders M, et al. Genetic testing for long-QT syndrome: distinguishing pathogenic mutations from benign variants. Circulation. 2009;120(18):1752-60.
17. Jons C, J OU, Moss AJ, Reumann M, Rice JJ, Goldenberg I, et al. Use of mutant-specific ion channel characteristics for risk stratification of long QT syndrome patients. Sci Transl Med. 2011;3(76):76ra28.
18. Grunnet M, Behr ER, Calloe K, Hofman-Bang J, Till J, Christiansen M, et al. Functional assessment of compound mutations in the KCNQ1 and KCNH2 genes associated with long QT syndrome. Heart Rhythm. 2005;2(11):1238-49.
19. Yang T, Chung SK, Zhang W, Mullins JG, McCulley CH, Crawford J, et al. Biophysical properties of 9 KCNQ1 mutations associated with long-QT syndrome. Circ Arrhythm Electrophysiol. 2009;2(4):417-26.
20. Kinoshita K, Komatsu T, Nishide K, Hata Y, Hisajima N, Takahashi H, et al. A590T mutation in KCNQ1 C-terminal helix D decreases IKs channel trafficking and function but not Yotiao interaction. J Mol Cell Cardiol. 2014;72:273-80.
21. Wedekind H, Schwarz M, Hauenschild S, Djonlagic H, Haverkamp W, Breithardt G, et al. Effective long-term control of cardiac events with beta-blockers in a family with a common LQT1 mutation. Clin Genet. 2004;65(3):233-41.

22. Pilichou K, Nava A, Basso C, Beffagna G, Bauce B, Lorenzon A, et al. Mutations in desmoglein-2 gene are associated with arrhythmogenic right ventricular cardiomyopathy. Circulation. 2006;113(9):1171-9.
23. Awad MM, Dalal D, Cho E, Amat-Alarcon N, James C, Tichnell C, et al. DSG2 mutations contribute to arrhythmogenic right ventricular dysplasia/cardiomyopathy. Am J Hum Genet. 2006;79(1):136-42.
24. Syrris P, Ward D, Asimaki A, Evans A, Sen-Chowdhry S, Hughes SE, et al. Desmoglein-2 mutations in arrhythmogenic right ventricular cardiomyopathy: a genotype-phenotype characterization of familial disease. Eur Heart J. 2007;28(5):581-8.
25. Schlipp A, Schinner C, Spindler V, Vielmuth F, Gehmlich K, Syrris P, et al. Desmoglein-2 interaction is crucial for cardiomyocyte cohesion and function. Cardiovasc Res. 2014;104(2):245-57.
26. Groeneweg JA, Bhonsale A, James CA, te Riele AS, Dooijes D, Tichnell C, et al. Clinical Presentation, Long-Term Follow-Up, and Outcomes of 1001 Arrhythmogenic Right Ventricular Dysplasia/Cardiomyopathy Patients and Family Members. Circ Cardiovasc Genet. 2015;8(3):437-46.
27. Richards S, Aziz N, Bale S, Bick D, Das S, Gastier-Foster J, et al. Standards and guidelines for the interpretation of sequence variants: a joint consensus recommendation of the American College of Medical Genetics and Genomics and the Association for Molecular Pathology. Genet Med. 2015;17(5):405-24.

Chapter 2:
Diagnostic yield of a cardiac arrhythmia gene panel in a Brugada syndrome cohort

Eline Simons[a], Ewa Sieliwonczyk[a], Maaike Bastiaansen[a], Bert Vandendriessche[a], Dogan Akdeniz[a], Hanne Boen[a], Ilyas Louarroudi[a], Dieter De Cleen[b], Hilko Miljoen[c], Hein Heidbuchel[c], Wim Huybrechts[c], Pieter Koopman[d], Emeline Van Craenenbroeck[c], Joris Schurmans[d], Sophie Van Malderen[e], Gaelle Vermeersch[f], Philippe Vanduynhoven[g], Johan Saenen[c], Dorien Schepers[a], Bart Loeys[a], Maaike Alaerts[a]

[a] Cardiogenetics Research Group, Centre of Medical Genetics, University of Antwerp and Antwerp University Hospital, Antwerp, Belgium.
[b] Department of Cardiology, AZ KLINA, Brasschaat, Belgium
[c] Department of Cardiology, University Hospital Antwerp, Edegem, Belgium; Department GENCOR-Heart Rhythm Disorders, University of Antwerp, Antwerp, Belgium
[d] Department of Cardiology, Hartcentrum Hasselt, Jessa Hospital, Hasselt, Belgium
[e] Department of Cardiology, AZ Monica, Deurne, Belgium
[f] Electrophysiology Unit, ZNA Heart Centre Middelheim, Antwerpen, Belgium
[g] Department of Cardiology, Arrhythmia Clinic, Algemeen Stedelijk Ziekenhuis Aalst, Aalst, Belgium.

Abstract

Background and Aims: Brugada syndrome (BrS) is a rare inherited cardiac arrhythmia disorder characterized by a typical ST-segment elevation on an electrocardiogram (ECG) and is associated with an increased risk of ventricular fibrillation and sudden cardiac death (SCD). The main and only gene considered to be definitively causal for BrS is *SCN5A*, encoding the cardiac sodium channel, although other ion channel and related genes have been associated with the disease as well. We aimed to determine the diagnostic yield of a gene panel for inherited cardiac arrhythmias in a cohort of BrS patients.

Methods: We collected clinical history, ECG parameters and genetic results of 350 BrS patients (showing a type I BrS ECG) screened with a diagnostic cardiac arrhythmia gene panel (N=51 genes in 272 patients, N=60 in 78 patients) at the Center of Medical Genetics Antwerp.

Results: In our cohort (38% females), 15% of BrS patients showed a spontaneous type I ECG and according to the Shanghai criteria 46% of the cohort has a definite BrS diagnosis with a score ≥3.5. In total 142 (40%) patients carried a variant of uncertain significance (VUS) or a (likely) pathogenic variant in one of the investigated genes. Most variants were found in *SCN5A*, followed by *CACNA1C*. One hundred and nine BrS patients carried a VUS, 10 a likely pathogenic (LP) and 22 a pathogenic (P) variant, of which 15 the same known founder mutation in *SCN5A*. Of the 16 unique P/LP variants, 14 were found in the *SCN5A* gene and the other two in *LMNA* and *SCN2B.* Patients harbouring a P/LP variant had a significantly longer PR interval and QRS segment, more often a spontaneous Type I ECG, developed more ventricular fibrillations, had more often a familial history and had a higher Shanghai score.

Conclusion: In a cohort of 350 patients, the overall diagnostic yield is 9.4% which increases to 17.5% in BrS patients with a definite diagnosis following the Shanghai criteria and 19% in patients with a family history of BrS and/or SCD.

Key words: Brugada syndrome, genetics, NGS panel, Shanghai Score

What's New?

- Extensive genetic testing in a cohort of 350 Brugada patients revealed a (likely) pathogenic variant in 9% of the patients.
- Additional supporting evidence is provided for a role of *LMNA* and *SCN2B* in BrS pathogenesis.
- The yield of (likely) pathogenic variants is higher in patients with a definite BrS diagnosis (Shanghai criteria) and in patients with a family history of BrS and/or SCD.

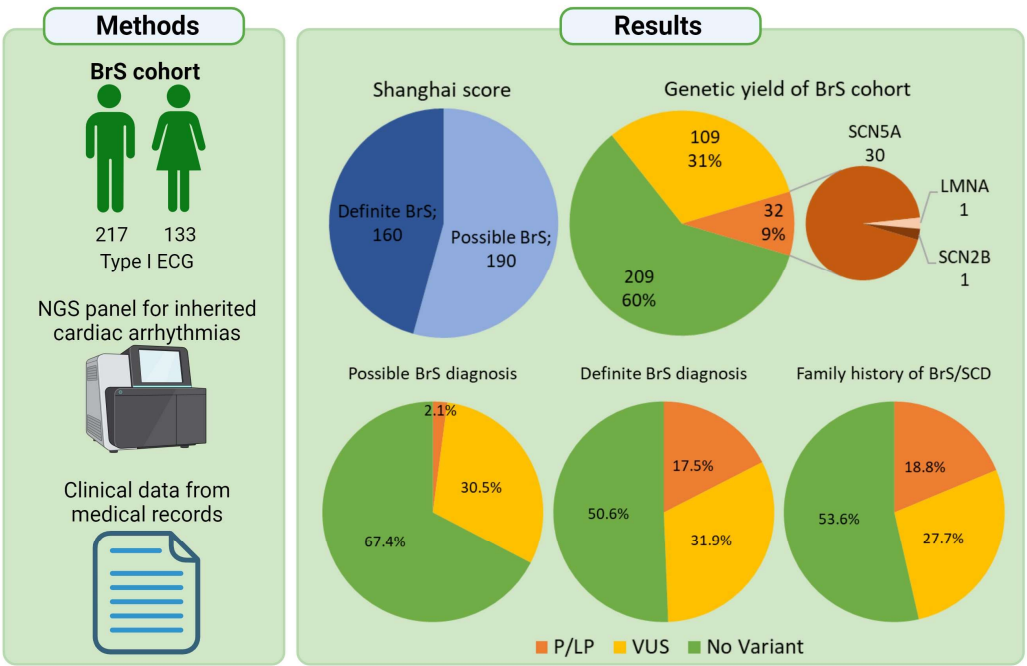

Introduction

Brugada syndrome (BrS) is a rare inherited cardiac arrhythmia disorder with a prevalence of approximately 1/2000 and it is 8 to 10 times more prevalent in men (1). BrS is diagnosed by a typical ST-segment elevation in more than one right precordial lead (V1-V3) on an electrocardiogram (ECG), either occurring spontaneously or after administration of a sodium channel blocker like ajmaline or flecainide (2). The clinical presentation ranges from no symptoms at all to heart palpitations, syncopes and ventricular fibrillation that can eventually lead to sudden cardiac death (SCD), indicating the well-known reduced penetrance and variable expressivity in BrS. The first gene reported as causal for BrS is *SCN5A*, encoding the cardiac specific voltage gated sodium channel Nav1.5, which is responsible for the fast depolarisation of the cardiac action potential (3). Loss-of-function variants in *SCN5A* are found in approximately 20-25 % of the BrS patients. Other genes have been associated with the disease (listed in Table 1), but these are not (yet) considered as definitively causal (4, 5). These genes encode sodium (*SCN5A, SCN10A, SCN1B, SCN2B, SCN3B*), calcium (*CACNA1C, CACNA2C1, CACNB1*) and potassium channels (*HCN4, KCND2, KCND3, KCNE3, KCNE5, KCNJ8*) and their associated proteins.

In 2016, the Shanghai score system to diagnose BrS, was proposed in the HRS/EHRA/APHRS/SOLAECE J-Wave Syndrome Consensus Report (6). This scoring system includes several parameters such as the ECG type I pattern (spontaneous, fever-induced or after provocation), clinical and familial history and genetic test results. Each parameter is given a certain number of points, based on severity, and when the sum of these points reaches 3.5 or above, a definite BrS diagnosis is established (6). Historically, this scoring system was used only for diagnostic purposes but more recently, it is also being tested as a risk stratification tool. At present only patients at high risk of arrhythmic events can be identified while the predictive capability for asymptomatic and intermediate-risk patients remains modest (7, 8).

To find potential pathogenic variants in patients, next-generation sequencing (NGS) panels are commonly used in molecular diagnostics. Genes associated with inherited cardiac arrhythmia (ICA) disorders, such as long/short QT syndrome (L/SQTS), BrS, catecholaminergic polymorphic ventricular tachycardia (CPVT) and arrhythmogenic (right ventricular) cardiomyopathy (ARVC/ACM) are combined in these panels (9), due to the genetic overlap between these disorders. At our genetic centre, a multigene NGS panel (Primary Electrical Disease PED panel) is used to screen for variants in 51 or 60 genes related to ICA (9).

Table 1: Genes associated with BrS

Gene	**Gene name**	**Ref.**
ABCC9	ATP Binding Cassette Subfamily C Member 9	(10)
ANK2	Ankyrin 2	(11)
CACNA1C	Calcium Voltage-Gated Channel Subunit Alpha1 C	(12)
CACNA2D1	Calcium Voltage-Gated Channel Auxiliary Subunit Alpha2delta 1	(13)
CACNB2B	Calcium Voltage-Gated Channel Auxiliary Subunit Beta 2	(12)
FGF12	Fibroblast Growth Factor 12	(14)
GPD1L	Glycerol-3-Phosphate Dehydrogenase 1 Like	(15)
HCN4	Hyperpolarization Activated Cyclic Nucleotide Gated Potassium Channel 4	(16)
HEY2	Hes Related Family BHLH Transcription Factor With YRPW Motif 2	(17)
KCND2	Potassium Voltage-Gated Channel Subfamily D Member 2	(18)
KCND3	Potassium Voltage-Gated Channel Subfamily D Member 3	(19)
KCNE3	Potassium Voltage-Gated Channel Subfamily E Regulatory Subunit 3	(20)
KCNE5	Potassium Voltage-Gated Channel Subfamily E Regulatory Subunit 5	(21)
KCNH2	Potassium Voltage-Gated Channel Subfamily H Member 2	(22)
KCNJ8	Potassium Inwardly Rectifying Channel Subfamily J Member 8	(23)
LMNA	Lamin A/C	(24)
LRRC10	Leucine Rich Repeat Containing 10	(25)
MYBPC3	Myosin Binding Protein C3	(26)
PKP2	Plakophilin 2	(27)
RANGRF	RAN Guanine Nucleotide Release Factor	(28)
SCN1B	Sodium Voltage-Gated Channel Beta Subunit 1	(29)
SCN2B	Sodium Voltage-Gated Channel Beta Subunit 2	(30)
SCN3B	Sodium Voltage-Gated Channel Beta Subunit 3	(31)
SCN5A	Sodium Voltage-Gated Channel Alpha Subunit 5	(3)
SEMA3A	Semaphorin 3A	(32)
SLMAP	Sarcolemma Associated Protein	(33)
TPM1	Tropomyosin 1	(34)
TRPM4	Transient Receptor Potential Cation Channel Subfamily M Member 4	(35)

Here we present a BrS cohort of 350 patients who were screened for variants in the PED panel genes. We investigate the diagnostic yield of our PED panel and use the Shanghai scoring system to diagnose the patients.

Material and methods

Ethics

This study was approved by the Ethical Committee of the Antwerp University Hospital (EC20/20/257). All patients signed an informed consent.

Clinical evaluation

Medical records of 520 patients with possible BrS, who were referred to our Centre of Medical Genetics Antwerp for genetic testing were collected over 32 medical centres across Belgium. Family history and clinical data were investigated. 350 patients met the diagnostic criteria for BrS, showing a type I BrS ECG either spontaneously, during fever or provoked with a sodium channel blocker and were index patients in their family. 158 were patients at the Antwerp University Hospital. For 175 patients ECG recordings were available for both PR interval and QRS segment analysis. Patients' Shanghai score was calculated following the guidelines drafted in the 2016 HRS/EHRA/APHRS/SOLAECE J-Wave Syndrome Consensus Report (6). In Supplementary Table 1, the proposed score system is presented. A score ≥3.5 points is classified as definite BrS, between 2 and 3 points is a possible BrS diagnosis and below 2 points is non-diagnostic.

Genetic testing

Genomic DNA was extracted from blood using standard procedures. Amplification of the target regions was performed using the PED MASTR Plus assay (n=272, Multiplicom; including 51 genes; see Proost et al. (9), Supplementary Table 2) or the Twist Human Core Exome kit spiked-in with additional custom probes (n=78, Twist Bioscience; selection of 60 genes for analysis, Supplementary Table 2), according to the manufacturer's instructions. This was followed by NGS-sequencing on a NextSeq or NovaSeq instrument (Illumina). Data analysis was performed using the SeqNext module of Sequence Pilot (JSI Medical Systems) detecting variants in the coding exons, including exon/intron boundaries up to 15 intronic nucleotides, of the set of PED genes. For all samples, minimum 99% of the targeted region was covered at ≥30x. The list of genes and their respective transcripts are given in Supplementary Table 2. Variants were classified following the ACMG guidelines (36).

Statistical analysis

Groups were compared either using the non-parametric Kruskal-Wallis test followed by pairwise Mann-Whitney U test or the Fisher's exact test. Statistical analysis was performed in R.

Results

Clinical characteristics of the patient population

Our population comprises 350 patients of which 133 (38%) are female. Most of the patients (80.3%) only showed a type I ECG after provocation with a sodium channel blocker, while 52 (14.9%) had a spontaneous type I ECG and 10 (2.9%) showed a type I ECG during fever. A history of sudden cardiac death (SCD) and/or BrS in first- or second-degree relatives was observed in 112 patients (32%). Fifty-five patients (15.7%) suffered a suspected cardiac syncope while 13 patients (3.7%) were documented with ventricular fibrillation (VF) and/or polymorphic ventricular tachycardia (VT) and 9 (2.5%) suffered from (aborted) cardiac arrest. An implantable cardioverter defibrillator (ICD) was implanted in 114 (32.6%) patients of whom 9 (7.9%) received an appropriate shock while 11 (9.6%) had an inappropriate shock. Sixty-one patients (17.4%) were documented with atrial fibrillation. One hundred and sixty patients (45.7%) had a definite BrS diagnosis according to the Shanghai scoring system, the median calculated Shanghai score for the whole population was 3. ECG analysis of 175 patients (50%) showed a median PR interval of 160 ms (normal range 120 – 200 ms) and median QRS segment of 104 ms (normal range <200 ms).

Table 2: Summary of the BrS Cohort

	All Patients	**Patients without variant**	**Patients carrying VUS**	**Patients harbouring P/LP variant**	**P-value**
Total	350	209 (59.4%)	109 (31.4%)	32 (9.1%)	
Female (%)	133 (38%)	78 (37.3%)	46 (42.2%)	9 (28.1%)	
Diagnosis					
Spontaneous Type I ECG	52 (14.9%)	20 (9.6%)	19 (17.4%)	13 (40.6%)	**<0.0001**
Type I ECG during fever	10 (2.9%)	7 (3.3%)	2 (1.8%)	1 (3.1%)	ns
Provoked Type I ECG	281 (80.3%)	176 (84.2%)	88 (80.7%)	17 (53.1%)	**<0.001**
Family History	112 (32%)	60 (28.7%)	31 (28.4%)	21 (65.6%)	**<0.001**
Family History of BrS	77 (22%)	40 (19.1%)	20 (18.3%)	17 (53.1%)	

	All Patients	Patients without variant	Patients carrying VUS	Patients harbouring P/LP variant	P-value
Unexplained SCD<45 yrs in 1st or 2nd degree relative	46 (13.1%)	24 (11.5%)	15 (13.8%)	7 (21.9%)	
Clinical symptoms					
Suspected cardiac syncope	55 (15.7%)	26 (12.4%)	22 (20.2%)	7 (21.9%)	ns
Atrial Fibrillation	61 (17.4%)	40 (19.1%)	17 (15.6%)	4 (12.5%)	ns
Major adverse event	23 (6.6%)	16 (7.7%)	2 (1.8%)	5 (15.6%)	
VF/VT	13 (3.7%)	8 (3.8%)	1 (0.9%)	4 (12.5%)	**<0.05**
Cardiac arrest	9 (2.5%)	7 (3.4%)	2 (1.8%)	0 (0%)	ns
ICD shock	9 (2.5%)	6 (2.9%)	2 (1.8%)	1 (3.1%)	ns
ECG data	175 (50%)	98 (46.9%)	57 (52.3%)	20 (62.5%)	
PR interval (ms) [IQR]	160 [148 – 174]	160 [148 – 172]	158 [144 – 170]	181 [162 – 207]	**<0.01**
QRS segment (ms) [IQR]	104 [92 – 116]	103 [90 – 114]	100 [92 – 114]	110 [108 – 125]	**<0.01**
Electrophysiology study	102 (30%)	58 (27.8%)	33 (30.3%)	11 (34.4%)	ns
Induction VF/VT	13/102 (12.7%)	7/58 (12.1%)	5/33 (15.2%)	2/11 (18.2%)	ns
Implantable cardioverter defibrillator	114 (32.6%)	64 (30.6%)	36 (33%)	14 (43.8%)	ns
Appropriate shock	9/114 (7.9%)	6/64 (9.4%)	2/36 (5.6%)	1/14 (7.1%)	ns
Inappropriate shock	11/114 (9.6%)	5/64 (7.8%)	5/36 (13.9%)	1/14 (7.1%)	ns
Median Shanghai score *[IQR]*	3 [2 – 4]	2 [2 – 4]	3 [2 – 4]	4.5 [4 – 6.5]	**<0.0001**

	All Patients	Patients without variant	Patients carrying VUS	Patients harbouring P/LP variant	P-value
Variant in *SCN5A*	46 (13.1%)		16 (14.7%)	30 (93.8%)	**<0.0001**

% are compared to the total number of patients per group unless otherwise specified
VUS: Variant of unknown significance, P/LP: Pathogenic or likely pathogenic, BrS: Brugada syndrome, SCD: sudden cardiac death, VF/VT: ventricular fibrillation/tachycardia, IQR: interquartile range

Cardiac arrhythmia PED gene panel yield

In total 141 patients (40.3 %) carried a variant of uncertain significance (VUS, class 3), likely pathogenic (LP, class 4) or pathogenic (P, class 5) variant (Table 2, Table 4). One hundred and nine patients (31.1%) carried a VUS, 10 patients (2.9%) a LP variant and 22 patients (6.3%) a P variant. Twenty-three patients (6.6%) carried two or more VUS and in 8 patients (2.3%) with a P/LP variant one or more VUS were observed. All the variants we discovered in 35 different genes are depicted in Figure 1 and listed in Supplementary Table 3.

In our cohort most variants were detected in the *SCN5A* gene, with 46 patients (13.1%) carrying a *SCN5A* variant, 16 (4.6%) a VUS, and 30 (8.6%) a (L)P variant. 28 different variants in the *SCN5A* gene were observed of which 6 are classified as pathogenic, 8 are likely pathogenic and the other 14 are considered VUS. One pathogenic variant (c.4813+3_4813+6dupGGGT) detected in 15 patients of this cohort is a founder mutation we described in 2021 (37). The location of the variants in the *SCN5A* gene is depicted in Figure 1E. The different types of variants are spread across the different regions of the $Na_V1.5$ protein with at the c-terminal region only the presence of VUS. Other (L)P variants were observed in the *LMNA, SCN2B* and *KCNE1* genes (Table 3). One pathogenic variant is found in *LMNA* (p.(Arg331Gln)), encoding the Lamin-A/C protein in a patient with a positive ajmaline test, prolonged PR interval and a familial history of SCD (father and grandfather). The likely pathogenic *SCN2B* variant p.(Val99Met) is harboured by a BrS patient who presented the ECG type I pattern after ajmaline provocation, with a history of SCD in her family (father at age 40 yrs and paternal grandfather at age 32 yrs) and an affected brother (type 1 BrS ECG) harbouring the variant as well. One class 5 variant (p.(Arg98Trp)) was detected in the *KCNE1* gene encoding minK, a voltage-gated

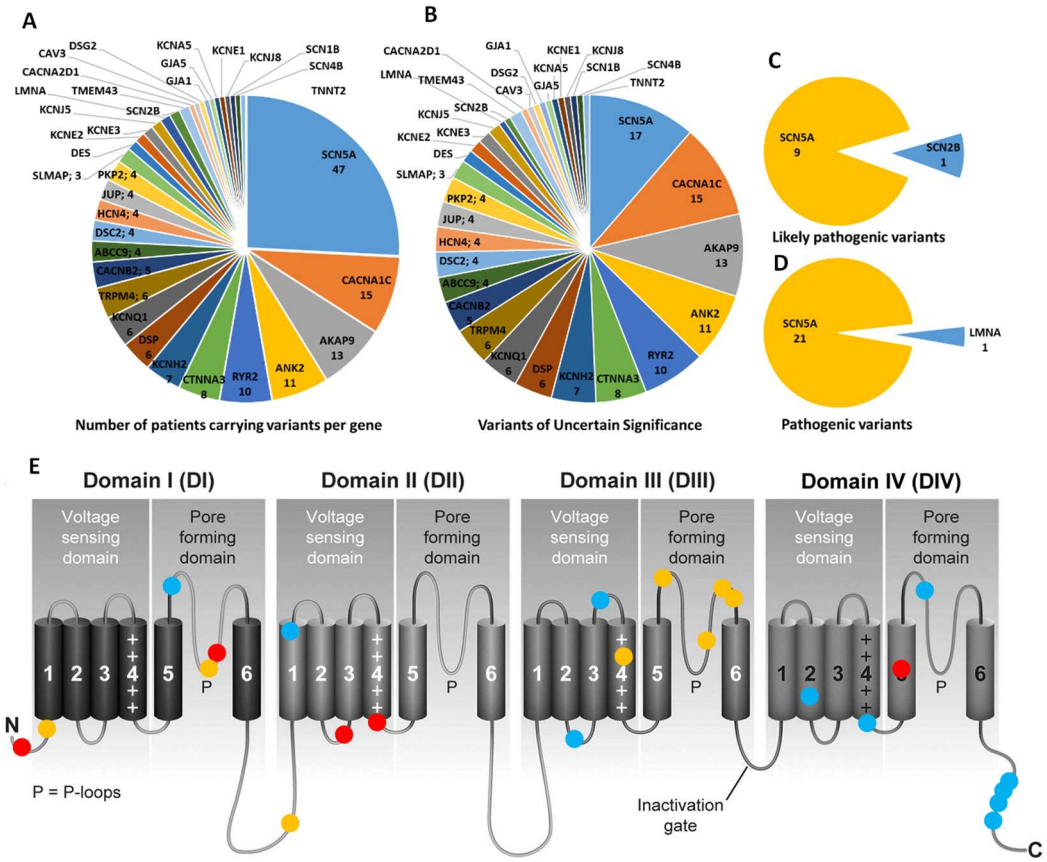

Figure 1: Overview of genes with variants. A) Pie chart of number of patients carrying variants per genes found. B-D) Pie chart of genes with Variants of uncertain significance, likely pathogenic and pathogenic variants, respectively. E) Overview of the variants found in the SCN5A gene (Intronic variants not included, adapted from (54)). Red dots: pathogenic variant, yellow dots: likely pathogenic variant, blue dots: VUS.

potassium channel β-subunit which primarily interacts with the Kv7.1 α-subunit. *KCNE1* is a known LQTS gene but has not yet been associated with BrS. The proband carrying this variant showed a type I ECG after provocation with ajmaline and no sign of long QT. Segregation analysis showed that both her daughter and brother with unknown clinical phenotype carried the *KCNE1* variant, while another brother with BrS (with ICD after resuscitation) doesn't carry it. This indicates that there might be another cause for the BrS phenotype in this family and therefore we classify this variant as VUS for BrS.

Table 3: Class 4 and 5 variants identified in the BrS cohort.

Gene	Variant	Variant	Variant Class	No.
LMNA	c.992G>A	p.(Arg331Gln)	5	1
SCN2B	c.295G>A	p.(Val99Met)	4	1
SCN5A	c.20delC	p.(Pro7Leufs*90)	5	1
	c.361C>T	p.(Arg121Trp)	4	1
	c.1099C>T	p.(Arg367Cys)	4	1
	c.1127G>A	p.(Arg376His)	5	1
	c.1855C>T	p.(Leu619Phe)	4	1
	c.2320delT	p.(Tyr774Thrfs*28)	5	2
	c.2466G>A	p.(Trp822*)	5	1
	c.3911C>T	p.(Thr1304Met)	4	1
	c.4132G>A	p.(Val1378Met)	4	1
	c.4258G>C	p.(Gly1420Arg)	4	1
	c.4296G>T	p.(Arg1432Ser)	4	2
	c.4297G>T	p.(Gly1433Trp)	4	1
	c.4813+3_4813+6dupGGGT		5	15
	c.4978A>G	p.(Ile1660Val)	5	1
KCNE1	c.292C>T	p.(Arg98Trp)	5*	1

*Pathogenic variant for Long QT syndrome, VUS (Class 3) for BrS

Genotype-phenotype correlations

To investigate genotype-phenotype correlations, we divided our cohort into three groups: 'No Variant', 'VUS' and 'Pathogenic or likely pathogenic variant (P/LP)' (Table 2). We observed that a higher proportion of the patients with a P/LP variant presented with a spontaneous type I ECG-pattern compared to the VUS and no variant group (41% vs 17% and 10%, p=0.000067) and have more positive family histories of BrS/SCD (66%) compared to the VUS and no variant groups (28% and 29% respectively, p=0.00029). Regarding clinical symptoms, only the occurrence of VF/VT was significantly more prevalent in the P/LP group (13% compared to 4% in the no variant group and 1% in the VUS group, p=0.023). Also in terms of ECG parameters, we found a significant prolongation of the PR interval from 181 ms in the P/LP group vs 160 ms in the no variant and 158 ms in the VUS group (p=0.0012). With a median value of 110 ms, the QRS segment was also significantly prolonged in the class 4/5 group compared to the no variant and class 3 group (103 ms and 100 ms respectively, p=0.0023)(Figure 2). Electrophysiological studies (EPS) were performed in 102 patients of which 13 (12.7%)

developed VF/VT. There was no significant difference in occurrence over the different genotype groups.

The subpopulation of patients with a P/LP variant had a median Shanghai score of 4.5, which is significantly higher compared to the two other groups ($p=2.9x10^{-10}$) and indicates a definite BrS diagnosis. Even if we leave the P/LP mutation status out of the Shanghai score, the median in this group (median = 4) is still significantly different from the patients without any variant or with a VUS (Shanghai score of 2 and 3 respectively) ($p=7.6x10^{-6}$, Figure 2).

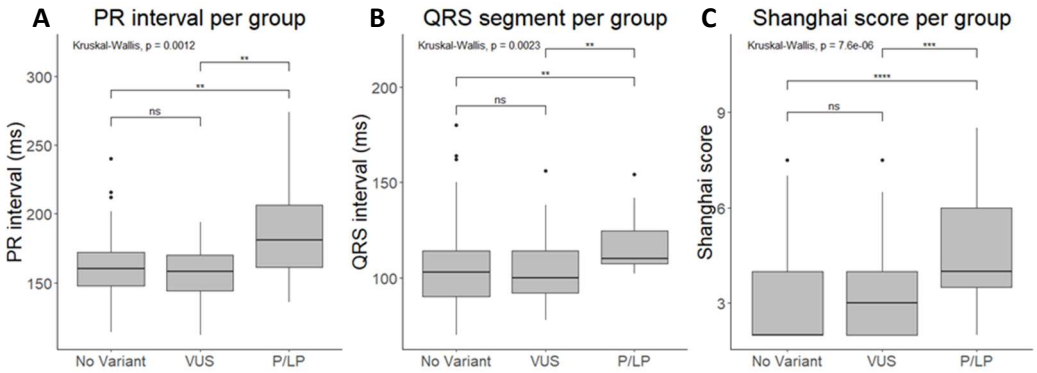

*Figure 2: ECG parameters and Shanghai score per variant group. A, B) Boxplot of the PR interval and QRS segment (median with Interquartile range, n per group: No variant = 98, VUS = 57, P/LP = 20). C) Boxplot of the Shanghai score without mutation status (median with Interquartile range, n per group is: No variant = 209, VUS = 109, P/LP = 32) . ns: not significant, *: p<0.05, **: p<0.01, ***: p<0.001, ****: p<0.0001*

Shanghai score

Another way to analyse our data is to divide the patients in groups based on their Shanghai score: possible BrS (2-3) and definite BrS (≥3.5) (Table 4). As clinical data is mostly included in this scoring system, it is only informative to look at the parameters that are not included such as gender, electrophysiology study, and ICD implantation. Here we only found a significant difference in ICDs implanted with 93 patients with definite BrS (58.1%) versus only 21 patients with a possible BrS diagnosis (11.1%) ($p=3.8x10^{-20}$). In patients with a definite BrS diagnosis (Shanghai ≥3.5) the diagnostic yield increases to 17.5% and when we look at the diagnostic yield in patients with familial history of SCD and/or BrS a percentage of 18.7% (21/112) is reached.

Table 4: Comparison based on Shanghai score

	All Patients	Possible BrS diagnosis (2-3)	Definite BrS diagnosis (≥3.5)	p-value
Total	350	190 (54.3%)	160 (45.7%)	
Female (%)	133 (38%)	83 (43.7%)	50 (31.3%)	**<0.05**
Variant	142 (40.6%)	63 (33.2%)	79 (49.4%)	**<0.01**
VUS	109 (31.1%)	58 (30.5%)	51 (31.9%)	ns
P/LP	32 (9.1%)	4 (2.1%)	28 (17.5%)	**<0.0001**
***SCN5A* variant**	46 (13.1%)	10 (5.3%)	36 (22.5%)	**<0.0001**
VUS	16 (4.6%)	7 (3.7%)	9 (5.6%)	ns
P/LP	30 (8.6%)	3 (1.6%)	27 (16.9%)	**<0.0001**
Electrophysiology study	102 (29.1%)	48 (25.3%)	54 (33.8%)	Ns
Induction VF/VT	13/102 (9.0%)	4/48 (8.3%)	10/54 (18.5%)	ns
Implantable cardioverter defibrillator	114 (32.6%)	21 (11.1%)	93 (58.1%)	**<0.0001**
Appropriate shock	9/114 (7.9%)	0/21 (0%)	9/93 (9.7%)	ns

% are compared to the total number of patients per group unless otherwise specified
VUS: Variant of unknown significance, P/LP: Pathogenic or likely pathogenic, BrS: Brugada syndrome, SCD: sudden cardiac death, VF/VT: ventricular fibrillation/tachycardia, CI: confidence interval, ICD: Implantable cardioverter defibrillator
Even if we leave out the mutation status from the Shanghai score (minus 0.5), the p-values remained exactly the same

Discussion

In this study we aimed to evaluate the yield of our NGS cardiac arrhythmia PED panel (n=51 genes) used in the genetic diagnosis of BrS patients requesting a test at the Centre of Medical Genetics Antwerp. Overall, in our cohort of 350 patients we detected a (likely) pathogenic variant in 9.1%, with 8.6% carrying a P/LP variant in *SCN5A* and in 109 patients (31.4 %) a VUS was found. This (P/LP) diagnostic yield is substantially lower compared to the yield of around 15-30% reported in literature (38-42). Although this 15-30% might be an over-estimation because these papers were published before the introduction of the ACMG criteria in 2015 (36) - providing a more restricted set of rules to classify variants as P/LP - and studied smaller and more severely affected cohorts (44-130 probands). Kapplinger et al. combined the genetic results of 2100 BrS patients (tested in 9 centres) and found a yield ranging from 11% to 28% over the centres with an overall yield of 21% in the *SCN5A* gene (43). In 2022, Zaklyazminskaya et al. investigated the diagnostic yield ((likely) pathogenic variants) in genes encoding the

Nav1.5 channel (*SCN5A*, *SCN1B*, *SCN2B*, *SCN3B*, and *SCN4B*) in their cohort of 75 patients and reached 13% (44). They found only one VUS in *SCN4B* (not included in the yield calculation), whereas all other variants were detected in *SCN5A.* In our cohort, only 8.8% (31/350) of the patients carried a (L)P variant in the five sodium channel genes mentioned above with 30 patients harbouring a (L)P variant in *SCN5A* and one in *SCN2B.* In 2021 Milman et al. looked at the genotype-phenotype correlation in 392 BrS patients (45). Twenty-three percent of the patients carried *SCN5A* variants, with only 11% being (likely) pathogenic variants and 12% VUS which is higher compared to our data (8.6% P/LP and 4.6% VUS). An explanation for this difference lies in the population studied by Milman et al. which is part of the SABRUS patient cohort, all presenting with a first arrhythmic event. Regarding the phenotype, they also found a higher percentage of familial history of SCD in patients carrying a P/LP variant but unlike our observation no significant difference in the occurrence of a spontaneous type I ECG. The prolongation in PR interval and QRS segment we found in our P/LP variant carriers compared to the VUS and No Variant group, was also observed in other recent studies (46, 47). When we look in our cohort only at the patients with a family history of BrS and/or SCD, the diagnostic yield increases to 18.8% (21/112) which is more in line with previously mentioned reports.

In 2016, the Shanghai scoring system was introduced in order to diagnose BrS patients (6). The scoring system takes several characteristics into account such as familial history, cardiac (arrhythmia) events, genetics and the occurrence of type I ECG pattern. More severe cardiac events like VF/VT and cardiac arrest are awarded more points. In our cohort, 160 patients (45.3%) fulfilled the criteria for a definite BrS diagnosis and taking only this selection into account the genetic yield of our panel increased to 17.5% (28/160), supporting the value of the Shanghai score. Zhang et al. found a slightly higher yield of 22.9% in a BrS cohort of 262 definite BrS patients (48). The Shanghai score was designed as a scoring system for the diagnosis of BrS, but nowadays it is tested as a predictive tool as well. In 2018, Kawada et al. validated the scoring system and used it as a tool for risk stratification. They found that patients with a higher Shanghai score (≥4) were having a progressively higher risk for VT/VF, while patients that were asymptomatic and had a score <3.5 did not show any symptoms during their follow up (49). Two more studies validated the Shanghai score as a predictive value and one found that the score is good at predicting both the highest and lowest at-risk patients but it performs moderate in the groups with an intermediate risk, while the second study indicated that only high-risk patients could be predicted (7, 8). In combination with EPS it might help identifying patients with a higher risk for adverse cardiac events. Based on these publications, in our cohort there are 190 patients (54.3%, Shanghai score ≤3) with a low risk of development of sudden cardiac arrest and VT/VF, 14 patients (4%) have a

Shanghai score above 7 and as such a high risk for the development of arrhythmic events, while for the other 146 patients, risk stratification is unclear.

In 32 BrS patients we found P/LP variants of which 30 patients harboured 14 different P/LP variants in the *SCN5A* gene (6 P, 8 LP). Our P/LP cohort as such almost exclusively consists of *SCN5A* variant carriers (with clinical characteristics described in Table 2). The other two patients harboured a class 5 variant in *LMNA* and a class 4 variant in the *SCN2B* gene.

The pathogenic variant (p.(Arg331Gln)) located in the *LMNA* gene was discovered in a proband with a provoked type I ECG and no clinical symptoms except for a prolonged PR interval. The variant is a known founder mutation discovered in 23 Dutch probands and 35 family members showing a mild and variable phenotype ranging from atrioventricular conduction disturbances, supraventricular arrhythmias to dilated cardiomyopathy but without any record of a BrS type I ECG (50). A role for *LMNA* in BrS was first described in 2020, when the p.(Arg216Cys) variant was found in a male BrS patient who experienced a cardiac arrest at the age of 31 and showed a spontaneous type I ECG pattern. The patient itself did not show laminopathy features but two family members carrying the same variant presented with mild signs of conduction disturbances (24). This indicates that the variant (p.(Arg331Gln)) we have found could play a role in the BrS phenotype of our patient (also without overt laminopathy features), but considering the complex genetic background of BrS this will likely not be the sole causal variant. The class 4 variant p.(Arg98Trp) in the *SCN2B* gene is carried by an asymptomatic female patient with a provoked type I ECG. *SCN2B*, a β-subunit of $Na_v1.5$, was first associated with BrS in 2013 by Riuro et al. where they found a variant (p.(Asp211Gly)) that reduced sodium current by reduced surface expression (30). We detected another class 5 variant: p.(Arg98Trp) in the *KCNE1* gene, a known LQTS gene (51) , in a BrS proband showing a type I ECG after provocation with ajmaline but without any clinical symptoms or QTc prolongation. In this family the daughter and brother carried this variant, but their clinical status is not yet known. Another brother with a Brugada type I ECG who was successfully resuscitated after SCD at age 44, does not carry the variant. This *KCNE1* (51) p.(Arg98Trp) variant was reported as pathogenic in several LQTS patients (clinical and functional reappraisal in (52)), but has not yet been associated with BrS. Most likely, this variant is not the causal variant in this family, but nevertheless it could play a modulating role in the development of BrS and therefore we classify this variant as a VUS for BrS.

Comparing three ‘genetic groups’ in our cohort: patients carrying ‘no variant’, ‘VUS’ or a ‘P/LP variant’ (Table 2), a significantly higher proportion of the P/LP patients presented with a spontaneous type I ECG-pattern, had a family history of BrS/SCD, experienced

VF/VT and had a significantly longer PR interval and QRS segment. This underscores the true pathogenic role of these variants. Differences between the VUS and no variant groups were not significant. Some of these VUS might turn out to be pathogenic variants if more data become available, but many of them might have no pathogenic effect on their own. It is now generally accepted that the genetic architecture of BrS is complex and more likely polygenic (53), so likely the detected VUS and (likely) pathogenic variants cause the BrS phenotype in our patients in combination with untyped and/or still unknown genetic variation. Currently, these VUS are documented and when possible functionally investigated. When in the future knowledge is gained on the (polygenic) genetic architecture, they can be re-analysed for pathogenicity on their own or in combination with other variants.

For 78 patients in our cohort whole exome sequencing (WES) was performed and nine extra arrhythmia related genes analysed (Supplementary Table 2). Three VUS in *SCN10A* and one VUS in *RRAD* were detected (see Supplementary Table 3). For one patient the VUS in *SCN10A* was the only variant found, but the other three patients also carried another VUS in one of the 51 screened PED panel genes. The nine extra genes have rather limited evidence to be involved in BrS, so screening them in all patients would mainly have increased the yield of VUS (with an estimated 5% (4/78)). Nevertheless, these VUS could play a role in BrS causation in combination with other genetic variants.

As debated by Hosseini et al. (4) *SCN5A* is currently considered the only causal gene for BrS. In our cohort as well, almost all of the P/LP variants were indeed found in the *SCN5A* gene (30/32). Therefore, some might say that screening *SCN5A* is the most informative screening for BrS patients. However, additional knowledge or evidence for other genes playing a role in the development of BrS can only be achieved after thorough investigation of the genetic background of patients.

Limitations of our study

One limitation of our approach is the retrospective character of the study, with missing data for some of the parameters we investigated and often no possibility to follow-up on these. We also collected data using patient's medical records gathered in different hospitals, so we are aware there will be some variability in the way of recording data. Although in all participating hospitals family members of BrS patients are contacted for clinical examination and - if applicable - segregation analysis, this is not always successful, reducing the possibility to reclassify some of the VUS.

Conclusion

In a cohort of 350 BrS patients, the overall diagnostic yield was 9.4%, which increases to 17.5% in BrS patients with a definite diagnosis according to the Shanghai score (28/160) and to 18.8% in patients with a family history of SCD or BrS (21/112). These results might serve as an indication for clinicians for genetic counselling and the decision to refer their BrS patients for genetic testing. Patients carrying a P/LP variant presented more often with a spontaneous type I ECG, familial history of BrS or SCD and showed prolonged PR interval and QRS segment compared to the other patients.

Author Contributions

Conceptualization: B.L., M.A. and E.Sim. Data Collection: E.Sim., E.Sie., M.B. and I.L. Data analysis: E.Sim. Manuscript writing: E.Sim., M.A. Manuscript editing & review: M.A., B.L., D.S.

Funding

Dr. Loeys holds a consolidator grant from the European Research Council ("Genomia" ERC-COG-2017-771945). D. Schepers is a postdoctoral fellow (12R5623N) of the FWO. E. Simons and E. Sieliwonczyk are research fellows supported by the FWO (1S25318N, 1192019N). This research is supported by GOA application 33933 and Methusalem-OEC grant "Genomed" 40709 from the University of Antwerp.

References

1. Priori SG, Wilde AA, Horie M, Cho Y, Behr ER, Berul C, et al. HRS/EHRA/APHRS expert consensus statement on the diagnosis and management of patients with inherited primary arrhythmia syndromes: document endorsed by HRS, EHRA, and APHRS in May 2013 and by ACCF, AHA, PACES, and AEPC in June 2013. Heart Rhythm. 2013;10(12):1932-63.
2. Antzelevitch C, Brugada P, Borggrefe M, Brugada J, Brugada R, Corrado D, et al. Brugada syndrome: report of the second consensus conference: endorsed by the Heart Rhythm Society and the European Heart Rhythm Association. Circulation. 2005;111(5):659-70.
3. Chen Q, Kirsch GE, Zhang D, Brugada R, Brugada J, Brugada P, et al. Genetic basis and molecular mechanism for idiopathic ventricular fibrillation. Nature. 1998;392(6673):293-6.
4. Hosseini SM, Kim R, Udupa S, Costain G, Jobling R, Liston E, et al. Reappraisal of Reported Genes for Sudden Arrhythmic Death: Evidence-Based Evaluation of Gene Validity for Brugada Syndrome. Circulation. 2018;138(12):1195-205.
5. Monasky MM, Micaglio E, Ciconte G, Pappone C. Brugada Syndrome: Oligogenic or Mendelian Disease? Int J Mol Sci. 2020;21(5).

6. Antzelevitch C, Yan GX, Ackerman MJ, Borggrefe M, Corrado D, Guo J, et al. J-Wave syndromes expert consensus conference report: Emerging concepts and gaps in knowledge. J Arrhythm. 2016;32(5):315-39.
7. Probst V, Goronflot T, Anys S, Tixier R, Briand J, Berthome P, et al. Robustness and relevance of predictive score in sudden cardiac death for patients with Brugada syndrome. Eur Heart J. 2021;42(17):1687-95.
8. Rodriguez-Manero M, Baluja A, Hernandez J, Munoz C, Calvo D, Fernandez-Armenta J, et al. Validation of multiparametric approaches for the prediction of sudden cardiac death in patients with Brugada syndrome and electrophysiological study. Rev Esp Cardiol (Engl Ed). 2022;75(7):559-67.
9. Proost D, Saenen J, Vandeweyer G, Rotthier A, Alaerts M, Van Craenenbroeck EM, et al. Targeted Next-Generation Sequencing of 51 Genes Involved in Primary Electrical Disease. J Mol Diagn. 2017;19(3):445-59.
10. Hu D, Barajas-Martinez H, Terzic A, Park S, Pfeiffer R, Burashnikov E, et al. ABCC9 is a novel Brugada and early repolarization syndrome susceptibility gene. Int J Cardiol. 2014;171(3):431-42.
11. Allegue C, Coll M, Mates J, Campuzano O, Iglesias A, Sobrino B, et al. Genetic Analysis of Arrhythmogenic Diseases in the Era of NGS: The Complexity of Clinical Decision-Making in Brugada Syndrome. PLoS One. 2015;10(7):e0133037.
12. Antzelevitch C, Pollevick GD, Cordeiro JM, Casis O, Sanguinetti MC, Aizawa Y, et al. Loss-of-function mutations in the cardiac calcium channel underlie a new clinical entity characterized by ST-segment elevation, short QT intervals, and sudden cardiac death. Circulation. 2007;115(4):442-9.
13. Burashnikov E, Pfeiffer R, Barajas-Martinez H, Delpon E, Hu D, Desai M, et al. Mutations in the cardiac L-type calcium channel associated with inherited J-wave syndromes and sudden cardiac death. Heart Rhythm. 2010;7(12):1872-82.
14. Hennessey JA, Marcou CA, Wang C, Wei EQ, Wang C, Tester DJ, et al. FGF12 is a candidate Brugada syndrome locus. Heart Rhythm. 2013;10(12):1886-94.
15. London B, Michalec M, Mehdi H, Zhu X, Kerchner L, Sanyal S, et al. Mutation in glycerol-3-phosphate dehydrogenase 1 like gene (GPD1-L) decreases cardiac Na+ current and causes inherited arrhythmias. Circulation. 2007;116(20):2260-8.
16. Ueda K, Hirano Y, Higashiuesato Y, Aizawa Y, Hayashi T, Inagaki N, et al. Role of HCN4 channel in preventing ventricular arrhythmia. J Hum Genet. 2009;54(2):115-21.
17. Bezzina CR, Barc J, Mizusawa Y, Remme CA, Gourraud JB, Simonet F, et al. Common variants at SCN5A-SCN10A and HEY2 are associated with Brugada syndrome, a rare disease with high risk of sudden cardiac death. Nat Genet. 2013;45(9):1044-9.
18. Perrin MJ, Adler A, Green S, Al-Zoughool F, Doroshenko P, Orr N, et al. Evaluation of genes encoding for the transient outward current (Ito) identifies the KCND2 gene as a cause of J-wave syndrome associated with sudden cardiac death. Circ Cardiovasc Genet. 2014;7(6):782-9.
19. Giudicessi JR, Ye D, Tester DJ, Crotti L, Mugione A, Nesterenko VV, et al. Transient outward current (I(to)) gain-of-function mutations in the KCND3-encoded Kv4.3 potassium channel and Brugada syndrome. Heart Rhythm. 2011;8(7):1024-32.

20. Delpon E, Cordeiro JM, Nunez L, Thomsen PE, Guerchicoff A, Pollevick GD, et al. Functional effects of KCNE3 mutation and its role in the development of Brugada syndrome. Circ Arrhythm Electrophysiol. 2008;1(3):209-18.
21. Ohno S, Zankov DP, Ding WG, Itoh H, Makiyama T, Doi T, et al. KCNE5 (KCNE1L) variants are novel modulators of Brugada syndrome and idiopathic ventricular fibrillation. Circ Arrhythm Electrophysiol. 2011;4(3):352-61.
22. Verkerk AO, Wilders R, Schulze-Bahr E, Beekman L, Bhuiyan ZA, Bertrand J, et al. Role of sequence variations in the human ether-a-go-go-related gene (HERG, KCNH2) in the Brugada syndrome. Cardiovasc Res. 2005;68(3):441-53.
23. Medeiros-Domingo A, Tan BH, Crotti L, Tester DJ, Eckhardt L, Cuoretti A, et al. Gain-of-function mutation S422L in the KCNJ8-encoded cardiac K(ATP) channel Kir6.1 as a pathogenic substrate for J-wave syndromes. Heart Rhythm. 2010;7(10):1466-71.
24. Armaroli A, Balla C, Trabanelli C, Selvatici R, Brieda A, Sette E, et al. Lamin A/C Missense Mutation R216C Pinpoints Overlapping Features Between Brugada Syndrome and Laminopathies. Circ Genom Precis Med. 2020;13(2):e002751.
25. Huang L, Tang S, Chen Y, Zhang L, Yin K, Wu Y, et al. Molecular pathological study on LRRC10 in sudden unexplained nocturnal death syndrome in the Chinese Han population. Int J Legal Med. 2017;131(3):621-8.
26. Pappone C, Monasky MM, Ciconte G. Epicardial ablation in genetic cardiomyopathies: a new frontier. Eur Heart J Suppl. 2019;21(Suppl B):B61-B6.
27. Cerrone M, Lin X, Zhang M, Agullo-Pascual E, Pfenniger A, Chkourko Gusky H, et al. Missense mutations in plakophilin-2 cause sodium current deficit and associate with a Brugada syndrome phenotype. Circulation. 2014;129(10):1092-103.
28. Kattygnarath D, Maugenre S, Neyroud N, Balse E, Ichai C, Denjoy I, et al. MOG1: a new susceptibility gene for Brugada syndrome. Circ Cardiovasc Genet. 2011;4(3):261-8.
29. Watanabe H, Koopmann TT, Le Scouarnec S, Yang T, Ingram CR, Schott JJ, et al. Sodium channel beta1 subunit mutations associated with Brugada syndrome and cardiac conduction disease in humans. J Clin Invest. 2008;118(6):2260-8.
30. Riuro H, Beltran-Alvarez P, Tarradas A, Selga E, Campuzano O, Verges M, et al. A missense mutation in the sodium channel beta2 subunit reveals SCN2B as a new candidate gene for Brugada syndrome. Hum Mutat. 2013;34(7):961-6.
31. Hu D, Barajas-Martinez H, Burashnikov E, Springer M, Wu Y, Varro A, et al. A mutation in the beta 3 subunit of the cardiac sodium channel associated with Brugada ECG phenotype. Circ Cardiovasc Genet. 2009;2(3):270-8.
32. Boczek NJ, Ye D, Johnson EK, Wang W, Crotti L, Tester DJ, et al. Characterization of SEMA3A-encoded semaphorin as a naturally occurring Kv4.3 protein inhibitor and its contribution to Brugada syndrome. Circ Res. 2014;115(4):460-9.
33. Ishikawa T, Sato A, Marcou CA, Tester DJ, Ackerman MJ, Crotti L, et al. A novel disease gene for Brugada syndrome: sarcolemmal membrane-associated protein gene mutations impair intracellular trafficking of hNav1.5. Circ Arrhythm Electrophysiol. 2012;5(6):1098-107.
34. Mango R, Luchetti A, Sangiuolo R, Ferradini V, Briglia N, Giardina E, et al. Next Generation Sequencing and Linkage Analysis for the Molecular Diagnosis of a Novel Overlapping Syndrome Characterized by Hypertrophic Cardiomyopathy and Typical Electrical Instability of Brugada Syndrome. Circ J. 2016;80(4):938-49.

35. Liu H, Chatel S, Simard C, Syam N, Salle L, Probst V, et al. Molecular genetics and functional anomalies in a series of 248 Brugada cases with 11 mutations in the TRPM4 channel. PLoS One. 2013;8(1):e54131.
36. Richards S, Aziz N, Bale S, Bick D, Das S, Gastier-Foster J, et al. Standards and guidelines for the interpretation of sequence variants: a joint consensus recommendation of the American College of Medical Genetics and Genomics and the Association for Molecular Pathology. Genet Med. 2015;17(5):405-24.
37. Sieliwonczyk E, Alaerts M, Robyns T, Schepers D, Claes C, Corveleyn A, et al. Clinical characterization of the first Belgian SCN5A founder mutation cohort. Europace. 2021;23(6):918-27.
38. Priori SG, Napolitano C, Gasparini M, Pappone C, Della Bella P, Brignole M, et al. Clinical and genetic heterogeneity of right bundle branch block and ST-segment elevation syndrome: A prospective evaluation of 52 families. Circulation. 2000;102(20):2509-15.
39. Priori SG, Napolitano C, Gasparini M, Pappone C, Della Bella P, Giordano U, et al. Natural history of Brugada syndrome: insights for risk stratification and management. Circulation. 2002;105(11):1342-7.
40. Crotti L, Marcou CA, Tester DJ, Castelletti S, Giudicessi JR, Torchio M, et al. Spectrum and prevalence of mutations involving BrS1- through BrS12-susceptibility genes in a cohort of unrelated patients referred for Brugada syndrome genetic testing: implications for genetic testing. J Am Coll Cardiol. 2012;60(15):1410-8.
41. Selga E, Campuzano O, Pinsach-Abuin ML, Perez-Serra A, Mademont-Soler I, Riuro H, et al. Comprehensive Genetic Characterization of a Spanish Brugada Syndrome Cohort. PLoS One. 2015;10(7):e0132888.
42. Schulze-Bahr E, Eckardt L, Breithardt G, Seidl K, Wichter T, Wolpert C, et al. Sodium channel gene (SCN5A) mutations in 44 index patients with Brugada syndrome: different incidences in familial and sporadic disease. Hum Mutat. 2003;21(6):651-2.
43. Kapplinger JD, Tester DJ, Alders M, Benito B, Berthet M, Brugada J, et al. An international compendium of mutations in the SCN5A-encoded cardiac sodium channel in patients referred for Brugada syndrome genetic testing. Heart Rhythm. 2010;7(1):33-46.
44. Zaklyazminskaya E, Shestak A, Podolyak D, Komoliatova V, Makarov L, Novitskaya A, et al. Diagnostic yield and variant reassessment in the genes encoding Nav1.5 channel in Russian patients with Brugada syndrome. Front Pharmacol. 2022;13:984299.
45. Milman A, Behr ER, Gray B, Johnson DC, Andorin A, Hochstadt A, et al. Genotype-Phenotype Correlation of SCN5A Genotype in Patients With Brugada Syndrome and Arrhythmic Events: Insights From the SABRUS in 392 Probands. Circ Genom Precis Med. 2021;14(5):e003222.
46. Ciconte G, Monasky MM, Santinelli V, Micaglio E, Vicedomini G, Anastasia L, et al. Brugada syndrome genetics is associated with phenotype severity. Eur Heart J. 2021;42(11):1082-90.
47. Wijeyeratne YD, Tanck MW, Mizusawa Y, Batchvarov V, Barc J, Crotti L, et al. SCN5A Mutation Type and a Genetic Risk Score Associate Variably With Brugada Syndrome Phenotype in SCN5A Families. Circ Genom Precis Med. 2020;13(6):e002911.
48. Zhang ZH, Barajas-Martinez H, Xia H, Li B, Capra JA, Clatot J, et al. Distinct Features of Probands With Early Repolarization and Brugada Syndromes Carrying SCN5A Pathogenic Variants. J Am Coll Cardiol. 2021;78(16):1603-17.

49. Kawada S, Morita H, Antzelevitch C, Morimoto Y, Nakagawa K, Watanabe A, et al. Shanghai Score System for Diagnosis of Brugada Syndrome: Validation of the Score System and System and Reclassification of the Patients. JACC Clin Electrophysiol. 2018;4(6):724-30.
50. Hoorntje ET, Bollen IA, Barge-Schaapveld DQ, van Tienen FH, Te Meerman GJ, Jansweijer JA, et al. Lamin A/C-Related Cardiac Disease: Late Onset With a Variable and Mild Phenotype in a Large Cohort of Patients With the Lamin A/C p.(Arg331Gln) Founder Mutation. Circ Cardiovasc Genet. 2017;10(4).
51. Splawski I, Tristani-Firouzi M, Lehmann MH, Sanguinetti MC, Keating MT. Mutations in the hminK gene cause long QT syndrome and suppress IKs function. Nat Genet. 1997;17(3):338-40.
52. Garmany R, Giudicessi JR, Ye D, Zhou W, Tester DJ, Ackerman MJ. Clinical and functional reappraisal of alleged type 5 long QT syndrome: Causative genetic variants in the KCNE1-encoded minK beta-subunit. Heart Rhythm. 2020;17(6):937-44.
53. Hoeksema WF, Amin AS, Bezzina CR, Wilde AAM, Postema PG. Novelties in Brugada Syndrome: Complex Genetics, Risk Stratification, and Catheter Ablation. Card Electrophysiol Clin. 2023;15(3):273-83.
54. de Lera Ruiz M, Kraus RL. Voltage-Gated Sodium Channels: Structure, Function, Pharmacology, and Clinical Indications. J Med Chem. 2015;58(18):7093-118.

Supplementary Table 1: Proposed Shanghai Score System for Diagnosis of Brugada Syndrome (6)

	Points
*I. ECG (12-Lead/Ambulatory)**	
A. Spontaneous type 1 Brugada ECG pattern at nominal or high leads	3.5
B. Fever-induced type 1 Brugada ECG pattern at nominal or high leads	3
C. Type 2 or 3 Brugada ECG pattern that converts with provocative drug challenge	2
II. Clinical History[+]	
A. Unexplained cardiac arrest or documented VF/ polymorphic VT	3
B. Nocturnal agonal respirations	2
C. Suspected arrhythmic syncope	2
D. Syncope of unclear mechanism/unclear etiology	1
E. Atrial flutter/fibrillation in patients <30 years without alternative etiology	0.5
III. Family History	
A. First- or second-degree relative with definite BrS	2
B. Suspicious SCD (fever, nocturnal, Brugada aggravating drugs) in a first- or second-degree relative	1
C. Unexplained SCD <45 years in first- or second- degree relative with negative autopsy	0.5
IV. Genetic Test Result	
A. Probable pathogenic mutation in BrS susceptibility gene	0.5

**Only award points once for highest score within this category. One item from this category must apply*.
[+]*Only award points once for highest score within this category*.
VF: ventricular fibrillation, VT: ventricular tachycardia, BrS: Brugada syndrome, SCD: sudden cardiac death

Supplementary Table 2: Overview of the genes included in the gene panel for inherited cardiac arrhythmias.

Gene	Disease	Transcript	Alternative transcript
ABCB4*	AF	ENST00000265723	
ABCC9	SQTS, AF	ENST00000261200	ENST00000261201: Exon 38
ACTN2*	AF, VF	ENST00000542672	ENST00000366578: Exon 8
AKAP9	LQTS	ENST00000356239	
ANK2	LQTS	ENST00000357077	ENST00000506722: Exon 2
CACNA1C	BrS, LQTS, SQTS, IVF associated	ENST00000347598	ENST00000399634: Exon 8 ENST00000344100: Exon 32 ENST00000399595: Exon 38 ENST00000399617: Exon 43
CACNA2D1	BrS, SQTS, IVF associated	ENST00000356860	
CACNB2	BrS, SQTS, IVF associated, ERS	ENST00000324631	ENST00000396576: Exon 1 ENST00000377329: Exon 1 ENST00000377315: Exon 1 ENST00000282343: Exon 1 ENST00000352115: Exon 7

Gene	Disease	Transcript	Alternative transcript
			ENST00000377319: Exon 6
CALM1	CPVT, LQTS	ENST00000356978	
CALM2*	LQTS	ENST00000272298	ENST00000456319: Exon 2
CALM3*	LQTS	ENST00000291295	
CASQ2	CPVT	ENST00000261448	
CAV3	LQTS	ENST00000343849	
CTNNA3	ARVC/D	ENST00000433211	
DES	ARVC/D	ENST00000373960	
DPP6	IVF	ENST00000377770	ENST00000332007: Exon 1 ENST00000404039: Exon 1 ENST00000406326: Exon 6
DSC2	ARVC/D	ENST00000280904	ENST00000251081: Exon 16
DSG2	ARVC/D	ENST00000261590	
DSP	ARVC/D	ENST00000379802	
GJA1	AF, SIDS	ENST00000282561	
GJA5	AF	ENST00000271348	
GNB5*	ID with cardiac arrhytmia	ENST00000261837	
GPD1L	BrS	ENST00000282541	
HCN4	BrS, SSS	ENST00000261917	
JUP	ARVC/D	ENST00000393931	
KCNA5	AF	ENST00000252321	
KCND3	BrS	ENST00000315987	
KCNE1	LQTS	ENST00000399286	
KCNE2	LQTS, AF	ENST00000290310	
KCNE3	BrS	ENST00000310128	
KCNE5	BrS	ENST00000372101	
KCNH2	LQTS, SQTS	ENST00000262186	ENST00000330883: Exon 1 ENST00000430723: Exon 9
KCNJ2	LQTS (andersen Tawil syndrome), SQTS, AF	ENST00000243457	
KCNJ5	LQTS	ENST00000529694	
KCNJ8	BrS, SQTS, IVF associated, ERS	ENST00000240662	

Gene	Disease	Transcript	Alternative transcript
KCNK17*	CCD	ENST00000373231	ENST00000453416: Exon 5
KCNQ1	LQTS, SQTS, AF	ENST00000155840	
LMNA	arrythmogenic CM	ENST00000368300	
NKX2.5	ASD & AV conduction defect, Ebstein ASD +/- AV block	ENST00000329198	ENST00000521848: Exon 2
NOS1AP	LQTS	ENST00000361897	ENST00000493151: Exon 1
NPPA	AF	ENST00000376480	
PKP2	ARVC/D	ENST00000070846	
PLN	arrythmogenic CM	ENST00000357525	
PPA2*	sudden cardaic failure	ENST00000341695	
PRKAG2	WPW	ENST00000287878	
RANGRF	BrS	ENST00000226105	
RRAD*	BrS	ENST00000299759	
RYR2	ARVC/D, CPVT	ENST00000366574	
SCN1B	BrS	ENST00000262631	ENST00000415950: Exon 3
SCN2B	BrS, AF	ENST00000278947	
SCN3B	BrS, IVF associated	ENST00000392770	
SCN4B	LQTS	ENST00000324727	
SCN5A	BrS, LQTS, IVF, AF	ENST00000333535	ENST00000413689: Exon 6
SCN10A*	BrS	ENST00000449082	
SLMAP	BrS	ENST00000295952	
SNTA1	LQTS	ENST00000217381	
TGFB3	ARVC/D	ENST00000238682	
TMEM43	ARVC/D	ENST00000306077	
TRDN	CPVT	ENST00000398178	
TRPM4	HB type 1B	ENST00000252826	

AF: atrial fibrillation; ARVC/D: arrhythmogenic right ventricular cardiomyopathy/dysplasia; ASD&AV: atrial septal defect and atrioventricular; BrS: Brugada syndrome; CCD: cardiac conduction disorder; CM: cardiomyopathy; CPVT: catecholaminergic polymorphic ventricular tachycardia; ERS: early repolarization syndrome; HB: heart block; ID: intellectual disability; IVF: idiopathic ventricular fibrillation; LQTS: long QT

syndrome; SIDS: sudden infant death syndrome; SQTS: short QT syndrome; SSS: sick sinus syndrome; VF: ventricular fibrillation: WPW: Wolff-Parkinson-White syndrome
* These genes are only included in the gene panel containing 60 genes and variants detected in these genes were not included in the general analysis because not all patients (only n= 78) were tested for them.

Supplementary Table 3: Variants detected in BrS patients

Gene	c.notation	p.(notation)	Variant Class	No.
ABCC9	c.1987C>T	p.(Arg663Cys)	3	1
	c.2158G>A	p.(Gly720Ser)	3	1
	c.2885A>T	p.(Asp962Val)	3	1
	c.4205C>G	p.(Ser1402Cys)	3	1
AKAP9	c.752T>G	p.(Leu251Arg)	3	1
	c.1259A>G	p.(Gln420Arg)	3	1
	c.3736A>G	p.(Arg1246Gly)	3	1
	c.4075C>G	p.(Gln1359Glu)	3	1
	c.4091A>T	p.(Glu1364Val)	3	1
	c.4225A>G	p.(Asn1409Asp)	3	1
	c.4927A>C	p.(Ile1643Leu)	3	1
	c.4960_4961delAG	p.(Arg1654Glyfs*23)	3	1
	c.5204T>G	p.(Leu1735Arg)	3	1
	c.5668A>T	p.(Thr1890Ser)	3	1
	c.7816T>G	p.(Leu2606Val)	3	1
	c.10013C>G	p.(Pro3338Arg)	3	1
	c.11085T>G	p.(His3695Gln)	3	1
ANK2	c.4373A>G	p.(Glu1458Gly)	3	1
	c.5615C>T	p.(Ser1872Leu)	3	1
	c.5737C>T	p.(Arg1913Cys)	3	1
	c.7283C>T	p.(Ser2428Leu)	3	1
	c.7894G>A	p.(Val2632Ile)	3	1
	c.7897G>T	p.(Asp2633Tyr)	3	1
	c.8645C>T	p.(Thr2882Ile)	3	1
	c.9223T>A	p.(Ser3075Thr)	3	1
	c.9526G>T	p.(Asp3176Tyr)	3	1
	c.10084T>A	p.(Ser3362Thr)	3	1
	c.11516G>C	p.(Ser3839Thr)	3	1
CACNA1C	c.76G>A	p.(Ala26Thr)	3	1
	c.107C>T	p.(Ala36Val)	3	1
	c.178C>T	p.(Arg60Trp)	3	1
	c.202G>A	p.(Ala68Thr)	3	1

Gene	c.notation	p.(notation)	Variant Class	No.
	c.974A>G	p.(Gln325Arg)	3	1
	c.1342G>A	p.(Asp448Asn)	3	1
	c.1721A>G	p.(Lys574Arg)	3	1
	c.2861G>A	p.(Gly954Asp)	3	1
	c.3391G>A	p.(Val1131Ile)	3	1
	c.3446C>T	p.(Thr1149Met)	3	1
	c.5086G>A	p.(Ala1696Thr)	3	1
	c.5452G>A	p.(Ala1818Thr)	3	1
	c.6235G>A	p.(Gly2079Ser)	3	1
	c.6416A>G	p.(Asn2139Ser)	3	1
	Duplication exon146-49		3	1
CACNA2D1	c.1663-5C>G		3	1
	c.104T>C	p.(Leu35Pro)	3	1
	c.1018G>A	p.(Ala340Thr)	3	1
CACNB2	c.1171C>T	p.(Pro391Ser)	3	1
	c.1207G>A	p.(Val403Ile)	3	1
	c.1735G>A	p.(Val579Met)	3	1
CAV3	c.376C>T	p.(Arg126Cys)	3	1
	c.137G>C	p.(Ser46Thr)	3	1
	c.392C>T	p.(Ala131Val)	3	1
	c.719C>T	p.(Thr240Ile)	3	1
CTNNA3	c.796C>T	p.(Pro266Ser)	3	1
	c.2201C>G	p.(Ala734Gly)	3	1
	c.2501G>T	p.(Arg834Leu)	3	2
	c.2638_2639insA	p.(Ile880Asnfs*9)	3	1
DES	c.216C>A	p.(Ser72Arg)	3	1
	c.1147C>T	p.(Arg383Cys)	3	1
	c.154G>A	p.(Val52Ile)	3	1
DSC2	c.713A>G	p.(Asp238Gly)	3	1
	c.1322C>T	p.(Ala441Val)	3	1
	c.2393G>T	p.(Arg798Leu)	3	1
DSG2	c.1072G>A	p.(Ala358Thr)	3	1
	c.347A>G	p.(Asp116Gly)	3	1
	c.2720G>A	p.(Arg907His)	3	1
DSP	c.4775A>G	p.(Lys1592Arg)	3	1
	c.5324G>T	p.(Arg1775Ile)	3	1
	c.7604A>G	p.(Asp2535Gly)	3	1
	c.8128G>T	p.(Ala2710Ser)	3	1

Gene	c.notation	p.(notation)	Variant Class	No.
GJA1	c.868A>G	p.(Thr290Ala)	3	1
GJA5	c.1025G>A	p.(Arg342Gln)	3	1
HCN4	c.458A>G	p.(Glu153Gly)	3	1
	c.3125C>T	p.(Pro1042Leu)	3	1
	c.3304C>T	p.(Arg1102Cys)	3	1
	c.3502_3505delTTTG	p.(Phe1168Glyfs*12)	3	1
JUP	c.56C>T	p.(Thr19Ile)	3	1
	c.427G>A	p.(Ala143Thr)	3	1
	c.460G>A	p.(Glu154Lys)	3	1
	c.634C>G	p.(Leu212Val)	3	1
KCNA5	c.1580C>T	p.(Thr527Met)	3	1
KCNE1	c.292C>T	p.(Arg98Trp)	5	1
KCNE2	c.260A>G	p.(Tyr87Cys)	3	1
	c.369_370delCT	p.(Ter124Ilefs*15)	3	1
KCNE3	c.2T>C	p.?	3	1
	c.139C>T	p.(Arg47Trp)	3	1
KCNH2	c.524C>A	p.(Ala175Asp)	3	1
	c.526C>T	p.(Arg176Trp)	3	1
	c.1120G>T	p.(Val374Phe)	3	1
	c.2717C>T	p.(Ser906Leu)	3	1
	c.2904G>A	p.(Pro968=)	3	1
	c.3107G>A	p.(Gly1036Asp)	3	1
	c.3251C>T	p.(Pro1084Leu)	3	1
KCNJ5	c.514G>A	p.(Ala172Thr)	3	1
	c.1150_1168delCCACTGCT	p.(Pro384Leufs*45)	3	1
KCNJ8	c.601G>A	p.(Val201Ile)	3	1
KCNQ1	c.136G>A	p.(Ala46Thr)	3	1
	c.160_168dupATCGCGCCC	p.(Ile54_Pro56dup)	3	1
	c.211G>T	p.(Ala71Ser)	3	1
	c.1195G>T	p.(Ala399Ser)	3	1
	c.1388G>C	p.(Ser463Thr)	3	1
	c.1876G>A	p.(Gly626Ser)	3	1
LMNA	c.161C>T	p.(Thr54Met)	3	1
	c.992G>A	p.(Arg331Gln1)	5	1
PKP2	c.374G>A	p.(Arg125Lys)	3	1
	c.1031T>C	p.(Leu344Pro)	3	1
	c.1568C>T	p.(Ala523Val)	3	1
	c.2330T>C	p.(Ile777Thr)	3	1

Gene	c.notation	p.(notation)	Variant Class	No.
RRAD*	c.695C>T	p.(Thr232Ile)	3	1
RYR2	c.1727A>G	p.(His576Arg)	3	1
	c.2050C>A	p.(Pro684Thr)	3	1
	c.4188G>A	p.(Asp1396Asn)	3	1
	c.5638G>A	p.(Glu1880Lys)	3	1
	c.6022+5G>A		3	1
	c.9667G>A	p.(Glu3223Lys)	3	1
	c.10541A>T	p.(His3514Leu)	3	1
	c.12859T>C	p.(Tyr4287His)	3	1
	c.13379A>G	p.(Gln4460Arg)	3	1
	c.13712C>T	p.(Thr4571Met)	3	1
SCN10A*	c.926T>C	p.(Leu309Pro)	3	1
	c.3674T>C	p.(Ile1225Thr)	3	1
	c.3739A>G	p.(Lys1247Glu)	3	2
SCN1B	c.637C>A	p.(Pro213Thr)	3	1
SCN2B	c.82C>T	p.(Arg28Trp)	3	1
	c.295G>A	p.(Val99Met)	4	1
SCN4B	c.362T>C	p.(Leu121Pro)	3	1
SCN5A	c.20delC	p.(Pro7Leufs*90)	5	1
	c.361C>T	p.(Arg121Trp)	4	1
	c.393-5C>A		3	1
	c.841G>A	p.(Val281Met)	3	1
	c.1099C>T	p.(Arg367Cys)	4	1
	c.1127G>A	p.(Arg376His)	5	1
	c.1855C>T	p.(Leu619Phe)	4	1
	c.2199C>A	p.(Phe733Leu)	3	1
	c.2320delT	p.(Tyr774Thrfs*28)	5	2
	c.2466G>A	p.(Trp822Ter)	5	1
	c.3667-14G>A		3	1
	c.3784G>A	p.(Gly1262Ser)	3	3
	c.3878T>C	p.(Phe1293Ser)	3	1
	c.3911C>T	p.(Thr1304Met)	4	1
	c.4132G>A	p.(Val1378Met)	4	1
	c.4258G>C	p.(Gly1420Arg)	4	1
	c.4296G>T	p.(Arg1432Ser)	4	2
	c.4297G>T	p.(Gly1433Trp)	4	1
	c.4299+6T>C		3	2
	c.4720G>A	p.(Glu1574Lys)	3	1

Gene	c.notation	p.(notation)	Variant Class	No.
	c.4813+3_4813+6dupGGGT		5	15
	c.4913G>A	p.(Arg1638Gln)	3	1
	c.4978A>G	p.(Ile1660Val)	5	1
	c.5065G>C	p.(Asp1689His)	3	1
	c.5513T>C	p.(Met1838Thr)	3	1
	c.5540G>A	p.(Arg1847His)	3	1
	c.5561T>C	p.(Leu1854Pro)	3	1
	c.5968G>C	p.(Val1990Leu)	3	1
SLMAP	c.1637G>T	p.(Arg546Leu)	3	1
	c.1889A>G	p.(Gln630Arg)	3	1
	c.2300A>G	p.(Gln767Arg)	3	1
TMEM43	c.333G>A	p=	3	1
	c.844A>G	p.(Thr282Ala)	3	1
TRPM4	c.95G>A	p.(Gly32Glu)	3	1
	c.1294G>A	p.(Ala432Thr)	3	2
	c.1744G>A	p.(Gly582Ser)	3	2
	c.2117G>A	p.(Arg706His)	3	1

* Variants is these genes were not included in the analysis because not all patients (only n= 78) were tested for them

Chapter 3:
Generation of two induced pluripotent stem cell (iPSC) lines (BBANTWi006-A, BBANTWi007-A) from Brugada syndrome patients carrying an *SCN5A* mutation

Eline Simons, Aleksandra Nijak, Bart Loeys, Maaike Alaerts

Cardiogenetics Research Group, Center of Medical Genetics, University of Antwerp and Antwerp University Hospital, Antwerp, Belgium.

Published in Stem Cell Research DOI: 10.1016/j.scr.2022.102719

Abstract

Brugada syndrome (BrS) is an inherited primary electrical disorder of the heart. 25% of BrS patients carry a mutation in the *SCN5A* gene, encoding the cardiac specific voltage-gated sodium channel Nav1.5. Here we report two iPSC lines (BBANTWi006-A, BBANTWi007-A) of a brother and a sister carrying an *SCN5A* mutation (c.4813 + 3_4813 + 6dupGGGT) causing BrS. iPSCs were generated from dermal fibroblasts and reprogrammed with the Cytotune®-iPS 2.0 Sendai Reprogramming Kit (Invitrogen). The generated iPSCs showed a normal karyotype, expressed pluripotency markers, were differentiated into cells of the three germ layers and carried the original genotype.

Resource Table

Unique stem cell lines identifier	BBANTWi006-A BBANTWi007-A
Alternative name(s) of stem cell lines	BrS9 C7 (BBANTWi006-A) BrS10 C3 (BBANTWi007-A)
Institution	University of Antwerp
Contact information of distributor	Maaike Alaerts – maaike.alaerts@uantwerpen.be
Type of cell lines	iPSC
Origin	Human
Additional origin info required	BBANTWi006-A: 50 yrs, Male, Caucasian BBANTWi007-A: 46 yrs, Female, Caucasian
Cell Source	Dermal Fibroblasts
Clonality	Clonal
Associated disease	Brugada Syndrome
Gene/locus	*SCN5A* c.4813+3_4813+6dupGGGT
Date archived/stock date	23/10/2018 (BBANTWi006-A) 26/12/2018 (BBANTWi007-A)
Cell line repository/bank	Hpscreg https://hpscreg.eu/cell-line/BBANTWi006-A https://hpscreg.eu/cell-line/BBANTWi007-A
Ethical approval	This study was approved by the Ethics committee of Antwerp University Hospital (18/05/059).

Resource utility

Because the invasiveness of a heart biopsy often prohibits the use of native cardiomyocytes to investigate the pathomechanism of cardiac arrhythmias including Brugada syndrome, iPSC-derived cardiomyocytes provide an alternative to study the underlying disease mechanisms, including the variable expressivity and reduced penetrance observed in family members carrying the same mutation.

Resource Details

Brugada syndrome (BrS) is an inherited primary electrical disorder of the heart with a prevalence of approximately 1/2000 and accounts for about 4 % of all sudden cardiac deaths (SCD) (1). Following symptoms can be observed: heart palpitations, syncopes and

SCD. Mutation carriers show a variability in symptoms, even within one family. Up to 25% of the BrS patients carry a mutation in the *SCN5A* gene, encoding Nav1.5, the alpha subunit of the cardiac specific voltage gated sodium channel, which plays an important role in the generation of the action potential upstroke. Here, we present two iPSC lines generated from fibroblasts from BrS patients carrying an *SCN5A* mutation (c.4813 + 3_4813 + 6dupGGGT). This mutation has been reported twice but was not yet studied in cardiomyocytes (2,3). The clinical spectrum of mutation carriers ranges from asymptomatic over abrupt syncopes to a significant number of SCD (4). To study the mechanism of this phenotypical variability, two iPSC lines from *SCN5A* founder mutation carrier siblings are generated (Table 1), one from a symptomatic patient (BBANTWi006-A) and one from an asymptomatic (BBANTWi007-A) mutation carrier and will be differentiated into iPSC-derived cardiomyocytes.

In this study, fibroblasts, collected through a skin biopsy from two BrS patients were transduced with Sendai virus to deliver Oct3/4, Sox2, Klf4 and hc-MYC to the cells. iPSC colonies appeared approximately 20 days after transduction and were manually picked five times before expanding them. iPSCs expressed pluripotency markers Oct3/4, Nanog, Tra-1-60, Tra-1-81 confirmed with immunocytochemistry staining (Fig. 1A and B) and NANOG, POU5F1, DNTM3B and SOX2 detected with RT-qPCR (Fig. 1C). Mutation analysis was performed with Sanger sequencing and confirmed the presence of the *SCN5A* mutation in the patient cell lines (Fig. 1D). Spontaneous differentiation to mesodermal, ectodermal and endodermal layers was proven with the formation of embryoid bodies followed by RT-qPCR (Fig. 1G). SNP array analysis indicated that the genotypes of donor cells (fibroblasts or blood cells) and iPSCs were consistent with each other (Fig. 1H). CNV analysis revealed no clinically relevant duplications or deletions (Fig. 1E and F, duplications in green, deletions in purple). A more detailed overview of the deletions and duplications, including genes located within the CNVs can be found in Supplementary Table 1 and 2. Absence of the Sendai vector was tested with a RT-PCR and Mycoplasma contamination was also excluded.

Table 1: Characterization and validation

Classification	Test	Result	Data
Morphology	Photography Bright field	Normal	Available with author
Phenotype	Qualitative analysis: *Immunocytochemistry*	Positive for: Oct3/4, Nanog, Tra1-60, Tra1-81	Figure 1 panel A and B
	Quantitative analysis: *RT-qPCR*	Expression of POU5F1, NANOG, SOX2 and DNMT3B	Figure 1 panel C
Genotype	HumanCytoSNP-12 array	Resolution 72kb, no major copy number variations	Figure 1 Panel E and F
Identity	HumanCytoSNP-12 array	>99,9% of identical SNPs	Figure 1 Panel H
	STR analysis	N/A	N/A
Mutation analysis (IF APPLICABLE)	Sequencing	Heterozygous *SCN5A* c.4813+3_4813+6dupGGGT	Figure 1 panel D
	Southern Blot OR WGS	N/A	N/A
Microbiology and virology	Mycoplasma	Mycoplasma testing by PCR: Negative	Available with author
Differentiation potential	e.g. Embryoid body formation *with RT-qPCR*	Expression of markers from each germ layer	Figure 1 panel G
List of recommended germ layer markers	Expression of these markers has to be demonstrated at mRNA (RT PCR) or protein (IF) levels, at least 2 markers need to be shown per germ layer	Ectoderm: PAX6 & MAP2 Mesoderm: NKX2.5 & ACTA2 (A-SMA) Endoderm: SOX17 & CXCR4 Reference genes: GAPDH & ACTB	Figure 1 panel G

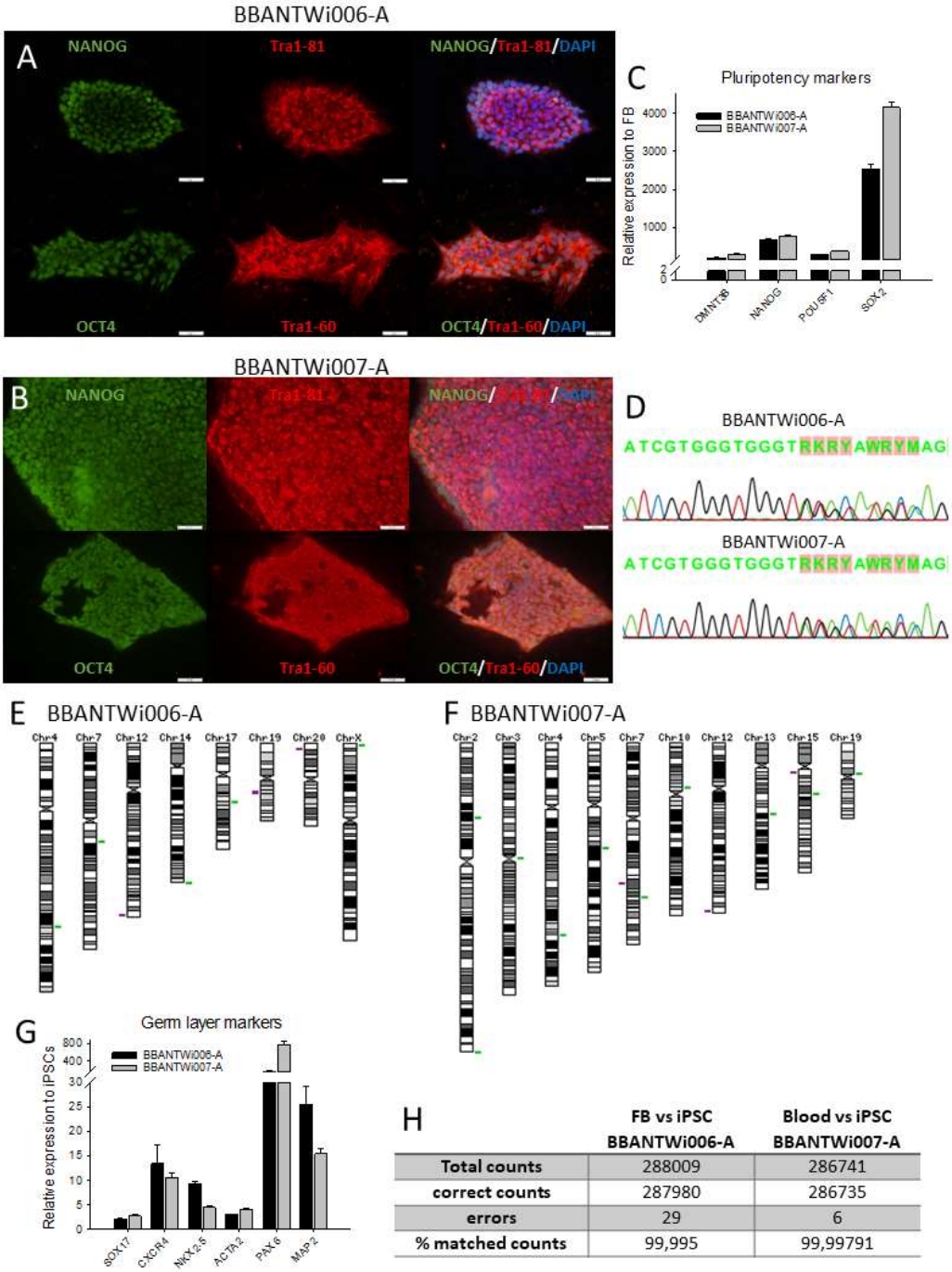

H

	FB vs iPSC BBANTWi006-A	Blood vs iPSC BBANTWi007-A
Total counts	288009	286741
correct counts	287980	286735
errors	29	6
% matched counts	99,995	99,99791

Figure 1: Characterization of 2 iPSC lines BBANTWi006-A, BBANTWi007-A

Materials and Methods

Fibroblast culture and iPSC culture

A punch biopsy from the inner side of the upper arm was taken from the patient. The biopsy was cut in smaller pieces and incubated with collagenase and trypsine for 1 h in 37 °C. Afterwards fibroblasts were cultured in RPMI medium (Life Technologies) supplemented with 15% FBS (Life Technologies), 1% sodium pyruvate (Life Technologies), 100 U/mL Pen/Strep (Life Technologies) and 0,1% primocin (InvivoGen Europe). Fibroblasts were plated in one well of a 6-well plate and after two days, the cells were transduced with the CytoTune™-iPS 2.0 Sendai Reprogramming Kit (Life Technologies) following the manufacturer's protocol. After seven days, cells were plated on Matrigel (Corning). One day later, the medium switched from RPMI to E8 flex medium (Life Technologies). Colonies were manually picked and seeded on Matrigel coated 24-well plates and incubated at 37 °C/5%CO2/5%O2. After five rounds of picking, cells were chemically passaged as small clumps with Versene (EDTA 0,02%) (Lonza) every 4–5 days and expanded in a 1:5 ratio. Cells were supplemented with 1x Revitacell (Life Technologies) for 24 h after a picking/passage.

Embryoid body formation

iPSCs (p16-BBANTWi006-A, p16-BBANTWi007-A) were collected using Versene (EDTA 0,02%) (Lonza) for 5 min at room temperature (RT) followed by washing of the cells. 500.000 cells/well were seeded onto a 24-well low-attachment plate with E6 medium (Life Technologies) and incubated at 37 °C/5%CO2/5%O2 and half a medium change was performed every other day. After 14 days EBs were collected for RNA extraction.

RNA extraction and RT-qPCR

Total RNA was extracted from cell cultures (passage 10–15) using the Quick-RNA Miniprep Kit (Zymo-Research). cDNA was synthesized using SuperScript™ III First-Strand Synthesis System (Life Technologies). RT-qPCR was performed using Roche LightCycler480/BioRad CFX meastro with TaqMan® probes ((Life Technologies) (Table 2) and TaqMan® gene expression mastermix (Life Technologies) following manufacturer's protocol.

Sendai virus detection

SeV genome and transgenes detection in iPSCs (p16-BBANTWi006-A, p16-BBANTWi007-A) was performed with RT-PCR (94 °C 5 min, 34x (94 °C 15 s, 60 °C 30 s, 72 °C 45 s), 72 °C 10 min, 10 °C 1 min) using primers (IDT) (Table 2) provided in the manufacturer's protocol.

Immunocytochemistry

iPSCs (p22-BBANTWi006-A, p11-BBANTWi007-A) were fixed with ice cold methanol for 20 min at −20 °C and permeabilized with 0.1% triton X-100 (Sigma-Aldrich) at RT for 15 min. 5% goat serum (Jackson ImmunoResearch) was used as blocking buffer for 30 min at RT. Subsequently, iPSCs were incubated overnight with primary antibodies at 4 °C. After three washing steps, cells were incubated with secondary antibodies for 1 h at RT. DAPI (Life Technologies) was used to stain the nuclei of the iPSCs.

Mycoplasma detection

Contamination of mycoplasma was analyzed with the LookOut Mycoplasma PCR Detection Kit (Sigma-Aldrich) following manufacturer's protocol.

SNP array (CNV analysis – cell identity)

DNA sample was collected from fibroblasts or blood cells and iPSC clones (p16-BBANTWi006-A, p10-BBANTWi007-A). DNA was extracted using an automatic DNA extraction system Maxwell® RSC with Maxwell® RSC Cultured Cells DNA Kit (Promega), following manufacturer's protocol and DNA samples were stored at + 4 °C after extraction. HumanCytoSNP-12 array (Illumina) was run according to the manufacturer's protocol for the automated Infinium HD Assay Ultra on an iScan instrument. Results were visualized using Genome Studio software (Illumina) and identity between the iPSC clones and original cell line confirmed. Results were further analysed with CNV-WebStore, an in-house developed online available CNV Analysis tool (http://cnv-webstore.ua.ac.be).

Mutation analysis

SCN5A exon 27 was amplified in genomic DNA obtained from iPSCs and fibroblasts, by PCR (Touch down PCR: 94 °C 5 min, 20x (94 °C 45 s, 65 °C (Δ-0.5) 45 s, 72 °C 45 s), 15x (94 °C 45 s, 56 °C 45 s, 72 °C 45 s), 72 °C 1 min) in a Veriti Fast Thermal Cycler (Applied Biosystems). The mutation was verified with Sanger sequencing. Primers are listed in Table 2.

Table 2: Reagents details

Antibodies used for immunocytochemistry/flow-cytometry

	Antibody	Dilution	Company Cat #	RRID
Pluripotency Markers	Mouse anti-TRA-1-60	1:200	Cell Signaling Technology Cat# 4746	AB_2119059
	Mouse anti-TRA-1-81	1:200	Cell Signaling Technology Cat# 4745	AB_2119060

Antibodies used for immunocytochemistry/flow-cytometry				
	Antibody	**Dilution**	**Company Cat #**	**RRID**
	Rabbit anti-NANOG	1:500	Thermo Fisher Scientific Cat# PA1-097	AB_2539867
	Rabbit anti-Oct3/4	1:100	Santa Cruz Biotechnology Cat# sc-9081	AB_2167703
Secondary antibodies	Goat anti-Mouse IgM (AF555)	1:500	Thermo Fisher Scientific Cat# A-21426	AB_2535847
	Goat anti-Rabbit IgG (AF 488)	1:500	Thermo Fisher Scientific Cat# A-11034	AB_2576217

Primers			
	Target	**Size of band**	**Forward/Reverse primer (5'-3')**
Sendai virus Plasmids (PCR)	Sev	181bp	GGATCACTAGGTGATATCGAGC ACCAGACAAGAGTTTAAGAGATATGTATC
	KOS	528bp	ATGCACCGCTACGACGTGAGCGC ACCTTGACAATCCTGATGTGG
	Klf4	410bp	TTCCTGCATGCCAGAGGAGCCC AATGTATCGAAGGTGCTCAA
	c-MYC	532bp	TAACTGACTAGCAGGCTTGTCG TCCACATACAGTCCTGGATGATGATG
House-Keeping Genes (RT-qPCR)	GAPDH	93bp	Hs02758991_g1
	ACTB	63bp	Hs01060665_g1
Pluripotency Markers (RT-qPCR)	POU5F1	77bp	Hs04260367_gH
	NANOG	99bp	Hs04260366_g1
	SOX2	91bp	Hs01053049_s1
	DNMT3B	55bp	Hs00171876_m1
Differentiation markers (RT-qPCR)	SOX17	149bp	Hs00751752_s1
	CXCR4	153bp	Hs00607978_s1
	PAX6	76bp	Hs00240871_m1
	MAP2	98bp	Hs00258900_m1
	NKX2.5	64bp	Hs00231763_m1
	ACTA2	105bp	Hs00426835_g1
Genotyping	SCN5A	525bp	GGCTTTGGGCTCACTAGAGG GGGGTGAGAAATGCACTGAA

Declaration of Competing Interest

The authors declare that they have no known competing financial interests or personal relationships that could have appeared to influence the work reported in this paper

References

1. Antzelevitch, C., P. Brugada, M. Borggrefe, J. Brugada, R. Brugada, D. Corrado, I. Gussak, H. LeMarec, K. Nademanee, A. R. Perez Riera, W. Shimizu, E. Schulze-Bahr, H. Tan, and A. Wilde. 2005. 'Brugada syndrome: report of the second consensus conference: endorsed by the Heart Rhythm Society and the European Heart Rhythm Association', Circulation, 111: 659-70.
2. Hong, K., A. Guerchicoff, G. D. Pollevick, A. Oliva, R. Dumaine, M. de Zutter, E. Burashnikov, Y. S. Wu, J. Brugada, P. Brugada, and R. Brugada. 2005. 'Cryptic 5' splice site activation in SCN5A associated with Brugada syndrome', J Mol Cell Cardiol, 38: 555-60.
3. Rossenbacker, T., E. Schollen, C. Kuiperi, T. J. de Ravel, K. Devriendt, G. Matthijs, D. Collen, H. Heidbuchel, and P. Carmeliet. 2005. 'Unconventional intronic splice site mutation in SCN5A associates with cardiac sodium channelopathy', J Med Genet, 42: e29.
4. Sieliwonczyk, E., M. Alaerts, T. Robyns, D. Schepers, C. Claes, A. Corveleyn, R. Willems, E. M. Van Craenenbroeck, E. Simons, A. Nijak, B. Vandendriessche, G. Mortier, C. Vrints, P. Koopman, H. Heidbuchel, L. Van Laer, J. Saenen, and B. Loeys. 2021. 'Clinical characterization of the first Belgian SCN5A founder mutation cohort', Europace, 23: 918-27.

Appendix A. Supplementary data

Supplementary Table 1: Overview of the deletions and duplications in BBANTWi006-A

BBANTWi006-A				
Chromosome	**Location**	**Copy Number**	**Size**	**Genes in Region**
4	140,466,604-140,563,222	Duplication	96617	SETD7
7	75,348,505-75,374,880	Duplication	26374	HIP1
12	131,722,521-131,842,011	Deletion	119489	LINC02370
14	106,752,607-107,188,814	Duplication	436206	LINC00221
17	44,204,373-44,289,232	Duplication	84858	KANSL1, KANSL1-AS1
19	36,904,778-38,693,305	Deletion	1788526	HKR1, WDR87, ZNF529, ZNF571-AS1, ZNF793-AS1, LOC644189, SNORD152, ZFP82
20	3,843,668-3,897,014	Deletion	53345	MAVS
X	184,508-1,473,247	Duplication	1288738	CRLF2
X	1,520,995-2,704,609	Duplication	1183613	AKAP17A,P2RY8

Supplementary Table 2: Overview of the deletions and duplications in BBANTWi007-A

BBANTWi007-A				
Chromosome	**Location**	**Copy Number**	**Size**	**Genes in Region**
2	58,412,472-58,481,863	Duplication	69390	FANCL
2	242,517,966-ter	Duplication	681406	LINC01237
3	90,296,480-93,632,198	Duplication	3335717	PROS1
4	151,190,804-151,346,422	Duplication	155617	LRBA
5	82,484,885-82,737,843	Duplication	252957	XRCC4
7	110,468,988-110,580,701	Deletion	111712	IMMP2L
7	120,666,122-120,819,121	Duplication	152998	CPED1
10	35,148,739-35,456,389	Duplication	307649	CREM
12	131,722,521-131,830,332	Deletion	107810	LINC02415
13	55,236,342-55,428,049	Duplication	191706	
15	21,907,922-22,576,118	Deletion	668195	IGHV1OR15-1, REREP3, CXADRP2, LINC02203, LOC646214, MIR3118-2, MIR3118-3, MIR3118-4, MIR5701-1, MIR5701-2, MIR5701-3, NF1P2, POTEB, POTEB2, POTEB3
15	39,193,242-39,319,573	Duplication	126330	
19	23,794,032-23,837,145	Duplication	43112	ZNF675

Chapter 4:
Characterization of a Belgian *SCN5A* founder mutation in induced pluripotent stem cell derived cardiomyocyte models

Eline Simons[a], Aleksandra Nijak[a], Ewa Sieliwonczyk[a], Bert Vandendriessche[a], Dogan Akdeniz[a], Hanne Boen[a], Evy Majeur[b], Dieter Van de Sande[b], Erik Fransen[c], Peter Ponsaerts[d], Dirk Snyders[b], Alain Labro[b], Dorien Schepers[a], Bart Loeys[a], Maaike Alaerts[a]

[a] Cardiogenetics Research Group, Center of Medical Genetics, University of Antwerp and Antwerp University Hospital, Antwerp, Belgium

[b] Experimental Neurobiology Unit, Department of Biomedical Sciences, University of Antwerp, Antwerp, Belgium

[c] Center of Medical Genetics, University of Antwerp, Antwerp, Belgium.

[d] Laboratory of Experimental Hematology (LEH), Vaccine and Infectious Disease Institute (VAXINFECTIO), University of Antwerp, Antwerp, Belgium.

Abstract

Brugada syndrome (BrS) is a rare inherited cardiac arrhythmia disorder with symptoms varying from asymptomatic to life-threatening ventricular fibrillation. *SCN5A* is a key gene linked to BrS, encoding the cardiac Nav1.5 sodium channel. Prior research primarily relied on heterologous expression systems, but induced pluripotent stem cells (iPSCs) now offer a more comprehensive model of BrS by including cardiomyocyte (CM)-specific proteins and patient genetic background. Here, we focus on a specific *SCN5A* founder mutation (c.4813+3_4813+6dupGGGT) identified in over 25 Belgian families, leading to varying clinical manifestations and penetrance. Functional analysis of this mutation revealed the presence of three distinct mutant transcripts in heterologous expression systems.

In this study, iPSC-CMs of five BrS patients with different disease severity, two unrelated healthy control individuals and one isogenic control were created using a chemically defined monolayer-based differentiation protocol. At least two separate differentiations were performed of two different iPSC-clones per individual. Generated iPSC-CMs were characterized for expression of cardiomyocyte markers on RNA and protein levels with RT-qPCR and immunocytochemistry. Several techniques such as RT-qPCR, Western blot and patch clamp were deployed to investigate the effect of the *SCN5A* mutation on different levels.

The created iPSC-CMs expressed both CM specific structural markers and ion channel genes required for action potential (AP) generation. Expression studies revealed the presence of two mutant transcripts in BrS patient iPSC-CMs besides the wild type (WT) transcript but no significant difference in expression of the latter was observed between patients and controls. Sodium current density or AP characteristics did not show statistically significant differences between patient and control iPSC-CMs in general due to the high variability in the data. Sodium current density was also not correlated with clinical disease severity, while decreased AP amplitude and upstroke velocity and increased APD90c was observed with increasing clinical severity. Comparing iPSC-CMs of a severely affected patient and its isogenic control, the sodium current density and APD90c were significantly decreased.

Overall, we were able to model a Belgian *SCN5A* founder mutation and highlighted the added value of the use of iPSC-CMs as disease specific cell type. Due to the high variability in our results, arising from both intra- and interclonal differences, detection of statistically significant differences between patients and controls and between symptomatic and asymptomatic carriers was hampered, but we show that the use of

isogenic controls is a promising strategy to study the effect of the mutation under investigation.

Introduction

Brugada syndrome (BrS) is a rare inherited primary cardiac arrhythmia disorder with a prevalence of approximately 1/2000. It is diagnosed with a typical ST-segment elevation in more than one right precordial lead (V1-V3) on an electrocardiogram (ECG) either occurring spontaneously or after administration of a sodium channel blocker like ajmaline or flecainide (1). BrS patients show symptoms ranging from asymptomatic over heart palpitations, syncopes and ventricular fibrillations which could lead eventually to sudden cardiac death (SCD), indicating reduced penetrance and variable expression of the disorder.

SCN5A, encoding the cardiac specific voltage gated sodium channel $Na_v1.5$ is the only gene classified as a 'definitive evidence' gene for BrS (2). Loss-of-function variants in *SCN5A* are found in approximately 20-25% of the BrS patients. Another 5% of BrS cases is explained by pathogenic variants in other genes encoding cardiac ion channels and/or accessory proteins. Nav1.5 is responsible for the inward sodium current which underlies the fast depolarization phase of the action potential (AP) generated in cardiomyocytes (CMs). Variants in *SCN5A* have extensively been studied in heterologous expression systems such as HEK293 or CHO cells (3-6). Although these models have proven to be effective, they have some drawbacks as only the ion channel(s) under study are expressed, missing all other CM-specific AP related proteins. This disadvantage has been overcome by the more recent discovery of induced pluripotent stem cells (iPSCs) and further differentiation into iPSC-derived cardiomyocytes (iPSC-CMs) (7, 8). In addition, these models have the advantage of presenting the full genetic background of the donor. Several BrS iPSC-CM models of *SCN5A* pathogenic variants have been investigated (reviewed in (9)). These all presented with a reduction in sodium current density and some models also showed an effect on sodium channel kinetics, which was not always visible in heterologous expression systems. This underlines the added value of iPSC-CM as they express channel auxiliary subunits influencing the main channel. In most models AP recordings revealed a reduction in upstroke velocity and in some a reduction in amplitude, reflecting sodium current deficits (9).

This paper focuses on an *SCN5A* founder mutation (c.4813+3_4813+6dupGGGT in intron 27) identified in over 25 Belgian families with mutation carriers presenting large phenotypical heterogeneity described in Sieliwonczyk et al (10). The mutation was previously functionally modelled and reported to result in a loss-of-function of the $Na_v1.5$ channel (11, 12). Hong et al. studied a patient's lymphoblastoid cell line and found two transcript bands on PCR with sequencing revealing one wild type (WT) transcript and one transcript with a deletion of 96 base pairs (bp) in exon 27 caused by activation

of a cryptic splice site. This results in a deletion of 32 amino acids in the fourth domain of $Na_v1.5$ on protein level. Patch clamping of TSA cells expressing this mutant $Na_v1.5$ revealed complete absence of sodium current (11). Rossenbacker et al. performed an exon trapping experiment in COS-7 cells and found three different mutant transcripts, one with the deletion of 96 bp, another one with the retention of intronic GTGG and a third one where no splicing occurred. The latter results in an addition of 95 amino acids not native to the normal sequence before a stop codon is recognised. The GTGG retention leads to a frameshift incorporating 183 aberrant amino acids before termination (12). Since the mutation occurs after the last exon-exon junction, no NMD will occur (13) and the mutant transcripts can be translated.

Here we present the functional characterization of iPSC-CMs derived from three symptomatic (with syncopes/SCD) and two asymptomatic patients (BrS type-1 ECG pattern) carrying the *SCN5A* c.4813+3_4813+6dupGGGT mutation, one isogenic control (CRISPR correction of mutation in iPSC of symptomatic patient) and two unrelated healthy control individuals. Two iPSC clones of each individual were selected and several differentiations per clone were performed followed by investigation of electrophysiological characteristics (I_{Na} and AP) and *SCN5A* RNA/$Na_v1.5$ protein expression.

Material and methods

iPSC generation and culture

In Chapter 3 of this thesis, we describe the inhouse generation and validation of iPSCs starting from fibroblasts (14). In short, fibroblasts of two healthy control individuals (one male and one female) and five BrS patients were obtained from a skin biopsy from the inner side of the upper arm and were cultured in RPMI medium (Life Technologies) supplemented with 15% FBS (Life Technologies), 1% sodium pyruvate (Life Technologies), 100 U/mL Pen/Strep (Life Technologies) and 0,1% primocin (InvivoGen Europe) in a humidified incubator at 37°C/5% CO_2 . Fibroblasts were plated in a 6-well plate and two days later the cells were transduced with the CytoTune™-iPS 2.0 Sendai Reprogramming Kit (Life Technologies) following the manufacturer's protocol. Colonies were manually picked and seeded on Matrigel (Corning) coated plates at 37°C/5%CO_2/5%O_2. After 5 picking rounds, wells were passaged using 0,5mM EDTA/PBS (Life Technologies) and expanded. iPSCs were cultured in E8 flex (Life Technologies) or Stemflex medium (Life Technologies) and grown on Matrigel (corning) or Geltrex (Life Technologies). iPSCs were characterized as described in (14). In short, iPSCs were tested for pluripotency, *in vitro* differentiation potential, morphology, identity and the

presence of the mutation in case of the patients. iPSCs from patient BrS12 were corrected using CRISPR/Cas9 (outsourced to Synthego) to create an isogenic control.

Differentiation to iPSC derived cardiomyocytes

iPSCs were plated in 6-well plates and at 80-90% confluency (3/4/5 days after plating), cells were incubated with RPMI1640 medium (Life Technologies) supplemented with 6µM CHIR99021 (Axon Medchem), 1x B27 supplement without insulin (Life Technologies) and 1x Revitacell (Life Technologies) at 37°C/5%CO_2/5%O_2 for 2 days. After 48h medium was changed to RPMI 1640 supplemented with 2µM Wnt-59 (Selleck Chemicals GmbH) and 1x B27 supplement without insulin. At day 4, medium was replaced with RPMI1640 medium supplemented with 1x B27 supplement without insulin and Pen/Strep (Life Technologies). Medium was changed every other day. From day 8 on, medium was supplemented with 20 ng/mL thyroid hormone (T3) (T3 medium, Sigma Aldrich). From day 14 to day 20, cells were deprived from glucose to enrich the culture for iPSC-CM using lactate medium (RPMI1640 minus glucose (Life Technologies) supplemented with 500 µg/mL albumine (Sigma Aldrich), 213 µg/mL ascorbic acid (Sigma Aldrich), 5 mM lactate (Sigma Aldrich), 20 ng/mL T3). Cells were cultured in T3 medium till day 30-40 to perform functional characterization. Cells were dissociated using 1x TrypLE Select for 5-15 min in 37°C. iPSC-CM were washed twice using T3 medium to collect the cells.

Mutation analysis

Genomic DNA was obtained from iPSCs and fibroblasts and extracted using an automatic DNA extraction system Maxwell® RSC with Maxwell® RSC Cultured Cells DNA Kit (Promega), following supplier's protocol. DNA was used for PCR amplification followed by purification and sanger sequencing. Primers are listed in Supplementary Table 1.

Immunocytochemistry

iPSC-CM were fixed with 4% paraformaldehyde on day 33-38 for 15 min at room temperature (RT). Cells were permeabilized with 0,1% triton x-100 (Sigma Aldrich) for 15 min, blocked with 5% goat serum (Jackson ImmunoResearch) for 1h at RT and incubated overnight at 4°C with primary antibodies diluted in DAKO diluent (Agilent). The next day, cells were washed three times with PBS (Life Technologies) and incubated with the secondary antibodies (Supplementary Table 2). After two more washes with PBS, 1 µg/mL DAPI (Life Technologies) was added and incubated for 5 min. After two more washes, cover slips were mounted with Fluoromount-G (Life Technologies). Pictures were taken with an Olympus BX51 or with a Leica Dmi8 fluorescence microscope at 40x and 100x.

Electrophysiology

The electrophysiological experiments were executed between differentiation day 30-40. Cells were superfused at 1 mL/min with extracellular solution (ECS): 150 mM NaCl, 5.4 mM KCl, 1.8 mM $CaCl_2$, 1 mM $MgCl_2$, 15 mM glucose, 15 mM HEPES, 1 mM Na-pyruvate and adjusted at pH 7.4 with NaOH. Patch pipettes were pulled from 1.2 mm borosilicate glass capillaries (World Precision Instruments, Inc.) with a resistance of approximately 2MΩ using a P-2000 puller (Sutter Instrument Co.) and filled with an intracellular solution which consists of 150 mM KCl, 10 mM HEPES, 5 mM $MgCl_2$, 5 mM NaCl, 2 mM $CaCl_2$, 5 mM EGTA adjusted to pH 7.2 with KOH. Data was collected using the Axopatch 200B amplifier and a pClamp 10.7/Digidata 1440A acquisition system (Axon CNS Molecular Devices). Sodium current was recorded after passing a 5- or 10-kHz low pass filter, sampled at 10 or 20 kHz and digitized at room temperature (RT) in voltage clamp mode on singularized iPSC-CM using a whole cell (ruptured) patch. The cell is approached with a pipette and after contact and sealing of the cells, small pressure pulses rupture the membrane that attach to the pipette. The activation protocol consists of 21 sweeps with following voltage steps: holding potential of -90 mV, a prepulse of -130 mV for 80 ms, a depolarizing step of 40 ms ranging from 80 mV to -130 mV with 10 mV steps and a final step bringing the cell back to 0 mV. The inactivation protocol consists of 22 sweeps with following steps: a 100 ms prepulse of -130 mV, a 500 ms step starting at -135 mv and increasing per swipe with 5 mV to -30 mV and a final 50 ms step to 0 mV. The last protocol, inactivation of recovery, has 10 sweeps with following setup: a starting 40 ms pulse of -130 mV, a next 500 ms step depolarizes the cell to -10 mV, followed by a step to -130 mV for 0.5 to 500 ms increasing per sweep and a final 10 ms of -10 mV. Action potentials (AP) were recorded at RT on groups of cells or monolayers in current clamp mode using a perforated patch. Hereto, 0.84 mM Amphotericin B (Sigma Aldrich) was added to the intracellular solution.

Sodium current data was analysed using the pCLAMP10 software (Axon CNS Molecular devices). AP waveforms were extracted from pCLAMP and analysed using an in-house developed Matlab script. Following parameters were analysed: resting membrane potential (RMP), AP duration at 50% and 90% of repolarization (APD50, APD90), beats per minute (BPM), beat interval, AP amplitude and upstroke velocity. APD50 and APD90 were corrected for heart rate according the Fridericia formula: $APDc = APD/\sqrt[3]{beat\ interval/1000}$.

RNA collection and RT-qPCR

Total RNA was extracted from approximately 1.5x10^6 iPSC-CMs at day 35 using the Quick-RNA Miniprep Kit (Zymo-Research). From 1 ug RNA, cDNA was synthesized using

SuperScript™ III First-Strand Synthesis System (Life Technologies). RT-qPCR was performed using Roche LightCycler480/BioRad CFX maestro using qPCR 2X MasterMix Plus for SYBR® Assay No ROX (Tebubio) or TaqMan® gene expression mastermix (Life Technologies) following the manufacturer's protocol with in-house developed primers and probes (IDT) (Supplementary Table 1) or TaqMan® probes (Life Technologies) (Supplementary Table 3). Each reaction was performed in triplo and three reference genes (*ECHS1*, *RPL13A* and *GAPDH*) were used for normalization. Fold changes of the cardiac markers (*ANK2, ANK3, CAV3, GJA1, HCN4, KCND3, KCNH2, KCNJ2, KCNJ8, CACNA1C, RYR2, TNNI3, TNNT2, MLC2a, MLC2v, MYH6, MYH7* and *SCN5A*) are analyzed using a modified delta-delta-Ct method (15) in the qBase+ software (Biogazelle) and results are presented relative to the mean of all samples of control 1 (n=4) . Tissue expression levels of the left ventricle of a human heart are shown as a reference for normal tissue expression levels.
Expression levels of the different *SCN5A* transcripts were normalized using the same three reference genes (*ECHS1*, *RPL13A* and *GAPDH*). Following formulas are used to get the relative expression per transcript type: mutant deletion = 2^-(mean Ct $_{\text{deletion}}$ - mean Ct $_{\text{reference genes}}$), mutant insertion: 2^-(mean Ct $_{\text{insertion}}$ - mean Ct $_{\text{reference genes}}$), wild type: 2^-(mean Ct $_{\text{wild type}}$ - mean Ct $_{\text{reference genes}}$) - 2^-(mean Ct $_{\text{insertion transcript}}$ - mean Ct $_{\text{reference genes}}$). Because the probe detecting the wild-type transcript also detects the insertion transcript, while for insertion and deletion transcript we were able to design specific probes. Next, proportions were calculated to the total amount of *SCN5A* transcripts.

Western blot

Cytosolic and membrane proteins of approximately 5*10^6 iPSC-CMs were collected using the Mem-PER™ Plus Membrane Protein Extraction Kit (Life Technologies) following manufacturer's protocol. Protein concentrations were measured using the Pierce BCA protein assay (Life Technologies). At least 3.5µg membrane fraction of the protein extract was loaded and separated on a Tris-acetate 3-8% gel for 50 min at 200 V and transferred to a nitrocellulose membrane with the Pierce™ G2 Fast Blotter System (Life Technologies). Ponceau S (Bio-Connect) staining confirmed transfer of proteins. The membrane was blocked with 5% milk powder (MP) for 2h at room temperature on a shaker. Primary antibodies were diluted in 5% MP and incubated for 1 hour at RT followed by an overnight incubation at 4 °C. After washing the membrane, secondary antibodies diluted in 5% MP were incubated for 2 hours (Supplementary Table 2). Visualisation was achieved with femto or ECL solution (Life Technologies), following manufacturer's protocol. The area under the peak of both Nav1.5 and N^+/K^+ ATPase (reference membrane protein) was determined using ImageJ. The expression of Nav1.5

is calculated relative to the expression of N^+/K^+ ATPase. Results are displayed with the number of iPSC-CM samples that were analysed (n=) which is different for each cell line.

Statistical analysis

Several statistical tests were used depending on the assay and the comparisons made. In the text, the used statistical analysis method is mentioned with the abbreviations indicated in this section.

For comparison of patients versus controls in the patch clamp analyses, a linear mixed model (LMM_PC) was fitted with mutation status as fixed effect and sodium current density or AP characteristic as dependent variable. The random intercept included differentiation, nested within clone, nested within cell line. A log transformation was performed on the sodium current density results because they were highly skewed. An F-test with Kenward Roger correction was used to test for significance. For other patients vs controls comparisons, a linear mixed model (LMM) also fitted mutation status as fixed effect and qPCR panel data/*SCN5A* transcript expression/Nav1.5 membrane expression as dependent variable with a random intercept that included cell line followed by the F-test with Kenward Roger correction. A similar approach was used to test differences between symptomatic and asymptomatic patients (LMM_symp) where affected status was the fixed effect.

To determine whether there are overall statistical differences between all the iPSC-CM lines or between the patients themselves, a one-way ANOVA was used (ANOVA) followed by a TukeyHSD or Dunnett post hoc test. A 2-way ANOVA model that fitted the independent variables cell line, percentage of *SCN5A* transcript and the interaction between them was also performed. An independent sample t-test (t-test) was used to test the statistical differences between two groups, such as e.g. BrS12 vs BrS12 CRISPR.

To investigate the correlation between severity of the symptoms of patients (most severely affected patient was ranked 1, least severely affected as 5) and a certain y-value a Spearman's rank correlation test (Spearman) was used with correlation coefficient rho.

A Pearson correlation coefficient was calculated for WT *SCN5A* expression versus Nav1.5 protein expression and peak sodium current density.

For the interpretation of the variability of the results, the coefficient of variation (CV%) was calculated using the following formula: $CV\% = \frac{standard\ deviation}{mean} X\ 100\%$.

Results

Clinical and genetic profile of BrS patients and control individuals

Five BrS patients (BrS3, BrS8, BrS9, BrS10, BrS12) carrying the *SCN5A* founder mutation (c.4813+3_4813+6dupGGGT) and two healthy unrelated control individuals were recruited. BrS3, a male child, experienced sudden cardiac death at the age of 10. BrS8 (male, age 35) and BrS12 (male, age 36) both presenting with a positive ajmaline test are cousins (Figure 1, A). BrS8 is an asymptomatic carrier of the mutation while BrS12 experienced a syncope at the age of 25 and received an ICD which gave one appropriate shock. BrS9 (male, 54 years) and BrS10 (female, 50 years) are siblings (Figure 1, A). BrS9 showed a type I ECG after ajmaline provocation and presented with a syncope at the age of 30 for which an ICD was implanted, while BrS10 showed a spontaneous type I ECG but is asymptomatic. We can rank the BrS patients based on clinical severity starting with the most severe phenotype: BrS3 (SCD at age 10) - BrS12 (syncope and appropriate ICD shock) – BrS9 (syncope) - BrS10 (asymptomatic with spontaneous type I ECG) - BrS8 (asymptomatic with provoked type I ECG). Patients are shown in this order in all figures. The healthy control individuals, Control 1 and Control 2, are a 50-year-old male and a 33-year-old female, respectively. They were screened and tested negative with gene panels for cardiac arrhythmia, cardiomyopathy and thoracic aortic aneurysm. An isogenic control was created by CRISPR/Cas9 correction of the founder mutation in iPSCs of patient BrS12 (BrS12CRISPR).

Generation of iPSCs and iPSC-CMs

Fibroblasts from five BrS patients and two healthy control individuals were cultured from skin biopsies and reprogrammed into iPSCs, of which two (BrS9 and BrS10) are describe in Chapter 3 of this thesis (14). Three clones per cell line were fully validated with immunocytochemistry staining, morphology and *in vitro* trilineage differentiation potential as described before (14). Pluripotency was demonstrated through endogenous expression of Tra1-60, Tra1-81, Oct3/4 and Nanog (Figure 1, B). The *SCN5A* founder mutation was present (Figure 1, C) in all the generated patient iPSC clones and no relevant genomic aberrations were detected (no CNVs affecting genes involved in cardiovascular function or development, Supplementary Table 4).

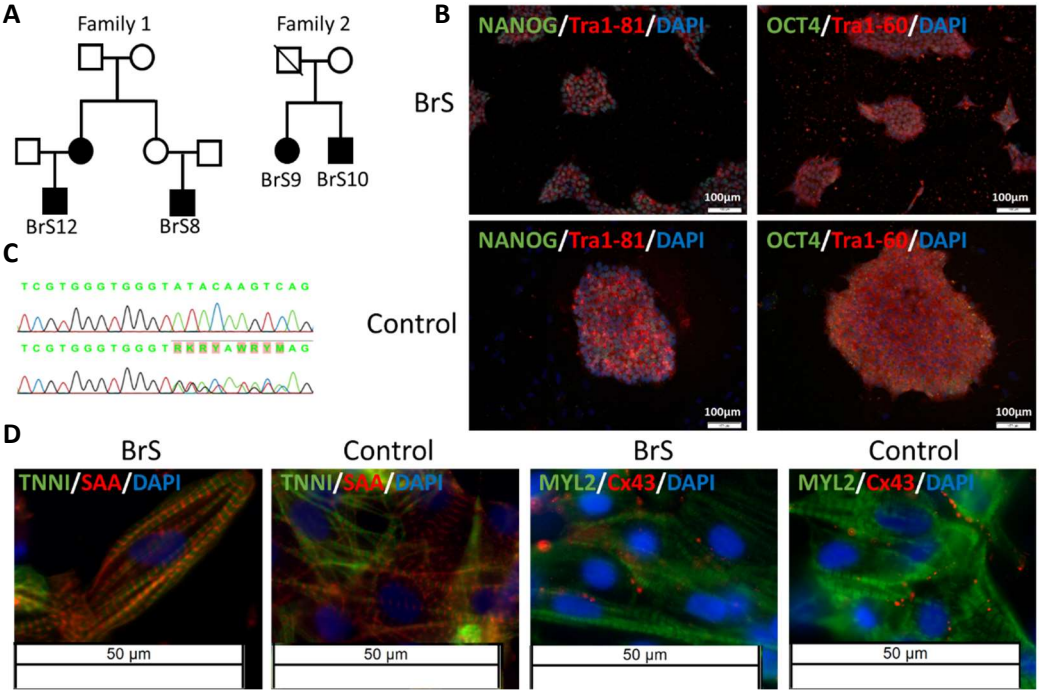

Figure 1: Characterization of iPSCs and iPSC-CMs of BrS patients and control individuals. A) Pedigree of two BrS families carrying the SCN5A founder mutation. B) Immunocytochemistry (ICC) staining of iPSC colonies of a BrS patient and a healthy control individual with pluripotency markers Nanog, Tra1-81, Oct4 and Tra1-60. DAPI was used to stain the nuclei. Scale bar equals 100 µm C) Sanger sequencing result of DNA of a BrS patient iPSC cell line showing the insertion of GTGG in intron 27 of SCN5A. D) ICC of iPSC-CMs of BrS patients and controls with cardiac specific markers Troponin I (TNNI), sarcomeric alpha actinin (SAA), myosin light chain 2 (MYL2) and connexin 43 (Cx43) at 100x. DAPI was used to stain the nuclei.

Two iPSC clones per individual were differentiated at least two times. Cardiomyocytes started beating between day 8 and day 12 of differentiation and were purified with a lactate treatment for 6 days, starting at day 14. CM-specific markers sarcomeric alpha-actinin, Troponin I, connexin 43 and myosin light chain 2 were detected by immunostaining in each iPSC-CM line in each differentiation and showed well-structured sarcomeres (Figure 1, D). RNA expression profiles of a panel of CM markers were similar across the different cell lines, only BrS12 showed a significantly higher expression for 10/19 markers (Figure 2, Supplementary Table 5). Excluding BrS12 from the analysis, there were no significant differences in expression (ANOVA $p>0.05$). Between patient and control iPSC-CMs, there was no significant difference in expression of any of these CM markers (LMM $p>0.05$, Supplementary Table 5).

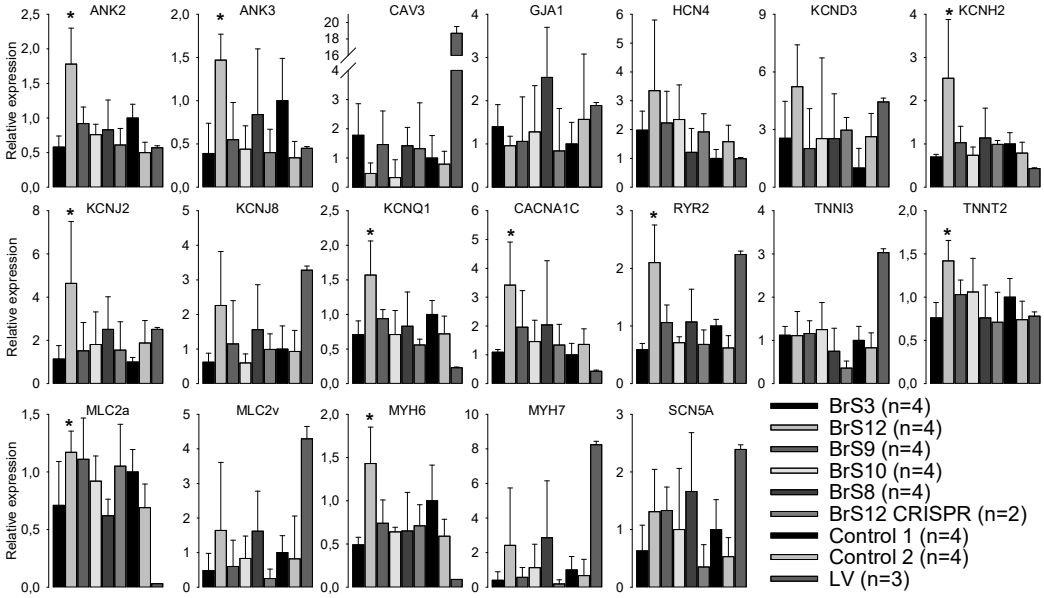

*Figure 2: RT-qPCR expression of 19 cardiomyocyte-specific markers in the iPSC-CMs. The graphs represent the relative expression normalized to 3 reference genes (GAPDH, RPL13A and ECHS1) and relative to the control line M45-50. As a reference, the expression in native left ventricular (LV) tissue we obtained from a donor heart is also shown. Results of two clones and their two differentiations are combined as one group (only for BrS12CRISPR n=2). In this qPCR assay, all transcripts of SCN5A are detected. LV: left ventricle, *Significantly increased expression for BrS12 compared to at least one other cell line.*

SCN5A/$Na_v1.5$ expression

At mRNA level, no significant difference in general *SCN5A* expression was observed between patients and control individuals (LMM p=0.13) (Figure 2). Since the mutation leads to the generation of alternative transcripts when expressed in heterologous expression systems, we investigated this in more detail in the iPSC-CMs. Using RT-qPCR and cDNA sequencing, we confirmed the presence of two of the described alternative transcripts in BrS patient iPSC-CMs: one with the 96 bp deletion in exon 27 ('deletion transcript') and the one with the GTGG insertion between exon 27 and 28 ('GTGG transcript', Figure 3, E). The presence of the latter indicates that NMD did not occur. This GTGG transcript was not observed in the unrelated controls or the isogenic control while the deletion transcript was detected, but only in negligible quantities (0.5-2.1%). In all BrS patients, of the total amount of *SCN5A* expressed, 24% to 34% was wild type transcript, 55% to 60% deletion transcript and 9 to 18% GTGG transcript (Figure 3, D). This proportion was not significantly different between the patients with different disease severity (2-way ANOVA p=0.34).

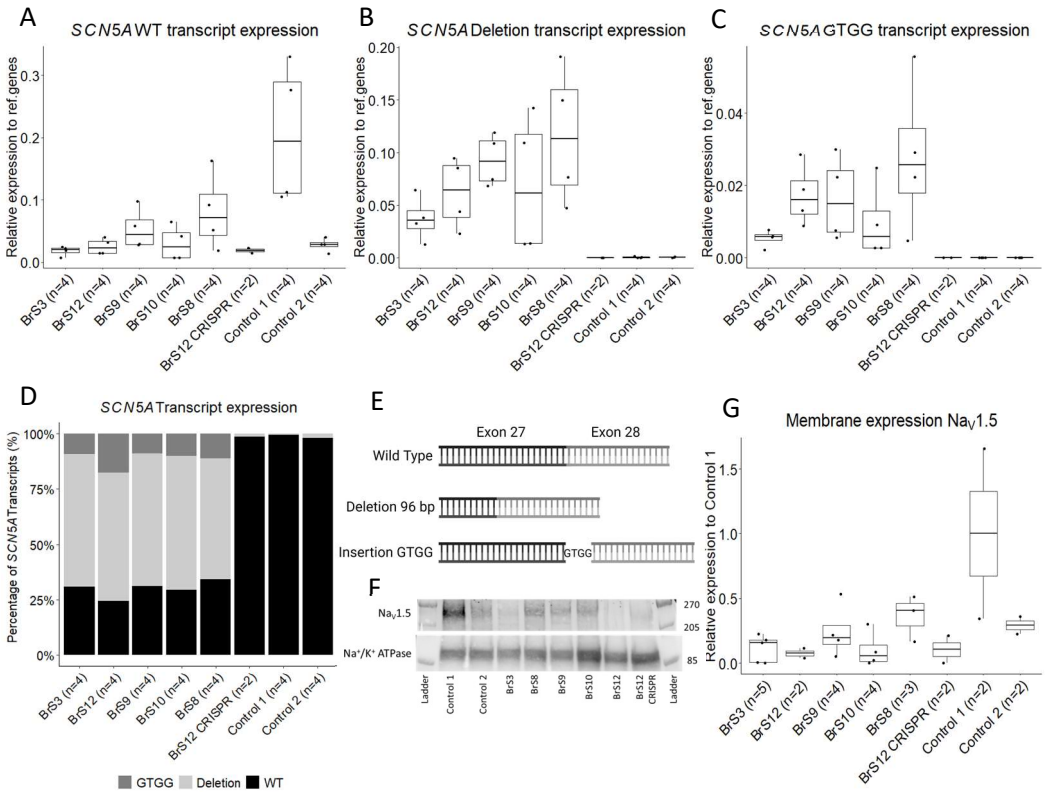

Figure 3: SCN5A and Nav1.5 expression in iPSC-CMs of BrS patients and controls. A-C) SCN5A transcript expression relative to the reference genes with WT (A), deletion (B) and GTGG (C) transcript. A correlation between severity and transcript expression was observed for the WT (rho= 0.45) and deletion (rho= 0.47) transcripts. D) Proportions of different SCN5A transcripts. There is no difference in expression of the transcripts over de different patients (p=0.34). E) Overview of the different transcripts of SCN5A observed in BrS patients. F-G) Western blot results of Nav1.5 membrane expression with Na^+/K^+ ATPase as reference membrane protein and relative to Control 1. No significant difference is observed in expression of Nav1.5 between patients and controls (p=0.18).

The expression of *SCN5A* WT transcript is not significantly different between patients and control individuals (LMM p=0.37) and no significant differences in expression are observed between the patients for the WT (ANOVA p=0.11), deletion (ANOVA p=0.21) and GTGG transcript (ANOVA p=0.16) (Figure 3, A, B and C). The *SCN5A* WT expression does not seem to differ between BrS12 and its isogenic control BrS12 CRISPR, but the low number of observations does not allow to perform statistical analysis for this comparison. When we rank the patients according to severity, there is a moderate trend of higher expression of WT *SCN5A* transcript towards the less severe patients (Spearman rho= 0.45, p=0.045, Figure 3, A). We see a similar moderate correlation for the deletion transcript (Spearman rho= 0.47, p= 0.036, Figure 3, B) but not for the GTGG transcript

(Spearman rho= 0.29, p=0.21, Figure 3, C). If we compare symptomatic (BrS3, BrS12 and BrS9) with asymptomatic patients (BrS10 and BrS12), we do not observe a significant difference in expression of any of the transcripts (WT: p= 0.39, deletion: p= 0.36, GTGG: p= 0.53, LMM_symp).

The three different *SCN5A* transcripts detected with qPCR could in theory translate into three different proteins. Western blot (WB) analysis of $Na_V1.5$ membrane expression showed one band with molecular weight between 205 and 270 kDa (Figure 3, F). The WT Nav1.5 protein has a molecular weight of 227 kDa which on WB cannot be separated from the 96bp deletion mutant channel with a theoretical weight of 223 kDa. The GTGG retention mutant channel has a theoretical weight of 196 kDa and is thus expected to show a separate band on WB, but this was not detected. Levels of $Na_V1.5$ membrane expression showed a pattern similar to the *SCN5A* WT transcript expression levels with no significant difference between the patients and control individuals (LMM p=0.18) (Figure 3, F and G). Expression of $Na_V1.5$ was similar in BrS12 and its isogenic control. Ranking the patients according to severity did not show a significant trend to higher membrane expression of $Na_V1.5$ in less severely affected patients (Spearman rho= 0.29, p= 0.24) and no difference was observed comparing symptomatic and asymptomatic patients (LMM_symp p= 0.57) (Figure 3, G).

There is no significant correlation between the expression of $Na_V1.5$ in the membrane and mRNA expression of total *SCN5A* (Pearson *r*=0.16, p=0.51) or *SCN5A* WT transcript only (Pearson *r*= 0.38, p=0.1) (Figure 5, A and B).

Sodium current

The effect of the mutation on the sodium current was measured in singularized iPSC-CMs using the patch clamp technique. When combining for each individual the data from all cells from both clones and their different differentiations, no significant decrease in sodium current density of the iPSC-CMs of the five patients compared to the three control individuals was revealed (LMM_PC p=0.59, Figure 4, A). Decreased sodium current is observed in the patient iPSC-CMs compared to control 1 and to BrS12CRISPR (I/V plot Figure 4, A and mean peak sodium current density Table 3), but this is not statistically significant (LMM_PC p=0.64 and 0.88 respectively) due to the high (within patient or control) variability in the data (Figure 4 F and G, Supplementary Figure 1, Supplementary Figure 2). Control 2 has a peak sodium current density comparable to BrS3 and BrS10 so not different from the patients (LMM_PC p=0.69). Comparing the sodium current density of the isogenic control BRS12CRISPR to the original patient BrS12 iPSC-CMs, we observed a significant increase in peak sodium current density from -152 pA/pF in BrS12 to -406 pA/pF in the isogenic control (t-test p<0.01).

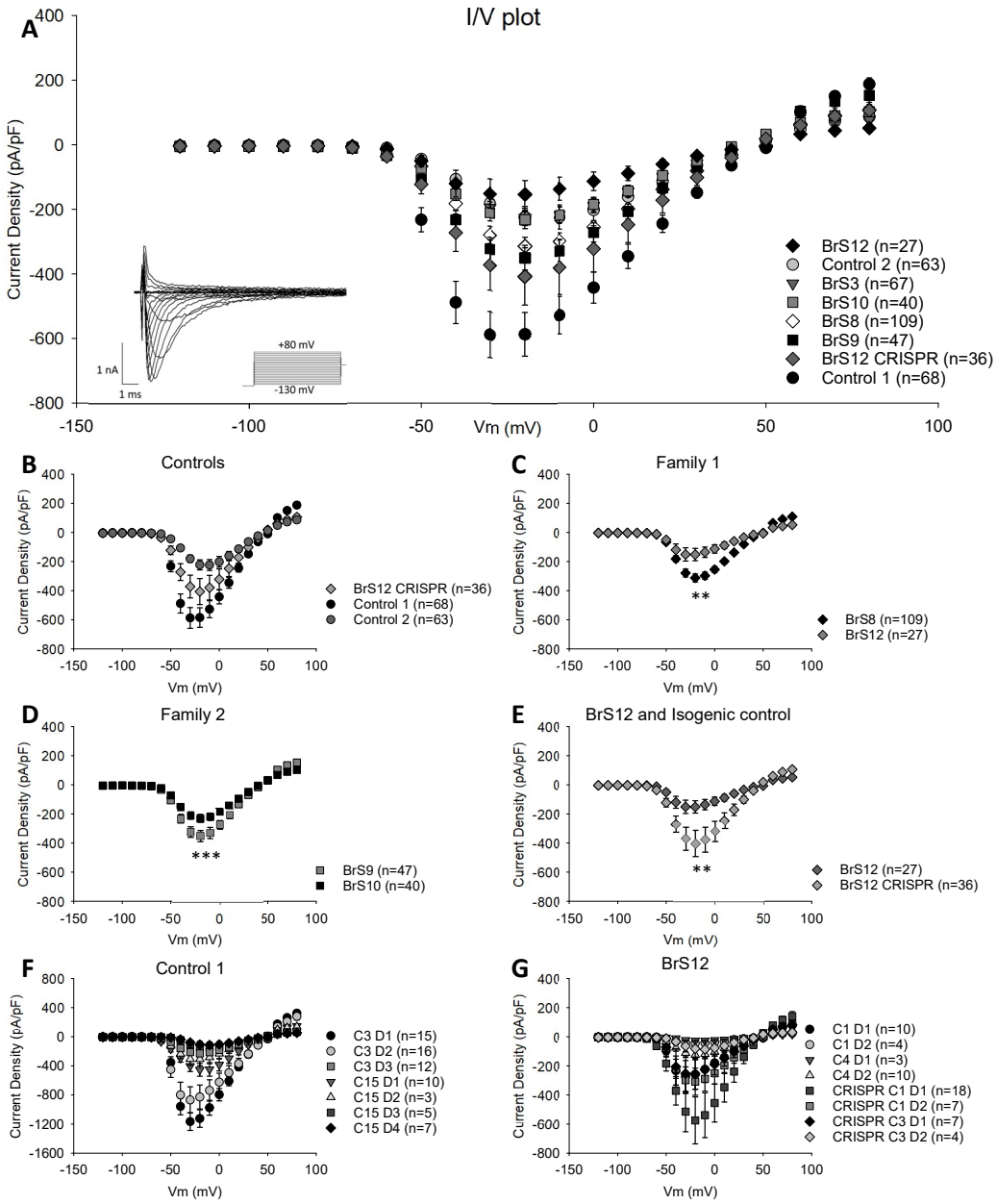

Figure 4: Sodium current density in BrS patient and control iPSC-CMs. A) Current-voltage (I-V) relationship of all patients and controls, with a representative trace of sodium current and the activation pulse protocol for voltage dependent sodium current density measurement. B) Sodium current density of the healthy controls and an isogenic control. C) Significant difference in peak sodium current ($p<0.01$) between BrS8 and BrS12 in Family 1. D) Significant difference between BrS9 and BrS10 in peak sodium current density ($p<0.001$) in Family 2. E) Significant increase in peak sodium current density comparing isogenic control BrS12CRISPR with BrS12 ($p<0.01$). F-G) Individual peak sodium current density results per clone and differentiation of Control 1 (G)

*and BrS12 (isogenic control included) (F). The number of recorded cells per cell line is displayed as (n=). Results are depicted as mean ± standard error of mean (SEM), '**' p<0.01, '***' p<0.001.*

Ranking the patients according to severity there is no correlation with the peak sodium current density (Spearman rho= -0.11, p= 0.057, Table 1) and there is no difference between symptomatic and asymptomatic patients (LMM_symp p= 0.72).

If we look within the families, we observe a significantly larger peak sodium current density in the asymptomatic BrS8 patient compared to the severely affected BrS12 patient (t-test p<0.01, Figure 4, C). In the second family however, asymptomatic BrS10, who has a spontaneous type I ECG, displays a significantly smaller peak current density compared to BrS9 who is symptomatic (t-test p<0.001, Figure 4, D).

Table 1: Peak sodium current density at -20mV per individual

	BrS3	BrS12	BrS9	BrS10	BrS8	BrS12 CRISPR	Control 1	Control 2
Mean (pA/pF)	-224,1	-151,8	-348,1	-230,3	-312,5	-406,1	-584,9	-222,8
SD	191,1	219,5	260,8	177,5	287,6	535,1	550,8	273,0
CV%	85	145	75	77	92	132	94	123
n	67	27	47	40	109	36	68	63

SD: standard deviation, CV: Coefficient of variation, n: number of recorded cells

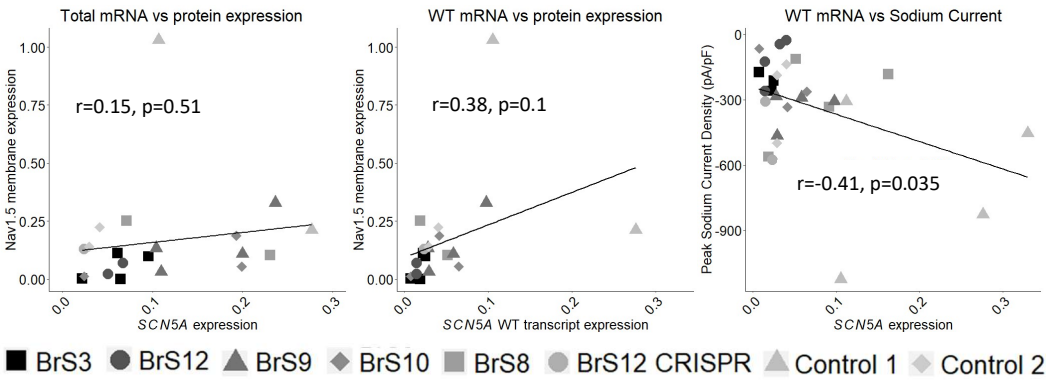

Figure 5: Scatter plots for SCN5A mRNA expression versus protein expression and sodium current density. A) Correlation of total SCN5A mRNA expression and $Na_V1.5$ protein expression (Pearson p=0.51). B) Correlation of WT SCN5A mRNA and $Na_V1.5$ protein expression (Pearson p=0.1). C) Correlation of SCN5A WT transcript expression and peak sodium current density (Pearson p=0.035).

No differences were observed regarding the voltage dependence of inactivation and recovery of inactivation of sodium current and both activation and inactivation kinetics were similar between controls and patients and within these groups (Supplementary Figure 3).

When we plot the expression of the WT *SCN5A* transcript versus the peak sodium current density, a moderate correlation is observed. Higher expression of the WT *SCN5A* transcript, results in larger peak current density (Pearson *r*= -0.41, p= 0.035, Figure 5, C).

Action potentials

Action potentials were also recorded from in most cases two differentiations of two clones per individual to investigate the effect of the mutation on AP characteristics such as AP duration at 50% or 90% of repolarization (APD50, APD90), AP amplitude and upstroke velocity (Table 2). Recordings were only included in the analysis when the resting membrane potential (RMP) was below -60 mV (Figure 6, A). During the analysis, a variable beat rate was noted (Figure 6, B), therefore, APD50 and APD90 were corrected using the Fridericia formula (APD50c and APD90c) (Figure 6, D and E). When comparing patient with control iPSC-CMs, no significant differences were observed for any of the AP characteristics (LMM_PC, Table 3). Again, a high variability in the data was observed.

BrS12 iPSC-CMs had a significantly lower beat rate compared to the isogenic control (22 beats per minute (bpm) vs 46 bpm, t-test p= 0.0009), a higher AP amplitude (112 mV vs 105mV, t-test p=0.004) and a shorter APD90c (307 ms vs 498 ms, t-test p=0.006, Figure 6, B, C, E).

Regarding the clinical severity of patients, a moderate correlation was found in AP amplitude, upstroke velocity and APD90c (Spearman rho= 0.31, p= $6.6x10^{-4}$; rho= 0.41, p= $3.3x10^{-6}$; rho= -0.40, p= $2.1x10^{-5}$, Table 3) with a higher amplitude, faster upstroke velocity and shorter APD90c in less severely affected patients. Asymptomatic patients showed a significantly faster upstroke velocity compared to the symptomatic ones (LMM_symp p= 0.026, Figure 6, F)

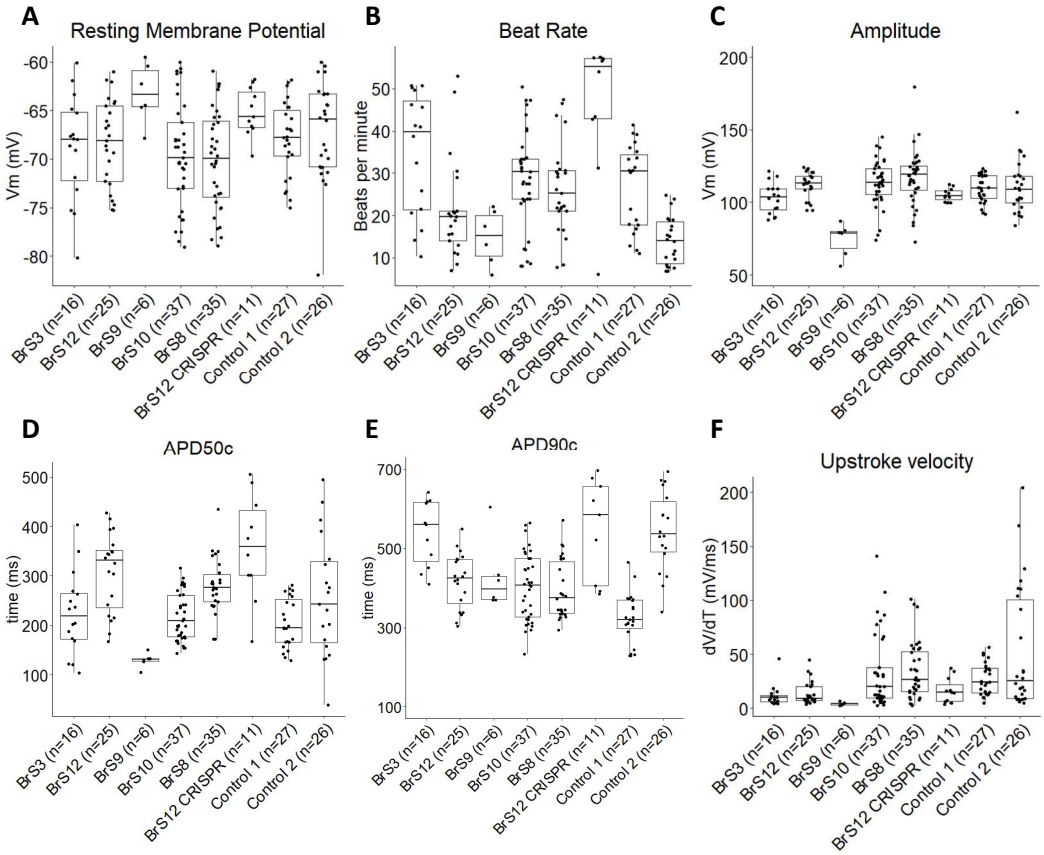

Figure 6: Action potential (AP) characteristics of BrS patient and control iPSC-CMs. A) Resting membrane potential filtered for RMP < -60 mV. B) Beat rate C) Amplitude of the AP, D-E) APD50 (D) and APD90 (E) corrected for beat rate with the Fridericia formula. F) Upstroke velocity of AP.

Table 2: AP characteristics of patient and control iPSC-CMs

		BrS3	BrS12	BrS9	BrS10	BrS8	BrS12 CRISPR	Control 1	Control 2
RMP (mV)	**Mean**	-69	-68	-63	-70	-70	-65	-68	-67
	SD	5	4	3	5	5	2	4	5
	CV%	8	7	5	8	7	4	6	7
Beat Rate (BPM)	**Mean**	35	22	15	29	26	46	27	14
	SD	14	12	6	11	11	17	10	6
	CV%	42	56	43	40	40	36	36	41
Amplitude (mV)	**Mean**	103	112	74	113	117	105	109	111
	SD	11	9	12	16	19	4	9	17
	CV%	10	8	15	14	16	4	9	16

		BrS3	BrS12	BrS9	BrS10	BrS8	BrS12 CRISPR	Control 1	Control 2
APD50c (ms)	**Mean**	225	308	130	217	280	357	205	257
	SD	83	79	15	48	56	107	50	121
	CV%	37	26	11	22	20	20	24	47
APD90c (ms)	**Mean**	615	418	429	403	395	566	323	552
	SD	140	69	90	85	75	131	63	105
	CV%	23	17	21	21	19	23	20	19
upstroke velocity (mV/ms)	**Mean**	12	14	4	33	35	17	27	53
	SD	10	11	1	34	26	12	15	57
	CV%	86	76	34	104	76	71	53	108
	n	16	25	6	37	35	11	27	26

SD: standard deviation, CV: Coefficient of variation, n: number of recorded cells, AP: Amplitude, RMP: Resting membrane potential, APD50c/APD90c: corrected action potential duration at 50/90% of repolarization.

Table 3: Statistical analysis of AP characteristics

AP characteristic	p-value Patient vs control[a] (LMM_PC)	Clinical severity Spearman Rho[b]	p-value Spearman[c]	p-value symptomatic vs asymptomatic[d] (LMM_symp)
RMP	0.22	-0.15	0.09	0.16
Beat Rate	0.59	0.01	0.88	0.67
Amplitude	0.51	0.31	**$6.6x10^{-4}$**	0.29
APD50c	0.17	0.12	0.23	0.35
APD90c	0.44	-0.40	**$2.1x10^{-5}$**	0.73
Upstroke velocity	0.49	0.41	**$3.3x10^{-6}$**	**0.026**

[a] Linear mixed model was used for the comparison of patients vs controls
[b] Spearmans rank correlation test investigated the correlation between patient severity and AP characteristics. Rho value indicates the correlation coefficient.
[c] p-value of the Spearmans rank correlation test
[d] linear mixed model to test the differences between symptomatic and asymptomatic patients.
AP: action potential, RMP: Resting membrane potential, APD50c/APD90c: corrected action potential duration at 50/90% of repolarization.

Variability

In our different analyses performed on the iPSC-CMs, we observe a large variability in the data, evidenced by large standard deviations (SD) and coefficients of variance (CV%),

hampering the detection of statistically significant differences between patient and control phenotypes. The use of two iPSC clones per individual combined with at least two separate differentiations of these clones is certainly partly responsible for this.

Regarding variability in *SCN5A* mRNA or Nav1.5 protein expression – where just one RNA or protein sample was taken and investigated per differentiation per clone (Figure 2, Figure 3) – the CV% per individual range from 27% to 97% (mean 57%; Supplementary Table 9) and from 33% to 141% (mean 79.5%; Supplementary Table 8) respectively. For the other CM markers in the qPCR panel, CV% vary across different genes with values ranging from 16% to 97% per individual (Supplementary Table 9). Investigating variability of peak sodium current and AP characteristics – where several measurements per differentiation per clone were taken (Figure 4, Figure 6) – a mean CV% of 100% (range 75-145%) is obtained for peak sodium current (Table 1) and mean CV% of 10.5% (range 4-16%), 20% (range 17-23%), 24% (range 11-47%), 41% (range 36-56%) and 72% (range 34-108%) are obtained for respectively AP amplitude, APD90c, APD50c, beat rate and upstroke velocity (Table 2).

Since the sodium current is dependent on one channel and as such influenced by less variables than APs, we focused on it to further investigate iPSC-CM inter- and intraclonal variability. We observed significant differences in sodium current density between differentiations of one clone (intraclonal) and between two clones of one individual (interclonal), however not for every cell line (Figure 4, F and G, Supplementary Figure 1). Significant interclonal differences were observed in BrS8 (C2 > C3, Clone 2 showed higher peak sodium current than C3; t-test $p=6x10^{-7}$), BrS10 (C10 > C3; t-test $p=3x10^{-8}$), BrS12 CRISPR (C1 > C3; t-test p=0.04), Control 1 (C3 > C15; t-test $p=2x10^{-5}$) and Control 2 (C3 > C2; t-test p=0.03) (Supplementary Table 6). Significant intraclonal differences were observed for BrS8 C2 (ANOVA p=0.03), BrS8 C3 (ANOVA p= 0.08), BrS12 C4 (t-test p=0.02), Control 1 C3 (ANOVA p=0.0001) and Control 1 C15 (ANOVA p=0.009) (Supplementary Table 7).

The linear mixed model used for statistical analysis of the patch clamp results, indicated that 18.3% of the observed variability in sodium current density is explained by the differentiation rounds, 16.1% is due to the use of different clones while only 3% is explained by the individual. This leaves 62.4% of the variation that is not captured by person, clone or differentiation and represents spread of the data measured per cell. The mean CV% for peak sodium current density when data are separated per differentiation is 75.5% (range 31-168%), investigated per clone this increases to 90% (range 51-145%) and per individual to 100% (range 75-145%).

Discussion

In this study, we investigated the effect of the *SCN5A* (c.4813+3_4813+6dupGGGT) Belgian founder mutation using patient and control iPSC-derived cardiomyocytes. Brugada syndrome is known for reduced penetrance and variable expressivity and this founder mutation is a clear example. Sieliwonczyk et al. describe its clinical spectrum in 25 Belgian families and found that 52% of the mutation carriers present with BrS, 65% with cardiac conduction defects, 11% with atrial dysrhythmia and 17% with no symptoms at all (10). We aimed to model this mutation in a disease-relevant iPSC-CM cell type, also to investigate if the phenotypic differences observed in the patients could be recapitulated at cellular level. We therefore selected five mutation carriers with different clinical symptoms, ranked them based on clinical phenotype severity and investigated correlation with cellular characteristics.

Previous research conducted in heterologous expression systems has demonstrated that this GGGT duplication in intron 27 results in the absence of sodium current and it can give rise to three mutant transcripts, with only one of these (with 96 bp of exon 27 deleted) observed in patient lymphocytes (11, 12). In the iPSC-CMs of our BrS patients, we detected the wild-type transcript and two mutant transcripts, the 96 bp deletion transcript and the one with intronic GTGG retention leading to a frameshift, representing on average 30%, 59% and 11% of transcripts respectively. With *SCN5A* (almost) not expressed in fibroblasts or PBMCs, this already shows the added value of studying the patient-specific physiologically relevant cell type of iPSC-CMs. In the control iPSC-CMs we did detect a tiny amount of the 96 bp deletion transcript as well (0.5-2.1%), showing that even in the WT transcript the cryptic splice site in exon 27 is used during splicing, but at extremely low level.

Though more than half of the total amount of *SCN5A* mRNA in patient iPSC-CMs is mutant transcript, we did not observe the expected reduction of WT transcript in patient compared to control iPSC-CMs in an allele-specific qPCR, not even between patient BrS12 and its isogenic control. In fact, *SCN5A* expression in Control 2 and BrS12CRISPR was lower than in any other individual. Within the BrS patient iPSC-CMs the amount of WT transcript was correlated with their clinical severity ranking, suggesting that higher WT transcript levels could explain reduced penetrance of clinical symptoms, but the low expression in control individuals questions the validity of relating RNA expression level with phenotype in this iPSC-CM model. The ratio between the three different transcripts did not differ over the BrS patients with different clinical severity of the disease.

Membrane expression of the channel $Na_V1.5$ was investigated on Western blot, but only an antibody that could not differentiate between WT and mutant protein was available

for use. WT (length 2016 amino acids, 227 kDa) and 96 bp deletion mutant channel (theoretical length 1984 amino acids, 223 kDa) would certainly be indistinguishable on the blot, but the GTGG retention mutant channel (theoretical length 1786 amino acids, 196 kDa) should have resulted in a separate band. This was not observed, supporting the hypothesis that this transcript is not translated to protein, although it is also possible that the expression of this mutant protein was too low to be visible on the blot. We did not observe a significant difference in $Na_V1.5$ expression between BrS patient and control iPSC-CMs or between BrS12 and its isogenic control, which would agree with presence of both (deletion) mutant and WT channel on the membrane. Then we would not expect a correlation between $Na_V1.5$ expression and patient clinical severity, which was indeed the case. But channel protein expression was quite low and variable and though the pattern of average protein expression resembled this of *SCN5A* mRNA expression, it did not show a correlation with mRNA expression per differentiation, neither with *SCN5A* WT alone nor with total *SCN5A* transcript. Based on our data we cannot conclude whether the mutant transcripts are translated into (non-functional) proteins that are transported to the membrane. Experiments expressing the single mutant transcripts in HEK293 cells to investigate protein expression are currently being performed.

Sodium current is the major cardiomyocyte characteristic affected by an *SCN5A*/$Na_V1.5$ mutation, and as such a focus of our functional investigations, but we did not observe a statistically significant difference in sodium current density between BrS patient and control iPSC-CMs in general. The two included unrelated healthy control individuals differ significantly in sodium current density with control 2 iPSC-CMs displaying sodium currents similar to the BrS patient iPSC-CMs. Even if we compare the patients only to control 1 expressing the largest current, we do not reach statistical significance due to high variability in the results, represented by CV% ranging from 75-145%. We specifically opted to use two different iPSC clones per individual and (at least) two differentiations of each clone to take into account the effect that random variation arising from somatic mutations that could occur during reprogramming and culturing and random variation in handling and environmental conditions during culture could have on the cellular phenotype, to be able to tease out robust mutation-related characteristics and differences. But this approach resulted in such variable results that reaching statistical significance was hampered. We observed highly variable data, both between two clones of one individual as well as within the same clone between differentiations. 18.3% of the observed variability in sodium current density was explained by the differentiation rounds, 16.1% by the use of different clones and only 3% by the individual. This leaves 62.6% of the variation that is not captured by person, clone or differentiation and represents spread of the data measured per cell. In our study also none of the AP

characteristics showed significant differences between BrS patient iPSC-CMs and control iPSC-CMs. Again, quite some variability was observed, depending on the characteristic. The CV% was below 20% for RMP and AP amplitude, 17% to 23% for APD90c, 11% to 47% for APD50c and 34% to 108% for the upstroke velocity of the AP. Upstroke velocity is known as a more difficult to measure and as such more variable characteristic.

In a literature search on BrS iPSC-CM models, we found that such variability has not been reported before. Even many recent papers do not use different clones of one individual and do not show individual results per round of differentiation to address this variability issue (16-19). Selga et al. did differentiate two clones of their patient cell line twice and mentioned that the results were similar so they could pool their data, but individual results per differentiation were not provided (20). Cai et al. used three control lines and two different clones of one BrS patient line, but no information was provided on the number of differentiations performed. iPSC-CMs of the two clones of the patient showed similar sodium current, APs and *SCN5A* mRNA and protein expression (21). Chai et al tackled the variability issue by performing the differentiations of iPSCs of a healthy individual, a severely affected and less severely affected long QT patient always together. They only compared data within one differentiation round and always found significant APD prolongation in the severely affected patient compared to the control or mildly affected patient and this over many differentiations performed over five years (22). However, such an approach is not always practically feasible. We also performed a separate analysis on our data comparing only patient and control iPSC-CMs that were differentiated at the same time, but still did not find a consistent significant difference in sodium current.

Part of the variability we observed, could be explained by the rather immature phenotype of iPSC-CM, which is known in the field. They rather resemble fetal cardiomyocytes, both structurally and electrophysiologically. Efforts have been made to improve this maturity state. In our protocol, we applied metabolic maturation by addition of thyroid hormone (T3) and we culture our cells up to at least 35 days to improve the maturity. However, this does not guaranty that every cell is in the same state at the same moment. When we compare the expression of cardiomyocyte specific markers of our iPSC-CMs to left ventricle tissue, we see that the expression profiles differ for half of the tested genes. This implies that, as expected, full maturity has not yet been obtained. It has to be noted though that the left ventricle tissue contains several other cell types such as endothelial cells and cardiac fibroblasts and also their expression of the marker genes is reflected in the qPCR results.

Although we observed no general significant differences between patient and control iPSC-CMs due to the high variability, we detected a significant decrease of peak sodium current density comparing severely affected patient BrS12 with its isogenic control. This isogenic cell line was restored to wild type evidenced by receding of the mutant transcripts. This supports the added value of the use of isogenic cell lines when studying functional characteristics of iPSC-CMs displaying high variability. At AP level, BrS12 displayed higher AP amplitude and shorter APD90c compared to the isogenic control but no difference in upstroke velocity or APD50c. Although in theory lower AP amplitude, slower upstroke velocity and shorter APD could be expected with loss of function sodium channel mutations, this has not consistently been shown in BrS cellular models and as such it is not clear how to interpret such differences. In several other studies isogenic controls of BrS iPSC-CM models have been generated and used for comparison. Liang et al. studied two BrS iPSC-CM models with *SCN5A* mutations and of one an isogenic control was generated that restored the AP and calcium transient properties as well as membrane expression levels to those of unrelated control iPSC-CMs (17). Similar results with isogenic controls were obtained by Li et al. and Zhong et al. where they investigated BrS iPSC-CM models with *SCN5A* and *CACNB2* mutations/variants respectively and found a recovery of expression, AP and current properties (16, 18). This indicates the added value of the use of isogenic controls in addition to (unrelated) healthy controls, as they carry the same genetic background of the patient, helping to pinpoint the effect of just the mutation.

In our study we also aimed to investigate if the phenotypic differences observed in the patients could be recapitulated at iPSC-CM level. Ranking the patients according to their disease severity did not show a significant correlation for $Na_V1.5$ membrane expression, sodium current density and APD50c. AP amplitude, APD90c and upstroke velocity correlated with disease severity, with more severely affected patients showing longer APD90c, lower AP amplitudes, and a slower upstroke velocity. In this case the trend in the two latter sodium-related AP parameters could be an indication of more dysfunctional sodium channels in patients with more severe symptoms, although as mentioned this is not backed up by a reduction in sodium current and channel kinetics showed no differences anywhere. Comparing more general symptomatic to asymptomatic patients did not reveal a significant difference in $Na_V1.5$ membrane expression, sodium current density or AP characteristics except for a faster upstroke velocity in asymptomatic patients. Failure to demonstrate significant correlations could again be due to the variability we observe in our results. This hampers the ability to model and record (small) cellular phenotypical differences that could explain the observed clinical differences in patients.

We also compared peak sodium current density between patients of the same family and did detect significant differences there. The asymptomatic patient BrS8 had a larger peak current in comparison to the symptomatic patient BrS12. In the second family, it was the other way around where the symptomatic patient BrS9 had a larger peak current compared to asymptomatic BrS10 with a spontaneous type I ECG. We based our clinical severity ranking on the presence of visible symptoms such as syncopes, but it is possible that a spontaneous type I ECG might be a more severe phenotypic expression of BrS than a provoked type I ECG in combination with a syncope (BrS9). When we change the ranking of BrS9 and BrS10, we observe a small rise in the correlation coefficient in WT and deletion *SCN5A* transcript expression but none of the other correlations changed in such a way that they became significant. Penttinen et al. also modelled iPSC-CMs of a symptomatic and asymptomatic BrS patient and did not find any significant differences (19). Sun et al. investigated a BrS family with a *SCN5A* variant creating iPSC-CMs of the proband with repeated syncopes, his asymptomatic brother and mother harbouring the variant and seven unaffected non-carrier family members and observed a milder phenotype for sodium current, calcium handling, AP characteristics and arrhythmic events in asymptomatic mutation carriers compared to the proband iPSC-CMs (23). Including unaffected family members could also be an interesting strategy to reduce variability.

As discussed, a limitation of our (and other) iPSC-CM studies is the immaturity of the cell type. Several methods have been developed to improve this maturity. We used longer cell culture and applied T3 hormone, but other biochemical additions such as fatty acids and dexamethasone or electrical or mechanical stimulation of the cells can improve the maturity state as well (24). Another way is co-culture of iPSC-CM with other cardiac cell types such as cardiac endothelial cells or fibroblasts and/or aggregation in 3D models to create engineered heart tissue, cardiac microtissues or organoids depending on the way of culture (25-27). However, the question remains if these approaches will reduce the variability to be able to model small phenotypical differences as the environment/development of organoids is less controllable and addition of other cell types might also introduce extra sources of variation. Another limitation in our study is regarding the recordings of APs that were performed at constant room temperature and not at the physiological temperature of 37 °C. Due to technical limitations we were not able to use pacing for AP recordings. The implementation of these two techniques might have decreased the variability of AP data.

In conclusion, our iPSC-CM model enabled us to investigate the effect of the *SCN5A* founder mutation at transcript level. Although for the functional investigations we are confronted with high inter- and intraclonal variability as well as general data variability,

hampering the detection of statistically significant differences, we show that the use of isogenic controls is a promising strategy to study the effect of the mutation under investigation.

References

1. Antzelevitch C, Brugada P, Borggrefe M, Brugada J, Brugada R, Corrado D, et al. Brugada syndrome: report of the second consensus conference: endorsed by the Heart Rhythm Society and the European Heart Rhythm Association. Circulation. 2005;111(5):659-70.
2. Hosseini SM, Kim R, Udupa S, Costain G, Jobling R, Liston E, et al. Reappraisal of Reported Genes for Sudden Arrhythmic Death: Evidence-Based Evaluation of Gene Validity for Brugada Syndrome. Circulation. 2018;138(12):1195-205.
3. Shinlapawittayatorn K, Dudash LA, Du XX, Heller L, Poelzing S, Ficker E, et al. A novel strategy using cardiac sodium channel polymorphic fragments to rescue trafficking-deficient SCN5A mutations. Circ Cardiovasc Genet. 2011;4(5):500-9.
4. Mikhailova VB, Karpushev AV, Vavilova VD, Klimenko ES, Tulintseva T, Yudina YS, et al. Functional Analysis of SCN5A Genetic Variants Associated with Brugada Syndrome. Cardiology. 2021.
5. Hu RM, Song EJ, Tester DJ, Deschenes I, Ackerman MJ, Makielski JC, et al. Expression defect of the rare variant/Brugada mutation R1512W depends upon the SCN5A splice variant background and can be rescued by mexiletine and the common polymorphism H558R. Channels (Austin). 2021;15(1):253-61.
6. Nijak A, Labro AJ, De Wilde H, Dewals W, Peigneur S, Tytgat J, et al. Compound Heterozygous SCN5A Mutations in Severe Sodium Channelopathy With Brugada Syndrome: A Case Report. Front Cardiovasc Med. 2020;7:117.
7. Takahashi K, Tanabe K, Ohnuki M, Narita M, Ichisaka T, Tomoda K, et al. Induction of pluripotent stem cells from adult human fibroblasts by defined factors. Cell. 2007;131(5):861-72.
8. Zwi L, Caspi O, Arbel G, Huber I, Gepstein A, Park IH, et al. Cardiomyocyte differentiation of human induced pluripotent stem cells. Circulation. 2009;120(15):1513-23.
9. Nijak A, Saenen J, Labro AJ, Schepers D, Loeys BL, Alaerts M. iPSC-Cardiomyocyte Models of Brugada Syndrome-Achievements, Challenges and Future Perspectives. Int J Mol Sci. 2021;22(6).
10. Sieliwonczyk E, Alaerts M, Robyns T, Schepers D, Claes C, Corveleyn A, et al. Clinical characterization of the first Belgian SCN5A founder mutation cohort. Europace : European pacing, arrhythmias, and cardiac electrophysiology : journal of the working groups on cardiac pacing, arrhythmias, and cardiac cellular electrophysiology of the European Society of Cardiology. 2021;23(6):918-27.
11. Hong K, Guerchicoff A, Pollevick GD, Oliva A, Dumaine R, de Zutter M, et al. Cryptic 5' splice site activation in SCN5A associated with Brugada syndrome. J Mol Cell Cardiol. 2005;38(4):555-60.

12. Rossenbacker T, Schollen E, Kuiperi C, de Ravel TJ, Devriendt K, Matthijs G, et al. Unconventional intronic splice site mutation in SCN5A associates with cardiac sodium channelopathy. J Med Genet. 2005;42(5):e29.
13. Popp MW, Maquat LE. Organizing principles of mammalian nonsense-mediated mRNA decay. Annu Rev Genet. 2013;47:139-65.
14. Simons E, Nijak A, Loeys B, Alaerts M. Generation of two induced pluripotent stem cell (iPSC) lines (BBANTWi006-A, BBANTWi007-A) from Brugada syndrome patients carrying an SCN5A mutation. Stem Cell Research. 2022;60:102719.
15. Hellemans J, Mortier G, De Paepe A, Speleman F, Vandesompele J. qBase relative quantification framework and software for management and automated analysis of real-time quantitative PCR data. Genome Biol. 2007;8(2):R19.
16. Li Y, Dinkel H, Pakalniskyte D, Busley AV, Cyganek L, Zhong R, et al. Novel insights in the pathomechanism of Brugada syndrome and fever-related type 1 ECG changes in a preclinical study using human-induced pluripotent stem cell-derived cardiomyocytes. Clin Transl Med. 2023;13(3):e1130.
17. Liang P, Sallam K, Wu H, Li Y, Itzhaki I, Garg P, et al. Patient-Specific and Genome-Edited Induced Pluripotent Stem Cell-Derived Cardiomyocytes Elucidate Single-Cell Phenotype of Brugada Syndrome. J Am Coll Cardiol. 2016;68(19):2086-96.
18. Zhong R, Schimanski T, Zhang F, Lan H, Hohn A, Xu Q, et al. A Preclinical Study on Brugada Syndrome with a CACNB2 Variant Using Human Cardiomyocytes from Induced Pluripotent Stem Cells. Int J Mol Sci. 2022;23(15).
19. Penttinen K, Prajapati C, Shah D, Rajan DK, Cherian RM, Swan H, et al. HiPSC-derived cardiomyocyte to model Brugada syndrome: both asymptomatic and symptomatic mutation carriers reveal increased arrhythmogenicity. BMC Cardiovasc Disord. 2023;23(1):208.
20. Selga E, Sendfeld F, Martinez-Moreno R, Medine CN, Tura-Ceide O, Wilmut SI, et al. Sodium channel current loss of function in induced pluripotent stem cell-derived cardiomyocytes from a Brugada syndrome patient. J Mol Cell Cardiol. 2018;114:10-9.
21. Cai D, Wang X, Sun Y, Fan H, Zhou J, Yang Z, et al. Patient-specific iPSC-derived cardiomyocytes reveal aberrant activation of Wnt/beta-catenin signaling in SCN5A-related Brugada syndrome. Stem Cell Res Ther. 2023;14(1):241.
22. Chai S, Wan X, Ramirez-Navarro A, Tesar PJ, Kaufman ES, Ficker E, et al. Physiological genomics identifies genetic modifiers of long QT syndrome type 2 severity. J Clin Invest. 2018;128(3):1043-56.
23. Sun Y, Su J, Wang X, Wang J, Guo F, Qiu H, et al. Patient-specific iPSC-derived cardiomyocytes reveal variable phenotypic severity of Brugada syndrome. EBioMedicine. 2023;95:104741.
24. Wu P, Deng G, Sai X, Guo H, Huang H, Zhu P. Maturation strategies and limitations of induced pluripotent stem cell-derived cardiomyocytes. Biosci Rep. 2021;41(6).
25. Lemoine MD, Mannhardt I, Breckwoldt K, Prondzynski M, Flenner F, Ulmer B, et al. Human iPSC-derived cardiomyocytes cultured in 3D engineered heart tissue show physiological upstroke velocity and sodium current density. Sci Rep. 2017;7(1):5464.
26. Giacomelli E, Meraviglia V, Campostrini G, Cochrane A, Cao X, van Helden RWJ, et al. Human-iPSC-Derived Cardiac Stromal Cells Enhance Maturation in 3D Cardiac

Microtissues and Reveal Non-cardiomyocyte Contributions to Heart Disease. Cell Stem Cell. 2020;26(6):862-79 e11.

27. Lee SG, Kim YJ, Son MY, Oh MS, Kim J, Ryu B, et al. Generation of human iPSCs derived heart organoids structurally and functionally similar to heart. Biomaterials. 2022;290:121860.

Supplementary Materials

Supplementary tables

Supplementary Table 1: Primers used for RT-qPCR cardiomyocyte marker panel and PCR mutation analysis of the SCN5A founder mutation.

Gene	Forward primer 5'-3'	Reverse primer 5'-3'
ANK2	TGGACTTCACAGCCAGGAAT	GCCTCGATCCAGTAAGAGCT
ANK3	ACCAAAGGAGGACAGCAACT	GAAAAGACAGACGACCACAGG
CACNA1C	TGACATCGAGGGAGAAAACT	ACATTAGACTTGACTGCGGC
CAV3	GACCCCAAGAACATTAACGAGG	GGACAACAGACGGTAGCACC
ECHS1	AAGGCCCTCAATGCACTTTG	ACTCAGGTTCTGCATTTCCTTG
GAPDH	TGCACCACCAACTGCTTAGC	GGCATGGACTGTGGTCATGAG
GJA1 (CX43)	GGTGACTGGAGCGCCTTAG	GCGCACATGAGAGATTGGGA
HCN4	ACCCATGCTACAGGACTTCC	GAAGAGCGCGTAGGAGTACT
KCND3	AAACAATCACAGGGACTGGC	ACACCATTGTCACCATGACC
KCNH2	TCCTTCTCCATCACCACCTC	AAATCGCCTTCTACCGGAAA
KCNJ2	GTGCGAACCAACCGCTACA	CCAGCGAATGTCCACACAC
KCNJ8	AGTGGAATGGAGAAAAGTGGT	TCCTCTGTCATCATCCTCCC
KCNQ1	ACAAAGTACTGCATGCGTCG	CATGAGAACCAACAGCTTCG
MLC2a	CACCGTCTTCCTCACACTCTT	AGGCACTCAGGATGGCTTC
MLC2v	GATGTTCGCCGCCTTCCCCGC	GCAGCGAGCCCCCTCCTAGT
MYH6	GATAGAGAGACTCCTGCGGC	CCGTCTTCCCATTCTCGGTT
MYH7	TCGTGCCTGATGACAAACAGGAGT	ATACTCGGTCTCGGCAGTGACTTT
RPL13A	CCTGGAGGAGAAGAGGAAAGAGA	TTGAGGACCTCTGTGTATTTGTCAA
RYR2	CATCGAACACTCCTCTACGGA	GGACACGCTAACTAAGATGAGGT
SCN5A	AGCTGGCTGATGTGATGGTC	CACTTGTGCCTTAGGTTGCC
TNNI3	TGTGGACAAGGTGGATGAAG	CCGCTTAAACTTGCCTCGAA
TNNT2	AGAGCGGAAAAGTGGGAAGA	CTGGTTATCGTTGATCCTGT
SCN5A mutation specific	ATCAACCTGCTCTTTGTGGC	CGTCGGGGAGAAGAAGTACT
SCN5A Exon 27 (genotyping)	GGCTTTGGGCTCACTAGAGG	GGGGTGAGAAATGCACTGAA

Supplementary Table 2: List of antibodies used for immunocytochemistry (ICC) staining or Western blot (WB) of iPSC-CMs and iPSCs.

Antibody	Cat nr.	Dilution ICC	Dilution WB
Anti-Sarcomeric Alpha Actinin	ab9465	1/300	
Anti-Cardiac Troponin I	ab47003	1/100	
Connexin 43	14-4759-82	1/100	
Anti-Myosin Light Chain 2	ab79935	1/300	
Nkx2.5	MA5-15551	1/500	
SCN5A Polyclonal Antibody	PA5-115620	1/200	1/200
Anti TRA-1-60	4746	1/200	
Anti TRA-1-81	4745	1/200	
Anti-NANOG	PA1-097	1/500	
Anti-Oct3/4	Sc-9081	1/100	
goat anti-rabbit IgG AF488	A11034	1/500	
goat anti-mouse IgG AF555	A21424	1/500	
Anti-Sodium Potassium ATPase	ab76020		1/1000
Goat Anti-Rabbit IgG -HRP Conjugate	1706515 (biorad)		1/5000 – 1/10000

Supplementary Table 3: TaqMan probes and custom fluorescent label probes for RT-qPR

Gene	Fluorescent label	TaqMan Probe/sequence
GAPDH	FAM	Hs02758991_g1
ECHS1	FAM	Hs00187943_m1
RPL13A	FAM	Hs03043885_g1
WT SCN5A	FAM	TCCATCGTGGGCACTGTGCT
GTGG SCN5A	FAM	TCTCCATCGTGGGTGGGCAC
Deletion SCN5A	HEX	TCTTCACAGGCACTGTGCTCTCG

Supplementary Table 4: Overview of detected CNVs (>100 kb)

Cell line	CNV type	CNV minimal region	CVN size	Genes in the region
BrS3	deletion	Chr1:2522392-2789108	266716	LOC100996583
	deletion	Chr4:34049908-34492968	443060	LINC02484, LINC02484
	duplication	Chr5:3520064-5454709	1934645	LINC01017, ADAMTS16
	deletion	Chr7:62699114-62940543	241429	MIR4283-2, MIR4283-1, LOC100287704
	duplication	Chr7:70186701-71168010	981309	AUTS2
	deletion	Chr8:141260967-141380181	119214	TRAPPC9
	deletion	Chr10:31516419-31795212	278793	LOC101929352
	deletion	Chr19:23619964-24070417	450453	RPSAP58, ZNF675
BrS8	deletion	Chr5:105642031-105830691	188660	
	duplication	Chr9:2382247-2625172	242925	VLDLR-AS1, VLDLR
	deletion	Chr11:90802950-90933499	130549	
	deletion	Chr16:32564812-32959259	394447	TP53TG3B, TP53TG3F, TP53TG3C, TP53TG3E, SLC6A10P, TP53TG3, LOC390705
	deletion	ChrX:7564428-7736547	172119	VCX
BrS9	duplication	Chr14:106997898-107146692	148794	LINC00221
	deletion	Chr19:36938398-38632752	1694354	SNORD152, LOC644189, HKR1, ZNF529, ZFP82, WDR87, ZNF571-AS1, ZNF793-AS1
	duplication	ChrX:191998-1465537	1273539	CRLF2

Cell line	CNV type	CNV minimal region	CVN size	Genes in the region
	duplication	ChrX:1530483-2697868	1167385	LINC00106, XG, AKAP17A, P2RY8, SLC25A6
BrS10	duplication	Chr2:242917734-243029573	111839	LINC01237
	duplication	Chr5:82500295-82685444	185149	XRCC4
	duplication	Chr10:35154346-35451598	297252	CREM
	duplication	Chr13:55256186-55414164	157978	
	deletion	Chr15:22335694-22562318	226624	POTEB2, CXADRP2, MIR3118-4, LINC02203, MIR5701-2, IGHV1OR15-1, POTEB3, MIR3118-2, MIR5701-3, REREP3, POTEB, LOC646214, MIR5701-1,NF1P2, MIR3118-3
	duplication	Chr15:39201066-39313182	106673	
BrS12	deletion	Chr1:99415713-100006117	590404	LINC01708
	deletion	Chr1:189478530-189807634	329104	
	deletion	Chr2:55055307-55167820	112513	EML6
	duplication	Chr14:22802820-22974256	171436	LOC105370401
	duplication	Chr17:44184828-44369335	164962	LRRC37A, NSFP1, ARL17B, ARL17A
	duplication	ChrX:353979-2697868	2343889	XGY2, IL3RA, CRLF2, AKAP17A, MIR6089
Control 1	deletion	Chr4:34049908-34397464	347556	LINC02484, LOC101928622

Cell line	CNV type	CNV minimal region	CVN size	Genes in the region
	deletion	Chr16:32624879-32855389	230510	TP53TG3
	duplication	Chr19:54737010-54841732	104722	LILRA4, LILRA3
	duplication	ChrX:48645256-48746726	101470	GLOD5, TIMM17B, PQBP1, ERAS
	duplication	ChrX:91752101-92408647	656546	PCDH11X
	duplication	ChrX:153606281-153781876	175595	CTAG1A, ATP6AP1, FLNA, FAM223B, FAM223A, CTAG1B, LAGE3
Control 2	deletion	Chr2:141722532-142196011	473479	LRP1B
	deletion	Chr2:242917734-243029573	111839	LINC01237
	duplication	ChrX:958808-1257358-198646	298550	CRLF2

Supplementary Table 5: Statistical analysis of RNA expression (qPCR) of cardiomyocyte markers

Gene	iPSC-CM ANOVA p-value[a]	Significant pairwise differences[b]	Patient/control comparison LMM p-value[c]	iPSC-CM + LV ANOVA p-value[d]	Significant differences towards LV[e]
ANK2	**$3.7x10^{-5}$**	BrS12 vs All iPSC-CM	0.41	**$1.9x10^{-6}$**	BrS12
ANK3	**0.0021**	BrS12 vs BrS3, BrS9, BrS10 & Control 2	0.66	**0.0013**	BrS12
CACNA1C	**0.049**	BrS12 vs Control 1	0.22	**0.020**	BrS12
CAV3	0.075		0.87	**$1.0x10^{-18}$**	All iPSC-CM
ECHS1	**0.0014**	BrS12 vs BrS8, BrS9, BrS12 CRISPR & Control 2	0.53	**$5.1x10^{-6}$**	All iPSC-CM
GAPD	0.52		0.55	0.56	
GJA1	0.17		0.55	0.20	
HCN4	0.14		0.18	0.097	
KCND3	0.088		0.36	0.088	
KCNH2	**0.0038**	BrS12 vs BrS3, BrS9, BrS10, Control 1 & Control 2	0.53	**0.0016**	BrS12
KCNJ2	**0.029**	BrS12 vs BrS3 & Control 1	0.36	**0.034**	
KCNJ8	0.14		0.54	**0.013**	BrS3, BrS10, Control 1, Control 2
KCNQ1	**0.0046**	BrS12 vs BrS3, BrS8, BrS10, BrS12 CRISPR & Control 2	0.49	**$3.8x10^{-4}$**	BrS9, BrS12, Control 1
MLC2a	**0.026**		0.97	**$4.7x10^{-5}$**	All iPSC-CM
MLC2v	0.52		0.53	**0.0028**	All iPSC-CM
MYH6	**0.0022**	BrS12 vs BrS3, BrS8, BrS9, BrS10, BrS12	0.93	**$1.1x10^{-4}$**	BrS9, BrS12, Control 1

Gene	iPSC-CM ANOVA p-value[a]	Significant pairwise differences[b]	Patient/control comparison LMM p-value[c]	iPSC-CM + LV ANOVA p-value[d]	Significant differences towards LV[e]
		CRISPR & Control 2			
MYH7	0.28		0.31	**$2.8x10^{-4}$**	All iPSC-CM
RPL13A	0.41		0.69	0.16	
RYR2	**$3.7x10^{-5}$**	BrS12 vs All iPSC-CM	0.40	**$4.2X10^{-6}$**	BrS3, BrS8, BrS9, BrS10, BrS12 CRISPR, Control 1 , Control 2
SCN5A	0.12		0.13	**0.024**	BrS3, BrS12 CRISPR, Control 2
TNNI3	0.25		0.16	**$7.2x10^{-6}$**	All iPSC-CM
TNNT2	**0.0093**	BrS12 vs BrS3, BrS8 & Control 2	0.36	**0.0065**	BrS12

[a] A one-way ANOVA was performed on the RT-qPCR panel results of the iPSC-CMs
[b] Significant differences were tested with a Tukey HSD post hoc test, only BrS12 showed different expression from the other cell lines.
[c] Patient and control iPSC-CMs did not show difference in cardiac marker expression, tested with a linear mixed model.
[d] A one-way ANOVA was performed on the RT-qPCR panel results of iPSC-CMs and LV
[e] Significant differences were tested with a Dunnett's post hoc test with LV as control group.
LV: Left ventricle

Supplementary Table 6: Peak sodium current density per clone of a cell line.

Cell Line	Mean (pA/pF)	SD	CV%	n	p-value t-test
BrS3 C1	-262	210	80	30	0.16
BrS3 C2	-193	171	89	37	
BrS8 C2	-433	314	73	58	**0.0000006**
BrS8 C3	-176	175	99	51	
BrS9 C3	-400	306	76	24	0.16
BrS9 C7	-293	196	67	23	
BrS10 C3	-65	60	92	13	**0.00000003**
BrS10 C10	-310	159	51	27	
BrS12 C1	-198	287	145	14	0.26
BrS12 C4	-102	101	98	13	
BrS12 CRISPR C1	-500	602	120	25	**0.04**
BrS12 CRISPR C3	-192	245	127	11	
Control 1 C15	-276	248	90	25	**0.00002**
Control 1 C3	-764	599	78	43	
Control 2 C2	-143	117	81	27	**0.03**
Control 2 C3	-282	337	119	36	

SD: standard deviation, CV%: Coefficient of variation, n: number of analysed cells

Supplementary Table 7: Peak sodium current density per individual differentiation of a cell line.

Cell Line	mean	SD	CV%	n	p-value t-test/ANOVA*
BrS3 C1 D1	-325,0	283,2	87	13	0.20
BrS3 C1 D2	-213,6	117,7	55	17	
BrS3 C2 D1	-174,2	156,5	90	8	0.42
BrS3 C2 D2	-259,8	218,6	84	9	
BrS3 C2 D3	-171,4	154,2	90	20	
BrS8 C2 D1	-332,9	257,8	77	29	**0.03**
BrS8 C2 D2	-561,8	347,6	62	24	
BrS8 C2 D3	-391,2	263,6	67	5	
BrS8 C3 D1	-183,3	227,6	124	10	**0.08**
BrS8 C3 D2	-112,9	89,0	79	5	
BrS8 C3 D3	-185,5	122,1	66	3	
BrS8 C3 D4	-127,7	167,3	131	23	
BrS8 C3 D5	-308,3	124,2	40	10	
BrS9 C3 D1	-466,1	357,8	77	15	0.11
BrS9 C3 D2	-291,0	152,5	52	9	
BrS9 C7 D1	-284,3	152,6	54	14	0.81
BrS9 C7 D2	-307,5	259,4	84	9	
BrS10 C3 D1	-65,2	60,3	92	13	
BrS10 C10 D1	-333,1	152,7	46	18	0.31
BrS10 C10 D2	-262,9	171,2	65	9	
BrS12 C1 D1	-258,9	322,8	125	10	0.07
BrS12 C1 D2	-44,7	23,1	52	4	
BrS12 C4 D1	-26,3	13,8	53	3	**0.02**
BrS12 C4 D2	-125,3	104,5	83	10	
BrS12 CRISPR C1 D1	-574,8	685,0	119	18	0.17
BrS12 CRISPR C1 D2	-308,6	246,7	80	7	
BrS12 CRISPR C3 D1	-254,7	283,9	111	7	0.20
BrS12 CRISPR C3 D2	-82,6	114,1	138	4	
Control 1 C3 D1	-1124,3	465,1	41	15	**0.0001**
Control 1 C3 D2	-828,1	656,8	79	16	
Control 1 C3 D3	-229,7	116,8	51	12	
Control 1 C15 D1	-454,5	278,3	61	10	**0.009**
Control 1 C15 D2	-307,7	94,0	31	3	
Control 1 C15 D3	-135,3	161,7	119	5	
Control 1 C15 D4	-108,2	74,8	69	7	
Control 2 C2 D1	-72,8	69,3	95	7	0.13
Control 2 C2 D2	-188,3	157,3	84	10	

Cell Line	mean	SD	CV%	n	p-value t-test/ANOVA*
Control 2 C2 D3	-148,0	71,8	48	10	
Control 2 C3 D1	-499,7	290,4	58	3	0.44
Control 2 C3 D2	-331,8	325,2	98	3	
Control 2 C3 D3	-358,2	232,2	65	9	
Control 2 C3 D4	-267,9	449,7	168	14	
Control 2 C3 D5	-99,3	122,3	123	7	

*A t-test was used when there were only two differentiations per clone, otherwise a one-way ANOVA was used

SD: standard deviation, CV%: Coefficient of variation, n: number of analysed cells

Supplementary Table 8: $Na_V1.5$ membrane expression

	BrS3	BrS12	BrS9	BrS10	BrS8	BrS12 CRISPR	Control 1	Control 2
Mean	0.11	0.08	0.24	0.10	0.36	0.11	1.00	0.29
SD	0.10	0.05	0.20	0.14	0.18	0.15	0.93	0.10
CV%	92	72	84	135	49	141	93	33
n	5	2	4	4	3	2	2	2

SD: standard deviation, CV: Coefficient of variation, n: number of analysed samples

Supplementary Table 9: Relative expression of cardiomyocyte markers

	n=4	BrS 3	BrS 12	BrS 9	BrS 10	BrS 8	BrS12 CRISPR	Control 1	Control 2
ANK2	**Mean**	0,58	1,78	0,92	0,76	0,83	0,61	1,00	0,50
	SD	0,16	0,52	0,24	0,15	0,43	0,24	0,20	0,15
	CV%	28	29	26	20	51	40	20	29
ANK3	**Mean**	0,39	1,47	0,55	0,44	0,84	0,40	1,00	0,34
	SD	0,35	0,30	0,43	0,27	0,76	0,27	0,49	0,19
	CV%	89	20	77	61	91	67	49	54
CAV3	**Mean**	1,78	0,47	1,46	0,33	1,42	1,32	1,00	0,79
	SD	1,08	0,36	1,15	0,61	0,63	1,57	0,77	0,44
	CV%	61	78	78	184	44	119	77	56
GJA1	**Mean**	1,40	0,96	1,06	1,28	2,54	0,84	1,00	1,57
	SD	0,51	0,22	1,03	1,07	1,16	0,98	0,50	1,51
	CV%	36	23	97	83	46	117	50	96
HCN4	**Mean**	1,98	3,35	2,23	2,35	1,21	1,92	1,00	1,58
	SD	0,66	2,45	1,10	1,20	0,83	0,63	0,31	0,57

	n=4	BrS 3	BrS 12	BrS 9	BrS 10	BrS 8	BrS12 CRISPR	Control 1	Control 2
	CV%	34	73	49	51	69	33	31	36
KCND3	**Mean**	2,55	5,23	2,01	2,53	2,53	2,97	1,00	2,63
	SD	1,92	2,18	2,08	4,20	2,33	0,66	1,02	1,21
	CV%	75	42	103	166	92	22	102	46
KCNH2	**Mean**	0,70	2,52	1,03	0,74	1,14	0,99	1,00	0,79
	SD	0,06	1,36	0,38	0,19	0,69	0,09	0,26	0,25
	CV%	8	54	37	25	61	9	26	32
KCNJ2	**Mean**	1,14	4,64	1,52	1,81	2,51	1,55	1,00	1,88
	SD	0,62	2,86	1,31	1,51	1,51	1,31	0,21	1,04
	CV%	55	62	86	83	60	84	21	55
KCNJ8	**Mean**	0,62	2,26	1,15	0,60	1,56	0,99	1,00	0,93
	SD	0,26	1,56	1,25	0,26	1,30	0,45	0,67	0,61
	CV%	42	69	109	43	83	45	67	66
KCNQ1	**Mean**	0,71	1,57	0,94	0,71	0,83	0,56	1,00	0,72
	SD	0,20	0,49	0,13	0,35	0,50	0,08	0,20	0,26
	CV%	28	31	14	48	60	15	20	36
CACNA1C	**Mean**	1,09	3,42	1,96	1,46	2,04	1,34	1,00	1,36
	SD	0,09	1,49	1,27	0,74	2,23	0,72	0,40	0,54
	CV%	9	44	65	51	109	53	40	40
RYR2	**Mean**	0,59	2,10	1,06	0,71	1,07	0,68	1,00	0,62
	SD	0,11	0,65	0,30	0,10	0,57	0,25	0,11	0,21
	CV%	18	31	29	14	53	37	11	34
SCN5A	**Mean**	0,63	1,31	1,33	1,00	1,66	0,35	1,00	0,53
	SD	0,45	0,73	0,41	1,06	1,02	0,39	0,52	0,33
	CV%	71	56	31	106	62	109	52	63
TNNI3	**Mean**	1,12	1,11	1,16	1,25	0,75	0,36	1,00	0,83
	SD	0,20	0,56	0,29	0,63	0,53	0,16	0,32	0,35
	CV%	18	50	25	50	71	45	32	41
TNNT2	**Mean**	0,76	1,42	1,03	1,06	0,76	0,71	1,00	0,74
	SD	0,18	0,24	0,17	0,39	0,38	0,35	0,22	0,21
	CV%	23	17	16	37	50	49	22	29
MLC2a	**Mean**	0,71	1,17	1,11	0,92	0,62	1,05	1,00	0,69
	SD	0,38	0,18	0,36	0,22	0,14	0,36	0,19	0,20
	CV%	54	16	32	24	23	35	19	30
MLC2v	**Mean**	0,48	1,64	0,60	0,83	1,62	0,25	1,00	0,82
	SD	0,50	1,97	0,76	0,65	1,16	0,27	0,49	1,24
	CV%	103	120	127	79	71	109	49	151

	n=4	BrS 3	BrS 12	BrS 9	BrS 10	BrS 8	BrS12 CRISPR	Control 1	Control 2
MYH6	**Mean**	0,49	1,43	0,74	0,64	0,65	0,71	1,00	0,59
	SD	0,09	0,42	0,27	0,05	0,45	0,24	0,41	0,20
	CV%	18	30	36	8	69	34	41	33
MYH7	**Mean**	0,40	2,42	0,57	1,13	2,86	0,19	1,00	0,67
	SD	0,49	3,32	0,57	1,35	3,29	0,24	0,78	0,94
	CV%	121	137	100	119	115	127	78	141
RPL13A	**Mean**	1,25	0,77	1,10	0,99	1,04	0,98	1,00	1,22
	SD	0,22	0,40	0,09	0,18	0,53	0,13	0,25	0,34
	CV%	17	52	8	18	51	13	25	28
ECHS1	**Mean**	0,89	1,10	0,82	1,00	0,88	0,77	1,00	0,86
	SD	0,05	0,05	0,04	0,11	0,16	0,06	0,12	0,05
	CV%	6	5	5	11	19	8	12	6
GAPDH	**Mean**	0,86	1,41	1,04	0,98	1,22	1,24	1,00	0,93
	SD	0,11	0,77	0,12	0,23	0,56	0,07	0,34	0,19
	CV%	13	55	12	23	46	5	34	20

SD: standard deviation, CV: Coefficient of variation, n: number of analysed samples

Supplementary Figures

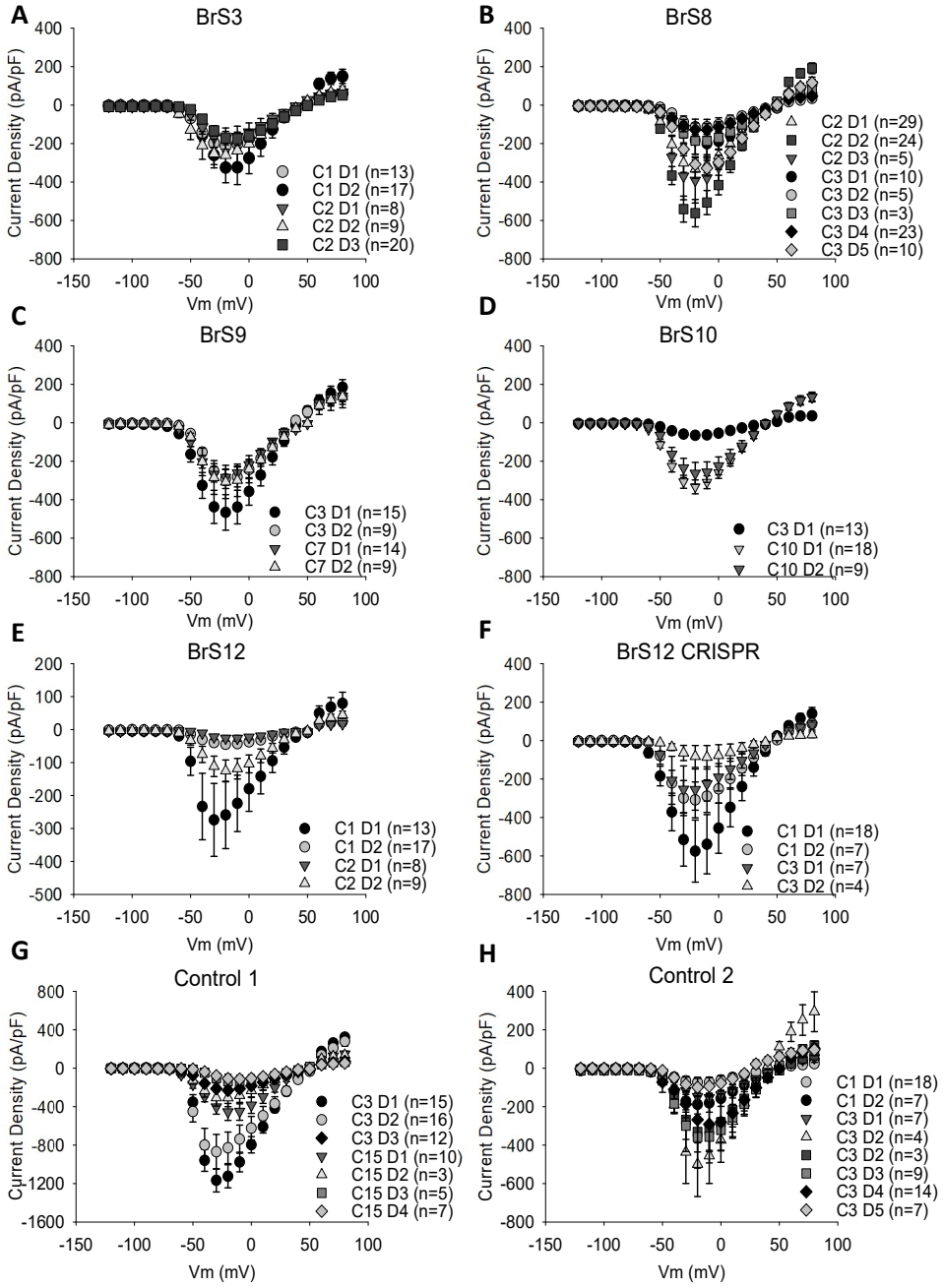

Supplementary Figure 1: Sodium Current Density in BrS patient and control iPSC-CMs. Peak sodium current density per individual differentiation per cell line. The amount of recorded cells per cell line is displayed as (n=). Results are depicted as mean ± standard error of mean (SEM).

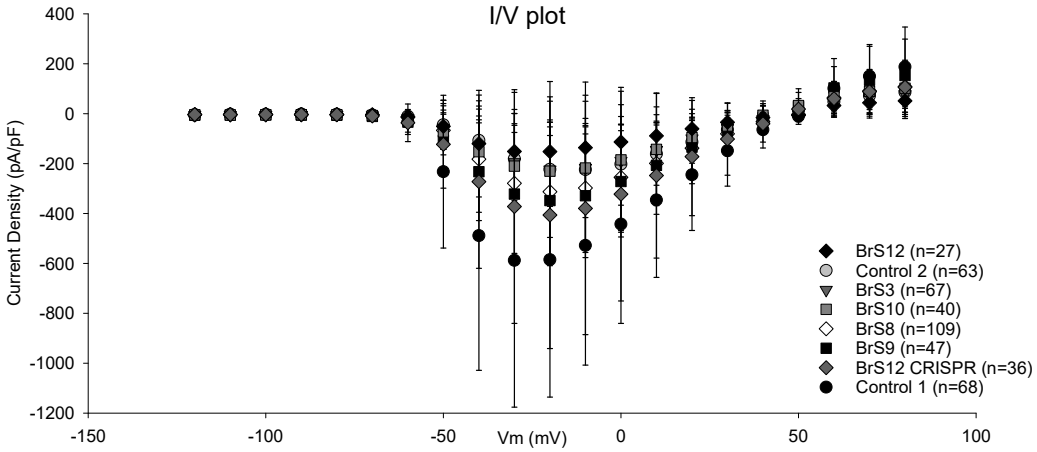

Supplementary Figure 2: Current-voltage (I-V) relationship of all patients and controls depicted as mean ± standard deviation.

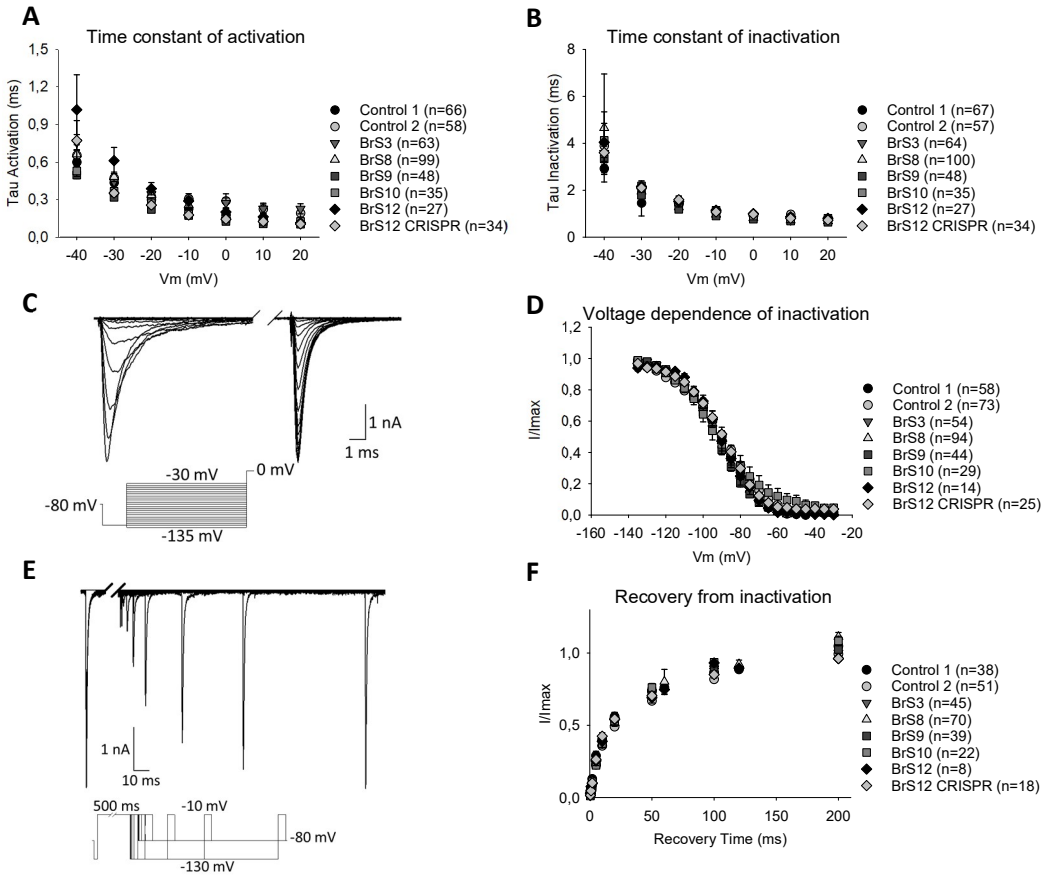

*Supplementary Figure 3: Sodium current characterization in BrS patient and control iPSC-CMs. A-**B**) Sodium current activation (A) and inactivation kinetics (B) calculated from the activation pulse protocol. C) Representative trace of sodium current inactivation with the used protocol. D) Voltage dependence of inactivation curve. E) Representative trace of recovery from sodium current inactivation with the used protocol. F) Recovery from inactivation curve. No differences were observed between patients and controls.*

General discussion

Inherited Cardiac Arrhythmias

Inherited cardiac arrhythmias (ICA) are a group of cardiac diseases that lead in worst case to sudden cardiac death (SCD). The most well-known inherited cardiac arrhythmias include long QT syndrome (LQTS), Brugada syndrome (BrS), catecholaminergic polymorphic ventricular tachycardia (CPVT), short QT syndrome (SQTS) and arrhythmogenic cardiomyopathy (ACM), previously known as arrhythmogenic right ventricular cardiomyopathy (ARVC). They share some common characteristics such as low prevalence, reduced penetrance and symptoms like syncope, ventricular fibrillation and SCD. Identification of a genetic cause is not complete for every ICA (1, 2). Genes involved in these diseases partially overlap and encode sodium, potassium and calcium ion channels and their associated proteins for LQTS, SQTS and BrS, desmosomal genes or genes encoding intercalated disc proteins for ACM and in genes playing a role in calcium homeostasis for CPVT. (Likely) pathogenic variants located in these genes are found in up to 80% of the LQT patients, 50% to 65% in CPVT and ACM cases while only 20% to 30% of the SQTQ and BrS patients harbour a known causal variant (2-5). This indicates that depending on the disease, up to 80% of the patients remains without a genetic diagnosis, making (genetic) counselling for the patients and their families more difficult. With the development of the next generation sequencing (NGS) technologies such as NGS panels, whole exome and genome sequencing (WES, WGS) more genes could be screened at the same time. This however did not solve the missing heritability observed in ICAs. One of the reasons for this are the variants of unknown significance (VUS) of which the impact on the functioning of the gene is currently not certain. These VUS could be causative for the disease, but currently there is not sufficient evidence yet. Another important factor that could partially explain this missing heritability is the more complex genetic architecture where (common) variants located in several genes do interact to cause the development of the disease. In addition, our knowledge on the effect of non-coding and e.g. (deep) intronic variants that could influence the expression level of genes and contribute to the disease mechanism, is currently far from complete.

The quest for causal variants of ICAs in the NGS era

Next generation sequencing technologies made it possible to sequence many genes, if not all, at the same time and even intronic sequences are processed with the WGS technique.

The worst possible outcome and how to proceed – Molecular autopsy

Sudden cardiac death (SCD) has an estimated annual incidence of 1:1000. In the young (<50 years) a genetic cause is suspected in up to 80% of the SCD cases, with inherited cardiac arrhythmia or cardiomyopathy among the main disease categories (6). Sudden death is often the first symptom that presents and when this event occurs, the patient itself (when he/she survives) and/or family members remain with many questions on the cause of this event and their own risk. This is where molecular and clinical diagnostics come into play. When the patient survived, a full clinical check-up and genetic analysis can be performed which might reveal diagnostic clues and answers for further treatment and management for the disease. If on the other hand the patient died, an autopsy or toxicology screen might provide insights in the underlying cause, but sometimes, for example in the case of inherited cardiac arrhythmias, no visible changes can be observed. In this instance looking into the genome by performing a molecular autopsy can unravel the cause of the cardiac arrest and inform the family members on their risk (7).

In **Chapter 1** a case of a man who died suddenly in his sleep is presented. It was impossible to perform an autopsy on this person but the molecular autopsy with a NGS panel investigating ICA genes revealed that he carried two missense variants in the *KCNQ1* and *DSG2* genes, both initially classified as VUS. Further segregation analysis in family members demonstrated the *de novo* occurrence of the *DSG2* variant which led to the reclassification of the variant to likely pathogenic following the ACMG guidelines (8), indicating the *DSG2* variant as most likely cause of SCD. Segregation analysis revealed that both the mother and daughter of the patient carried the *KCNQ1* variant and although this is a VUS, precautions must be taken in carriers of this variant to prevent or suppress any symptoms.

A recent consensus report on molecular testing in sudden cardiac death patients by Wilde et al. elaborates on when and how this should be performed (7). They advise to first screen for channelopathies either with an NGS panel or targeted WES/WGS, which can be extended to cardiomyopathies. Hypothesis-free WES/WGS however is not recommended. The implementation of a virtual WES panel analysis identified a disease-causing variant in 10% of 228 cardiac arrest survivors in a recent study (7, 9). In other studies (likely) pathogenic variants are found using NGS panels (10-12) or a virtual WES panel (13) in 10% to 34% of the cases (10-13). VUS were detected in 20% to 42% of the individuals (11-13). Looking outside of these virtual WES panel genes could potentially lead to the identification of novel candidate genes, but those would need further investigation. As NGS panels, WES and WGS will reach similar costs, choices have to be

made which one to use in a diagnostic setting. WGS provides information on the whole genome, including the non-coding part. This non-coding part plays a role in various processes that are not yet fully understood in a normal, healthy context, let alone in disease mechanisms, which will for now result in the detection of even more VUS. So more research needs to be performed on the non-coding part of the genome. However, efforts have been made in this field to study non-coding RNAs and epigenetic influences such as methylation, histone modification and 3D genome architecture (14). Combining the WGS data with transcriptome data will also improve the knowledge on regulatory mechanisms in diseases (15). WGS data collected at this moment, can in the future be re-evaluated when more information is available on disease mechanisms and in this way help to give a genetic diagnosis to patients later on. Several of this re-evaluation studies have been performed in different disease areas and found indeed an increase in diagnostic yield after several months/years (16-18).

Genetic complexity in Brugada syndrome

Brugada syndrome was first described in 1992 and is diagnosed by a typical ST segment elevation followed by a T wave inversion (Type I) in the right precordial leads of the electrocardiogram (ECG) (19). This occurs either spontaneously or after provocation with a sodium channel blocker such as ajmaline (19). It has a prevalence of 1 in 2000 and patients show symptoms such as syncopes, ventricular arrhythmias and sudden cardiac arrest. Several scoring systems, based on the Type I ECG, family history and occurrence of symptoms, have been developed to improve the diagnosis of BrS including the Shanghai , Sieira and Delise score (20-22). In approximately 20 to 30% of the patients a (likely) pathogenic variant is found, mostly a loss-of-function variant in the *SCN5A* gene encoding the alpha subunit of the cardiac voltage gated sodium channel $Na_v1.5$. Current treatment exists of the immediate treatment of fever, avoidance of specific drugs and in symptomatic patients an implantable cardioverter defibrillator should be considered.

Currently, only *SCN5A* is linked to BrS, although up to 43 genes have been associated with the disease (23, 24). It is reported that only up to 30% of the patients have a definite genetic diagnosis. In **Chapter 2** we genetically analysed a cohort of 350 BrS patients using a gene panel of 51 or 60 ICA associated genes. Clinical parameters were collected and the analysis of these data in correlation to the genotype revealed a higher incidence of ventricular arrhythmias in patients carrying a Pathogenic (P) or Likely pathogenic (LP) variant as well as more familial history and a higher Shanghai score. As previously reported, these BrS patients have a prolonged PR interval and QRS complex compared to the groups with only a VUS or no variant (25-27). Looking at the total genetic yield we found that 9% carried a P/LP mutation which is lower than the 20 to 30% that is generally

reported. If we diagnose the patients according to the Shanghai score, we have 160 patients with a definite BrS diagnosis and the molecular diagnostic yield in this group is 18%. All P/LP variant except two are located in *SCN5A,* currently considered as the only causal gene for BrS. The two LP variants are located in *LMNA/C* and *SCN2B,* providing additional supporting evidence for their role in BrS pathogenesis. VUS are found in 31% of the BrS patients and some of these variants might be causal, but there is currently a lack of evidence. *SCN5A* is the gene with the most VUS, followed by *CACNA1C* indicating that this gene also plays a role in the BrS pathology. Although the identification of a P/LP variant does not lead to a different clinical management, it does have an impact on the patient's family members. Those can be screened for the specific variant and with the help of genetic counselling, they can be informed on their risk for developing the disease. On top of that, preimplantation diagnostics can be provided if needed/wanted.

These results underline that the genetic architecture of BrS is not as straightforward as first thought. A monogenic Mendelian mode of inheritance with reduced penetrance has long been proposed. But more recently this idea is challenged and a more complex mode of inheritance is suggested where genetic modifiers and/or common variants play a role in the development of the disease. Genome wide association studies (GWAS) have demonstrated that single nucleotide polymorphisms (SNPs) in several loci such as the SC*N5A-SCN10A* and *HEY2* loci are associated with BrS (28). Additional loci also include genes encoding cardiac developmental transcription factors that are involved in the regulation of ion channel expression in the adult heart, including that of $Na_v1.5$ and genes encoding microtubule or myofiber associated proteins (29). The common *SCN5A* H558R polymorphism has been reported to improve sodium channel gating kinetics and trafficking of mutated channels possibly by restoring correct folding and to increase expression of $Na_v1.5$ by reduction of promotor methylation (30-32). However, this modifier will probably not have an effect on every type of *SCN5A* mutation as total loss of function mutations and truncating mutations often don’t lead to the production of repairable protein. Other types of genetic aberrations such as CNVs are rarely detected in BrS patients and most of them are located in *SCN5A* (33, 34). These data emphasize the complex and more oligogenic character of BrS (35, 36).

Overall with the NGS technique, many questions have been resolved, but many new questions have also been added. The number of variants that are detected is huge and scoring them for the possible impact they might have remains challenging. Therefore ACMG guidelines have been established to streamline the interpretation of variants. Numerous variants however are still under debate and are classified as VUS and to reclassify them, functional research is needed.

The hunt for functional evidence of pathogenicity

The genetic landscape of ICA is mainly populated by ion channel genes and its associated proteins although regulatory and structural genes play a role in these disorders as well. The effect of a variant in these ion channel is often studied in a heterologous expression system. Here a cell type such as HEK293, TSA201, COS-7, CHO or xenopus oocytes is transfected with a plasmid to express the gene with the variant of interest. In **Chapter 1**, the *KCNQ1* variant detected in the proband and his mother and daughter was classified as a VUS. To better understand the impact of this variant, it was modelled in HEK cells and patch clamp analysis did not reveal significant changes in electrophysiological function compared to wild type. This reassured both the mother and daughter that they don't have an increased risk of SCD and they could be taken of beta-blocker treatment. This case report emphasises the added value of a molecular autopsy followed by segregation analyses and functional investigation for family members. Unfortunately, not every VUS is as easily modelled and reclassified as either pathogenic or benign which makes an accurate risk assessment or management challenging. In a diagnostic setting, functional evidence mostly arises from literature and *in silico* pathogenicity prediction programs such as Polyphen and MutationTaster, although these results are not always concordant with functional testing (37, 38). *In vitro* and *in vivo* functional testing of VUS on the other hand is not (yet) routinely done in a diagnostic setting because most of the current analyses are not high throughput, have a high cost and are time-consuming. This is why collaborations with specific research laboratories are beneficial and the further development of novel high-throughput technologies will help in the future interpretation of VUS.

One advantage of heterologous expression systems (HES) is that you can easily investigate the molecular mechanism of a mutation although caution is needed as the results of these experiments could differ because of the variety of cell types (39). Another drawback of this method is that you cannot model the human complexity of ventricular cardiomyocytes (CM) in these expression systems as they are not all of human origin and don't possess the machinery to mimic CMs. Native human cardiomyocytes on the other hand are currently the best model to study BrS on a cellular level however these are not easily obtained from patients. One way to overcome this problem is by using the innovative induced pluripotent stem cell (iPSC) technique. These cells can be generated from different human cell types such as blood cells and skin fibroblasts and carry the full genetic background of the donor. Because of the pluripotent character they can be differentiated in all cell types of the human body, including cardiomyocytes, so called iPSC-derived cardiomyocytes (iPSC-CM). Some studies compare the use of heterologous expressions systems with iPSC-CMs to investigate the

effect of mutations on ion channels. De la Roche et al. for example found no changes in sodium channel inactivation properties in the HES while a small shift was observed in iPSC-CMs of a BrS patient (40). A similar minor difference in activation and inactivation shifts of sodium current curves between HES and iPSC-CMs was observed by Ma et al. for BrS a patient (41). In the **Introduction**, an overview of several iPSC-CM models of ICAs is given. iPSC-CM models have been used to increase the knowledge on the pathophysiological mechanisms of cardiac diseases as well as for development of therapies and drug treatment, not only in 2D models but also 3D models such as organoids, microtissues, engineered heart tissue and organ-on-a-chip. These *in vitro* tissue-like structures mimic even more closely the situation of a heart in the human body, which makes them an ideal model to study cardiac arrhythmia diseases such as BrS.

In **Chapter 3,** we described how we generated iPSC of BrS patients carrying a Belgian *SCN5A* founder mutation (c.4813+3_4813+6dupGGGT) starting from fibroblasts. This mutation has previously been described on molecular and clinical level (25, 42, 43). Molecularly this mutation leads to the generation of several mutant mRNA transcripts. Two of these result in a premature stop codon and one in a protein with a deletion of 32 amino acids that is reported to be non-functional. On a clinical level, mutation carriers show a variety of symptoms ranging from no symptoms at all over atrial dysrhythmias, cardiac conduction defect to ventricular fibrillations and sudden cardiac death. In **Chapter 4**, iPSC-CMs of five BrS patients with a different severity of the disease, two unrelated healthy controls and one isogenic control were generated and analysed on a molecular and electrophysiological level. In patients, two mutant transcripts were detected that were not observed in controls. However, this did not lead to a significant difference in membrane expression of $Na_v1.5$ between patient and controls. Additionally, the peak sodium current did not differ significantly between patient and control iPSC-CMs which was not expected as the mutant transcript is reported as not functional. One contributing factor is that one of the control cell lines showed sodium current densities more comparable with those of the patients than the current densities of the other control line and the isogenic control. Use of an isogenic control is of added value in mutation analysis investigations as the genetic background of this control is the same as that of the patient except for the mutation under investigation. As was shown in our results, the isogenic control indeed showed a 'normal' phenotype with an increased sodium current peak compared to the patient iPSC-CMs and the absence of mutant *SCN5A* transcripts. When the deviating control is excluded, statistically significant results between patients and control individuals were not obtained which can partly be explained by the high variability we observe not only in sodium current and action potential data but also in qPCR and western blot data. Variable results were found

within differentiations of one clone of an individual (intraclonal) and between two different clones of an individual (interclonal). Interclonal variability might arise from (small) genetic alterations that occur during the generation of the iPSCs while differences between several differentiations of the same clone could be the result of small culture condition changes, such as different batches of medium or small molecules. Although we tried to keep everything as equal as possible for the differentiations and differentiate as many cell lines as possible at the same time, this is not always practically feasible and can also be a source of variability.

Although iPSC-CM is a worthy alternative of native cardiomyocytes of a patient, some side notes should be considered. One important note is the maturity status of the generated iPSC-CMs, often they are only in culture for 30 to 60 days, which is considerably less compared to native CMs. This will result in structural immaturity with smaller and more round cells, less organised sarcomeres and no T-tubules (44, 45). Functionally, these immature iPSC-CMs resemble more the foetal state of the native CMs with a glucose metabolism instead of the fatty acid β-oxidation and action potentials characteristics such as less negative resting membrane potentials and a slower upstroke velocity (44, 45). Genes regulating these APs are also less or not expressed in iPSC-CM, such as the I_{K1} gene and structural genes are more expressed in their foetal isoform (44, 45). Efforts have been made to improve the maturity of the iPSC-CM culture with biochemical (dexamethasone, thyroid hormone (T3), fatty acid) or electrical stimulation, long-term culture and 3D-cultures (46, 47). In **Chapter 4**, T3 is used for the promotion of maturation together with a culture time of at least 35 days. With many differentiation protocols a mixture of several cardiac cell types is generated and to select on cardiomyocytes, glucose deprivation treatment is performed, which is based on the capability of CMs to switch from glucose as energy source to lactate for example (48). We applied this method for 6 days to purify our culture for CM. Although the protocol we used generated iPSC-CMs, this protocol was not always reproducible meaning that when we started a differentiation, this would not every time lead to (sufficient) beating cardiomyocytes after 14 days. Even when beating cardiomyocytes were observed, not every well of the 6-well plate differentiated as efficient since some wells did not show any beating activity. A study performed in 2019 elaborates on this reproducibility and tested five differentiation protocols where the percentage of successful differentiations varies from 35% to 95% (49).

The current differentiation and analysis methods allow us to investigate ICA in a cell type specific manner, although not as efficient as we wanted. To improve this efficiency, more robust protocols and high throughput methods should be developed and applied.

What will the future bring?

One common point in ICAs is that the underlying genetic background is still not fully understood. In case of BrS for example, still 70% of the patients don't have a genetic diagnosis. The answer of this missing heritability might lie in the more complex combination of genes that play a role in the development of the disease. Depending on the number of genes involved in the development of the disease, the term oligogenic or polygenic can be used. When just a few genes act together, this is called oligogenic. If many genes with a very small effect size are interacting, we refer to this as polygenic. The latter is mostly used for continuous traits that are also influenced by non-genetic factors. In combination with the oligogenic or polygenic inheritance, the use of polygenic risk scores has gained interest. A polygenic risk score gives an indication of your risk of a certain disease based on the presence of specific polymorphisms in specified genes. For BrS, some risk scores have been tested using up to 21 risk alleles which might in the future be used as a diagnostic tool to identify BrS patients at a high risk of developing a severe phenotype (29, 50, 51). Here, a multi-omics approach, where you look at the genome, transcriptome, epigenome and proteome will improve the further understanding.

With improved techniques such as NGS, novel insights in the genetic landscape of ICAs have been gained. But in many ICA patients, a clear genetic cause is not yet identified or VUS are detected. However, following the current ACMG guidelines, these are not considered causal because of lack of evidence. This is a major issue that can be tackled with advanced techniques that are being developed. The iPSC-CM field for example has proven its worth in modelling diseases and can now be used to evaluate the pathogenicity of variants in a patient-specific way or when combined with DNA editing techniques such as CRISPR/Cas9 more generally. Currently, the patch clamp method is still the golden standard to measure individual currents and action potentials of a cell. Although it is an accurate technique, it is labour intensive and low throughput. Automated patch clamp devices can overcome this and together with the Multi Electrode Array (MEA) will increase the throughput which will lead to a better understanding of disease mechanisms and interpretation of variants, including VUS. For example, a high-throughput screen of ion channel variants can be performed using an automated patch clamp system where 384 cells can simultaneously be recorded (52, 53). Similarly, MEA systems are also increasing their throughput with larger multi-well plates. These systems record extracellular field potentials similar to ECG recordings. By using specific stimulation protocols they can also record local extracellular action potentials (LEAP), similar to action potentials measured with the patch clamp technique (54). Another technique that improves the throughput is via the use fluorescent imaging in

combination with both genetically encoded calcium and voltage indicators (GECI/GEVI) (55, 56). They can be used to either follow the calcium flux in cells or changes in voltage over the cell membrane which results in calcium transient and action potential recordings respectively (55, 56) and can be scaled up using multi-well approaches. Fluorescent imaging can as well be applied to investigate VUS for example for possible trafficking deficiency variants (57).

The combination of these sophisticated analysis techniques as MEA, automated patch clamp and optical imaging with GEVIs and GECIs, will lead to novel insights regarding detected VUS. The current iPSC-CM models still show a more immature phenotype, where efforts have been made to improve the maturity with electrical, mechanical and biochemical stimulation. Together with the development of 3D iPSC-CM models with or without combination with other cardiac cell types, this will lead to models that more closely resemble the physiology of the human heart. One important remark that should be made is that there is some degree of variability which makes it difficult to pick up small phenotypical differences and might hamper the interpretation of VUS in the future.

In addition to the utility of *in vitro* models for advancing research, *in vivo* models will play a significant role in investigating ICAs. While several models, predominantly relying on mice, have already been established, the introduction of zebrafish represents a more recent development in the ICA research landscape. Despite anatomical differences in their hearts, zebrafish demonstrate electrophysiology more comparable to human than mice do. The integration of innovative techniques such as CRISPR/Cas9, GEVI/GECI, and refined imaging methods further elevates the potential of studying ICAs. These cutting-edge tools, in combination with zebrafish models, hold great promise for uncovering and classifying variants in ICAs.

Gaining deeper insights into the genetic architecture of ICAs is not only beneficial for genetic counseling of patients and their families but also promises advancements in our understanding of disease mechanisms. This, coupled with the development of innovative study models, will pave the way for the discovery of new and improved therapies for ICA, particularly where existing pharmacological treatments are limited. Additionally, these models can serve as robust testing platforms for newly developed drugs. A more personalized approach involves generating cell models directly from patients for patient-specific testing of therapies, offering a more individualized perspective on treatment efficacy.

One thing is certain: the genetic landscape of ICAs is far from fully understood and a combination of novel and innovative genetic and functional techniques will be needed to fill this knowledge gap.

References

1. Schwartz PJ, Ackerman MJ, Antzelevitch C, Bezzina CR, Borggrefe M, Cuneo BF, et al. Inherited cardiac arrhythmias. Nat Rev Dis Primers. 2020;6(1):58.
2. Gerull B, Brodehl A. Insights Into Genetics and Pathophysiology of Arrhythmogenic Cardiomyopathy. Curr Heart Fail Rep. 2021;18(6):378-90.
3. Schwartz PJ, Ackerman MJ, George AL, Jr., Wilde AAM. Impact of genetics on the clinical management of channelopathies. J Am Coll Cardiol. 2013;62(3):169-80.
4. Gray B, Behr ER. New Insights Into the Genetic Basis of Inherited Arrhythmia Syndromes. Circ Cardiovasc Genet. 2016;9(6):569-77.
5. Gollob MH, Redpath CJ, Roberts JD. The short QT syndrome: proposed diagnostic criteria. J Am Coll Cardiol. 2011;57(7):802-12.
6. Saenen JB, Van Craenenbroeck EM, Proost D, Marchau F, Van Laer L, Vrints CJ, et al. Genetics of sudden cardiac death in the young. Clin Genet. 2015;88(2):101-13.
7. Wilde AAM, Semsarian C, Marquez MF, Sepehri Shamloo A, Ackerman MJ, Ashley EA, et al. European Heart Rhythm Association (EHRA)/Heart Rhythm Society (HRS)/Asia Pacific Heart Rhythm Society (APHRS)/Latin American Heart Rhythm Society (LAHRS) Expert Consensus Statement on the State of Genetic Testing for Cardiac Diseases. Heart Rhythm. 2022;19(7):e1-e60.
8. Richards S, Aziz N, Bale S, Bick D, Das S, Gastier-Foster J, et al. Standards and guidelines for the interpretation of sequence variants: a joint consensus recommendation of the American College of Medical Genetics and Genomics and the Association for Molecular Pathology. Genet Med. 2015;17(5):405-24.
9. Grondin S, Davies B, Cadrin-Tourigny J, Steinberg C, Cheung CC, Jorda P, et al. Importance of genetic testing in unexplained cardiac arrest. Eur Heart J. 2022;43(32):3071-81.
10. Larsen MK, Christiansen SL, Hertz CL, Frank-Hansen R, Jensen HK, Banner J, et al. Targeted molecular genetic testing in young sudden cardiac death victims from Western Denmark. Int J Legal Med. 2020;134(1):111-21.
11. Christiansen SL, Hertz CL, Ferrero-Miliani L, Dahl M, Weeke PE, LuCamp, et al. Genetic investigation of 100 heart genes in sudden unexplained death victims in a forensic setting. Eur J Hum Genet. 2016;24(12):1797-802.
12. Lahrouchi N, Raju H, Lodder EM, Papatheodorou E, Ware JS, Papadakis M, et al. Utility of Post-Mortem Genetic Testing in Cases of Sudden Arrhythmic Death Syndrome. J Am Coll Cardiol. 2017;69(17):2134-45.
13. Shanks GW, Tester DJ, Ackerman JP, Simpson MA, Behr ER, White SM, et al. Importance of Variant Interpretation in Whole-Exome Molecular Autopsy: Population-Based Case Series. Circulation. 2018;137(25):2705-15.
14. Wang M, Tu X. The Genetics and Epigenetics of Ventricular Arrhythmias in Patients Without Structural Heart Disease. Front Cardiovasc Med. 2022;9:891399.
15. Andersen JD, Jacobsen SB, Trudso LC, Kampmann ML, Banner J, Morling N. Whole genome and transcriptome sequencing of post-mortem cardiac tissues from sudden cardiac death victims identifies a gene regulatory variant in NEXN. Int J Legal Med. 2019;133(6):1699-709.

16. Bartolomaeus T, Hentschel J, Jamra RA, Popp B. Re-evaluation and re-analysis of 152 research exomes five years after the initial report reveals clinically relevant changes in 18. Eur J Hum Genet. 2023.
17. Tan NB, Stapleton R, Stark Z, Delatycki MB, Yeung A, Hunter MF, et al. Evaluating systematic reanalysis of clinical genomic data in rare disease from single center experience and literature review. Mol Genet Genomic Med. 2020;8(11):e1508.
18. Machini K, Ceyhan-Birsoy O, Azzariti DR, Sharma H, Rossetti P, Mahanta L, et al. Analyzing and Reanalyzing the Genome: Findings from the MedSeq Project. Am J Hum Genet. 2019;105(1):177-88.
19. Brugada P, Brugada J. Right bundle branch block, persistent ST segment elevation and sudden cardiac death: a distinct clinical and electrocardiographic syndrome. A multicenter report. J Am Coll Cardiol. 1992;20(6):1391-6.
20. Kawada S, Morita H, Antzelevitch C, Morimoto Y, Nakagawa K, Watanabe A, et al. Shanghai Score System for Diagnosis of Brugada Syndrome: Validation of the Score System and System and Reclassification of the Patients. JACC Clin Electrophysiol. 2018;4(6):724-30.
21. Sieira J, Conte G, Ciconte G, Chierchia GB, Casado-Arroyo R, Baltogiannis G, et al. A score model to predict risk of events in patients with Brugada Syndrome. Eur Heart J. 2017;38(22):1756-63.
22. Delise P, Allocca G, Marras E, Giustetto C, Gaita F, Sciarra L, et al. Risk stratification in individuals with the Brugada type 1 ECG pattern without previous cardiac arrest: usefulness of a combined clinical and electrophysiologic approach. Eur Heart J. 2011;32(2):169-76.
23. Hosseini SM, Kim R, Udupa S, Costain G, Jobling R, Liston E, et al. Reappraisal of Reported Genes for Sudden Arrhythmic Death: Evidence-Based Evaluation of Gene Validity for Brugada Syndrome. Circulation. 2018;138(12):1195-205.
24. Campuzano O, Sarquella-Brugada G, Fernandez-Falgueras A, Cesar S, Coll M, Mates J, et al. Genetic interpretation and clinical translation of minor genes related to Brugada syndrome. Hum Mutat. 2019;40(6):749-64.
25. Sieliwonczyk E, Alaerts M, Robyns T, Schepers D, Claes C, Corveleyn A, et al. Clinical characterization of the first Belgian SCN5A founder mutation cohort. Europace. 2021;23(6):918-27.
26. Maury P, Rollin A, Sacher F, Gourraud JB, Raczka F, Pasquie JL, et al. Prevalence and prognostic role of various conduction disturbances in patients with the Brugada syndrome. Am J Cardiol. 2013;112(9):1384-9.
27. Robyns T, Nuyens D, Vandenberk B, Kuiperi C, Corveleyn A, Breckpot J, et al. Genotype-phenotype relationship and risk stratification in loss-of-function SCN5A mutation carriers. Ann Noninvasive Electrocardiol. 2018;23(5):e12548.
28. Bezzina CR, Barc J, Mizusawa Y, Remme CA, Gourraud JB, Simonet F, et al. Common variants at SCN5A-SCN10A and HEY2 are associated with Brugada syndrome, a rare disease with high risk of sudden cardiac death. Nat Genet. 2013;45(9):1044-9.
29. Barc J, Tadros R, Glinge C, Chiang DY, Jouni M, Simonet F, et al. Genome-wide association analyses identify new Brugada syndrome risk loci and highlight a new mechanism of sodium channel regulation in disease susceptibility. Nat Genet. 2022;54(3):232-9.

30. Shinlapawittayatorn K, Du XX, Liu H, Ficker E, Kaufman ES, Deschenes I. A common SCN5A polymorphism modulates the biophysical defects of SCN5A mutations. Heart Rhythm. 2011;8(3):455-62.
31. Matsumura H, Nakano Y, Ochi H, Onohara Y, Sairaku A, Tokuyama T, et al. H558R, a common SCN5A polymorphism, modifies the clinical phenotype of Brugada syndrome by modulating DNA methylation of SCN5A promoters. J Biomed Sci. 2017;24(1):91.
32. Poelzing S, Forleo C, Samodell M, Dudash L, Sorrentino S, Anaclerio M, et al. SCN5A polymorphism restores trafficking of a Brugada syndrome mutation on a separate gene. Circulation. 2006;114(5):368-76.
33. Mademont-Soler I, Pinsach-Abuin ML, Riuro H, Mates J, Perez-Serra A, Coll M, et al. Large Genomic Imbalances in Brugada Syndrome. PLoS One. 2016;11(9):e0163514.
34. Sonoda K, Ohno S, Ozawa J, Hayano M, Hattori T, Kobori A, et al. Copy number variations of SCN5A in Brugada syndrome. Heart Rhythm. 2018;15(8):1179-88.
35. Monasky MM, Micaglio E, Ciconte G, Pappone C. Brugada Syndrome: Oligogenic or Mendelian Disease? Int J Mol Sci. 2020;21(5).
36. Campuzano O, Sarquella-Brugada G, Cesar S, Arbelo E, Brugada J, Brugada R. Update on Genetic Basis of Brugada Syndrome: Monogenic, Polygenic or Oligogenic? Int J Mol Sci. 2020;21(19).
37. Leong IU, Stuckey A, Lai D, Skinner JR, Love DR. Assessment of the predictive accuracy of five in silico prediction tools, alone or in combination, and two metaservers to classify long QT syndrome gene mutations. BMC Med Genet. 2015;16:34.
38. Vivekanandam V, Ellmers R, Jayaseelan D, Houlden H, Mannikko R, Hanna MG. In silico versus functional characterization of genetic variants: lessons from muscle channelopathies. Brain. 2023;146(4):1316-21.
39. Li Y, Lang S, Akin I, Zhou X, El-Battrawy I. Brugada Syndrome: Different Experimental Models and the Role of Human Cardiomyocytes From Induced Pluripotent Stem Cells. J Am Heart Assoc. 2022;11(7):e024410.
40. de la Roche J, Angsutararux P, Kempf H, Janan M, Bolesani E, Thiemann S, et al. Comparing human iPSC-cardiomyocytes versus HEK293T cells unveils disease-causing effects of Brugada mutation A735V of Na(V)1.5 sodium channels. Sci Rep. 2019;9(1):11173.
41. Ma D, Liu Z, Loh LJ, Zhao Y, Li G, Liew R, et al. Identification of an I(Na)-dependent and I(to)-mediated proarrhythmic mechanism in cardiomyocytes derived from pluripotent stem cells of a Brugada syndrome patient. Sci Rep. 2018;8(1):11246.
42. Hong K, Guerchicoff A, Pollevick GD, Oliva A, Dumaine R, de Zutter M, et al. Cryptic 5' splice site activation in SCN5A associated with Brugada syndrome. J Mol Cell Cardiol. 2005;38(4):555-60.
43. Rossenbacker T, Schollen E, Kuiperi C, de Ravel TJ, Devriendt K, Matthijs G, et al. Unconventional intronic splice site mutation in SCN5A associates with cardiac sodium channelopathy. J Med Genet. 2005;42(5):e29.
44. Ahmed RE, Anzai T, Chanthra N, Uosaki H. A Brief Review of Current Maturation Methods for Human Induced Pluripotent Stem Cells-Derived Cardiomyocytes. Front Cell Dev Biol. 2020;8:178.
45. Wu P, Deng G, Sai X, Guo H, Huang H, Zhu P. Maturation strategies and limitations of induced pluripotent stem cell-derived cardiomyocytes. Biosci Rep. 2021;41(6).

46. Yang X, Rodriguez M, Pabon L, Fischer KA, Reinecke H, Regnier M, et al. Tri-iodo-l-thyronine promotes the maturation of human cardiomyocytes-derived from induced pluripotent stem cells. J Mol Cell Cardiol. 2014;72:296-304.
47. Wang L, Wada Y, Ballan N, Schmeckpeper J, Huang J, Rau CD, et al. Triiodothyronine and dexamethasone alter potassium channel expression and promote electrophysiological maturation of human-induced pluripotent stem cell-derived cardiomyocytes. J Mol Cell Cardiol. 2021;161:130-8.
48. Tohyama S, Hattori F, Sano M, Hishiki T, Nagahata Y, Matsuura T, et al. Distinct metabolic flow enables large-scale purification of mouse and human pluripotent stem cell-derived cardiomyocytes. Cell Stem Cell. 2013;12(1):127-37.
49. Sung TC, Liu CH, Huang WL, Lee YC, Kumar SS, Chang Y, et al. Efficient differentiation of human ES and iPS cells into cardiomyocytes on biomaterials under xeno-free conditions. Biomater Sci. 2019;7(12):5467-81.
50. Wijeyeratne YD, Tanck MW, Mizusawa Y, Batchvarov V, Barc J, Crotti L, et al. SCN5A Mutation Type and a Genetic Risk Score Associate Variably With Brugada Syndrome Phenotype in SCN5A Families. Circ Genom Precis Med. 2020;13(6):e002911.
51. Tadros R, Tan HL, Investigators E-N, El Mathari S, Kors JA, Postema PG, et al. Predicting cardiac electrical response to sodium-channel blockade and Brugada syndrome using polygenic risk scores. Eur Heart J. 2019;40(37):3097-107.
52. Obergrussberger A, Rinke-Weiss I, Goetze TA, Rapedius M, Brinkwirth N, Becker N, et al. The suitability of high throughput automated patch clamp for physiological applications. J Physiol. 2022;600(2):277-97.
53. Glazer AM, Wada Y, Li B, Muhammad A, Kalash OR, O'Neill MJ, et al. High-Throughput Reclassification of SCN5A Variants. Am J Hum Genet. 2020;107(1):111-23.
54. Hayes HB, Nicolini AM, Arrowood CA, Chvatal SA, Wolfson DW, Cho HC, et al. Novel method for action potential measurements from intact cardiac monolayers with multiwell microelectrode array technology. Sci Rep. 2019;9(1):11893.
55. Broyles CN, Robinson P, Daniels MJ. Fluorescent, Bioluminescent, and Optogenetic Approaches to Study Excitable Physiology in the Single Cardiomyocyte. Cells. 2018;7(6).
56. Koopman CD, Zimmermann WH, Knopfel T, de Boer TP. Cardiac optogenetics: using light to monitor cardiac physiology. Basic Res Cardiol. 2017;112(5):56.
57. Kozek KA, Glazer AM, Ng CA, Blackwell D, Egly CL, Vanags LR, et al. High-throughput discovery of trafficking-deficient variants in the cardiac potassium channel K(V)11.1. Heart Rhythm. 2020;17(12):2180-9.

List of abbreviations

ACM	Arrhythmogenic cardiomyopathy
ACMG	American college of medical genetics
AP	Action potential
APA	Action potential amplitude
APD50	Action potential duration at 50% repolarization
APD90	Action potential duration at 90% repolarization
ARVC	Arrhythmogenic right ventricular cardiomyopathy
BPM	beats per minute
BrS	Brugada syndrome
CHO	Chinese hamster ovary
CM	Cardiomyocyte
CNV	copy number variation
CPVT	Catecholaminergic polymorphic ventricular tachycardia
CV%	Coefficient of variation
ECG	Electrocardiogram
ESC	Embryonal stem cell
GECI	Genetically encoded calcium indicators
GEVI	Genetically encoded voltage indicators
GOF	Gain-of-function
GWAS	Genome-wide association study
HES	Heterologous expression system
ICA	Inherited cardiac arrhythmia
ICD	Implantable cardioverter defibrillator
iPSC	Induced pluripotent stem cell
iPSC-CM	Induced pluripotent stem cell-derived cardiomyocytes

LOF	Loss-of-function
LQTS	Long QT syndrome
MEA	Multi electrode array
$Na_V1.5$	Cardiac voltage-gated sodium channel α-subunit
NGS	Next-generation sequencing
NMD	Nonsense mediated decay
P/LP	(Likely) pathogenic
PCR	Polymare chain reaction
QTc	Heart rate-corrected QT interval
RMP	resting membrane potential
RT	Room temperature
RT-qPCR	Quantitative reverse transcription polymerase chain reaction
SCD	Sudden cardiac death
SD	Standard deviation
SNP	Single nucleotide polymorphism
SQTS	Short QT syndrome
T3	Triiodothyronine
VF	Ventricular fibrillation
VT	Ventricular tachycardia
VUS	Variant of uncertain significance
WES	Whole exome sequencing
WGS	Whole genome sequencing
WT	Wild type

Curriculum vitae

Personal information

Name	Eline Simons
Date of Birth	25/03/1992
Nationality	Belgian
Mail	eline.simons@uantwerpen.be

Education and Employment

2023 – present	Data Manager CellCarta, Belgium
2017 – 2023	PhD student Center of Medical Genetics, University of Antwerp, Belgium
2015 – 2017	Master in Biochemistry and Biotechnology: Molecular and Cellular Gene Biotechnology (great distinction) *Major: Molecular and cellular neuroscience, Minor: Research* University of Antwerp, Belgium
2013 – 2015	Bachelor in Biochemistry and Biotechnology University of Antwerp, Beglium
2010 – 2013	Bachelor in Medical Laboratory Technology (great distinction) Plantijn Hogeschool, Belgium

Additional education

2019	EMBL course 'Genome Engineering: CRISPR/Cas' Heidelberg, Germany; 17 – 22th March
2018	Permanent Education Course in Human Genetics Belgian Society for Human Genetics

Publications

Simons E, Loeys B, Alaerts M. *iPSC-Derived Cardiomyocytes in Inherited Cardiac Arrhythmias: Pathomechanistic Discovery and Drug Development*. Biomedicines. 2023 Jan 25;11(2):334. doi: 10.3390/biomedicines11020334. PMID: 36830871; PMCID: PMC9953535.

Simons E, Nijak A, Loeys B, Alaerts M. *Generation of two induced pluripotent stem cell (iPSC) lines (BBANTWi006-A, BBANTWi007-A) from Brugada syndrome patients carrying an SCN5A mutation.* Stem Cell Res. 2022 Feb 24;60:102719. doi: 10.1016/j.scr.2022.102719. Epub ahead of print. PMID: 35247843.

Nijak A, **Simons E**, Vandendriessche B, Van de Sande D, Fransen E, Sieliwończyk E, Van Gucht I, Van Craenenbroeck E, Saenen J, Heidbuchel H, Ponsaerts P, Labro AJ, Snyders D, De Vos W, Schepers D, Alaerts M, Loeys BL. Morpho-functional comparison of differentiation protocols to create iPSC-derived cardiomyocytes. Biol Open. 2022 Feb 15;11(2):bio059016. doi: 10.1242/bio.059016. Epub 2022 Feb 23. PMID: 35195246.

Simons E, Labro A, Saenen J, Nijak A, Sieliwonczyk E, Vandendriessche B, Dąbrowska M, Van Craenenbroeck EM, Schepers D, Van Laer L, Loeys BL, Alaerts M. *Molecular autopsy and subsequent functional analysis reveal de novo DSG2 mutation as cause of sudden death*. Eur J Med Genet. 2021 Nov;64(11):104322. doi: 10.1016/j.ejmg.2021.104322. Epub 2021 Aug 23. PMID: 34438094.

Sieliwonczyk E, Alaerts M, Robyns T, Schepers D, Claes C, Corveleyn A, Willems R, Van Craenenbroeck EM, **Simons E**, Nijak A, Vandendriessche B, Mortier G, Vrints C, Koopman P, Heidbuchel H, Van Laer L, Saenen J, Loeys B. *Clinical characterization of the first Belgian SCN5A founder mutation cohort.* Europace. 2020 Nov 22:euaa305. doi: 10.1093/europace/euaa305. Epub ahead of print. PMID: 33221854.

Nijak A, Labro AJ, De Wilde H, Dewals W, Peigneur S, Tytgat J, Snyders D, Sieliwonczyk E, **Simons E**, Van Craenenbroeck E, Schepers D, Van Laer L, Saenen J, Loeys B, Alaerts M. *Compound Heterozygous SCN5A Mutations in Severe Sodium Channelopathy With*

Brugada Syndrome: A Case Report. Front Cardiovasc Med. 2020 Jul 24;7:117. doi: 10.3389/fcvm.2020.00117. PMID: 32850980; PMCID: PMC7396896.

Conferences

Selected presentations

Genetics Retreat: NVHG Graduate Meeting
Kerkrade, The Netherlands; March 28-29th 2019
Study of the contribution of SCN10A mutations to the Brugada syndrome genetic architecture.

Poster presentations

GRC/GRS on Ion Channels: Molecular Mechanisms of Electrical Signaling in Health and Disease
South Hadley, MA, United States; June 9-15th 2022
Modeling of an SCN5A founder mutation in iPSC-derived cardiomyocytes.

European Society of Human Genetics (ESHG) 2022 Conference
Vienna, Austria; June 11-14th 2022
Diagnostic yield of a NGS panel in a Brugada syndrome cohort.

Frontiers in Cardiovascular Biomedicine 2022
Budapest, Hungary; April 29-30, May 1st 2022
Modeling of an SCN5A founder mutation in iPSC-derived cardiomyocytes.

BeSHG 21th annual meeting - Reproductive Genetics
Diegem, Belgium; September 17th 2021
Modeling of an SCN5A founder mutation in iPSC-derived cardiomyocytes.

EMBO Workshop: Cardiomyocyte Biology
Online event; May 30 - June 2nd 2021
Modeling of an SCN5A founder mutation in iPSC-derived cardiomyocytes

European Society of Human Genetics (ESHG) ESHG 2020.2: Live in Your Living Room
Online event; June 6-9th 2020
Electrophysiological characterization of a Brugada syndrome SCN5A Belgian founder mutation modelled in induced pluripotent stem cell cardiomyocytes.

BeSHG 19th annual meeting: Precision Medicine: Application of Genetics in Prevention and Treatment
Liège, Belgium; March 15th 2019
Study of the contribution of SCN10A mutations to the Brugada syndrome genetic architecture.

BWG-BRC: Cellular and molecular mechanisms underlying cardiovascular physiopathology
Louvain-La-Neuve, Belgium; November 16th 2018
Combined genetic and electrophysiological studies resolve an unexplained SCD case.

Genomics of Rare Disease
Wellcome Genome Campus, Hinxton, UK; March 26-28th 2018
Study of the contribution of SCN10A mutations to the Brugada syndrome genetic architecture.

Honors and awards

July 2022	FWO (Research Foundation – Flanders) travel grant for participation in a conference abroad
January 2018	FWO PhD Fellowship strategic basic research

Educational activities

Master thesis Dogan Akdeniz, *Use of CMOS-MEA chips for electrophysiological measurement of induced pluripotent stem cell derived cardiomyocytes (iPSC-CM),* University of Antwerp, 2020 – 2021

Bachelor thesis Melanie Cools, *Optimalisatie van het protocol voor differentiatie van iPSC naar cardiomyocyten,* AP Hogeschool, 2020 – 2021

Bachelor thesis Robbe Van Elsacker, *Optimalisatie van het protocol voor de differentiatie van iPSC's tot cardiomyocyten,* Karel de Grote Hogeschool, 2019 – 2020

Master thesis Thomas Font Freide, *Optimization of cardiomyocyte differentiation from induced pluripotent stem cells to create a cellular disease model for Brugada syndrome,* University of Antwerp, 2018 – 2019

Bachelor thesis Dago Arnouts, *Optimalisatie van een In-house qPCR panel ter vervanging van het TaqMan scorecard panel,* Karel de Grote Hogeschool, 2017 – 2018

Dankwoord

Nu deze thesis eindelijk geschreven is, neem ik graag nog even tijd om iedereen die me gesteund heeft in de afgelopen jaren te bedanken.

Als eerste zou ik graag Bart en Maaike willen bedanken dat ze mij de kans hebben gegeven om mijn master thesis op het labo te komen doen. Door het interessante onderwerp en de leuke werkomgeving heb ik dan ook niet lang getwijfeld om mij kandidaat te stellen voor de PhD positie die er vrij kwam. Bart, dankjewel om mij de kans te geven om dit doctoraat te starten en om me te ondersteunen met je uitgebreide wetenschappelijke kennis. Maaike, je opgewektheid, gedrevenheid en kennis hebben me altijd geïnspireerd om door te zetten. Je deur stond altijd open om binnen te springen wanneer het nodig was. En met de wispelturigheid van de differentiaties was het meer dan eens nodig om even te overleggen hoe we weer verder moesten gaan. Bedankt ook om door al het geschreven werk te gaan en dit toch steeds een niveautje hoger te tillen. Dorien, dankuwel om steeds je wetenschappelijke inzichten te delen en ook een luisterend oor aan te bieden op momenten dat dit wel eens nodig was.

Jolien en ik zijn tegelijk aan onze masterthesis begonnen op het CMG waar we onze ervaringen, frustraties en onhandige dagen meer dan eens met elkaar konden delen. De steun dat we aan elkaar hadden, heeft misschien ook wel geholpen bij de beslissing om beide een doctoraat te starten op het CMG, waarvoor dank! Samen met Melanie en Ewa zijn we dan ook effectief in 2017 gestart met ons doctoraat, waarna Ilse er al snel bijkwam. And not to forget, Ola!! Thank you for introducing me to the wonderful world of iPSCs, differentiations, Polish culture, German Christmas markets and many more amazing experiences! Wish you all the best, wherever you are in the world. Melanie, samen beginnen aan een doctoraat schept wel een band. Samen kunnen stressen voor het FWO, klagen op cellen die niet doen wat wij willen maar ook gewoon gezellige labomomentjes beleven, heeft het de afgelopen jaren zoveel leuker gemaakt. Dankuwel voor het steunpakket met de prachtige Mushu dat je samen met Jolien in elkaar hebt gestoken! Ewa, ik sta nog altijd versteld van je ongelofelijke wetenschappelijke kennis en interesse in zo veel uiteenlopende gebieden. Wat er ook voor gezorgd heeft dat ik jullie in Londen ben kunnen komen bezoeken en we een leuk weekendje hebben gehad. Ilse, wat een klein danske in het labo al niet kan voort brengen… onder andere een topreis naar Turkije waar we onze lachspieren zeker goed getraind hebben, goed hebben kunnen dansen aan paddenstoelen en we geleerd hebben dat het toch altijd de moeite waard is om eens onder de brug door te zwemmen ;). Dat we nog veel kunnen bla-bla-bla'en, dinerkes maken, feestjes en festivalleks doen en alles kunnen geven in de regen. En terwijl we allemaal gegroeid zijn door de jaren, zijn we toch ook wel een beetje blijven dutsen zoals op congressen waar er ringen in de afvoer belandden, knieën opzwollen, enkels omgeslagen werden, buikgriepjes voorkwamen en Corona toch ook van zich liet

horen. Anciens, bedankt voor zo veel leuke herinneringen van de afgelopen jaren. Maar er is zeker nog genoeg tijd om er veel meer bij te maken.

Ook de leden van het PED team mag ik niet vergeten te bedanken. Bert, jij kwam mee het PED team versterken om met zowel vissen als cellen te werken, moedige keuze! Hoewel de combinatie zeker niet voor de hand liggend is, was je toch altijd opgewekt als we in de week of het weekend samen aan de flow zaten, met af en toe zelf wat gezang erbij. Ook al kwam de Ferrari misschien je oren uit, toch bedankt om de StuBru pas op te zetten als ik uit het labo vertrok. Hanne, ook jou wil ik bedanken voor de leuke babbels aan de flow en je input tijdens de PED meetings. Dogan, als master student kwam je in onze groep en ik wil graag bedanken voor al de hulp die je toen gegeven hebt bij mijn celwerk. En bedankt om van tijd tot tijd overheerlijke baklava mee te nemen en ook te laten weten als het op de kar stond.

Al het werk zou natuurlijk ook niet gelukt zijn zonder het fantastische werk van onze laboranten. Laura, niet alleen dankuwel voor al uw hulp bij onder andere het celwerk, kleuringen, qPCR, extracties,… maar ook voor de fijne babbeltjes tussendoor! Maaike, bedankt om met al je kennis van western blot deze techniek voor je rekening te nemen. Jolien, ook jij bedankt voor je hulp met het celwerk en de leuke babbels. Jarl, Charlotte en Sofie, dankuwel ook aan jullie om het labo mee draaiende te houden!

Danku ook aan alle andere collega's van de cardiogenetica groep. Lotte, Joe, Jotte, Pauline, Merlijn, Lucia, Irene, Anne, Ivanna, Aline, Jeannette, Ilse en Silke dankuwel om samen zo een leuke werksfeer te creëren waar iedereen z'n plekje kan vinden.

Ik ben op het CMG begonnen in het hoekje achter de deur van bureau G230 met Dorien, Ilse L., Gerarda, Manou, Hanne, Elke en Elyssa. Maar zoals dat gaat met doctoraatsstudenten is het altijd een beetje een komen gaan waarna Lisse, Isabelle en Ana Regina de nieuwe bureaumaatjes werden. Dankuwel allemaal om een zo een fijne omgeving van te maken, met zeker de nodige babbeltjes, al dan niet werk gerelateerd. Maar plots was er sprake van een nieuw cellabo en een verhuis drong zich op. Wat eerst wat aanvoelde als een 'verbanning' naar het eerste verdiep, bleek uiteindelijk een aangename verrassing met een oase van rust en gezelligheid, als we het occasionele kindje dat in den bureau stond en het gehuil niet meerekenen. Laura M. dankuwel om als mijn buurvrouw naar mijn geklaag te luisteren als het schrijven toch weer eens niet zo vlot ging en voor de gezellige babbeltjes tussendoor. Nele, bedankt voor je enthousiasme dat zo aanstekelijk werkt, echt een plezier om met je samen in een bureau te zitten. Jotte, dankuwel om mijn paranimf te willen zijn! Ik had me er geen betere kunnen voorstellen. Met jouw vrolijkheid was het altijd fijn om naar het werk te komen. De toffe babbels die we hadden, die meer niet dan wel over het werk gingen en altijd

wel goed op de lachspieren werkten, waren ideaal als ontspanning tussendoor. Kathleen en Eef, ook jullie wil ik bedanken voor de fijne momentjes in onze bureau. Lucia and Irene, thank you for bringing some exotic vibes to our office. When you were talking in Spanish or Italian, it made me feel like I was on a holiday. Good luck and best wishes to all of you!!

Many thanks to all other colleagues at CMG for creating such a lovely and friendly environment. The cozy and relaxing lunches at CMG, lab days, after work drink and extra activities outside work would not have been the same without you all. Joe, Joe and Dale, a special thanks to you guys for organizing awesome CMG weekends with kayaking, hiking, hot tubs, microslaapjes and the famous high kick! Thank you Lisse, Tammy, Tycho, Farhan, Thomas, Evelien, Yentl, Liene, Ana Regina, Isabelle, Janah, Marc, Mathijs, Kirsten, Ellen E., Ellen S., An, Gerarda, Luna, Kevin and Arvid

Al mijn celwerk heb ik uitgevoerd op campus Drie Eiken in het gezellige labo van Prof. Ponsaerts. Bedankt om jullie labo met ons te delen en zo een leuke en aangename sfeer te creëren. Elise, Jonas en Julia, het was altijd fijn om bij jullie op het labo te komen en danku om ons met open armen te ontvangen.

Vele uren heb ik ook doorgebracht in het T-gebouw op de vijfde verdieping in het labo van Prof. Snyders en Prof. Labro. Dankuwel Dieter om me de kneepjes van het patchen te leren, hoewel ik niet zeker ben of ik het eigenlijk ooit echt heel leuk heb gevonden. Het was wel altijd fijn om niet alleen in het patch lokaal te moeten zitten en een muziekje op de achtergrond maakte het ook altijd weer leuker. Evy, echt een ongelofelijke merci! Zonder jou had ik nooit al die data hier in deze thesis kunnen genereren. En hoewel de cellen zeker niet altijd goed meewerkten, bleef je toch mee proberen. De babbeltjes tussendoor maakten het dan ook wel veel aangenamer zeker als het voor geen meter liep. Kenny, jij ook bedankt voor het fijne gezelschap op het labo, leuke lunches en de technische hulp als er weer ergens iets verkeerd liep bij het opzetten van de opstelling.

Een super dikke merci aan Daisy, hoe jij voor mij gesupporterd hebt gedurende die vele jaren PhD, dankuwel! Vanaf de eerste dag was je super enthousiast en heb jij mij door dik en dun gesteund. Een vriendschap die een start kent vele jaren terug op een dansvloer ergens in Antwerpen en die ons ondertussen op veel leuke en soms ook speciale plaatsten gebracht heeft, remember dat hostel in Berlijn ;). Mijn Homies en Bbitchatsjos, hoe kan ik jullie bedanken voor alles wat jullie voor mij betekenen? En dan te bedenken dat alles begonnen is met het memorabele zinnetje ‘Hallo, ik ben Marthe.’ Dankuwel om jullie luisterend oor te bieden wanneer het allemaal weer even tegenzat en me in mezelf te laten geloven, maar ook voor de zotte momenten samen zoals in Lapland, tijdens center parcs weekendjes, lunchkes, brunchkes, wijnavondjes, een stevig

feestje of gewoon een spelletjesmiddag met de rummiklub. Evelyne, Marthe, Emily, Nina en Sofie, dikke liefde voor jullie! Danku ook aan Elke, Emelie, Tim, Nick en Kenneth om naast leuke skireizen en gezellige diners me ook te steunen in mijn doctoraat. Ellen en Shana, nog niet super lang geleden hebben we elkaar leren kennen, maar wat ben ik er blij mee! Bedankt om er voor me te zijn en voor de nodige afleiding te zorgen wanneer het soms allemaal wat veel werd en een weekendje Disneyland helpt daar zeker ook bij. Wanneer zijn we nog eens weg met de partybak?! De Patronnekes wil ik ook nog graag bedanken voor de steun en leuke tijden de afgelopen jaren!

Ondertussen ben ik aan een nieuw hoofdstuk in mijn carrière begonnen bij CellCarta en mijn nieuwe collega's wil ik graag bedanken voor de fijne werkomgeving en de steun die ze mij de afgelopen periode hebben gegeven.

Wat ben ik ook blij met de familie die ik rond me heb. Dankuwel om steeds voor voldoende ontspanning te zorgen met leuke familiebijeenkomsten zoals verjaardagsfeestjes, Kerst, Pasen of welke gelegenheid dan ook. Een zwembad of springkasteel erbij maakt het plezier alleen maar groter en zeker niet alleen de kindjes maken er dan gebruik van. Bij deze dankuwel Bomma en Bompa, Nonkel Rudi, Tante Lea, Nonkel Lode, Tante Sonja, Nonkel Patrick, Phaedra, René, Evelyne, Filip, Jessie, Kimmy en de achterkleinkinderen.

Niet vergeten ook Nils en Allanah, mijn grote broer en zus. Ook jullie bedankt om er altijd te zijn en me te steunen en voor de onvermijdelijke plagerijtjes, memes en ook de Disneyquotes die te pas en te onpas boven komen. Elke keer als ik bij jullie ben samen met mama en papa, Kathleen, Kevin, Emiel, Nora, Tibo en Leon worden mijn batterijtjes weer helemaal opgeladen.

Ik heb het gevoel dat er hier al overdreven veel danku's en bedankt'en op de laatste pagina's staan, maar dat houdt me niet tegen om misschien wel de grootste danku uit te spreken voor Mama en Papa. Dankuwel om mij alle kansen te hebben gegeven om tot dit punt te komen, danku om er altijd te zijn voor mij, in mij te geloven en mij te steunen in alles wat ik doe. En een dikke merci voor al de maaltijden die jullie de laatste tijd hebben gemaakt voor mij.

Nog een laatste welgemeende danku aan iedereen die mij op eender welke manier dan ook gesteund heeft. En om het harde werk aan deze thesis niet voor niets te laten zijn, wil ik jullie misschien toch vragen om alsjeblieft ergens een paragraafje in deze thesis te lezen, Danku 😉.